

การกลายยีนแอมิโลมอลเทสจาก *Corynebacterium glutamicum* ATCC 13032

เพื่อปรับปรุงการทนความร้อนของเอนไซม์

นางสาวพิชชานันท์ นิ่มพิบูลย์



จุฬาลงกรณ์มหาวิทยาลัย

CHULALONGKORN UNIVERSITY

บทคัดย่อและแฟ้มข้อมูลฉบับเต็มของวิทยานิพนธ์ตั้งแต่ปีการศึกษา 2554 ที่ให้บริการในคลังปัญญาจุฬาฯ (CUIR)

เป็นแฟ้มข้อมูลของนิสิตเจ้าของวิทยานิพนธ์ ที่ส่งผ่านทางบัณฑิตวิทยาลัย

The abstract and full text of theses from the academic year 2011 in Chulalongkorn University Intellectual Repository (CUIR)

are the thesis authors' files submitted through the University Graduate School.

วิทยานิพนธ์นี้เป็นส่วนหนึ่งของการศึกษาตามหลักสูตรปริญญาวิทยาศาสตรดุษฎีบัณฑิต

สาขาวิชาเทคโนโลยีชีวภาพ

คณะวิทยาศาสตร์ จุฬาลงกรณ์มหาวิทยาลัย

ปีการศึกษา 2558

ลิขสิทธิ์ของจุฬาลงกรณ์มหาวิทยาลัย

MUTAGENESIS OF AMYLOMALTASE FROM *Corynebacterium glutamicum*
ATCC 13032 TO IMPROVE THERMOSTABILITY OF THE ENZYME

Miss Pitchanan Nimpiboon



A Dissertation Submitted in Partial Fulfillment of the Requirements
for the Degree of Doctor of Philosophy Program in Biotechnology

Faculty of Science

Chulalongkorn University

Academic Year 2015

Copyright of Chulalongkorn University

| | |
|-------------------|---|
| Thesis Title | MUTAGENESIS OF AMYLOMALTASE FROM <i>Corynebacterium glutamicum</i> ATCC 13032 TO IMPROVE THERMOSTABILITY OF THE ENZYME |
| By | Miss Pitchanan Nimpiboon |
| Field of Study | Biotechnology |
| Thesis Advisor | Professor Piamsook Pongsawasdi, Ph.D. |
| Thesis Co-Advisor | Associate Professor Jarunee Kaulpiboon, Ph.D. |

Accepted by the Faculty of Science, Chulalongkorn University in Partial
Fulfillment of the Requirements for the Doctoral Degree

..... Dean of the Faculty of Science
(Associate Professor Polkit Sangvanich, Ph.D.)

THESIS COMMITTEE

..... Chairman
(Assistant Professor Kanoktip Packdibamrung, Ph.D.)

..... Thesis Advisor
(Professor Piamsook Pongsawasdi, Ph.D.)

..... Thesis Co-Advisor
(Associate Professor Jarunee Kaulpiboon, Ph.D.)

..... Examiner
(Assistant Professor Saowarath Jantaro, Ph.D.)

..... Examiner
(Associate Professor Chanpen Chanchao, Ph.D.)

..... External Examiner
(Associate Professor Jarunya Narangajavana, Ph.D.)

พิชชานันท์ นิ่มพิบูลย์ : การกลายยีนแอมิโลมอลเตสจาก *Corynebacterium glutamicum* ATCC 13032 เพื่อปรับปรุงการทนความร้อนของเอนไซม์ (MUTAGENESIS OF AMYLOMALTASE FROM *Corynebacterium glutamicum* ATCC 13032 TO IMPROVE THERMOSTABILITY OF THE ENZYME) อ.ที่ปรึกษาวิทยานิพนธ์หลัก: ศ. ดร.เปี่ยมสุข พงษ์สวัสดิ์, อ.ที่ปรึกษาวิทยานิพนธ์ร่วม: รศ. ดร. จารุณี ควรพิบูลย์, 207 หน้า.

งานวิจัยนี้มีวัตถุประสงค์เพื่อปรับปรุงการทนความร้อนของเอนไซม์แอมิโลมอลเตสจาก *Corynebacterium glutamicum* ด้วยวิธีการกลายยีนแบบสุ่ม และการกลายยีนแบบเฉพาะตำแหน่ง จากผลการกลายยีนแบบสุ่มด้วยเทคนิค error-prone PCR พบว่าสามารถคัดเลือกเอนไซม์แอมิโลมอลเตสกลายที่ทนอุณหภูมิ 50 °ซ ได้ 1 โคลนในขณะที่เอนไซม์ดั้งเดิมสูญเสียแอกทิวิตีเกือบทั้งหมด ตรวจสอบพบว่าเอนไซม์กลายมีกรดอะมิโนกลายจากเอนไซม์ดั้งเดิม 1 ตำแหน่งคือ A406V เพื่อตรวจสอบว่าตำแหน่ง Ala406 มีผลต่อการทนความร้อนของเอนไซม์ จึงใช้เทคนิคการกลายยีนแบบเฉพาะตำแหน่งในการกลายยีนให้เป็น A406V และ A406L เมื่อนำเอนไซม์กลายทั้ง 2 ชนิดไปตรวจสอบลักษณะสมบัติพบว่าเอนไซม์กลาย A406V และ A406L เร่งปฏิกิริยา transglucosylation ได้สูงขึ้นจากเอนไซม์ดั้งเดิม มีอุณหภูมิ และ pH ที่เหมาะสม สำหรับปฏิกิริยา disproportionation และ cyclization เพิ่มขึ้นจากเอนไซม์ดั้งเดิม และสามารถทนอุณหภูมิที่ 35 °ซ และ 40 °ซ ได้ดีกว่า นอกจากนี้ผลของการทำ DSC พบว่าเอนไซม์กลายทั้ง 2 ชนิดมีรูปแบบการคงทนต่อความร้อนที่อุณหภูมิสูงกว่าเอนไซม์ดั้งเดิม โดยที่เอนไซม์ A406V แสดงผลของการเร่งปฏิกิริยา และทนต่อความร้อนได้ดีกว่า A406L จากการศึกษาทางจลนพลศาสตร์ของปฏิกิริยา disproportionation โดยเอนไซม์ A406V และ A406L มีค่า k_{cat}/K_m สูงขึ้นกว่าเอนไซม์ดั้งเดิม 2.9 และ 1.4 เท่า ตามลำดับ โดยมีการเพิ่มอย่างมีนัยสำคัญของ k_{cat} เมื่อตรวจสอบผลิตภัณฑ์ LR-CDs ของปฏิกิริยา cyclization พบว่าเอนไซม์ A406V สามารถผลิต LR-CDs ที่มีขนาดใหญ่และจำนวนที่มากขึ้นเมื่อเทียบกับเอนไซม์ดั้งเดิม โดยเฉพาะเมื่อเพิ่มระยะเวลา และอุณหภูมิในการบ่มให้สูงขึ้น ในส่วนที่สองของงาน ได้สร้างเอนไซม์กลายเพิ่มขึ้น เพื่อปรับปรุงการทนร้อนให้ดีขึ้น โดยใช้เทคนิคการกลายยีนเฉพาะตำแหน่ง เปลี่ยนกรดอะมิโน Ala406 ให้เป็น His (H), Arg (R) และ Phe (F) และเปลี่ยนที่ตำแหน่ง Asn287 ให้เป็น Tyr (Y) เมื่อตรวจสอบลักษณะสมบัติ พบว่า เอนไซม์กลายทั้ง 4 ชนิด A406H, A406R, A406F และ N287Y เร่งปฏิกิริยา transglucosylation ลดลงอย่างเห็นได้ชัด ในขณะที่ไม่สามารถตรวจวัดแอกทิวิตีของ cyclization ได้ เอนไซม์กลายทั้ง 4 ชนิด มี optimum pH สำหรับปฏิกิริยา disproportionation เพิ่มขึ้น โดยที่ เอนไซม์กลาย N287Y เพิ่มขึ้น 0.5 pH unit ขณะที่ เอนไซม์กลาย A406H, A406R, A406F เพิ่มขึ้น 1.0 pH unit ผลที่สำคัญคือเอนไซม์กลายทั้ง 4 ชนิด สามารถทนร้อนที่อุณหภูมิ 35 °ซ, 40 °ซ และ 45 °ซ ได้สูงกว่าเอนไซม์ดั้งเดิม เมื่อบ่มในระยะเวลา 3 ชม. และยังพบว่า เอนไซม์กลาย N287Y มี optimum temperature สำหรับปฏิกิริยา disproportionation เพิ่มขึ้น โดยเมื่อทำการตรวจสอบโครงสร้างด้วยวิธี circular dichroism และรูปแบบการคงทนต่อความร้อนด้วยเทคนิค DSC พบว่าโครงสร้างทุติยภูมิของเอนไซม์กลายแทบไม่เปลี่ยนแปลง แต่โครงสร้างตติยภูมิเปลี่ยนไปเมื่อเทียบกับเอนไซม์ดั้งเดิม จากผลทั้งหมด พบว่า เอนไซม์กลายที่ทนร้อนดีที่สุด และมีแอกทิวิตีสูงกว่าเอนไซม์ดั้งเดิมคือ A406V

สาขาวิชา เทคโนโลยีชีวภาพ

ปีการศึกษา 2558

ลายมือชื่อนิสิต

ลายมือชื่อ อ.ที่ปรึกษาหลัก

ลายมือชื่อ อ.ที่ปรึกษาร่วม

5273919423 : MAJOR BIOTECHNOLOGY

KEYWORDS: AMYLOMALTASE / RANDOM MUTAGENESIS / SITE-DIRECTED
MUTAGENESIS / THERMOSTABILITY / LARGE-RING CYCLODEXTRIN /
CORYNEBACTERIUM GLUTAMICUM

PITCHANAN NIMPIBOON: MUTAGENESIS OF AMYLOMALTASE FROM
Corynebacterium glutamicum ATCC 13032 TO IMPROVE THERMOSTABILITY OF
THE ENZYME. ADVISOR: PROF. PIAMSOOK PONGSAWASDI, Ph.D., CO-ADVISOR:
ASSOC. PROF. JARUNEE KAULPIBOON, Ph.D., 207 pp.

This work aims to improve thermostability of amyloamylase from a mesophilic *Corynebacterium glutamicum* (CgAM) by random and site-directed mutagenesis. From error prone PCR, a mutated CgAM with higher thermostability at 50 °C compared to the wild-type was selected and sequenced. The result showed that the mutant contains a single mutation of A406V. Site-directed mutagenesis was then performed to construct A406V and A406L. Both mutated CgAMs showed higher intermolecular transglucosylation activity with upward shift in optimum temperature and a slight increase in optimum pH for disproportionation and cyclization reactions. Thermostability of both mutated CgAMs at 35–40 °C was significantly increased with a higher peak temperature from DSC spectra when compared to the wild-type. A406V had a higher effect on activity and thermostability than A406L. The catalytic efficiency values k_{cat}/K_m of A406V- and A406L- CgAMs were 2.9 and 1.4 times higher than that of the wild-type, mainly due to a significant increase in k_{cat} . LR-CD products analysis demonstrated that A406V gave larger size CDs and higher product yield, especially at longer incubation time and higher temperature, in comparison to the wild-type enzyme. In the second part of the work, site-directed mutagenesis at Ala406 and Asn287 were performed in the attempt to construct more mutated CgAMs with higher thermostability. Substitutions of A406 by H, R and F and substitution of N287 by Y were performed. Transglucosylation activities of A406H, A406R, A406F and N287Y- CgAMs including starch transglucosylation and disproportionation were diminished while cyclization activity of all these four MT- CgAMs could not be detected. For disproportionation activity, the slight increase (+0.5 pH unit) in optimum pH was observed for N287Y-CgAM while a shift of 1.0 pH unit in optimum pH was also observed with A406H, A406R, and A406F- CgAMs, respectively. In addition, four MT- CgAMs showed higher effect on thermostability at 35 °C, 40 °C and 45 °C than that of WT- CgAM at a longer incubation for 3 h, a shift of +5 °C in optimum temperature was observed for N287Y- CgAM. The secondary structures of four mutated enzymes were closed to the WT from the result of circular dichroism spectra. However, three dimensional conformation may be changed as evidenced by thermal transition profiles from DSC measurements. From the overall results, A406V- CgAM was the best mutated enzyme with higher thermostability and higher activity than its WT counterpart.

Field of Study: Biotechnology

Student's Signature

Academic Year: 2015

Advisor's Signature

Co-Advisor's Signature

ACKNOWLEDGEMENTS

I would like to express my deepest gratitude to my advisor, Professor Piamsook Pongsawasdi, and my co-advisor, Associate Professor Jarunee Kaulpiboon for her generous advices, technical helps, guidance, attention and support throughout this thesis. Without their kindness and understanding, this work could not be accomplished. My appreciate is also expressed to Assistant Professor Kaukarun Krusong, for their valuable comment and insight concerning. My gratitude is also extended to Prof. Dr. Shun-ichi Kidokoro and Dr. Shigeyoshi Nakamura at Department of Bioengineering, Nagaoka University of Technology, Japan for their valuable suggestion, technical helps and DSC support.

The Department of Biochemistry, Faculty of Science gave support for chemicals and instruments. Sincere thanks and appreciation are also extened to Assistant Professor Dr. Kanoktip Packdibamrung, Associate Professor Dr. Chanpen Chanchao, Assistant Professor Dr.Saowarath Jantaro and Associate Professor Dr. Jarunya Narangajavana who serve as the members of the Doctoral committees, for their helpful suggestions and comments.

My thanks also go to all members in the Starch and Cyclodextrin Research Unit and friends in Department of the Biochemistry and Biotechnology program, for their assistance and friendship especially to Dr. Wischada Jongmevasna, Dr. Surachai Yaiyen, Dr. Santana Nakapong, Dr. Wiriya Srisimararat, Dr. Aporn Bualung, Dr. Bongkoj Boonburapong, Dr. Ajiraporn Kongpol, Miss Wanitcha Rachadech, Miss Nattaya Anurutphan, Miss Aornsiri Polla, Miss Phattanit Tripetch and Mr. Sayan Prakobpetch.

Finally, the greatest gratitude is expressed to my parents and my family for their infinite love, encouragement, will power and heartiness support throughout my life.

Pitchanan Nimpiboon received the Overseas Research Experience Scholarship for Graduate student supported by the Graduate School, Program in Biotechnology, and Faculty of Science, Chulalongkorn University, the Sakura Exchange Program in Science Scholarship supported by Japan Science and Technology Agency (JST) on DSC work at the Department of Bioengineering, Nagaoka University of Technology, Japan. The Financial supports from the IIAC of the CU Centenary Academic Development Project and Thailand Research Fund Grant number IRG 5780008 are acknowledged.

CONTENTS

| | Page |
|---|-------|
| THAI ABSTRACT | iv |
| ENGLISH ABSTRACT..... | v |
| ACKNOWLEDGEMENTS | vi |
| CONTENTS..... | vii |
| LIST OF TABLES | xiii |
| LIST OF FIGURES | xiv |
| ABBREVIATIONS | xviii |
| CHAPTER I..... | 1 |
| INTRODUCTION | 1 |
| 1.1 Starch | 1 |
| 1.2 Starch-degrading enzymes | 1 |
| 1.3 The 4- α -glucanotransferase (4 α GTase) group..... | 5 |
| 1.4 The structure of amylomaltase..... | 8 |
| 1.5 Physiological roles of amylomaltase | 18 |
| 1.6 Large ring cyclodextrins (LR-CDs)..... | 20 |
| 1.7 Application of amylomaltase and LR-CDs..... | 21 |
| 1.8 Error-prone PCR..... | 31 |
| 1.9 Background and the Objectives of this study | 32 |
| CHAPTER II..... | 34 |
| MATERIALS AND METHODS..... | 34 |
| 2.1 Equipments | 34 |
| 2.2 Chemicals | 35 |
| 2.3 Enzyme, Restriction enzymes and Bacterial strains | 38 |
| 2.4 Random mutagenesis | 39 |
| 2.4.1 Cultivation and extraction of recombinant plasmid pET-19b <i>CgAM</i> | 39 |
| 2.4.2 Agarose gel electrophoresis..... | 39 |
| 2.4.3 Modification of <i>CgAM</i> gene using error-prone PCR technique..... | 40 |
| 2.4.4 Restriction enzyme digestion | 40 |

| | Page |
|--|------|
| 2.4.5 Ligation of the PCR product with vector pET-19b | 41 |
| 2.4.6 Preparation of competent cells for electroporation (Sambrook and Russel, 2001) | 41 |
| 2.4.7 Plasmid transformation..... | 42 |
| 2.4.8 The colony PCR technique..... | 42 |
| 2.5 The screening for thermostability of MT-CgAMs..... | 43 |
| 2.6 Nucleotide sequencing | 43 |
| 2.7 Site-directed mutagenesis | 44 |
| 2.8 The expression of recombinant wild-type WT- and MT-CgAMs | 46 |
| 2.9 Expression and purification of WT- and MT-CgAMs | 46 |
| 2.9.1 Cells cultivation and crude extract preparation | 46 |
| 2.9.2 Purification of recombinant WT- and MT-CgAMs | 47 |
| 2.10 Enzyme assay..... | 48 |
| 2.10.1 Starch degrading activity..... | 48 |
| 2.10.2 Starch transglucosylation activity | 49 |
| 2.10.3 Disproportionation activity..... | 49 |
| 2.10.4 Cyclization activity..... | 50 |
| 2.10.5 Coupling activity | 50 |
| 2.10.6 Hydrolysis activity | 51 |
| 2.11 Protein determination..... | 51 |
| 2.12 Polyacrylamide gel electrophoresis (PAGE) | 51 |
| 2.12.1 SDS-polyacrylamide gel electrophoresis (SDS-PAGE)..... | 51 |
| 2.12.2 Coomassie blue staining..... | 52 |
| 2.13 Characterization of AM | 52 |
| 2.13.1 Effect of pH and temperature on activity and stability | 52 |
| 2.13.2 Substrate specificity | 53 |
| 2.13.3 Analysis of kinetic parameters | 53 |
| 2.13.4 Circular dichroism spectrometer | 53 |
| 2.13.5 Differential scanning calorimetry..... | 54 |

| | Page |
|---|------|
| 2.14 Synthesis and analysis of LR-CDs | 55 |
| CHAPTER III | 56 |
| RESULTS | 56 |
| 3.1 Random mutagenesis for improvement of thermostability of amyloamylase from <i>Corynebacterium glutamicum</i> (CgAM)..... | 56 |
| 3.1.1 Extraction of recombinant plasmid pET-19b CgAM..... | 56 |
| 3.1.2 Modification of CgAM gene using error-prone PCR technique..... | 56 |
| 3.1.3 Transformation | 57 |
| 3.1.4 Screening for thermostability of CgAM..... | 57 |
| 3.1.5 Nucleotide sequencing | 58 |
| 3.2 Site directed mutagenesis at A406V and A406L-CgAM | 68 |
| 3.3 The expression of recombinant wild-type WT- and MT-CgAMs | 68 |
| 3.4 Protein pattern of crude amyloamylase | 69 |
| 3.5 Purification of WT- and MT-CgAMs..... | 76 |
| 3.5.1 Preparation of crude AMs | 76 |
| 3.5.2 Purification by Histrap FF TM column..... | 76 |
| 3.5.3 Determination of enzyme purity of AMs | 77 |
| 3.6 Effect of mutation on enzyme characteristics..... | 81 |
| 3.6.1 Various activities of amyloamylases..... | 81 |
| 3.6.2 Optimum conditions and thermostability | 81 |
| 3.6.2.1 Effect of temperature | 81 |
| 3.6.2.2 Effect of pH | 82 |
| 3.6.2.3 Effect of temperature stability | 82 |
| 3.6.3 Enzyme conformation | 87 |
| 3.6.4 Differential scanning calorimetry..... | 89 |
| 3.6.5 Substrate specificity | 91 |
| 3.6.6 Determination of kinetic parameters | 91 |
| 3.6.7 Synthesis of LR-CDs..... | 95 |
| 3.6.7.1 Effect of pH and temperature on LR-CDs product profiles | 95 |

| | Page |
|---|------|
| 3.6.7.2 Effect of incubation time and temperature on LR-CDs production yield | 98 |
| 3.7 Site directed mutagenesis for improvement of thermostability of <i>CgAM</i> | 100 |
| 3.7.1 Extraction of recombinant plasmid pET-19b - <i>CgAM</i> | 101 |
| 3.7.2 Modification of <i>CgAM</i> gene by a single point mutation | 101 |
| 3.7.3 Transformation | 101 |
| 3.7.4 Nucleotide sequencing | 102 |
| 3.7.5 The expression of recombinant wild-type WT- and four MT- <i>CgAMs</i> .. | 114 |
| 3.7.5.1 The condition for soluble protein expression | 119 |
| 3.7.6 Purification of WT- and the four MT- <i>CgAMs</i> | 129 |
| 3.7.6.1 Preparation of crude AMs | 129 |
| 3.7.6.2 Purification by Histrap FF TM column | 129 |
| 3.7.6.3 Determination of enzyme purity of AMs | 130 |
| 3.8 Effect of mutation on enzyme characteristics | 133 |
| 3.8.1 Various activities of amyloamylase | 133 |
| 3.8.2 Optimum conditions and thermostability | 133 |
| 3.8.2.1 Effect of temperature | 133 |
| 3.8.2.2 Effect of pH | 134 |
| 3.8.2.3 Effect of temperature stability | 134 |
| 3.8.3 Enzyme conformation | 143 |
| 3.8.4 Differential scanning calorimetry | 145 |
| 3.8.5 Substrate specificity | 147 |
| CHAPTER IV | 149 |
| DISCUSSION | 149 |
| 4.1 Mutagenesis for the improvement of thermostability of <i>CgAM</i> gene | 150 |
| 4.1.1 Modification of <i>CgAM</i> gene using error-prone PCR technique | 150 |
| 4.1.2 Site directed mutagenesis | 151 |
| 4.1.3 Expression of WT- and MT- <i>CgAMs</i> | 152 |
| 4.2 Purification of recombinant WT- and MT- <i>CgAMs</i> | 153 |

| | Page |
|--|------|
| 4.3 Characterization of recombinant WT- and MT-CgAMs | 154 |
| 4.3.1 Molecular weight..... | 154 |
| 4.3.2 Various activities of amylomaltase | 155 |
| 4.3.3 Enzyme conformation | 159 |
| 4.3.4 Optimum conditions and thermostability | 163 |
| 4.3.5 Differential scanning calorimetry..... | 165 |
| 4.4 Synthesis of LR-CDs | 166 |
| 4.4.1 Effect of pH and temperature on LR-CD product profiles..... | 166 |
| 4.4.2 Effect of incubation time and temperature on LR-CD production yield | 167 |
| CHAPTER V | 169 |
| CONCLUSIONS..... | 169 |
| REFERENCES | 172 |
| APPENDICES | 187 |
| APPENDIX 1: Preparation for polyacrylamide gel electrophoresis | 188 |
| APPENDIX 2: Preparation for buffer solution..... | 191 |
| APPENDIX 3: Preparation of solution for cell preparation and enzyme | 192 |
| APPENDIX 4: Preparation for Iodine solution | 194 |
| APPENDIX 5: Preparation of Bradford solution | 195 |
| APPENDIX 6: Preparation for bicinchoninic acid assay | 196 |
| APPENDIX 7: Preparation for DNS reagent..... | 197 |
| APPENDIX 8: Bacterial media culture | 198 |
| APPENDIX 9: Abbreviation for amino acid residues | 199 |
| (Voet and Voet, 2004) | 199 |
| APPENDIX 10: Standard curve for protein determination by Bradford's method..... | 200 |
| APPENDIX 11: Standard curve of glucose determination by glucose | 201 |
| APPENDIX 12: Standard curve of starch degrading activity assay..... | 202 |
| APPENDIX 13: Standard curve for glucose determination by bicinchoninic..... | 203 |
| APPENDIX 14: Restriction map of pET-19b | 204 |

| | Page |
|---|------|
| APPENDIX 15: Structures of the amino acids commonly found in protein..... | 205 |
| VITA..... | 207 |



LIST OF TABLES

| | Page |
|---|------|
| Table 1.1 Enzymes belonging to the α -amylase family and four highly conserved region. | 4 |
| Table 1.2 Physicochemical properties of native small-ring CDs and LR-CDs. (Endo, 2011)..... | 24 |
| Table 1.3 A Studies of inclusion complex formation between pure LR-CD or mixture | 29 |
| Table 1.4 Studies of inclusion complex formation between pure LR-CD or mixture | 30 |
| | |
| Table 3.1 Purification of WT-, A406V- and A406L-CgAMs..... | 78 |
| Table 3.2 Specific activities of WT-, A406V- and A406L-CgAMs ^a | 83 |
| Table 3.3 Kinetic parameters of WT-, A406V- and A406L-CgAMs derived from the disproportionation reaction using maltotriose as the substrate ^a | 94 |
| Table 3.4 Purification of WT-, A406H-, A406R-, A406F- and N287Y-CgAMs... | 131 |
| Table 3.5 Specific activities of WT-, A406H-, A406R-, A406F- and N287Y-CgAMs..... | 136 |
| Table 3.6 Temperature stability of crude WT- and MT-CgAMs..... | 139 |

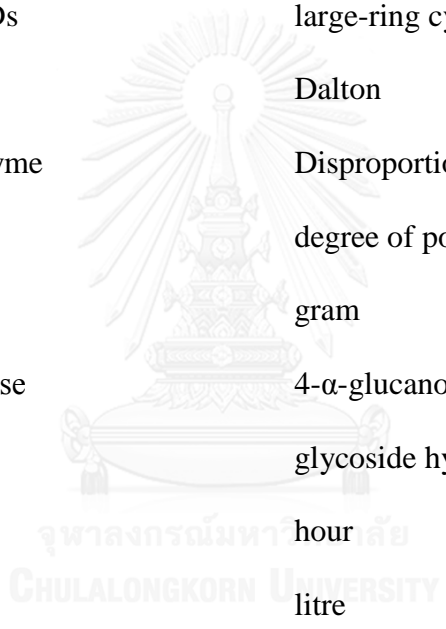
LIST OF FIGURES

| | Page |
|---|------|
| Figure 1.1 Different actions of starch-degrading enzymes. | 3 |
| Figure 1.2 The summarized action of 4 α GTase groups; | 7 |
| Figure 1.3 Fold pattern of AM from <i>T. aquaticus</i> | 10 |
| Figure 1.4 Molecular surfaces of (A) α -amylase isozyme II of porcine pancreas in | 11 |
| Figure 1.5 Binding mode of acarbose to AM. (A) acarbose bound to the active site..... | 15 |
| Figure 1.6 Three-dimensional model structure of CgAM with acarbose (in red) bound at the active site generated by PDB Swiss Viewer Program. The site of mutagenesis (Ala406 and Asn287) in this study is shown ... | 17 |
| Figure 1.7 Roles of 4 α GTase in glucan utilization by bacteria (Takaha and Smith, 1999) | 19 |
| Figure 1.8 Molecular structures of α -CD, β -CD, γ -CD, CD9 and CD14 side view and..... | 22 |
| Figure 1.9 Solid state structure of CD26. (A) Structure of CD26 indicating the ... | 23 |
| Figure 1.10 LR-CDs as an artificial chaperone for protein refolding by acting as the | 27 |
| Figure 1.11 Action of AM on starch (starch transglucosylation activity) in the | 28 |
| Figure 1.12 Different conditions of PCR and error prone PCR | 31 |
| | |
| Figure 3.1 Agarose gel electrophoresis of recombinant plasmid <i>CgAM</i> | 59 |
| Figure 3.2 Agarose gel electrophoresis of amplified DNA obtained from error- prone | 60 |
| Figure 3.3 Agarose gel electrophoresis of the product from colony PCR technique..... | 61 |
| Figure 3.4 Agarose gel electrophoresis of recombinant <i>CgAM</i> gene inserted in pET- | 62 |
| Figure 3.5 Screening for thermostability of MT- <i>CgAM</i> s obtained from random .. | 63 |

| | | |
|--------------------|---|-----|
| Figure 3.6 | Nucleotide sequence of MT-CgAM (clone number 50-11) compared with | 64 |
| Figure 3.7 | The deduced amino acid sequence of MT-CgAM (from clone number | 67 |
| Figure 3.8 | Expression of recombinant WT-CgAM in <i>E. coli</i> BL21 (DE3) at | 70 |
| Figure 3.9 | SDS-PAGE of crude enzyme from WT-CgAM induced by 0.4 mM IPTG at various times. | 71 |
| Figure 3.10 | Expression of recombinant A406V-CgAM in <i>E. coli</i> BL21 (DE3) at .. | 72 |
| Figure 3.11 | SDS-PAGE of crude enzyme from A406V-CgAM induced by 0.4 mM IPTG at various times. | 73 |
| Figure 3.12 | Expression of recombinant A406L-CgAM in <i>E. coli</i> BL21 (DE3)..... | 74 |
| Figure 3.13 | SDS-PAGE of crude enzyme from A406L-CgAM induced by 0.4 mM IPTG at various times. | 75 |
| Figure 3.14 | Purification profile of WT-CgAM by HisTrap FF TM column | 79 |
| Figure 3.15 | SDS-PAGE of recombinant AMs from each purification step, stained by coomassie blue..... | 80 |
| Figure 3.16 | Effect of temperature (A) and pH (B) for WT- (solid line), A406V-..... | 84 |
| Figure 3.17 | Effect of temperature (A) and pH (B) for WT- (solid line), A406V-..... | 85 |
| Figure 3.18 | Effect of temperature stability of WT- (solid line), A406V- (dashed line)..... | 86 |
| Figure 3.19 | Circular dichroism spectra and the predicted secondary structural | 88 |
| Figure 3.20 | Thermal transition curves of WT- (black line), A406V- (blue line) and | 90 |
| Figure 3.21 | Substrate specificity of WT-, A406V- and A406L-CgAMs in | 92 |
| Figure 3.22 | Lineweaver-Burk plot of recombinant WT-, A406V- and A406L- | 93 |
| Figure 3.23 | HPAEC analysis of LR-CDs synthesized at different pH by WT-..... | 96 |
| Figure 3.24 | HPAEC analysis of LR-CDs synthesized at different temperature | 97 |
| Figure 3.25 | HPAEC analysis of LR-CDs synthesized by WT-, A406V- and A406L-..... | 99 |
| Figure 3.26 | The superimposed structures of CgAM (Green) on <i>T. aquaticus</i> | 103 |
| Figure 3.27 | Agarose gel electrophoresis of recombinant plasmid pET-19b CgAM | 104 |

| | |
|--|-----|
| Figure 3.28 Agarose gel electrophoresis of amplified DNA containing <i>CgAM</i> gene..... | 105 |
| Figure 3.29 Agarose gel electrophoresis of PCR product from pET-19b vector..... | 106 |
| Figure 3.30 Nucleotide sequence alignment of A406H, A406R, A406F and N287Y- | 107 |
| Figure 3.31 The deduced amino acid sequence alignment of A406H, A406R, A406F | 112 |
| Figure 3.32 SDS-PAGE of crude enzyme from A406H- <i>CgAM</i> induced by 0.4 mM IPTG at various times | 115 |
| Figure 3.33 SDS-PAGE of crude enzyme from A406R- <i>CgAM</i> induced by 0.4 mM IPTG at various times | 116 |
| Figure 3.34 SDS-PAGE of crude enzyme from N287Y- <i>CgAM</i> induced by 0.4 mM IPTG at various times | 117 |
| Figure 3.35 SDS-PAGE of crude enzymes and cell pellets from WT- and MT- <i>CgAMs</i> after induced with 0.4 mM IPTG at 37 °C for 2 h | 118 |
| Figure 3.36 Expression of recombinant A406R- <i>CgAM</i> in <i>E. coli</i> BL21 (DE3) | 121 |
| Figure 3.37 SDS-PAGE of crude enzyme expressed from cells harboring A406R- <i>gAM</i> . Cells were cultivated in LB broth after induced with 0.4 mM IPTG at various times (condition1). | 122 |
| Figure 3.38 Expression of recombinant A406R- <i>CgAM</i> in <i>E. coli</i> BL21 (DE3) | 123 |
| Figure 3.39 SDS-PAGE of crude enzyme expressed from cells harboring A406R-124 | |
| Figure 3.40 Expression of recombinant A406R- <i>CgAM</i> in <i>E. coli</i> BL21 (DE3) | 125 |
| Figure 3.41 SDS-PAGE of crude enzyme expressed from cells harboring A406R-126 | |
| Figure 3.42 Expression of recombinant A406R- <i>CgAM</i> in <i>E. coli</i> BL21 (DE3) | 127 |
| Figure 3.43 SDS-PAGE of crude enzyme expressed from cells harboring A406R-128 | |
| Figure 3.44 SDS-PAGE of recombinant AMs stained by coomassie blue from each purification step..... | 132 |
| Figure 3.45 Effect of temperature (A) and pH (B) for WT- (black line), A406H-.. | 137 |
| Figure 3.46 (A) HPAEC analysis of the LR-CD products. 0.2% (w/v) pea starch was | 138 |
| Figure 3.47 Effect of temperature stability of WT- (black line), A406H- (blue line)..... | 140 |

| | |
|---|-----|
| Figure 3.48 Effect of temperature stability of WT- (black line), A406H- (blue line)..... | 141 |
| Figure 3.49 Effect of temperature stability of WT- (black line), A406H- (blue line)..... | 142 |
| Figure 3.50 Circular dichroism spectra and the predicted secondary structural | 144 |
| Figure 3.51 Thermal transition curves of WT- (black line), A406H- (blue line) and | 146 |
| Figure 3.52 Substrate specificity of WT-, A406H-, A406R-, A406F- and N287Y-148 | |
| Figure 4.1 Proposed binding of acarbose in the active site of CgAM | 157 |
| Figure 4.2 Proposed of the hydrogen bonding interactions between the amino group | 158 |
| Figure 4.3 The superimposed structures of WT- (cyan), A406V- (purple) and A406L-CgAMs (red). The enzyme structures are displayed as secondary structure generated by PDB Swiss Viewer Program. The important residues 406 are displayed as stick and colored. The active center of CgAM is located at the center of the modeled oligosaccharide shown in red. | 161 |
| Figure 4.4 Three-dimensional modeling structure of AM from <i>C. glutamicum</i> (CgAM) generated by PDB Swiss Viewer Program (A) WT-CgAM and (B) N287Y- CgAM. The active center of CgAM is located at the center of acarbose shown in red. | 162 |

ABBREVIATIONS

| | |
|------------------|---------------------------------|
| A | absorbance |
| AM | amylomaltase |
| BSA | bovine serum albumin |
| °C | degree Celsius |
| CDs | cyclodextrins |
| LR-CDs | large-ring cyclodextrins |
| Da | Dalton |
| D-enzyme | Disproportionation enzyme |
| DP | degree of polymerization |
| g | gram |
| 4 α GTase | 4- α -glucanotransferase |
| GH | glycoside hydrolases family |
| h | hour |
| l | litre |
| μ g | microgram |
| μ l | microlitre |
| M | molar |
| mA | milliampere |
| min | minute |
| mg | milligram |
| ml | millilitre |
| mM | millimolar |

| | |
|------|------------------------------------|
| MW | molecular weight |
| n.d. | not detectable |
| PAGE | polyacrylamide gel electrophoresis |
| rpm | revolution per minute |
| SDS | sodium dodecyl sulfate |
| U | unit |



CHAPTER I

INTRODUCTION

1.1 Starch

Carbohydrate is an essential component of all living organisms. Besides cellulose, starch is a polymer of α -1, 4-D-glucans which occurs widely in nature. This polymer serves the function as carbon store of plants when glucose is plenty. Plant can utilize starch which consists of two types of molecules: the linear-helical amylose and the branched amylopectin. The dominant industrial sources of starch are potato, wheat, maize, rice and tapioca, which are economically important crops. In the last century, the emergence of a large-scale starch industrial processing to produce various saccharides of beneficial use was occurred. The acid hydrolysis of starch has been shifted to the use of starch-degrading enzymes to produce maltodextrin, modified starch and glucose in the past decades. Many organisms could produce extracellular or intracellular enzymes which are able to convert glycogen or starch into carbon sources as energy for the cells (Figure 1.1). Besides the use in starch industry, starch-converting enzymes are also used in several other industrial applications, such as laundry and dish detergents or as anti-staling in baking industry (Van Der Maarel *et al.*, 2002).

1.2 Starch-degrading enzymes

The α -amylase family comprises of carbohydrate-metabolizing enzymes which fulfil the following requirements; (i) act on α -glycosidic bonds to produce α -

anomeric mono- or oligosaccharides; (ii) hold a TIM or $(\beta/\alpha)_8$ barrel structure; (iii) have four conserved regions in their primary structures which contain all the catalytic and most of the important substrate-binding sites ; and (iv) have 2-3 Asp and Glu residues as catalytic site (Table 1.1) (Kuriki *et al.*, 2006; Takata *et al.*, 1992).

The α -amylase family can be divided into 4 groups: (i) endoamylases; (ii) exoamylases; (iii) debranching enzymes; and (Gotsev and Ivanov) transferases (Van Der Maarel *et al.*, 2002). The first three groups are hydrolases. Endoamylase such as α -amylase (EC 3.2.1.1), is able to randomly hydrolyze the α -1,4-glycosidic bonds in the inner part (endo-action) of starch chain (amylose or amylopectin) to produce various length of oligosaccharide as products. Exoamylase which hydrolyzes glycosidic bond from the non-reducing end residues (exo-action) of starch chain to produce glucose, maltose or β -limit dextrin. The example of this group is β -amylase (EC 3.2.1.2), which is able to cleave α -1,4-glycosidic bonds to produce maltose while glucoamylase or amyloglucosidase (EC 3.2.1.3) hydrolyzes both of α -1,4 and α -1,6 glycosidic bonds to produce glucose. The third group is debranching enzyme that can exclusively hydrolyze α -1,6-glycosidic bonds by exo-action, the examples are isoamylase (EC 3.2.1.68) (Abe *et al.*, 1999) and pullulanase type I (EC 3.2.1.41) (Ben Messaoud *et al.*, 2002), which produce linear oligo/polysaccharides. The last one is transferase group such as 4- α -glucanotransferase (4 α GTase) group, acts by breaking an α -1, 4-link and transfers the resulting glucan moiety to an acceptor molecule through formation of a new α -1,4- link (Takaha and Smith, 1999) the main examples of 4 α GTase group are cyclodextrin glycosyltransferase (CGTase, EC 2.4.1.19) and amyloamylase (AM, EC 2.4.1.25). These enzymes mainly show transglycosylation

reaction to produce cyclic oligosaccharide with 6, 7, 8 unit of glucose or higher, while their hydrolytic activity are very low (Van Der Maarel *et al.*, 2002).

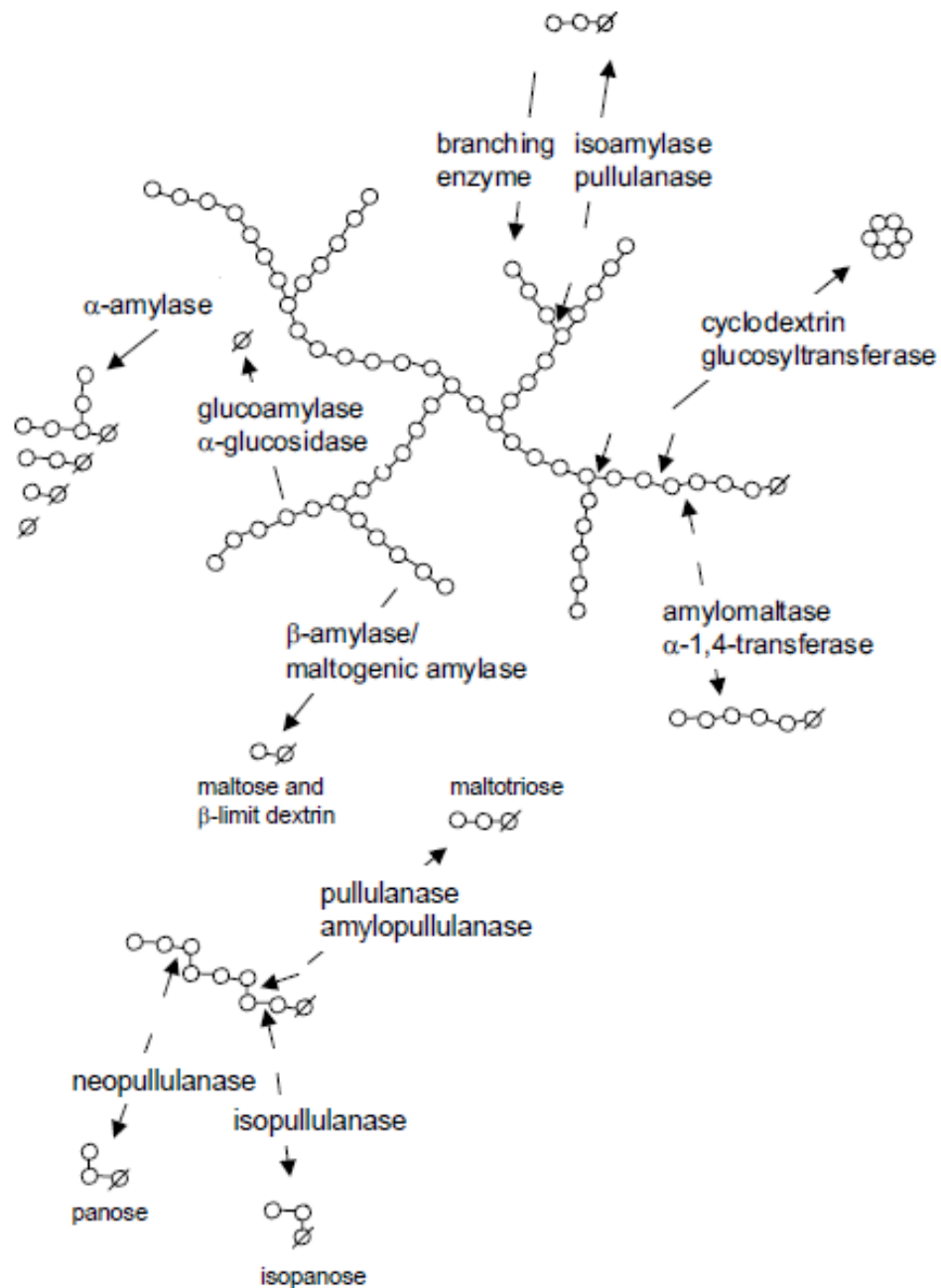


Figure 1. 1 Different actions of starch-degrading enzymes.

Glucose molecules are indicated as circle while reducing ends are marked by a line through the circle (Turner *et al.*, 2007).

Table 1. 1 Enzymes belonging to the α -amylase family and four highly conserved region. The three invariable catalytic sites are highlighted. Numbering of amino acid at the amino-terminal end of each enzyme. (Modified from van der Marrel *et al.*, 2002 and Kuriki *et al.*, 2006)

| Enzyme | Origin | Region 1 | Region 2 | Region 3 | Region 4 | Accession No. |
|-----------------------------|------------------------------------|-----------|---------------|----------|------------|---------------|
| α -amylase | <i>Aspergillus oryzae</i> | 117DVVANH | 202GLRIDTVKH | 230EVLID | 292FVENHD | I506277A |
| CGTase | <i>Bacillus macerans</i> | 135DFAPNH | 225GTRFDVAKH | 258EWFLL | 324FIDNHD | P31835 |
| Pullulanase | <i>Klebsiella aerogenes</i> | 600DVVYNH | 671GFRFDLMGY | 704EGWD | 827YVSKHD | P07811 |
| Isoamylase | <i>Pseudomonas amyloclavata</i> | 292DVVYNH | 371GFRFDLASV | 435EPWA | 505FIDVHD | AAA25855 |
| Branching enzyme | <i>Escherichia coli</i> | 335DWVPGH | 401ALRVDAVAS | 458EEST | 521LPLSHD | ACI76450 |
| Neopullulanase | <i>Bacillus stearothermophilus</i> | 242DAVFNH | 324DWRLDVANE | 357EIIWH | 419LLGSHD | AAK15003 |
| Amylopullulanase | <i>Thermococcus aerophilus</i> | 487DGVFNH | 593GWRLDVANE | 626ELWG | 698LLGSHD | P3839 |
| α -glucosidase | <i>Saccharomyces cerevisiae</i> | 106DLVINH | 210GFRIDTAGL | 276EVAH | 344YIENHD | P07265 |
| Oligo-1,6-glucosidase | <i>Bacillus cereus</i> | 98DLVVNH | 195GFRMDVINP | 255EMPGL | 324YWNHD | P21332 |
| Dextran glucosidase | <i>Streptococcus mutans</i> | 98DLVVNH | 190GFRMDVIDM | 236ETWG | 308FWNHD | AAA26939 |
| Amylomaltase | <i>Thermus aquaticus</i> | 213DMPIFV | 289LVRLDHFGR | 340EDLG | 390YTGTHD | O87172 |
| Glycogen debranching enzyme | <i>Homo sapiens</i> | 298DVVYNH | 504GVRLDNCCHS | 534ELFT | 603MDITHD | NP_000019 |
| Amylosucrase | <i>Neisseria polysaccharaea</i> | 190DFIFNH | 290ILRMDAVAF | 336EAIIV | 396YVVRSHD | CAA09772 |

1.3 The 4- α -glucanotransferase (4 α GTase) group

The 4 α GTase belongs to α -amylase super-family and has been assigned to glycoside hydrolase (GH) family 13, 57 and 77 (Henrissat, 1991; Kaper *et al.*, 2005), mainly involved in starch metabolism, is a specific group of transferase which catalyzes the transfer of α -1,4-D-glucan from starch donor to an acceptor molecule, such as glucose or another α -1,4-D-glucan with a free 4-OH group (Kaper *et al.*, 2007; Kaper *et al.*, 2005; Takaha and Smith, 1999). This group can be divided into three types; CGTase (Type I), Disproportionating enzyme (D-enzyme) or amyloamylase (Type II) and Glycogen debranching enzyme (GDE) (α -1,6-glucosidase/ 4- α -glucanotransferase) (EC 3.2.1.33 + EC 2.4.1.25) (Type III), respectively (Takaha and Smith, 1999). AM and D-enzyme are classified as GH77 while CGTase and α -amylase are part of GH13 (Kaper *et al.*, 2004). GH77 enzymes are efficient 4 α -GTases with remarkably low hydrolytic activities than those of GH13 (Takaha and Smith, 1999). AM shows similar catalytic reaction to CGTase but it is an intracellular enzyme which forms cycloamyloses (CAs) or large-ring cyclodextrin (LR-CDs) as the major cyclization product, while the final products of CGTase consist mainly of small cycloamyloses or small-ring cyclodextrins with 6-8 glucose units. In *E. coli*, the smallest substrate that AM recognizes is maltotriose (Palmer *et al.*, 1976) while maltose is reported as smallest substrate for plant D-enzyme (Takaha and Smith, 1999). AM (EC 2.4.1.25) catalyzes intramolecular and intermolecular transglucosylation reactions. Four reactions can be catalyzed by AM, including disproportionation, cyclization, coupling and hydrolysis. The summarized action of 4 α GTase is as shown in Figure 1.2. Disproportionation reaction is an intermolecular transglucosylation reaction in which some part from a linear glucan is transferred to

another linear glucan acceptor to produce oligosaccharides with variable length. Cyclization reaction is unique for AM, an intramolecular glucan transfer reaction within a single linear glucan molecule to produce cyclic α -1,4-glucan, product called cycloamyloses (CAs) or large-ring cyclodextrins (LR-CDs), this reaction is reversible by a reaction called coupling. In addition, this enzyme also shows a weak hydrolytic activity whereby ring opening of LR-CDs occurs (Fujii *et al.*, 2005a, 2007; Kaper *et al.*, 2007; Takaha and Smith, 1999).



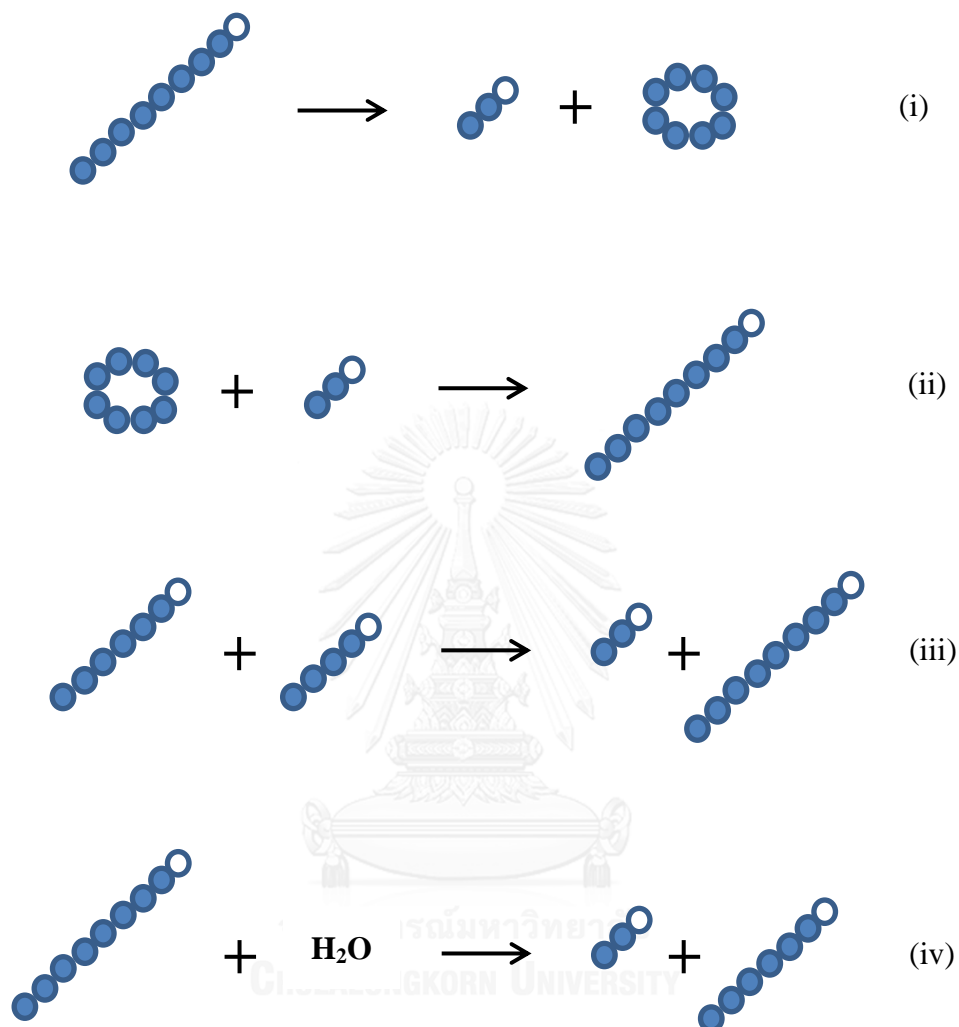


Figure 1. 2 The summarized action of 4 α GTase groups;

(i) Cyclization reaction, (ii) Coupling reaction, (iii) Disproportionation reaction and (Gotsev and Ivanov) Hydrolysis reaction. Glucose molecules are indicated as dark circle while reducing ends are marked by white circle (modified from (Takaha and Smith, 1999)).

1.4 The structure of amyломaltase

AM was first found in *Escherichia coli* as a maltose-inducible enzyme which is essential for the metabolism of maltose (Monod and Torriani, 1950). AM genes have been cloned from many organisms such as *Streptococcus pneumoniae* (Stassi *et al.*, 1981), *E. coli.*, (Pugsley and Dubreuil, 1988), *Clostridium butyricum* NCIMB 7423 (Goda *et al.*, 1997), hyperthermophilic archaeon *Thermococcus litoralis* (Goda *et al.*, 1997), *Thermus aquaticus* ATCC 33923 (Terada *et al.*, 1999), *Aquifex aeolicus* (Bhuiyan *et al.*, 2003), *Pyrobaculum aerophilum* IM2 (Kaper *et al.*, 2005), *Thermus brockianus* (Bo-young *et al.*, 2006), *Thermus filiformis* (Kaewpathomsri *et al.*, 2015) and *Corynebacterium glutamicum* ATCC 13032 (Srisimarath *et al.*, 2011). A similar enzyme to AM in plants called disproportionating enzyme (D-enzyme), is found in barley (Yoshio *et al.*, 1986), potatoes (Takaha *et al.*, 1993) and cassava tubers (Tantanarat *et al.*, 2014).

At present, only five AMs have been determined for their X-ray structures. AM from *T. brockianus* (Jung *et al.*, 2011), *Thermococcus litoralis* (Imamura *et al.*, 2003), *T. aquaticus* (Przylas *et al.*, 2000b), *T. maritima* (Roujeinikova *et al.*, 2002) and *Thermus thermophilus* (Lamour *et al.*, 2006) have been crystallized and 3D-structures identified. Even though almost all crystal structures are similarly assembled but the C-terminal part are different in length. The AM structure has two main domains, A and B. It contains several insertions between the strands of the central (α/β)₈-barrel localized in domain A. All insertions are presented at the C-terminal side of the barrel, where the substrate binding site also is located. These insertions are divided into three subdomains (subdomain B1, B2 and B3), in order to facilitate comparison to related enzymes (Figure 1.3). The insertions between the third and

fourth barrel strand of the central barrel (domain A) and between the fourth and fifth strand build subdomain B1. Subdomain B2 consists of a large insertion between the second and third barrel strand. The remaining insertions, between the first and second strand, between the seventh and eighth strand and after the eighth barrel strand build subdomain B3. Thus, subdomains B1 to B3 form an almost continuous ring around the C-terminal edge of the barrel and might participate in binding the large amylose substrates (Przylas *et al.*, 2000a). Subdomain B2 is present in AM and plant D-enzyme but absent in CGTase and α -amylase. Therefore, it is suggested that this domain has a unique role in AM (Fujii *et al.*, 2005a; Przylas *et al.*, 2000a).

In AM, the active-site cleft is partially covered by a long extended unique loop (250s loop) formed by residues 247-255 between subdomain B1 (Figure 1.4C and 1.4D). Two hydrophobic side chains, Tyr-250 and Phe-251, are located at the tip of the loop and point towards subdomain B3. This loop might be important for binding of substrates and dissociation of products (Figure 1.4D). On the other side of the active site groove, the 460s loop and Tyr-54 derived from the loop might restrict the formation of smaller cyclic products (Figure 1.4C) (Przylas *et al.*, 2000a). The co-crystal structure of *T. aquaticus* AM with acarbose (Przylas *et al.*, 2000a) demonstrated that acarbose molecule bound at two binding sites, the catalytic site and the second binding site. All AMs have seven conserved residues in their structure: the three catalytic residues Asp-293, Glu-340 and Asp-395 and residues Tyr-59, Asp-213, Arg-291 and His-394 (numbering in AM of *T. aquaticus*). These seven residues build up the core of the catalytic cleft. The presence of these core residues except for Tyr-59 is also found in the four conserved motifs of family 13 α -amylase, this supports a similar reaction mechanism for AM and other enzymes of this family,

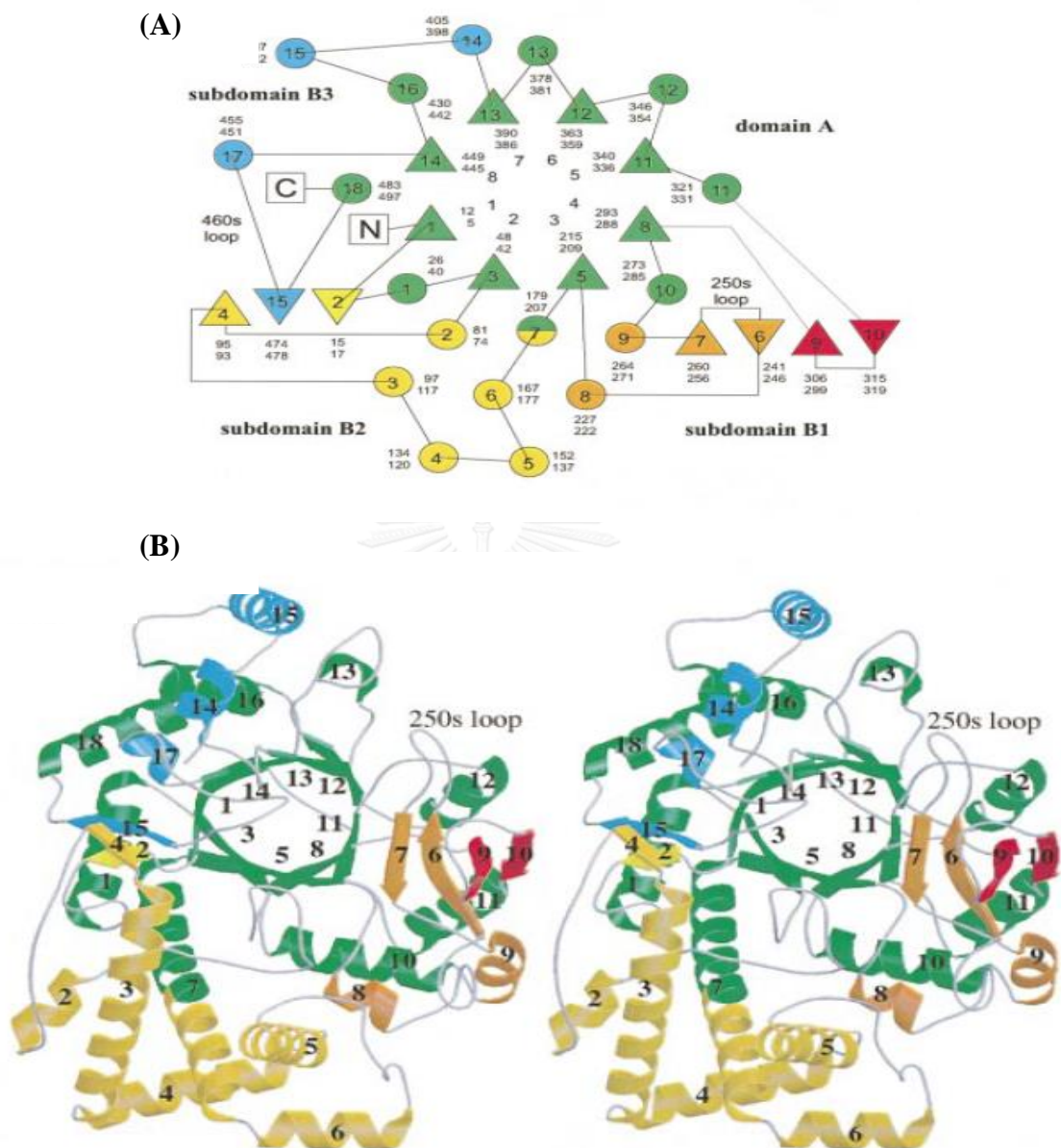


Figure 1. 3 Fold pattern of AM from *T. aquaticus*.

(A) Topography diagram. β -sheet and helices are represented by tri-angles and circles. Number 1-8 in the center stand for the position of the first to eight barrel strand. Domain A is colored in green, while subdomain B1-B3 is in red, yellow and blue, respectively. (B) Ribbon presents the fold AM as in (a) (Przylas *et al.*, 2000b).

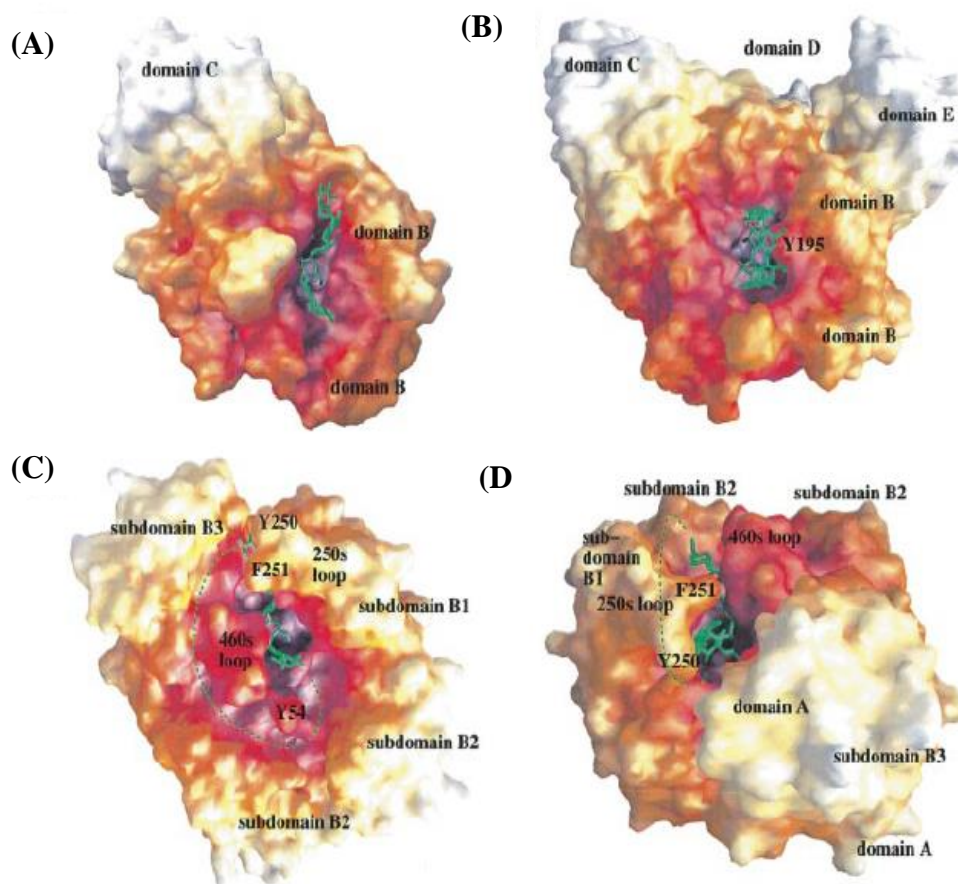


Figure 1. 4 MOLECULAR SURFACES OF (A) α -amylase isozyyme II of porcine pancreas in complex with a maltohexaose (part of a larger inhibitor) (Machius *et al.*, 1996); (B) CGTase from *Bacillus circulans* strain 8 complexed with β -cyclodextrin derivative (Schmidt *et al.*, 1998) and (C), (D) AM from *Thermus aquaticus* with a modeled binding mode of a maltohexaose. The surfaces are colored according to the distance to the center of mass. The domains, subdomains and two loops, the 250s loop and the 460s loop, are labeled. The bound or modeled inhibitors are shown in green. Possible binding paths for a cycloamylose product to AM are indicated as broken green line in (C) and (D). The active center of AM is located at the center of the modeled oligosaccharide in (C) and (D). (Przylas *et al.*, 2000a).

as previously indicated by homologous signature of the amino acid sequences. A mechanism involving a covalent intermediate, Glu-340 protonates the glycosidic oxygen atom of the scissile bond and a planer oxocarbenium-like transition state is formed. The Asp-293 is the nucleophile which attacks the C1 atom of the substrate under formation of the covalent intermediate. The Asp-395 presumably exerts strain on the substrate in the Michaelis complex and specifically stabilized the planer oxocarbenium-like transition state (Barends *et al.*, 2007). Obviously, the environment of the three acidic residues plays an important role in governing reaction specificity. For the other four additional conserved amino acid residues of amylomaltase (Tyr-59, Asp-213, Arg-291 and His-394), they are also part of catalytic cleft.

From 3D structure of AM, catalytic site is divided into subsites. The tyrosine residue in the catalytic subsite -1 (Figure 1.5A) helps to orientate the sugar by forming a stacking interaction with the hexose ring, while His-394 and Arg-291 interact with the O₂ atom of the substrate hexose in the -1 subsite. Asp-213 is part of a hydrogen bonding network that shows some flexibility in the substrate-bound and intermediate structure (Uitdehaag *et al.*, 1999). As has been previously noticed on the basis of sequence comparisons, the histidine residue of the first conserved region (His-122 of α -amylase, Table 1.1), which is conserved in most α -amylase family members, but is not presented in AM. In addition, the co-crystal structure with acarbose showed that the acarviosine moiety was not bound to subsites -1 and +1, as in the related family 13 enzymes (the glycosidic linkage is broken between subsites -1 and +1). Instead, the inhibitor occupies -3 to +1 of the active center (Figure 1.5A) (Srisimarat *et al.*, 2012). In this co-crystal structure of AM with acarbose, a second glucan binding site which is located in a groove close to the active center was

suggested. The distance between the reducing end of the maltotetraose part and the non-reducing end of the substrate analog bound to the active site is ~ 14 Å. Hydrophobic contacts of Tyr-54 with glucose unit B and Tyr-101 with unit C of the inhibitor are probable the most interactions that determine the conformation and binding of the inhibitor to this (Figure 1.5B). The acarbose winds around Tyr-54, which is highly solvent-exposed in the unliganded structure. Tyr-101 is involved in a hydrophobic stacking interaction with glucose unit C. Overall, the second acarbose has significantly fewer interactions with the protein compared to the acarbose bound to the active site (Figure 1.5A). In addition to Tyr-250, Phe-251 and Tyr-54 (Figure 1.4C), the hydrophobic side chains of Tyr-101 are solvent exposed and located near the catalytic cleft along an alternative glucan binding groove. These side chains may be involved in stacking interactions with the hydrophobic face of the glucan rings of the substrate. For the formation of cyclic products, the non-reducing end of glucan chain has to fold back to the active center. In *T. aquaticus* AM, the secondary binding site around Tyr-54 might help to form a curved conformation of the amylose chain in this region, which would favor the formation of cyclic products. Thus, one putative binding pathway for the smallest large-ring cyclodextrin products is obtained by connection the two acarbose molecules bound to AM as indicated in Figure 1.4C by a broken green line. The path indicated in Figure 1.4C has a length of about 110 Å. Large-ring cyclodextrin consisting of n glucose units which form a planer ring have a length of $\sim 4.6n$ (Å) and a radius of $\sim 0.73n$ (Å), assuming that the distance of two neighboring glucose units is about 4.6 Å. Therefore, an extended CD22 ring has a radius of about 16 Å and a length of ~ 100 Å, the dimensions that fit within 110 Å in length from the obtained 3D structure of *T. aquaticus* AM (Przylas *et al.*, 2000a). An

alternative pathway appears possible, which goes around the 250s loop (broken green line in Figure 1.4D). The flexibility of the 250s loop conformation might be important for binding of substrates and dissociation of products. It also clear that the formation of small cyclic products like cyclodextrins is sterically hindered by the presence of this loop near the active site. If the LR-CD product wraps around the 250s loop during the cyclization reaction, the minimum ring size might be restricted to about 18 residues by the size of this loop (Figure 1.4D) (Przylas *et al.*, 2000a).

Our research group has previously reported the cloning and characterization of a novel AM from a mesophilic *C. glutamicum*. The *C. glutamicum* amyloamylase gene (*CgAM*) had an ORF of 2,121 bp and was deduced into a protein with 706 amino acids (Srisimarath et al., 2013). *CgAM* is larger in size with a low amino acid sequence identity to those well characterized AMs from *Thermus*. The enzyme was crystallized (Srisimarath *et al.*, 2013) and the 3D-structure showed the $(\alpha\beta)_8$ barrel with the unique 420s loop lied over the active site as similar to AMs from *Thermus* (Figure 1.6). However, *CgAM* had an additional domain not found in *Thermus* AMs around N-terminus residues 2-173, functional analysis of this part by sequence deletion is now carried out. We hope to publish the 3D-structure with this functional analysis soon. In Fig. 1.6, the location of the mutated residues in this study, A406 and N287, was shown.

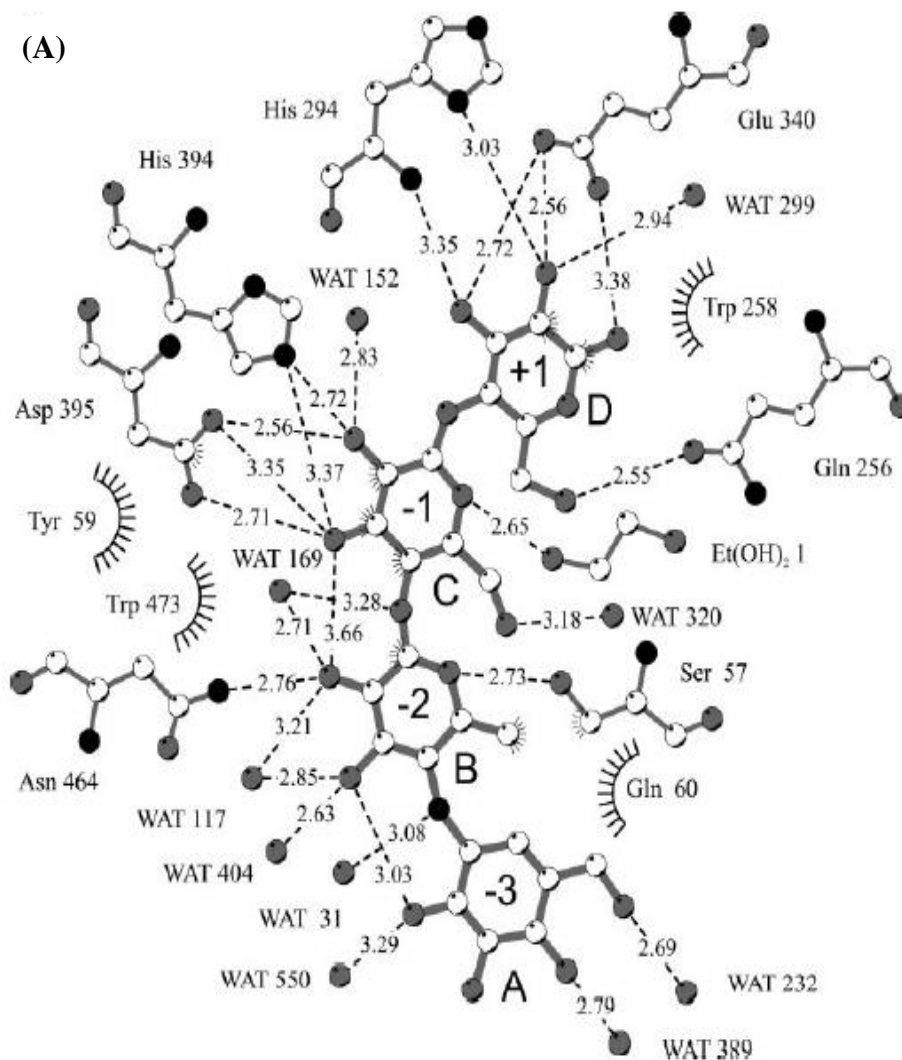


Figure 1. 5 Binding mode of acarbose to AM. (A) acarbose bound to the active site cleft and (B) acarbose near Tyr 54. Oxygen atoms are shaded gray and nitrogen atom black. Hydrogen bonding interactions are shown by dashed lines and the interatomic distance is given (Przylas *et al.*, 2000b).

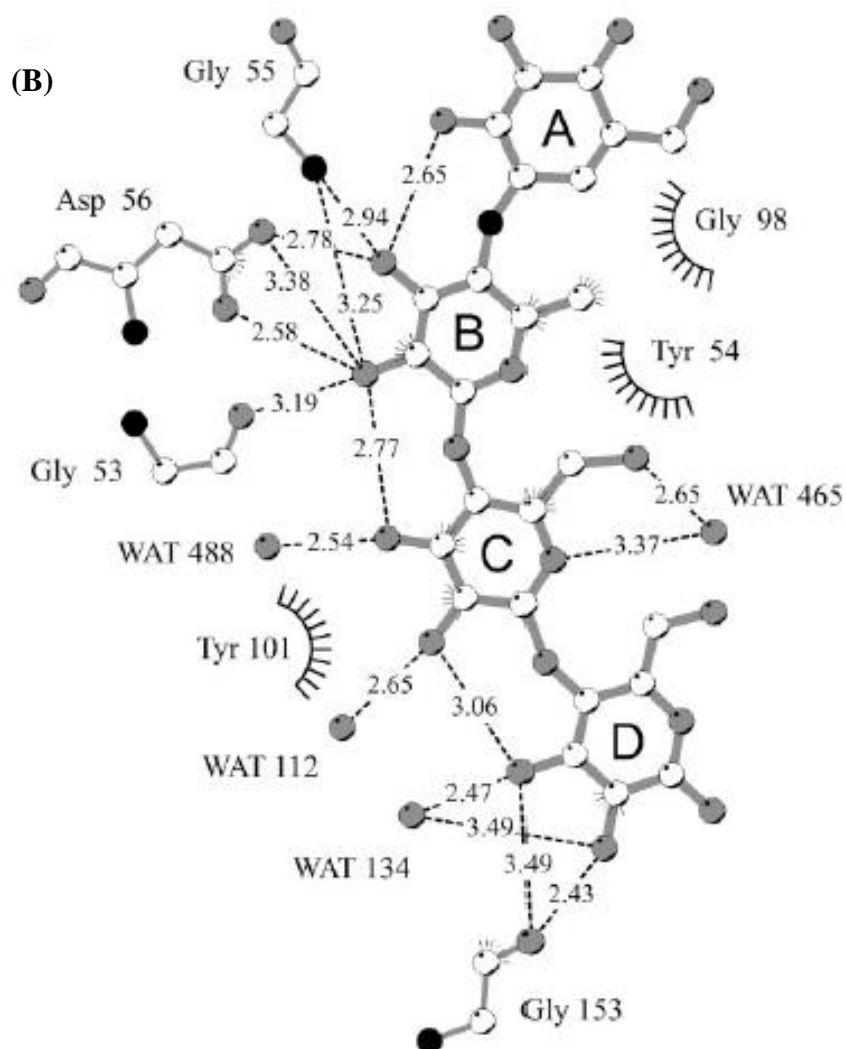


Figure 1.5 (continue) Binding mode of acarbose to AM. (A) acarbose bound to the active site cleft and (B) acarbose near Tyr 54. Oxygen atoms are shaded gray and nitrogen atom black. Hydrogen bonding are shown by dashed lines and the interatomic distance is given (Przylas *et al.*, 2000b).

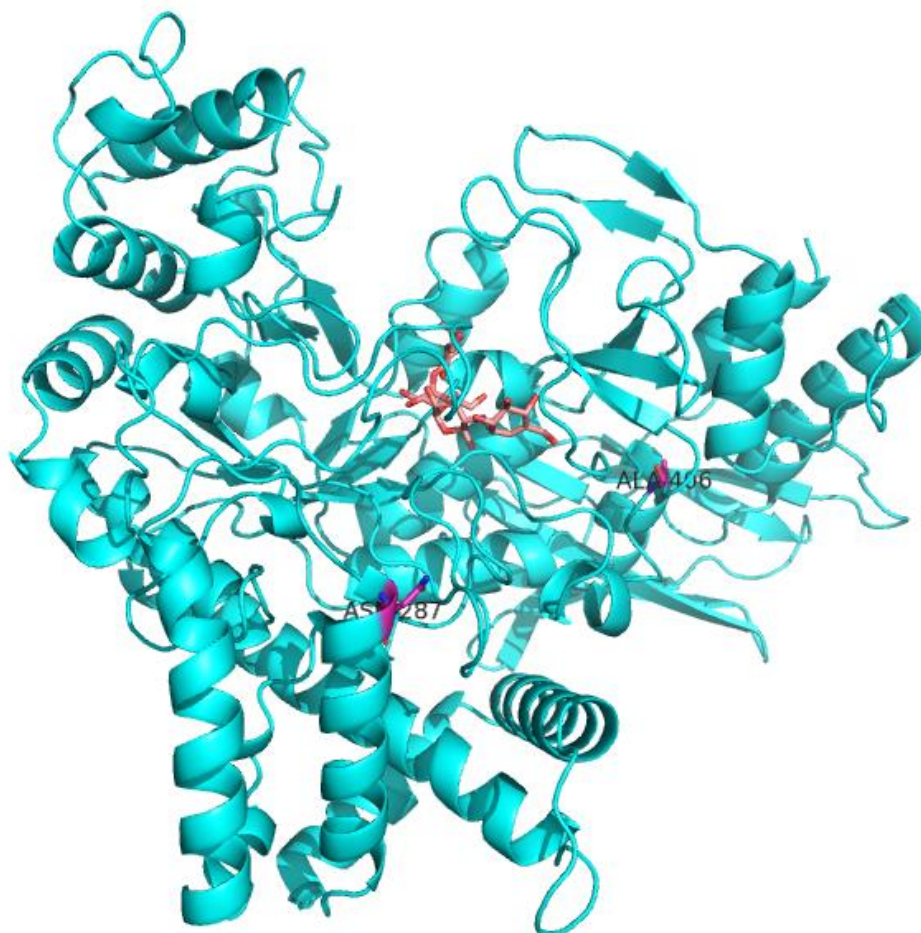


Figure 1. 6 Three-dimensional model structure of CgAM with acarbose (in red) bound at the active site generated by PDB Swiss Viewer Program. The site of mutagenesis (Ala406 and Asn287) in this study is shown (Krusong *et al.*) unpublished result

1.5 Physiological roles of amyloamylase

In *Escherichia coli*, AM (4 α GTase) is a part of maltooligosaccharide transport and utilization system which includes maltodextrin phosphorylase and maltose transport proteins (Schwartz, 1987). The role of AM apparently to convert short maltooligosaccharides into longer chain of which glucan phosphorylase can act on (Figure 1.6). This phosphorylase, like that in plant, degrades maltooligosaccharides to maltotetraose. The genes for AM and glucan phosphorylase constitute the *malPQ* operon. A similar operon structure was also found in *S. pneumoniae* (Lacks *et al.*, 1982), *Klebsiella pneumonia* (Bloch and Raibaud, 1986) and *C. butyricum* (Goda *et al.*, 1997), so the function of these AMs is expected to be the same as the *E. coli* enzyme. On the other hand, the genes for AM found in the genome of *Haemophilus influenzae* (Fleischmann *et al.*, 1995) and *Aquifex aeolicus* (Deckert *et al.*, 1998) are part of the glycogen operon, which include genes for glycogen synthesis and degradation. Furthermore, these organisms do not have the genes homologous to *E. coli malE*, *malF*, *malG* which are involved in the transport of maltooligosaccharides into the cytoplasm. All these observations suggest that *H. influenzae* and *A. aeolicus*, amyloamylase may not be involved in exogenous maltooligosaccharide utilization, but is involved in glycogen metabolism. Thus, the physiological role of amyloamylase may be different in each organism (Takaha and Smith, 1999).

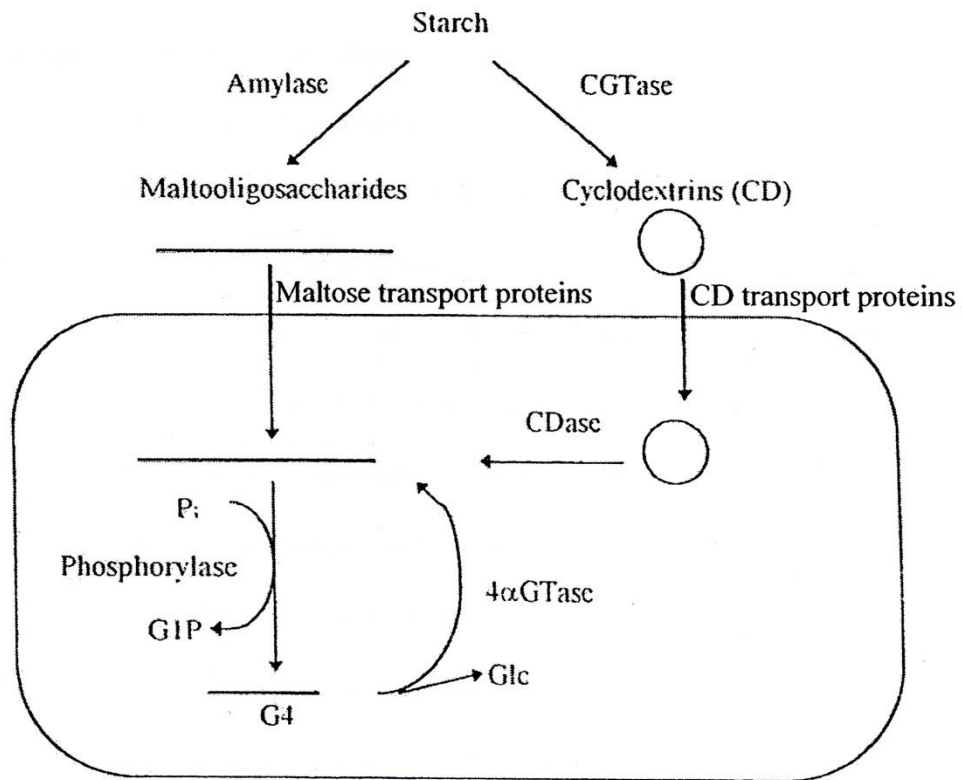


Figure 1. 7 Roles of 4αGTase in glucan utilization by bacteria (Takaha and Smith, 1999)

1.6 Large ring cyclodextrins (LR-CDs)

LR-CDs are cyclic oligosaccharides which compose of more than 9 D-glucose units, however, the smallest LR-CD produced by AM contains 16 units of glucose. Interestingly, LR-CDs are produced with different degrees of polymerization (DP) depending on the source of enzyme, AM from *E. coli* or *T. aquaticus*, D-enzyme from potato, GDE from *Saccharomyces cerevisiae* and CGTase can produce LR-CDs which have the minimum DP of 17, 22, 17, 11 and 9, respectively (Taira *et al.*, 2006; Takaha and Smith, 1999). In addition, it was reported that LR-CDs of DP 9 to 16 are produced in the initial phase of CGTase (cyclodextrin glycosyltransferase, a type 1 of 4 α GTase which catalyzes formation of small-ring CDs) after that it is converted into smaller CDs: CD6 or α -CD, CD7 or β -CD and CD8 or γ -CD (Figure 1.7) (Qi *et al.*, 2007; Taira *et al.*, 2006). CD10 to CD21 have been separated and purified from LR-CD mixture produced by the initial action of CGTase (Ueda *et al.*, 2002). And the larger ones from CD22 to CD39 have also been purified from LR-CD mixture produced by AM from *Thermus aquaticus* ATCC 3392 (Terada *et al.*, 1999). Due to flexibility, LR-CDs from variety of structures. In CD10 and CD14, the macrocyclic rings are deformed elliptical shapes and cavity shape is a narrow groove (Figure 1.7). CD14 is a boat-like shape, CD9 has an intermediate structure between that of small-ring CDs and CD10 and CD14, it displays a distorted elliptical macrocyclic ring without a band flips (Figure 1.7) (Endo, 2011). CD26 has a structure where two antiparallel V-amylose helices are bound through band flips (Figure 1.8). Table 1.2 lists some of the physicochemical properties of CD6 to CD39 (Endo, 2011). The aqueous solubilities of LR-CDs, except for CD9, CD10, CD14 and CD26, were higher than those of α -, β - and γ -CD. This may be a consequence of high

structural flexibility, on the basis of the formation of intramolecular and intermolecular hydrogen bonds. There are no marked differences in specific rotation among various LR-CDs (CD10 to CD39).

1.7 Application of amyloamylase and LR-CDs

Recently, AM have been explored for their potential applications. A first application of AM is to use for the production of LR-CDs with a degree of polymerization (DP) from 16 up to about a hundred of glucose (Bhuiyan *et al.*, 2003; Kaper *et al.*, 2004; Srisimarat *et al.*, 2011; Taira *et al.*, 2006; Terada *et al.*, 1999). They are hydrophilic outside, thus dissolves in water, exhibit helical structure and hydrophobic channel which can form inclusion complex with a large variety of hydrophobic guest molecules such as drug molecules, alcohol, fatty acids and detergent (Larsen, 2002; Przylas *et al.*, 2000a; Taira *et al.*, 2006). The most interesting property of LR-CDs is their higher solubility in water, in comparison to small-ring CDs. Therefore LR-CDs could have potential role in the stabilization and solubilization of guest compounds, insoluble or unstable food ingredients and drug molecules for chemical, cosmetics, food, pharmaceutical applications (Endo *et al.*, 2002; Kaper *et al.*, 2004; Larsen, 2002; Tomono *et al.*, 2002). The first report about inclusion complex of LR-CD is the effect of complex formation with CD9 on the solubility of drugs that are poorly soluble or insoluble in water. This study reported the inclusion complexes between CD9 with spironolactone and digtoxin (Miyazawa, 1994). In addition, the inclusion complex of CD9 and C₇₀ (Buckminster fullerene) could also be prepared and an effective solubilization of this molecule in water has been observed (Furuishi *et al.*, 1998). Nevertheless, since the LR-CDs are able to

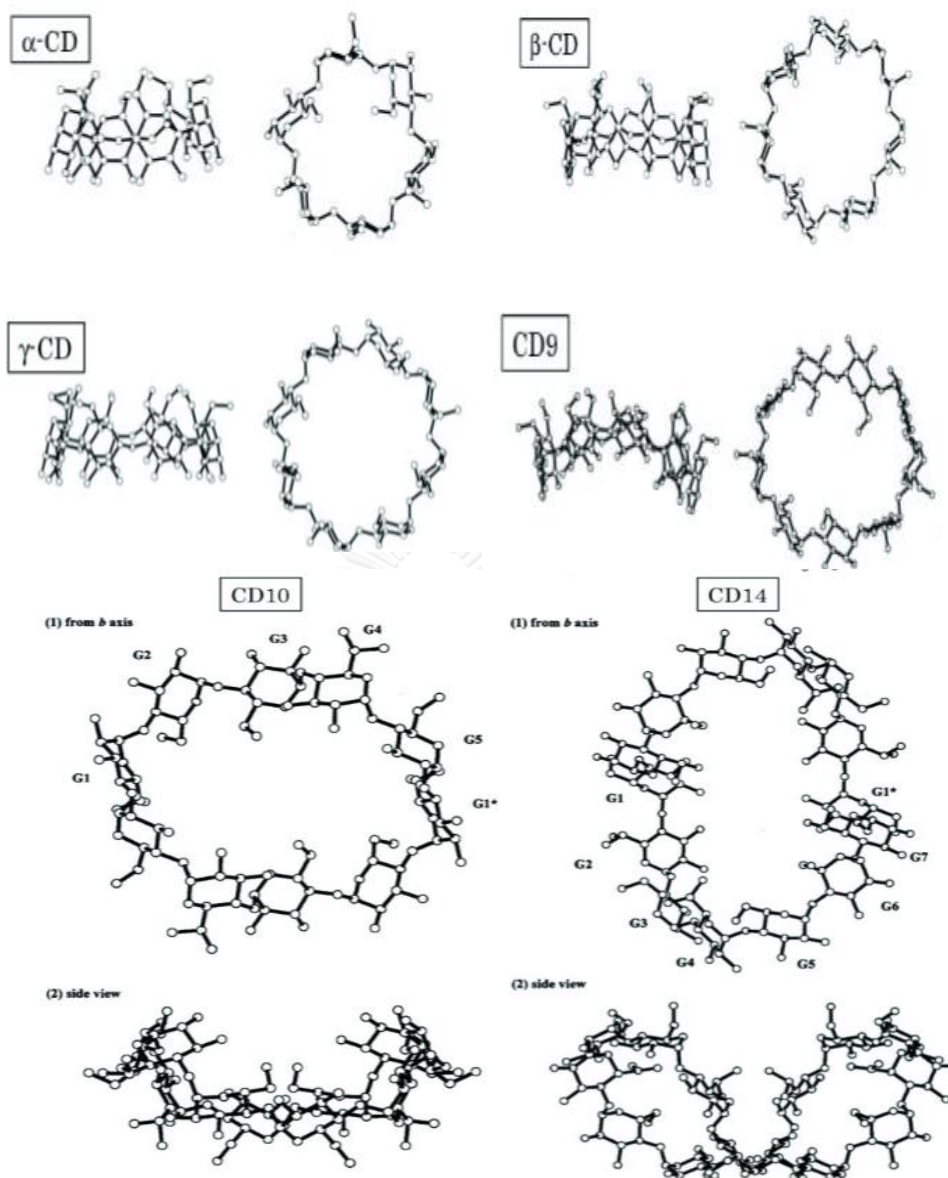


Figure 1. 8 Molecular structures of α -CD, β -CD, γ -CD, CD9 and CD14 side view and top (Endo, 2011).

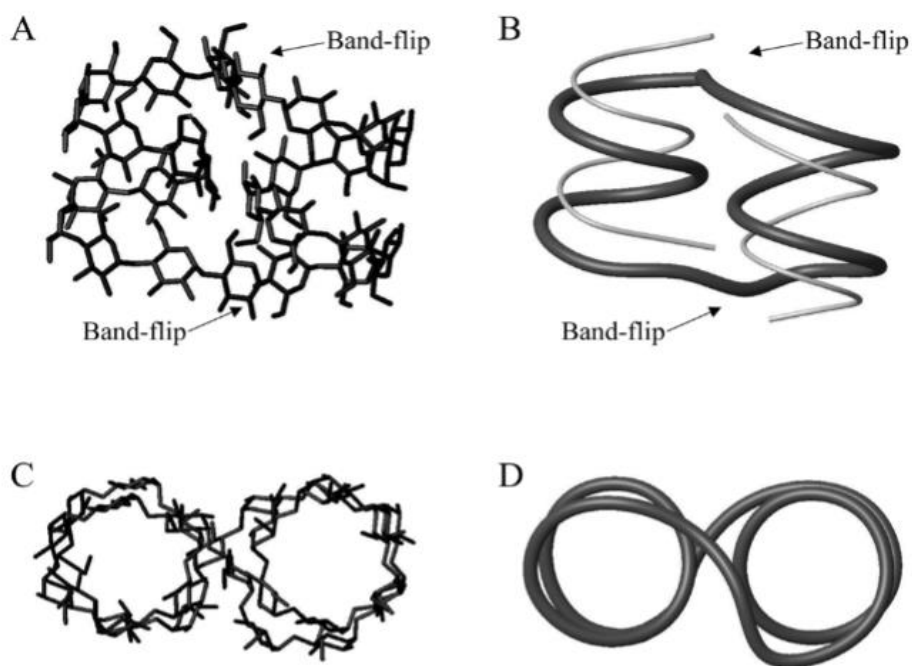


Figure 1. 9 Solid state structure of CD26. (A) Structure of CD26 indicating the position of the band-flips and the V- amylose like segments. (B) Same structure as a, the thick dark tube traces the position of C1, whereas the thin grey tube traces the position of C6. The band-flipped positions are clearly seen. (C) CD26 viewed from the top. (D) Same structure as C, the thick dark tube traces the position of C1 (Larsen, 2002). A band flip was defined as a 180° inverted glycoside linkage (Taira *et al.*, 2006).

Table 1. 2 Physicochemical properties of native small-ring CDs and LR-CDs. (Endo, 2011)

| | Theoretical ^{a)} molecular weight | Aqueous ^{b)} solubility (g/100 mL) | Surface ^{b)} tension (mN/m) | Specific rotation [α] _D ²⁵ | Half-life of ^{c)} ring opening (h) | | Theoretical ^{a)} molecular weight | Aqueous ^{b)} solubility (g/100 mL) | Surface ^{b)} tension (mN/m) | Specific rotation [α] _D ²⁵ | Half-life of ring opening (h) |
|--------------|--|---|--|---|---|------|--|---|--|---|-------------------------------------|
| α -CD | 972.8 | 14.5 | 72 | +147.8 | 33 | CD23 | 3729.2 | >100 | 73 | +196.6 | 2.7 |
| β -CD | 1135.0 | 1.85 | 73 | +161.1 | 29 | CD24 | 3891.4 | >100 | 73 | +196.0 | 2.6 |
| γ -CD | 1297.1 | 23.2 | 73 | +175.9 | 15 | CD25 | 4053.5 | >100 | 73 | +190.8 | 2.8 |
| CD9 | 1459.3 | 8.19 | 72 | +187.5 | 4.2 | CD26 | 4215.7 | 22.4 | 73 | +201.4 | 2.9 |
| CD10 | 1621.4 | 2.82 | 72 | +204.9 | 3.2 | CD27 | 4377.8 | >125 | 72 | +189.4 | 2.8 |
| CD11 | 1783.5 | >150 | 72 | +200.8 | 3.4 | CD28 | 4539.9 | >125 | 72 | +191.2 | 2.6 |
| CD12 | 1945.7 | >150 | 72 | +197.3 | 3.7 | CD29 | 4702.1 | >125 | 72 | +190.2 | 2.5 |
| CD13 | 2107.8 | >150 | 72 | +198.1 | 3.7 | CD30 | 4864.2 | >125 | 72 | +189.1 | 2.3 |
| CD14 | 2270.0 | 2.30 | 73 | +199.7 | 3.6 | CD31 | 5026.4 | >125 | 71 | +189.0 | 2.4 |
| CD15 | 2432.1 | >120 | 73 | +203.9 | 2.9 | CD32 | 5188.5 | >125 | 71 | +192.7 | 2.4 |
| CD16 | 2594.2 | >120 | 73 | +204.2 | 2.5 | CD33 | 5350.6 | >125 | 71 | +192.1 | 2.2 |
| CD17 | 2756.4 | >120 | 72 | +201.0 | 2.5 | CD34 | 5512.8 | >125 | 72 | +189.6 | 2.2 |
| CD18 | 2918.5 | >100 | 73 | +204.0 | 3.0 | CD35 | 5674.9 | >125 | 71 | +193.7 | 2.1 |
| CD19 | 3080.7 | >100 | 73 | +201.0 | 3.4 | CD36 | 5837.1 | >100 | 71 | +190.6 | 1.9 |
| CD20 | 3242.8 | >100 | 73 | +199.7 | 3.4 | CD37 | 5999.2 | >100 | 71 | +189.9 | 1.8 |
| CD21 | 3405.0 | >100 | 73 | +205.3 | 3.2 | CD38 | 6161.3 | >100 | 71 | +190.1 | 1.9 |
| CD22 | 3567.1 | >100 | 73 | +197.7 | 2.6 | CD39 | 6323.5 | >100 | 70 | +188.1 | 1.8 |

a) Calculated as $162.1406 * n$, where n is the number of glucopyranose unit.

b) Observed at 25 °C.

c) In 1 mol/L HCl at 50 °C.



present a variety of cavity sizes, compared to the conventional cyclodextrins, they may be useful for special applications. Moreover, it is very large cyclodextrins even a nanotube/V-amylose-like cavity (Larsen, 2002). Furthermore, Takaha and Smith, 1999 reported that the LR-CDs with a degree of polymerization larger than 50, showed the ability to form complexes with butanol, octanol and oleic acid. In addition, LR-CDs (DP22 to DP45 or larger than DP50) as the ingredient of the commercial 'Protein refolding kit' have the ability to strip a detergent molecule from protein-detergent complex and then assist the protein refolding to native conformation or active state (Figure 1.9) (Machida *et al.*, 2000). Furthermore, it was also reported in 2003 that the LR-CDs mixture provided an efficient method for refolding denatured antibody to correct active structure (Machida *et al.*, 2003). The interaction between LR-CDs mixture with DPs of 20 to 50 and drugs such as prednisolone, cholesterol, digoxin, digotoxin and nitroglycerin were evaluated (Tomono *et al.*, 2002), although nitroglycerin did not interact with the LR-CDs mixture, the solubilities of prednisolone, cholesterol, digoxin, digotoxin were enhanced by the presence of the LR-CDs mixture and the phase solubility diagrams showed the occurrence of complex formations. In particular, the LR-CDs mixture showed the highest solubilization effect for cholesterol in comparison with β - and γ -CD (Tomono *et al.*, 2002). Table 1.3 summarizes studies on the inclusion complex formation between LR-CD or mixture of LR-CDs and guest compounds (Endo, 2011).

A second application of AM is in the production of prebiotics or glucosides. The enzyme from *Thermotoga maritima* is used in combination with a maltogenic amylase from *Bacillus stearothermophilus* to produce isomalto-oligosaccharides (IMOs) from starch (Lee *et al.*, 2002). IMOs are non-digestible oligosaccharides

which can be used as a substitute sugar to improve the intestinal microflora, or prevent dental caries. The synthesis of an anticariogenic maltooligosylsucrose by AM has been recently reported (Saehu *et al.*, 2013). This oligosaccharide can be applied as sucrose substitute, cannot be utilized by *Streptococcus mutans*, a flora known to cause dental caries in humans and experimental animals. AM has also been used to modify the genistin, a major isoflavone in soybean to enhance its water solubility (Li *et al.*, 2005).

A third application is in the production of thermoreversible starch gel by disproportionation reaction that is of commercial interest since it can be used as a substitute for gelatin in food products. This product could be dissolved in water and formed gel after heating and cooling. The gel could be dissolved again by a new heating step. The action of AMs on starch was as shown in Figure 1.10, starch transglucosylation activity will transfer short chain of glucosyl group to yield shortened or elongated starch side chain (Hansen *et al.*, 2008; Kaper *et al.*, 2005; Kaper *et al.*, 2004; Lee *et al.*, 2006). Such thermoreversible starch gel is very similar to gelatin, a product derived from the bone marrow of cow. Due to its animal origin, gelatin suffers from a disputable reputation and is not accepted by vegetarians and certain religious groups as a food ingredient (Kaper *et al.*, 2005). In addition, the AM-treated starch was used to improve food products, such as improvement of creaminess of low-fat yoghurt (Alting *et al.*, 2009) and combination with xanthan gum for fat substitution in reduced-fat mayonnaise (Mun *et al.*, 2009).

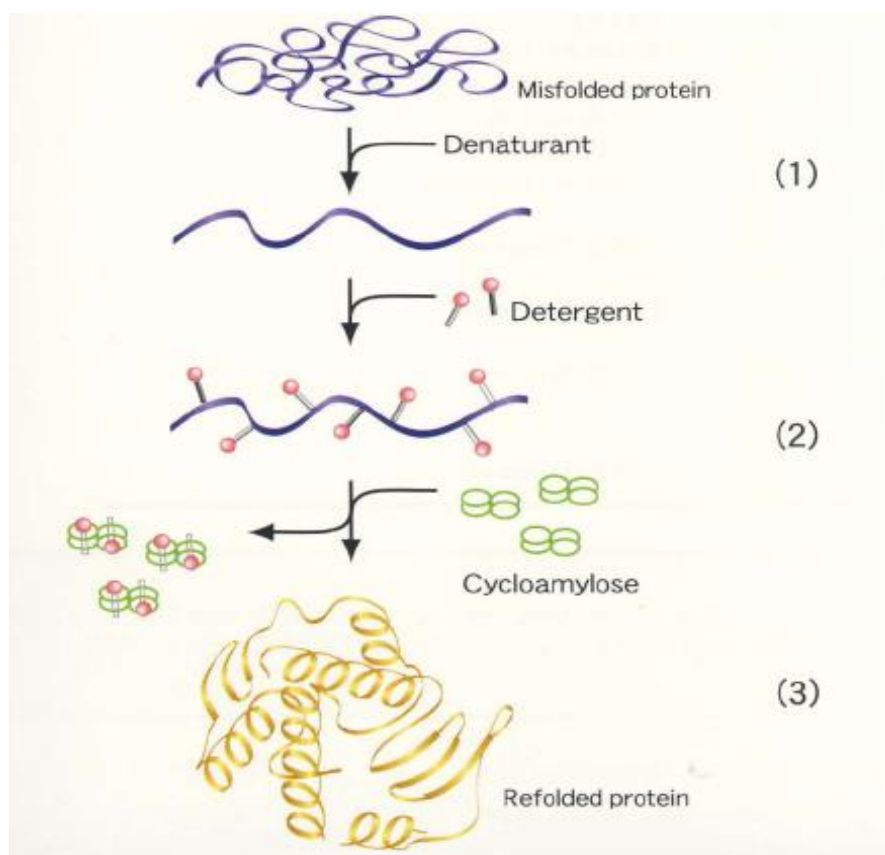


Figure 1. 10 LR-CDs as an artificial chaperone for protein refolding by acting as the ability to strip a detergent molecule from protein-detergent complex and then assist the protein refolding to native conformation or active state.

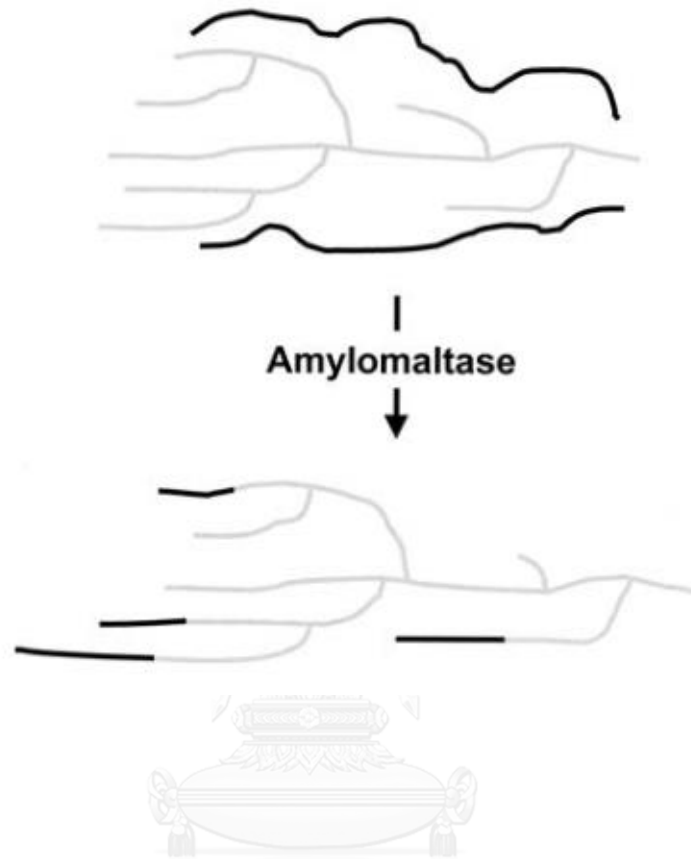


Figure 1. 11 Action of AM on starch (starch transglucosylation activity) in the explanation of forming a thermoreversible starch gel. The black and gray lines represent amylose and amylopectin, respectively. Some side chains of the final products have been shortened while others have been elongated (Kaper *et al.*, 2004).

Table 1. 3A Studies of inclusion complex formation between pure LR-CD or mixture of LR-CDs and guest compounds.

| CD | (Ref.no.) | Indicator or Method | Compound |
|--------------|----------------------|---|---|
| (Pure LR-CD) | | | |
| CD9 | (10) | Enhancement of solubility (UV/VIS absorption) | Anthracene Amphotericin B. Ajmalicine Ajmaline Carbamazepine Digitoxin Spironolactone 9, 10-Dibromoanthracene Perylene-3,4,9,10-tetracarboxylic Dianhydrate Spironolactone |
| | | Solubility method | Spironolactone |
| CD9 | (51, 53) (50, 52) | Enhancement of solubility Spectrophotometry | Fullerene C ₆₀ Fullerene C ₇₀ |
| CD9 | (45) | Enhancement of solubility (Spectrophotometry) | Reserpine [2,2]-Paracyclophane Perylene Triphenylene 1,8-Naphthalic anhydride Naphthalene-1,4,5,8-Tetracarboxylic dianhydride Digitoxin Gitoxin Digoxin Methyldigoxin Lanatoside C G-Strophanthin Proscillaridin A |
| | | Solubility method and NMR | Digitoxin |
| CD9 | (87) | Simple precipitation | 1,5-Cyclooctadiene Cyclononane Cyclodecanone Cycloundecanone Cyclododecanone Cyclotridecanone Cyclopentadecanone |
| | | Power X-ray diffraction DSC | Cycloundecanone Cyclododecanone |
| CD9 – CD13 | (46-48) | Capillary electrophoresis | Benzoate 2-Methyl benzoate 3-Methyl benzoate 4-Methyl benzoate 2,4-Dimethyl benzoate 2,5-Dimethyl benzoate 3,5-Dimethyl benzoate 3,5-Dimethoxy benzoate Salicylate 3-Phenyl propionate 4-tert-Butyl benzoate Ibuprofen anion 1-Adamantane carboxylate |

Table 1. 4 Studies of inclusion complex formation between pure LR-CD or mixture of LR-CDs and guest compounds.

| CD | (Ref.no.) | Indicator or Method | Compound |
|---|-----------|--|--|
| (Pure LR-CD) | | | |
| CD14 – CD17 | (49) | Capillary electrophoresis | Salicylate 4-tert-Butyl benzoate Ibuprofen anion |
| CD21 – CD32 | (56) | Isothermal titration Calorimetry (ITC) | Iodine |
| CD9 | (55) | X-ray crystallography | Cycloundecanone |
| CD12 | (54) | NMR | Single wall carbon nanotube (SWNT) |
| CD26 | (57, 88) | X-ray crystallography | NH ₄ I ₃ Ba(I ₃) ₂ Undecanoic acid Dodecanol |
| (Mixture of LR-CDs) | | | |
| CA(S) [*] and CA(L) ^{**} | (89) | Spectrofluorometry | 8-Anilino-1-naphthalene sulfonic acid |
| CA(S) [*] and CA(L) ^{**} | (25, 89) | Simple precipitation | 1-Octanol 1-Butanol Oleic acid |
| CA (with oligomerization Degree of 22 to around 60) | (64) | Enhancement of solubility (Spectrophotometry) | Fullerene C ₆₀ |
| CD21 – CD40 | (90) | ITC | Sodium dodecyl sulfate Sodium myristoyl sulfate |
| CA | (91) | Simple precipitation | SB3-14 ^{***} SB3-16 ^{****} |

1.8 Error-prone PCR

Error-prone PCR is a technique commonly used for random mutagenesis in the attempt to improve the protein or enzyme functions of interest, without a structural understanding of the target protein/enzyme. The technique involves reducing the fidelity of DNA polymerase during PCR of the targeting gene by adding manganese ion ($MnCl_2$) and biasing the dNTP concentration (Figure 1.11). After the implementation of error prone PCR the mutant gene is in abundant concentration and thus has an extremely high likelihood of ligating into a viable plasmid. These random matching “errors” in the global transcription factors will presumably lead to desirable mutations ultimately causing increase in current output. Following the ligation step, the random variants will be screened and selected. On the other hand, the original strand can be sorted out and eliminated by enzymatic digestion, leaving behind the PCR product of the mutated gene (Fujii *et al.*, 2004; Mabrouk *et al.*, 2013; Melzer *et al.*, 2015; Pritchard *et al.*, 2005).

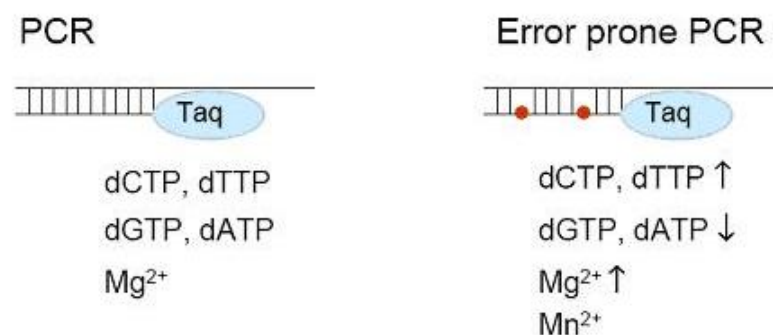


Figure 1. 12 Different conditions of PCR and error prone PCR .

1.9 Background and the Objectives of this study

In our previous study, a novel AM from *C. glutamicum* (a mesophilic bacteria) was cloned and characterized. The *C. glutamicum* AM gene (*CgAM*) had an ORF of 2,121 bp and was deduced into a protein with 706 amino acids. *CgAM* could produce LR-CDs with a DP of 18-55 and the enzyme was stable at temperature only up to 30 °C (Srisimarat *et al.*, 2012; Srisimarat *et al.*, 2011). It is well accepted that the thermostable enzymes with favorable properties have a great potential for industrial use e.g. as stable catalysts in food processing: clarification of fruit juice, dough making and starch processing (Lehmann *et al.*, 2000). In this work, our aim is to increase thermostability of *CgAM*, however, due to low similarity of *CgAM* to AMs from *Thermus* with known 3D-structures, random mutagenesis through the error-prone PCR is a method of choice for introducing mutation in this enzyme (Fujii *et al.*, 2005b; Pritchard *et al.*, 2005). We here describe screening for the highest thermostable mutated clone from random mutagenesis, sequencing to identify the site of mutation, investigating the importance of this residue by site directed mutagenesis and comparing properties of the mutated *CgAMs* to that of the wild-type enzyme.

The Objectives

1. To modify the AM gene from *C. glutamicum* ATCC 13032 by random and/or site-directed mutagenesis to increase thermostability of this enzyme
2. To clone and express the mutated AM gene in *Escherichia coli*
3. To purify and characterize the selected mutated AM from *E.coli*
4. To identify the amino acid residues involved in thermostability of AM by site-directed mutagenesis
5. To characterize and optimize the enzymatic reaction for production of LR-CDs



CHAPTER II

MATERIALS AND METHODS

2.1 Equipments

Amicon : Ultra-15 ml Centrifugal Filter Units (30 kDa cut off)

Autoclave : Model H-88LL, Kokusan Ensinki Co., Ltd., Japan

Autopipette : Pipetman, Gilson, France

Centrifuge, refrigerated centrifuge : Model Avanti™ J30-11, Beckman Instrument
Inc., USA

Electrophoresis unit :

- Mini protein, Bio-Rad, USA
- Submarine agarose gel electrophoresis unit, Bio-Rad, USA

Fraction collector : Frac-920, GE Healthcare Bio-Sciences AB, Sweden

Gene Pluser® /*E.coli* Pulser™ Cuvettes : Bio-Rad, USA

Gel Document : SYNGEND, England

HisTrap FF™ chromatography column was from GE Healthcare (United Kingdom)

HPAEC DX-600 : Dionex Corp., Sunnydale, USA

Column : Carbopac PA-100™ 4 x 250 mm

Plused amperometry detector : DIONEW ED40

Autosampler : DIONEX AS40

Column oven : DIONEX ICS-3000 SP

Incubator, waterbath : Model M20S, Lauda, Germany and BioChiller 2000,

FOTODYNE Inc., USA and ISOTEMP 210, Fisher Scientific, USA

Incubator shaker : Innova™ 4080, New Brunswick Scientific, USA

Light box : 2859 SHANDON, Shandon Scientific Co., Ltd., England

Laminar flow : HT123, ISSCO, USA

Magnetic Stirrer : Model Fisherbrand, Fisher Scientific, USA

Membrane filter : polyethersulfone (PES), pore size 0.45 µm, Whatman, England

Microcalorimeter : Model VP-DSC, Microcal, LLC 22 Industrial, USA

Microcentrifuge : Eppendorf, Germany

pH meter : Model PHM95, Radiometer Copenhagen, Denmark

Peristaltic : Pump P-1, GE Healthcare Bio-Scientific AB, Sweden

Power supply : Model POWER PAC 300, Bio-Rad, USA

Shaking waterbath : Model G-76, New Brunswick Scientific Co., Inc., USA

Sonicator : Bendelin, Germany

Spectropolarimeter : J-815 CD spectrometer, Jasco, Japan

Spectrophotometer : Biomate 3, Thermo scientific, USA

Spectrophotometer : DU Series 650, Beckman, USA

Vortex : Model K-550-GE, Scientific Industries, Inc, USA

2.2 Chemicals

N-acetylimidazole (NAI) : Sigma, USA

Acrylamide : Merck, Germany

Agar : Merck, Germany

Agarose : SEKEM LE Agarose, FMC Bioproducts, USA

Ammonium persulphate : Sigma, USA

Ammonium sulphate : Carlo Erba Reagent, Italy

Ampicillin : Sigma, USA

L-aspartic acid : Fluka, Switzerland

Bovine serum albumin : Sigma, USA

Boric acid : Merck, Germany

Bromphenol blue : Merck, Germany

Casein hydrolysate : Merck, Germany

Coomassie brilliant blue G-250 : Sigma, USA

Coomassie brilliant blue R-250 : Sigma, USA

Copper sulfate : Carlo Erba Reagenti, Italy

4,4'-Dicarboxy-2,2'-biquinoline : Sigma, USA

Dimethyl sulfoxide (DMSO) : Merck, Germany

di-Potassium hydrogen phosphate anhydrous : Carlo Erba Reagenti, Italy

1 kb DNA ladderTM : New England BioLabs Inc., USA and Fermentas, Canada

dNTP : Stratagene, USA

Ethidium bromide : Sigma, USA

Ethyl alcohol absolute : Carlo Erba Reagenti, Italy

Ethylene diamine tetraacetic acid (EDTA) : Merck, Germany

Gel extraction kit : GeneAids Biotech Ltd., Taiwan

Glacial acetic acid : Carlo Erba Reagenti, Italy

Glucose : BDH, England

Glucose liquicolor (Glucose oxidase kit) : HUMAN, Germany

Glycerol : Merck, Germany

Glycine : Sigma, USA

Hydrochloric acid : Carlo Erba Reagenti, Italy

Iodine : Baker chemical, USA

Isopropyl β -D-1-thiogalactopyranoside (IPTG): Sigma, USA

Maltose : BDH, England

Maltotriose : Fluka, Switzerland

Maltotetraose : Wako Pure Chemical Industries ,Japan

Maltopentaose : Wako Pure Chemical Industries ,Japan

Maltohexose : Wako Pure Chemical Industries ,Japan

Maltoheptaose : Wako Pure Chemical Industries , Japan

β -Mercaptoethanol : Fluka, Switzerland

N,N'-Methylene-bis-acrylamide : Sigma, USA

N,N,N',N'-Tetramethyl-1, 2-diaminoethane (TEMED) : Carlo Erba Reagenti, Italy

Pea starch : Emsland-Starke GmbH, Germany

Peptone : Scharlau microbiology, Spain

Phenol : Fisher Scientific, England

Phenylmethylsulfonyl fluoride (PMSF) : Sigma, USA

Plasmid Mini Kit : GeneAids Biotech Ltd., Taiwan

Potassium iodide : Mallinckrodt, USA

Potassiumphosphate monobasic : Carlo Erba Reagenti, Italy

Sodium acetate : Merck, Germany

Sodium carbonate anhydrous : Carlo Erba Reagenti, Italy

Sodium chloride : Carlo Erba Reagenti, Italy

Sodium citrate : Carlo Erba Reagenti, Italy

Sodium dodecyl sulfate : Sigma, USA

Sodium hydroxide : Merck, USA

Soluble starch (potato) : Scharlau microbiology, Spain

Standard LR-CD : Ezaki Glico Co. Ltd. (Japan)

Standard protein marker : Amersham Pharmacia Biotech Inc., USA

Tris (hydroxymethyl)-aminomethane : Carlo Erba Reagenti, Italy

Tryptone : Scharlau microbiology, Spain

Yeast extract : Scharlau microbiology, Spain

2.3 Enzyme, Restriction enzymes and Bacterial strains

Corynebacterium glutamicum ATCC 13032, Thailand Institute of Scientific and Technological Research, Thailand

Glucoamylase from *Aspergillus niger* : Fluka, Switzerland

E.coli BL21 (DE3) : Novagen, Germany

ExTaq DNA polymerase : Takara, Japan

PfuTurbo[®] DNA polymerase : Promega, USA

Plasmid pET-19b : Novagen, Germany

Restriction enzymes : New England BioLabs Inc., USA and Fermentas, Canada

RNaseA : Sigma, USA

T4 DNA ligase : New England BioLabs Inc., USA

2.4 Random mutagenesis

2.4.1 Cultivation and extraction of recombinant plasmid pET-19b *CgAM*

A single colony of recombinant *E. coli* BL21 (DE3) clones, harboring the AM gene from *C. glutamicum* (*CgAM*) (Srisimarath *et al.*, 2011) was cultured in 5 ml LB broth medium (0.5% NaCl, 0.5% Yeast extract and 1% Tryptone, w/v) containing 100 $\mu\text{g}\cdot\text{ml}^{-1}$ ampicillin at 37 °C with 250 rpm rotary shaking for overnight (16-18 h). One percent (v/v) starter was transferred into 80 ml fresh LB containing 100 $\mu\text{g}\cdot\text{ml}^{-1}$ and further cultivated at the same condition for overnight. The cell culture was collected by centrifugation at 10,000 x g for 5 min. The recombinant plasmid pET-19b vector harboring *CgAM* was extracted by Plasmid Mini Kit (GeneAids, Taiwan). The concentration of plasmid was determined by spectrophotometric method ($A_{260/280}$) and agarose gel electrophoresis.

2.4.2 Agarose gel electrophoresis

Electrophoresis through agarose is the standard method used to separate, identify and purify DNA fragments. The agarose powder (1%) was added to 100 ml electrophoresis buffer (89 mM Tris-HCl, 8.9 mM boric acid and 2.5 mM EDTA, pH 8.0) in an Erlenmeyer flask and heated until complete solubilization in a microwave oven. The agarose solution was cooled down to 60 °C until all air bubbles were completely eliminated, then poured into an electrophoresis mold. When ready, the DNA samples were mixed with one-fifth volume of the desired gel-loading buffer (0.025% bromophenol blue, 40% ficoll 400 and 0.5% SDS) and slowly loaded the mixture into agarose gel. Electrophoresis was performed at constant voltage of 10 volt/cm until the faster migration dye (bromophenol blue) migrated to approximately

1 cm from the bottom of the gel. The gel was stained with 2.5 µg/ml ethidium bromide solution for 5 min and destained to remove unbound ethidium bromide in distilled water for 10 min. DNA fragments on agarose gel were visualized under a long wavelength UV light and photographed using Gel Document apparatus. The molecular weight of DNA sample was compared with the relative mobility of the standard 1 kb DNA ladder™ fragment.

2.4.3 Modification of *CgAM* gene using error-prone PCR technique

Mutated *CgAM* genes (MT- *CgAMs*) were firstly constructed by PCR-mediated random mutagenesis which is based on error-prone PCR technique. In this technique, the recombinant plasmid pET-19b containing *CgAM* gene was extracted as described in section 2.4.1 to be used as a template DNA and oligonucleotide primers used were :

*CgAM*_FWD : [5'-GGGAATTCCATATGACTGCTCGCAGATTTTTGAATG-3']

And *CgAM*_REV : [5'-CCGCTCGAGCTAATCTCGCTTGCTTGCCTTTGCC-3'].

MT-*CgAMs* was amplified by *Taq* DNA polymerase in the presence of 50-200 µM MnCl₂ and biasing the dNTP concentration (0.2 mM of dATP and dGTP; 1 mM of dCTP and dTTP). PCR conditions were an initial denaturation at 95 °C for 2 min, followed by 30 cycles of amplification, each at 95 °C for 1 min, 60 °C for 30 sec, and 72 °C for 5 min.

2.4.4 Restriction enzyme digestion

The PCR product of each MnCl₂ concentration and plasmid vector pET-19b were separately double digested with *Nde* I and *Xho* I in the reaction mixture of 20 µl

containing 1x NEB buffer 4 (New England BioLabs., USA), 1 µg BSA, 10 U of *Nde* I, 20 U of *Xho* I and 50 µg of DNA template. The reaction was performed at 37 °C for 16 h, then resolved by agarose gel electrophoresis and eluted from the gels.

2.4.5 Ligation of the PCR product with vector pET-19b

The purified digested PCR and vector pET-19b were then ligated at 16 °C overnight in the 10 µl reaction mixture that composed of 1x ligation buffer (New England BioLabs., USA), 5 U of T4 DNA ligase, 30 µg of PCR product and 50 µg of pET-19b.

2.4.6 Preparation of competent cells for electroporation (Sambrook and Russel, 2001)

A fresh overnight culture of *E.coli* BL21 (DE3) was inoculated into 100 ml of LB medium with 1% inoculum size. The cell culture was cultivated with shaking at 250 rpm until A_{600} reached 0.5 to 0.6. The culture was chilled on ice for 15 min and the cells were harvested by centrifuge at 5,000 xg for 15 min at 4 °C. The cells were washed with 100 ml of cold water, spun down and washed again with 50 ml of cold water. After centrifugation, the cells were resuspended in approximately 15 ml of 10% glycerol in distilled water and centrifuged at 5,000 xg for 15 min at 4 °C. Finally the cell suspension was divided into 40 µl aliquots and store at -80 °C until used.

2.4.7 Plasmid transformation

The recombinant plasmids from section 2.4.5 were introduced into a competent of *E.coli* strain BL21 (DE3) by electroporation. In the electroporation step, 0.2 cm cuvettes and sliding cuvette holder were chilled on ice. The Gene Pulser® apparatus was set to the 25µF capacitor, 2.5 kV and the pulse controller unit was set to 200Ω. Competent cells, which were prepared as described in section 2.4.6 were gently thawed on ice. One to five microliter of recombinant plasmid from section 2.4.5 was mixed with 40 µl of the competent cells and then placed on ice for 1 min. This mixture was transferred to a chilled cuvette. The cuvette was applied one pulse at the above settings. Subsequently, one milliliter of LB medium (1% tryptone, 0.5% yeast extract and 0.5% NaCl) was added immediately to the cuvette. The cells were quickly resuspended, then the cell suspension was transferred to new tube and incubated at 37 °C for 1 hour with shaking. Finally, the suspension was spread onto the LB agar plates containing 100 µg/ml ampicillin. After incubation at 37 °C for 16 hours, the colonies were picked.

2.4.8 The colony PCR technique

Colony PCR is a convenient high-throughput method for determining the presence or absence of insert DNA in plasmid constructs. The individual colonies was picked and added directly to the PCR reaction, the initial heating step causes the release of the plasmid DNA from the cell, so it can serve as template for the amplification reaction. The oligonucleotide primers used were as show below:

CgAM_FWD : [5'-GGGAATTCCATATGACTGCTCGCAGATTTTTGAATG-3']
and *CgAM_REV* : [5'-CCGCTCGAGCTAATCTCGCTTGCTTGCCTTTGCC-3'].

The PCR conditions were an initial denaturation at 94 °C for 3 min, followed by 30 cycles of amplification, each at 94 °C for 30 sec, 50 °C for 1 min, and 72 °C for 3 min. To verify the insertion of PCR product into pET-19b was determined by agarose gel electrophoresis as described in section 2.4.2

2.5 The screening for thermostability of MT-CgAMs

Thirty mutated clones (MT-CgAMs) from each mutated libraries obtained from each MnCl₂ concentration (at 50, 100 and 200 μM) were randomly screened for thermostability of AM. In the first step, the crude enzymes from wild-type (WT) and mutants (MT) were determined for disproportionation activity with maltotriose substrate at 40 °C and the activity was detected by glucose oxidase method of which the glucose product develops pink color as described in section 2.10.3. Then the MT-CgAMs with higher disproportionation activity than the WT-CgAM were selected for temperature stability test at 40 °C and 50 °C.

2.6 Nucleotide sequencing

About 50-100 ng of the recombinant plasmid pET-19b from selected MT-CgAM clone obtained from section 2.5 was subjected to automated DNA sequencing (Macrogen, Korea). The sequencing was performed using primers of T7 promoter for DNA sequence at 5'-terminus and T7 terminator for DNA sequence at 3'-terminus of the inserted *CgAM* gene, respectively. The obtained DNA sequence was used to design primers f2CGAM and r2CGAM for determining the residual sequence which was localized in the middle of the gene. The primers used were as show below.

CgAM_FWD2 : [5'- TCT ACT CTG TGC GTT CCA CGT TG -3']

CgAM_REV2 : [5'- CCT GCG AGT TCT GCT TAT AGG -3']

2.7 Site-directed mutagenesis

Mutagenesis was carried out by PCR amplification using a pair of oligonucleotide with a desired point mutation and the recombinant plasmid as a template. The PCR product was digested with *Dpn* I endonuclease (target sequence: 5'-GA_{CH₃}[^]TC-3') which is specific for methylated as well as hemimethylated DNA. This enzyme is used to digest the parental DNA template to select for mutation-containing synthesized DNA. DNA isolated from almost all *E.coli* strains is dam methylated and therefore susceptible to *Dpn* I digestion. The nicked plasmid of the *Dpn* I-treated was then transformed into the host *E.coli* competent cells.

The recombinant plasmid pET-19b containing *CgAM* gene was extracted as described in section 2.4.1 to be used as a template DNA and the following synthetic oligonucleotides as primers for mutagenesis work at A406 to be substituted by Val (V) and Leu (L), His (H), Arg (R) and Phe (F). In addition, at N287 to be substituted by Tyr (Y). For mutagenic PCR primer, primerX server was used to design the primer based on *E.coli* codon usage. The sequences of mutagenic primers were shown below. The underlined letters were coded for the mutated residues.

A406V_FWD[5'-CTCAGCCACGTACTTGTTCCGGATGCGTCAG-3']

A406V_REV[5'- CTGACGCATCCGGAACAAAGTACGTGGCTGAG-3']

A406L_FWD[5'-CAGAACCTCAGCCACGTACTTCTGCCGGATGCGTCAGTGG-3']

A406L_REV[5'-CCACTGACGCATCCGGCCAGAAGTACGTGGCTGAGGTTCTG-3'].

A406H_FWD[5'- GAACCTCAGCCACGTACTTCATCCGGATGCGTCAGTGGGC -3']

A406H_REV[5'- GCCCACTGACGCATCCGGATGAAGTACGTGGCTGAGGTTC -3'].

A406R_FWD[5'- CTCAGCCACGTACTTCGTCCGGATGCGTCAGTGG -3']

A406R_REV[5'- CCACTGACGCATCCGGACGAAGTACGTGGCTGAG -3']

A406F_FWD[5'- CTCAGCCACGTACTTTTTCCGGATGCGTCAGTGGGC -3']

A406F_REV[5'- GCCCACTGACGCATCCGGAAAAAGTACGTGGCTGAG -3']

N287Y_FWD[5'-CATCATTGAGCGCTATGACGTCTACGCTGC -3']

N287Y_REV[5'-GCAGCGTAGACGTCATAGCGCTCAATGATG -3']

PCR was performed in a 50 µl reaction mixture containing 50-100 ng of the recombinant plasmid, 1x *Pfu* buffer with MgSO₄, 0.1 µmole of each dNTP, 10 pmoles of each primer and 1 U of *Pfu* DNA polymerase. the PCR conditions were an initial denaturation at 95 °C for 2 min, followed by 16 cycles of amplification : 1 min at 95 °C, 1 min at 60 °C and followed by final elongation at 72 °C for 12 min. Then, 30 µl of PCR product was transferred to a new tube and settled on ice for 2 min, then incubated with 1 µl (10 U) of *Dpn* I for 1 hour at 37 °C.

The *Dpn* I digested PCR product was prepared for transformation by gently mixed with competent *E.coli* BL21 (DE3) cells. The transformation was performed as described in section 2.4.7 Cells containing the recombinant mutated plasmids plasmid

were picked and the mutated plasmids were further extracted. To confirm the mutation, the plasmids were extracted and checked their size by agarose gel electrophoresis as described in section 2.4.1 and 2.4.2. The point of mutation was further confirmed by nucleotide sequencing as in section 2.6 and compared with the WT-*CgAM* gene.

2.8 The expression of recombinant wild-type WT- and MT-*CgAMs*

The *E. coli* BL21 (DE3) containing recombinant plasmid *CgAM* was cultivated in LB broth containing 100 µg/ml of ampicillin antibiotic. The enzyme production was induced with 0.4 mM IPTG for 0, 1, 2, 3, 4, 5 and 6 h. The growth rate was followed by A_{600} . The 1.5 ml of cell suspension was taken from recombinant clone *CgAMs* grown at 0.4 mM IPTG at various times and then harvested by centrifugation. The cell pellets were resuspended in 150 µl of extraction buffer, then sonicated and centrifuged to get crude supernatant, disproportionation activity in crude extract was assayed as described in section 2.10.3. The protein pattern of cells during IPTG induction was followed. The 8 µg protein of crude enzymes from WT-, MT-*CgAMs* were subjected to electrophoresis on 7.5% SDS-polyacrylamide gel.

2.9 Expression and purification of WT- and MT-*CgAMs*

2.9.1 Cells cultivation and crude extract preparation

A single colony of *E. coli* BL21 (DE3) recombinants harboring the WT-*CgAM* or MT-*CgAMs* were inoculated and cultured in LB medium (0.5% NaCl, 0.5% yeast extract and 1% tryptone, w/v) containing 100 µg/ml ampicillin. Incubation at 37 °C with 250 rpm rotary shaking was performed as previously described

(Srisimararat *et al.*, 2011). The expression of WT-CgAM and MT-CgAMs was induced by adding 0.4 mM of IPTG when A_{600} of the culture reached 0.4-0.6. In the case of mutated clones occurring in clusion body protein problem, these mutated clones were growth under 4 condition : condition 1 and 2 : cells were cultivated at 37 °C in LB broth and LB broth containing 1% of glucose, respectively, cells were grown until A_{600} reached 0.4-0.6, the enzyme production was induced with 0.4 mM IPTG; condition 3 : cells were cultivated at 37 °C in LB broth containing 1% of glucose, cells were grown until A_{600} reached 0.4-0.6, the enzyme production was induced with 1 mM IPTG, then the temperature was changed to 16 °C for protein expression. In condition 4 : cells were cultivated at 37 °C in Auto Induction Media (AIM) containing lactose until A_{600} reached 0.4-0.6, the temperature was then changed to 16 °C for protein expression without IPTG induction. After optimum time for gene expressions, cells were harvested by centrifugation at 6,000 xg for 15 min, then washed by 0.85% NaCl and extraction buffer, respectively. Bacterial cells were resuspended in extraction buffer then disrupted by sonication of 30% pulse for 1 min and stopped for 2 min, then repeated sonication process for 15 cycles. Bacterial cell debris was removed by centrifugation at 12,000 x g, 4 °C for 60 min. The supernatant which contained crude CgAM was collected and then dialyzed against 20 mM phosphate buffer, pH 7.4 before determination of enzyme activity and protein concentration as described in section 2.10 and 2.11, respectively.

2.9.2 Purification of recombinant WT- and MT-CgAMs

The crude extract from 2.9.1 was initially purified by HisTrap FFTM at 4 °C. The HisTrap FFTM was equilibrated with at least 5 times column volume of 20 mM

phosphate buffer, pH 7.4 containing 0.5 M NaCl and 20 mM imidazole at the flow rate of 1 ml/min. The dialyzed protein solution from section 2.9.1 was applied to HisTrap FFTM column (1 ml, two columns consecutively) and washed with the same buffer until A_{280} of eluent decreased to baseline. The bound protein was eluted by 500 mM imidazole in the same buffer at the flow rate of 1 ml/min. Fractions of 3 ml were collected and the enzyme activity was determined. The active fractions were pooled and dialyzed against 20 mM phosphate buffer, pH 7.4 before determination of the enzyme activity and protein concentration as described in section 2.10 and 2.11, respectively.

2.10 Enzyme assay

Amylomaltase activity was determined by five types of assay as described below.

2.10.1 Starch degrading activity

The enzyme activity was determined by measuring the degraded starch in the reaction using iodine method (Srisimarath *et al.*, 2012).

Fifty microliter of enzyme solution was added into 100 μ l of 0.75% (w/v) soluble potato starch and 100 μ l of 50 mM phosphate buffer, pH 6.0. Incubation was at 30 for 10 min and stopped by adding 500 μ l of 1 N HCl. One hundred μ l of reaction was withdrawn and mixed with 900 μ l of iodine solution (0.005% I_2 in 0.05% KI, (w/v)), The absorbance was measured at 660 nm.

One unit of enzyme was defined as the amount of enzyme which degraded starch (1 mg/ml) in 10 min incubation time under the assay conditions used.

2.10.2 Starch transglucosylation activity

The enzyme activity was determined by the ability to transfer glucosyl group from starch donor to maltose acceptor. The remained starch was detected by adding iodine solution (modified from (Park *et al.*, 2007).

The reaction mixture contained enzyme solution (100 μ l), 0.2% (w/v) soluble starch (250 μ l), 1.0% (w/v) maltose (50 μ l) and 50 mM phosphate buffer pH 6.0 (600 μ l). The reaction mixture was incubated at 30 °C for 10 min, and terminated by heating the solution at 100 °C for 10 min. Aliquot of 100 μ l was withdrawn and mixed with 1.0 ml of iodine solution (0.02% I₂ in 0.2% KI (w/v). The absorbance was measured at 600 nm.

One unit of enzyme was defined as the amount of enzyme that produced 1% decrease in the color of starch-iodine complex per min under the assay conditions used.

2.10.3 Disproportionation activity

This activity was measured by the glucose oxidase method as described (Srisimarat *et al.*, 2012) with slight modification.

The 50 μ l reaction mixture containing 5% (w/v) maltotriose and enzyme in 50 mM phosphate buffer, pH 6.0 was incubated at 40 °C for 10 min and stopped the reaction by boiling. The glucose oxidase reagent was added to a final volume of 1.0 ml, then incubated at 30 °C for 10 min and measured the absorbance at 505 nm.

One unit was defined as the amount of enzyme which produced 1 μ mol of glucose per min under the described conditions.

2.10.4 Cyclization activity

This activity was measured by high performance anion exchange chromatography with pulsed amperometric detection (HPAEC-PAD)

The reaction mixture containing pea starch and enzyme was incubated at pH 6.0, 30 °C for 90 min as previously described (Srisimarat *et al.*, 2012). Analysis of LR-CD products was by HPAEC after addition of 8 U of glucoamylase and incubated at 40 °C for 12 h.

One unit of enzyme was defined as the amount of enzyme which produced 1 nC of CD31 per min under the described conditions.

2.10.5 Coupling activity

This activity is a reverse of cyclization activity, measured by glucose oxidase method (Miwa *et al.*, 1972).

The 100 µl reaction mixture containing, each 20 µl of 3 mg/ml of LR-CDs and 1 mg/ml of cellobiose as the substrates was incubated with the enzyme in 50 mM phosphate buffer, pH 6.0 at 30 °C for 10 min. The reaction was stopped by boiling, then 8 U of glucoamylase was added, incubated at 40 °C for 30 min and inactivated by boiling. The glucose oxidase reagent was added to a final volume of 1.0 ml, then incubated at 30 °C for 10 min and measured the absorbance at 505 nm.

One unit was defined as the amount of enzyme which produced 1 µmol of glucose per min under the described conditions.

2.10.6 Hydrolysis activity

This activity was performed by bicinchoninic acid (BCA) method as described (Srisimarath *et al.*, 2012) with slight modification. The reaction mixture containing LR-CDs and enzyme was incubated at pH 6.0, 30 °C for 10 min. After stopped the reaction, BCA solution was added and incubated before measuring the absorbance at 562 nm.

One unit was defined as the amount of enzyme required for the production of 1 μ mol of reducing sugar (as glucose) per min under the described conditions.

2.11 Protein determination

Protein concentration was determined by (Bradford, 1976) method, using bovine serum albumin (BSA) as standard.

One hundred μ l of sample was mixed with 1 ml of Bradford working solution that contained Coomassie blue G-250, left for 10 min, and the absorbance was measured at 595 nm.

2.12 Polyacrylamide gel electrophoresis (PAGE)

2.12.1 SDS-polyacrylamide gel electrophoresis (SDS-PAGE)

The denaturing gel was performed on a 5% (w/v) stacking gel and 7.5% (w/v) separating gel that consisted of 0.1% SDS (w/v), electrophoresis was carried out on a Bio-Rad Mini-Protein III gel apparatus (Bio-Rad Laboratories, Hercules, MA, USA) using the Laemmli buffer system. The sample buffer was added into samples and boiled for 5 min prior to loading into the gel. The electrophoresis was run at constant current of 20 mA per slab from anode to cathode at room temperature.

2.12.2 Coomassie blue staining

After electrophoresis, the gel was stained for proteins with coomassie blue R-250 staining solution (1% Coomassie blue R-250, 45% methanol and 10% glacial acetic acid) at room temperature for 3 h. And then, it was destained with destaining solution (10% methanol and 10% glacial acetic acid) until the background was cleared.

2.13 Characterization of AM

2.13.1 Effect of pH and temperature on activity and stability

The effects of pH and temperature on activity and stability of WT- and MT-CgAMs were performed by disproportionation and cyclization reactions. The protein concentration of each enzyme was fixed at 15 μ g for disproportionation reaction and 0.3 mg for cyclization reaction.

For disproportionation reaction, optimum temperature was determined at pH 6.0, in the temperature range of 25 to 70 °C, using condition as described in section 2.10.3. Temperature stability was determined by measuring remaining activity after the enzyme was pre-incubated at 35 °C up to 180 min. Optimum pH was determined at 45 °C in different buffer of pH 4.0 to 9.0.

For cyclization reaction, optimum temperature was investigated at pH 6.0, in the temperature range of 25 to 50 °C, using condition as described in section 2.10.4. Optimum pH was determined at 30 °C in different buffer of pH 5.0 to 9.0.

Buffers used were: acetate for pH 4.0-6.0, phosphate for pH 6.0-8.0 and Tris-HCl for pH 8.0-9.0, all at 50 mM concentration.

2.13.2 Substrate specificity

Specificity for malto-oligosaccharide substrates (maltose, G2 to maltoheptaose, G7) was determined by disproportionation reaction as described in section 2.10.3. The reaction mixture contained 50 mM substrate and 0.2 U of starch transglucosylation activity. After incubation, disproportionation activity was determined by glucose oxidase method.

2.13.3 Analysis of kinetic parameters

The kinetic parameters for disproportionation reaction were investigated. The purified WT- or MT-CgAM was incubated in 50 mM phosphate buffer, pH 6.0, with various concentrations of maltotriose (0 to 40 mM) at 45 °C for 5 min, and then stopped by boiling for 10 min. The product was detected by glucose oxidase method. The kinetic parameters K_m and V_{max} were determined from a Lineweaver-Burk plot, and then the k_{cat} and k_{cat}/K_m values were calculated.

2.13.4 Circular dichroism spectrometer

The spectra were obtained using a spectropolarimeter (J-815 CD spectrometer, Jasco, Japan). A protein of 0.2 mg/ml was used for the measurement in the wavelength range of 190-250 nm at 25 °C. Each CD spectrum was monitored in three scans at 20 nm/min with constant time at 2 sec and 2 nm bandwidth.

The CD spectra of AMs were calculated from the method of (Kelly *et al.*, 2005). The Mean Residue Weight (MRW) for estimating the quantity of the peptide bond in protein is as shown in equation (1).

$$\text{MRW} = \frac{M}{(N-1)} \quad (1)$$

Where M stands for the molecular weight of the polypeptide chain (Da), N stands for the number of amino acid residues in the chain and N - 1 stands for the number of peptide bonds. The mean residue ellipticity (MRE) at each of wavelength λ ($[\theta]_{\text{mrw},\lambda}$) is given by equation (2).

$$[\theta]_{\text{mrw},\lambda} = \frac{\text{MRW} \times \theta\lambda}{10 \times dc} \quad (2)$$

Where $\theta\lambda$ = ellipticity (degrees) at each of wavelength λ

d = the path length of the cuvette (cm)

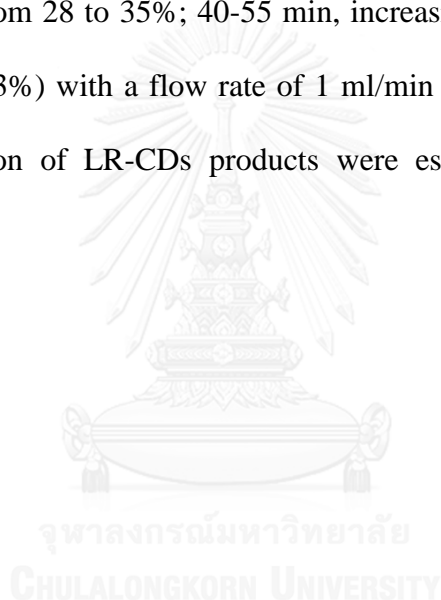
and c is the protein concentration (g/mL). The unit of MRE and molar ellipticity is $\text{deg.cm}^2.\text{dmol}^{-1}$. (Kelly *et al.*, 2005). The protein secondary structures were predicted using the Dichroweb online server program.

2.13.5 Differential scanning calorimetry

Samples for Differential scanning calorimetry (DSC) were prepared by dissolving the lyophilized enzyme samples in 50 mM phosphate buffer, pH 6.1 and dialyzed for 18 h. Samples were determined for protein concentration, and degassed (Islam *et al.*, 2009). Then DSC measurements were performed using a VP-DSC MicroCalorimeter (Microcal, USA) at a scan rate of 45, 60 or 90 K/h in the temperature range of 283-373 K. Protein concentration used was around 1.8 mg/ml for both WT- and MT-CgAMs. Thermal transition curve was obtained from a plot of heat capacity against temperature.

2.14 Synthesis and analysis of LR-CDs

LR-CD products were analyzed by HPAEC-PAD (ICS 5000 system (Dionex)) using a Carbopac PA-100 column (4 x 250mm). The sample solution was prepared as described in section 2.10.4. and 2.13.1. Then, 25 μ l of sample was injected into the column (Carbopac PA-100, 4 x 250 mm, Dionex, USA) and eluted with a linear gradient of 200 mM sodium nitrate in 150 mM NaOH (0-2 min, increasing from 4 to 8%; 2-10 min, increasing from 8 to 10%; 10-20 min, increasing from 18 to 28%; 20-40 min, increasing from 28 to 35%; 40-55 min, increasing from 35-45%; 55-60 min, increasing from 45-63%) with a flow rate of 1 ml/min (Srisimarat *et al.*, 2011). The size and concentration of LR-CDs products were estimated by comparison with standard LR-CDs.



CHAPTER III

RESULTS

3.1 Random mutagenesis for improvement of thermostability of amylomaltase from *Corynebacterium glutamicum* (CgAM)

In this work, random mutagenesis of *CgAM* gene using error-prone PCR technique was employed in the aim to increase thermostability of the enzyme *CgAM*.

3.1.1 Extraction of recombinant plasmid pET-19b *CgAM*

The recombinant plasmid pET-19b harboring *CgAM* gene was extracted and checked by agarose gel electrophoresis (Figure 3.1, Lane 1). After double digestion with *Nde* I and *Xho* I, the result showed that the size of pET-19b vector and *CgAM* gene were around 5.7 kb and 2.1 kb, respectively (Figure 3.1, Lane 2). The ratio of A260/280 values was 1.8 indicated that the purity of this extracted recombinant plasmid was sufficient to be used as template for further PCR amplification.

3.1.2 Modification of *CgAM* gene using error-prone PCR technique

The recombinant plasmid harboring *CgAM* gene was used as a DNA template for random mutagenesis by using error-prone PCR. The product from the PCR amplification in the presence of various concentrations of manganese ion (MnCl_2) ranging from 50 to 200 μM was found as a single band on agarose gel electrophoresis shown in Figure 3.2. The size of PCR product was 2.1 kb as expected for *CgAM* gene. The PCR product of each MnCl_2 concentration (at 50, 100 and 200 μM) were purified and subjected to digestion with the restriction enzymes *Nde* I and *Xho* I before ligated

with *Nde* I-*Xho* I digested pET-19 vector (Appendix Restriction map of pET-19b) by T4 DNA ligase, resulting in the three mutated libraries.

3.1.3 Transformation

The recombinant plasmid gene was constructed and transformed into the competent cells of *E. coli* BL21 (DE3) by electroporation as described in section 2.4.7. Two hundred microliters of the transformant, *E. coli* BL21 (DE3) containing pET-19b vector harboring mutated *CgAM* gene, was spread on LB agar plate containing 100 µg/ml of ampicillin and incubated at 37 °C for overnight. The colony PCR technique as described in section 2.4.8 was used for randomly detection of the recombinant clones. The agarose gel electrophoresis of the product from colony PCR technique is shown in Figure 3.3. The size of PCR product is 2.1 kb corresponded to the expected size of the *CgAM* gene. To verify the insertion of PCR product into pET-19b, the transformant was picked for plasmid extraction and digested with *Nde* I and *Xho* I as described in section 2.4.4. The agarose gel electrophoresis pattern of the recombinant plasmid containing *CgAM* gene is shown in Figure 3.4.

3.1.4 Screening for thermostability of *CgAM*

Thirty mutated clones (MT-*CgAM*) from each mutated libraries obtained from each MnCl₂ concentration were determined for disproportionation activity in the first step. The crude enzymes from wild-type (WT) and mutants (MT) were determined for disproportionation activity with maltotriose substrate at 40 °C and the activity was detected by glucose oxidase method of which the glucose product develops pink color. The mutants with higher activity than the wild-type (Figure 3.5A) about 17

mutated clones were selected. Then we further screened for thermostability at 40 °C (Figure 3.5B) and 50 °C (Figure 3.5C). After pre-incubation at 50 °C for 30 min, a MT-CgAM clone (number 50-11) obtained from error-prone PCR using 50 µM of MnCl₂ showed highest thermostability, significantly higher than the wild-type which showed no activity. The specific activity of this MT-CgAM was 12.3 U/mg while that of the WT was only 1.84 U/mg.

3.1.5 Nucleotide sequencing

To characterize the mutated *CgAM* gene, the gene was sequenced by using the primers of T7 promotor and T7 terminator which can sequence through the 5'-terminus and 3'-terminus of the inserted *CgAM* gene in plasmid, respectively. The sequence was extended by using primer fCgAM2 and rCgAM2 as described in section 2.6 and searched for overlapping regions. The nucleotide sequence and the deduced amino acid sequence alignment of MT-CgAM gene (clone number 50-11) was compared with the WT-CgAM as shown in Figures 3.6 and 3.7. The result showed that two mutations at nucleotide positions of 1217 and 1425 were changed from C to T and A to G, respectively. However, the amino acid sequence of the MT-CgAM gene from this clone was then determined as only a single point mutation at residue 406 from Ala (A) to Val (V).

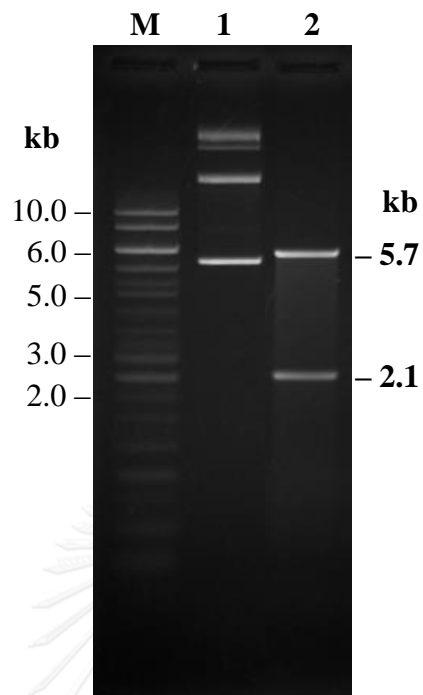


Figure 3. 1 Agarose gel electrophoresis of recombinant plasmid *CgAM*.

The DNA samples were separated on 1% agarose gel and visualized by ethidium bromide staining.

Lane M = GeneRuler™ 1 kb DNA ladder (Fermentas, Canada)

Lane 1 = Recombinant plasmid *CgAM*

Lane 2 = Recombinant plasmid *CgAM* after double digestion with *Nde* I and *Xho* I

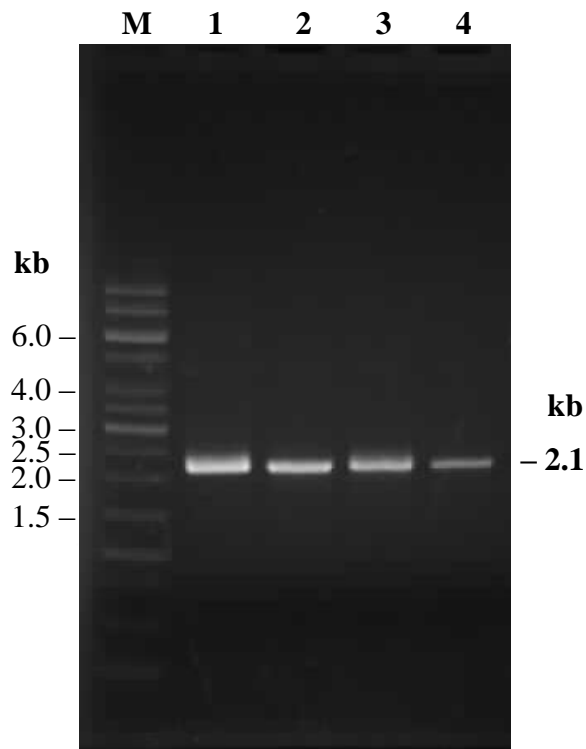


Figure 3. 2 Agarose gel electrophoresis of amplified DNA obtained from error-prone PCR. Various Mn^{2+} concentrations were added into PCR reaction. The DNA samples were separated on 1% agarose gel and visualized by ethidium bromide staining.

Lane M = GeneRuler™ 1 kb DNA ladder (Fermentas, Canada)

Lane 1 = PCR product with the addition of 50 μM $MnCl_2$

Lane 2 = PCR product with the addition of 100 μM $MnCl_2$

Lane 3 = PCR product with the addition of 200 μM $MnCl_2$

Lane 4 = PCR product without $MnCl_2$ addition

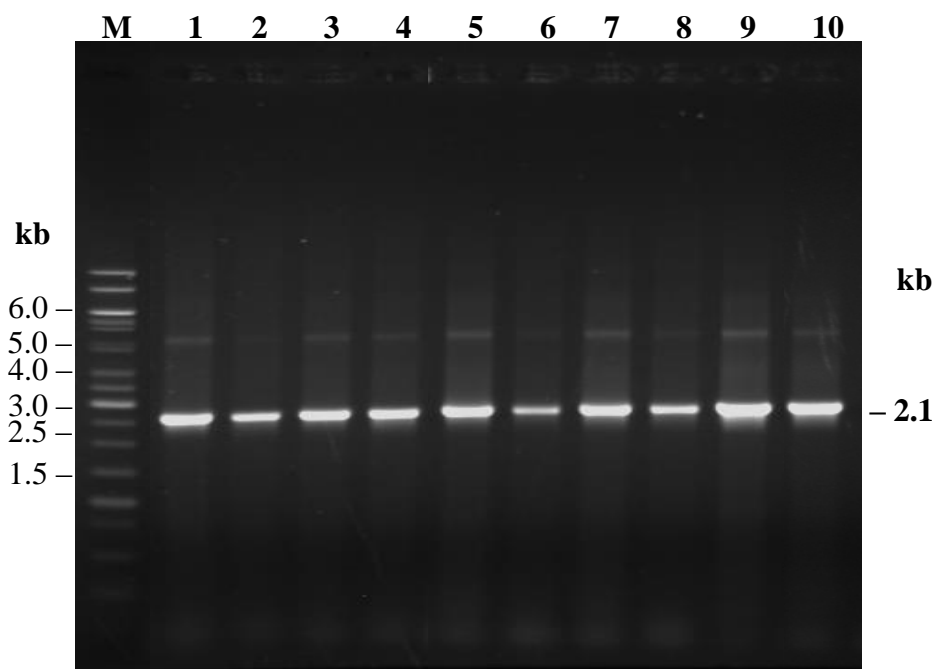


Figure 3. 3 Agarose gel electrophoresis of the product from colony PCR technique. The DNA samples were separated on 1% agarose gel and visualized by ethidium bromide staining.

Lane M = GeneRuler™ 1 kb DNA ladder (Fermentas, Canada)

Lane 1-10 = PCR product from ten mutated clones obtained from error-prone PCR with the addition of 50 μ M MnCl₂

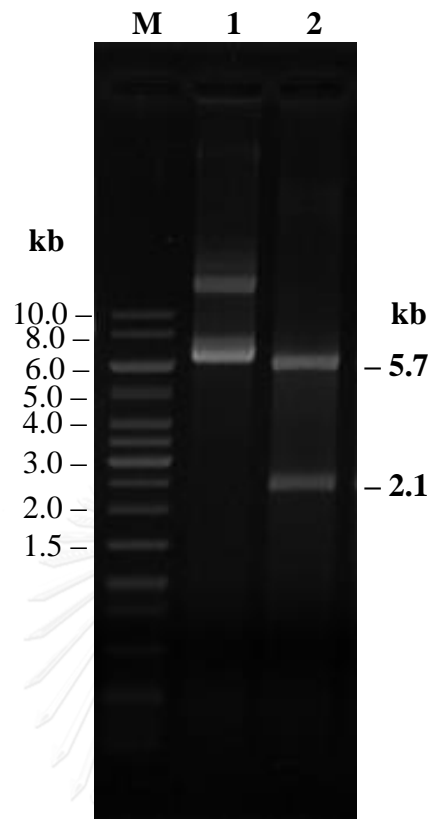


Figure 3. 4 Agarose gel electrophoresis of recombinant *CgAM* gene inserted in pET-19b vector. The DNA samples were separated on 1% agarose gel and visualized by ethidium bromide staining.

Lane M = GeneRuler™ 1 kb DNA ladder (Fermentas, Canada)

Lane 1 = Recombinant plasmid *CgAM* from a mutated clone

Lane 2 = pET-19b vector harboring *CgAM* gene, digested with *Nde* I and *Xho* I

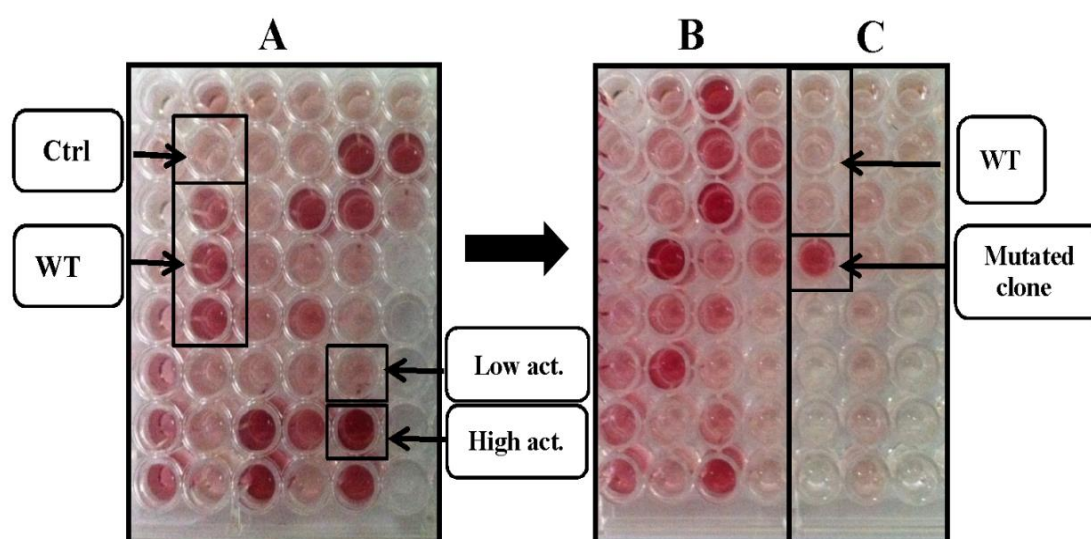


Figure 3. 5 Screening for thermostability of MT-CgAMs obtained from random mutagenesis using error-prone PCR technique. Left panel (A) is the activity of WT- and MT-CgAMs on disproportionation reaction. Then MT- clones with high activity were selected for temperature stability monitoring at 40 °C (B) and 50 °C (C). The experiments were performed as described in section 2.5. Ctrl, control with no enzyme added.

| | | |
|-------------|--|-----|
| WT-CgAM | ATGACTGCTCGCAGATTTTGAATGAACTCGCCGATCTCTACGGCGTAGCAACTTCCTAC | 60 |
| mutant50-11 | ATGACTGCTCGCAGATTTTGAATGAACTCGCCGATCTCTACGGCGTAGCAACTTCCTAC | 60 |
| | ***** | |
| WT-CgAM | ACTGATTACAAAGGTGCCCATATTGAGGTCAGCGATGACACATTAGTGAAAATCCTGCGT | 120 |
| mutant50-11 | ACTGATTACAAAGGTGCCCATATTGAGGTCAGCGATGACACATTAGTGAAAATCCTGCGT | 120 |
| | ***** | |
| WT-CgAM | GCTCTGGGTGTGAATTTAGATACAAGCAACCTCCCAACGATGACGCTATCCAACGCCAA | 180 |
| mutant50-11 | GCTCTGGGTGTGAATTTAGATACAAGCAACCTCCCAACGATGACGCTATCCAACGCCAA | 180 |
| | ***** | |
| WT-CgAM | ATTGCCCTCTTCCATGATCGAGAGTTCACTCGCCACTGCCTCCATCGGTGGTTCAGTT | 240 |
| mutant50-11 | ATTGCCCTCTTCCATGATCGAGAGTTCACTCGCCACTGCCTCCATCGGTGGTTCAGTT | 240 |
| | ***** | |
| WT-CgAM | GAAGGTGATGAACTAGTTTTCCCGGTGCATGTGCACGACGGTTCCTGCAGATGTCCAC | 300 |
| mutant50-11 | GAAGGTGATGAACTAGTTTTCCCGGTGCATGTGCACGACGGTTCCTGCAGATGTCCAC | 300 |
| | ***** | |
| WT-CgAM | ATCGAATTGGAAGACGGCAGCGCGGATGTTTCTCAGGTGGAAAACGGACAGCGCCA | 360 |
| mutant50-11 | ATCGAATTGGAAGACGGCAGCGCGGATGTTTCTCAGGTGGAAAACGGACAGCGCCA | 360 |
| | ***** | |
| WT-CgAM | CGGGAATTGATGGGATTAGGTGGGGCAGGCATCGTTTAAGATTCTGGTGATCTCCCC | 420 |
| mutant50-11 | CGGGAATTGATGGGATTAGGTGGGGCAGGCATCGTTTAAGATTCTGGTGATCTCCCC | 420 |
| | ***** | |
| WT-CgAM | TTGGGTTGGCACAAGCTTCACCTTAAATCCAATGAACGCTCAGCTGAGTGGGTTTGATC | 480 |
| mutant50-11 | TTGGGTTGGCACAAGCTTCACCTTAAATCCAATGAACGCTCAGCTGAGTGGGTTTGATC | 480 |
| | ***** | |
| WT-CgAM | ATCACCCCGGCTCGTCTGTCTACTGCTGATAAGTATCTTGATTCCCCTCGCAGTGGTGTC | 540 |
| mutant50-11 | ATCACCCCGGCTCGTCTGTCTACTGCTGATAAGTATCTTGATTCCCCTCGCAGTGGTGTC | 540 |
| | ***** | |
| WT-CgAM | ATGGCGCAGATCTACTCTGTGCGTTCCACGTTGTCGTGGGCATGGGTGATTTCAATGAT | 600 |
| mutant50-11 | ATGGCGCAGATCTACTCTGTGCGTTCCACGTTGTCGTGGGCATGGGTGATTTCAATGAT | 600 |
| | ***** | |
| WT-CgAM | TTAGGAACTTGGCAAGTGTGGTTGCCAGGATGGAGCAGACTTCCTGCTCATCAACCCC | 660 |
| mutant50-11 | TTAGGAACTTGGCAAGTGTGGTTGCCAGGATGGAGCAGACTTCCTGCTCATCAACCCC | 660 |
| | ***** | |
| WT-CgAM | ATGCACGCTGCAGAGCCGCTGCCTCCTACTGAGGACTCTCCTTATCTGCCACAACCAGG | 720 |
| mutant50-11 | ATGCACGCTGCAGAGCCGCTGCCTCCTACTGAGGACTCTCCTTATCTGCCACAACCAGG | 720 |
| | ***** | |
| WT-CgAM | CGCTTTATCAACCCGATCTACATTCGGGTAGAAGATATCCGGAGTTTAATCAGCTTGAG | 780 |
| mutant50-11 | CGCTTTATCAACCCGATCTACATTCGGGTAGAAGATATCCGGAGTTTAATCAGCTTGAG | 780 |
| | ***** | |

Figure 3. 6 Nucleotide sequence of MT-CgAM (clone number 50-11) compared with that of the WT-CgAM using Clustal X (1.81) multiple sequence alignment.

```

WT-CgAM      ATTGATCTACGCGATGATATCGCAGAGATGGCTGCGGAATTCGCGAACGCAATCTGACC 840
mutant50-11 ATTGATCTACGCGATGATATCGCAGAGATGGCTGCGGAATTCGCGAACGCAATCTGACC 840
*****

WT-CgAM      TCAGACATCATTGAGCGCAATGACGCTCTACGCTGCAAAGCTTCAAGTGTGCGCGCCATT 900
mutant50-11 TCAGACATCATTGAGCGCAATGACGCTCTACGCTGCAAAGCTTCAAGTGTGCGCGCCATT 900
*****

WT-CgAM      TTTGAAATGCCTCGTTCCAGCGAACGTGAAGCCAACCTTGTCTCCTTCGTGCAACGGGAA 960
mutant50-11 TTTGAAATGCCTCGTTCCAGCGAACGTGAAGCCAACCTTGTCTCCTTCGTGCAACGGGAA 960
*****

WT-CgAM      GGCCAAGGTCTTATTGATTTGCGCACCTGGTGCGCGGACCGCGAAACTGCACAGTCTGAA 1020
mutant50-11 GGCCAAGGTCTTATTGATTTGCGCACCTGGTGCGCGGACCGCGAAACTGCACAGTCTGAA 1020
*****

WT-CgAM      TCTGTCCACGGAAGTCTGAGCCAGACCGCGATGAGCTGACCATGTTCTACATGTGGTTGCAG 1080
mutant50-11 TCTGTCCACGGAAGTCTGAGCCAGACCGCGATGAGCTGACCATGTTCTACATGTGGTTGCAG 1080
*****

WT-CgAM      TGGCTATGTGATGAGCAGCTGGCGGCAGCTCAAAGCGCGCTGTCGATGCCGGAATGTGCG 1140
mutant50-11 TGGCTATGTGATGAGCAGCTGGCGGCAGCTCAAAGCGCGCTGTCGATGCCGGAATGTGCG 1140
*****

WT-CgAM      ATCGGCATCATGGCAGACCTGGCAGTTGGTGTGCATCCAGGTGGTGTGATGCCCAGAAC 1200
mutant50-11 ATCGGCATCATGGCAGACCTGGCAGTTGGTGTGCATCCAGGTGGTGTGATGCCCAGAAC 1200
*****

WT-CgAM      CTCAGCCACGTAAGTCTGCTGCGTCAAGTGGGCGCCCCACCAGATGGATAACAACCAG 1260
mutant50-11 CTCAGCCACGTAAGTCTGCTGCGTCAAGTGGGCGCCCCACCAGATGGATAACAACCAG 1260
*****

WT-CgAM      CAGGGCCAAGACTGGTCCCAGCCACCATGGCATCCAGTGCCTCTTGCAGAGGAAGGCTAC 1320
mutant50-11 CAGGGCCAAGACTGGTCCCAGCCACCATGGCATCCAGTGCCTCTTGCAGAGGAAGGCTAC 1320
*****

WT-CgAM      ATTCGGTGGCGTAATCTGCTGCGCACTGTGCTGCGTCACTCCGCGGAATCCGCGTGGAC 1380
mutant50-11 ATTCGGTGGCGTAATCTGCTGCGCACTGTGCTGCGTCACTCCGCGGAATCCGCGTGGAC 1380
*****

WT-CgAM      CACGTTCTTGGTTTGTTCAGGCTCTTTGTCATGCCACGCATGCAATCCCTGCTACGGGC 1440
mutant50-11 CACGTTCTTGGTTTGTTCAGGCTCTTTGTCATGCCACGCATGCAATCCCTGCTACGGGC 1440
*****

WT-CgAM      ACCTATATCCGCTTCGACCATAATGCGTTGGTAGGCATTCTAGCCCTAGAAGCAGAATC 1500
mutant50-11 ACCTATATCCGCTTCGACCATAATGCGTTGGTAGGCATTCTAGCCCTAGAAGCAGAATC 1500
*****

```

Figure 3.6 (continued) Nucleotide sequence of *MT-CgAM* (clone number 50-11) compared with that of the *WT-CgAM* using Clustal X (1.81) multiple sequence alignment.

```

WT-CgAM          GCAGGCGCCGTTGTTCATTGGTGAAGATCTGGGAACGTTTGAGCCTTGGGTACAAGATGCA 1560
mutant50-11     GCAGGCGCCGTTGTTCATTGGTGAAGATCTGGGAACGTTTGAGCCTTGGGTACAAGATGCA 1560
*****

WT-CgAM          TTGGCTCAGCGTGGCATCATGGGCACCTCGATCCTATGGTTCGAGCATCCCCAAGCCAG 1620
mutant50-11     TTGGCTCAGCGTGGCATCATGGGCACCTCGATCCTATGGTTCGAGCATCCCCAAGCCAG 1620
*****

WT-CgAM          CCGGGTCCTCGCCGCCAGGAAGAGTATCGTCCGCTGGCCTTGACCACTGTGACCACTCAT 1680
mutant50-11     CCGGGTCCTCGCCGCCAGGAAGAGTATCGTCCGCTGGCCTTGACCACTGTGACCACTCAT 1680
*****

WT-CgAM          GATCTCCCTCCGACTGCTGGTTATTTGGAGGGCGAGCACATTGCTCTTCGTGAGCGATTG 1740
mutant50-11     GATCTCCCTCCGACTGCTGGTTATTTGGAGGGCGAGCACATTGCTCTTCGTGAGCGATTG 1740
*****

WT-CgAM          GGGGTGCTCAACACTGATCCTGCTGCAGAACTCGCTGAGGATCTGCAGTGGCAAGCGGAG 1800
mutant50-11     GGGGTGCTCAACACTGATCCTGCTGCAGAACTCGCTGAGGATCTGCAGTGGCAAGCGGAG 1800
*****

WT-CgAM          ATCCTTGATGTGCGAGCATCTGCCAACGCATTGCCAGCCCGGAATACGTGGGACTCGAA 1860
mutant50-11     ATCCTTGATGTGCGAGCATCTGCCAACGCATTGCCAGCCCGGAATACGTGGGACTCGAA 1860
*****

WT-CgAM          CGCGATCAGCGCGGTGAGTTGGCTGAGCTGTTGGAAGGCCTGCACACTTTCGTTGCGAAA 1920
mutant50-11     CGCGATCAGCGCGGTGAGTTGGCTGAGCTGTTGGAAGGCCTGCACACTTTCGTTGCGAAA 1920
*****

WT-CgAM          ACCCCTCAGCACTGACCTGTGTCTGCTTGGTAGACATGGTCGGTGAAAAGCGGGCACAG 1980
mutant50-11     ACCCCTCAGCACTGACCTGTGTCTGCTTGGTAGACATGGTCGGTGAAAAGCGGGCACAG 1980
*****


WT-CgAM          AATCAGCCGGGCACAACGAGGGATATGTATCCCAACTGGTGTATCCCACTGTGTGACAGC 2040
mutant50-11     AATCAGCCGGGCACAACGAGGGATATGTATCCCAACTGGTGTATCCCACTGTGTGACAGC 2040
*****

WT-CgAM          GAAGGCAACTCCGTGCTCATTGAATCGCTGCGTGAAAATGAGCTGTATCACCGTGTGGCA 2100
mutant50-11     GAAGGCAACTCCGTGCTCATTGAATCGCTGCGTGAAAATGAGCTGTATCACCGTGTGGCA 2100
*****

WT-CgAM          AAGGCAAGCAAGCGAGATTAG 2121
mutant50-11     AAGGCAAGCAAGCGAGATTAG 2121
*****

```

Figure 3.6 (continued) Nucleotide sequence of *MT-CgAM* (clone number 50-11) compared with that of the *WT-CgAM* using Clustal X (1.81) multiple sequence alignment.



```

WT-CgAM          MTARRFLNELADLYGVATSYTDYKGAHIEVSDDTLVKILRALGVNLDTSNLPNDDAIQRQ 60
mutant50-11      MTARRFLNELADLYGVATSYTDYKGAHIEVSDDTLVKILRALGVNLDTSNLPNDDAIQRQ 60
*****

WT-CgAM          IALFHDREFTRPLPPSVVAVEGDELVFPVHVDGSPADVHIELEDGTQRDVSQVENWTAP 120
mutant50-11      IALFHDREFTRPLPPSVVAVEGDELVFPVHVDGSPADVHIELEDGTQRDVSQVENWTAP 120
*****

WT-CgAM          REIDGIRWGEASFKIPGDPLGWHLHLKSNERSAECGLIITPARLSTADKYLDSPRSGV 180
mutant50-11      REIDGIRWGEASFKIPGDPLGWHLHLKSNERSAECGLIITPARLSTADKYLDSPRSGV 180
*****

WT-CgAM          MAQIYSVRSTLSWGMGDFNDLGNLASVVAQDGADFLINPMHAAEPLPPTEDSPYLPTR 240
mutant50-11      MAQIYSVRSTLSWGMGDFNDLGNLASVVAQDGADFLINPMHAAEPLPPTEDSPYLPTR 240
*****

WT-CgAM          RFINPIYIRVEDIPEFNQLEIDLRRDIAEMAAEFRRNLTSDIERNVYAAKLQVLRAI 300
mutant50-11      RFINPIYIRVEDIPEFNQLEIDLRRDIAEMAAEFRRNLTSDIERNVYAAKLQVLRAI 300
*****

WT-CgAM          FEMPRSSEEREANFVSFVQREGQGLIDFATWCADRETAQSESVHGTEPDRDELTMFYMWLQ 360
mutant50-11      FEMPRSSEEREANFVSFVQREGQGLIDFATWCADRETAQSESVHGTEPDRDELTMFYMWLQ 360
*****

WT-CgAM          WLCDEQLAAAQKRAVDAGMSIGIMADLAVGVHPPGADAQNLSHVLIPDASVGAPPDGYNQ 420
mutant50-11      WLCDEQLAAAQKRAVDAGMSIGIMADLAVGVHPPGADAQNLSHVLIPDASVGAPPDGYNQ 420
*****

WT-CgAM          QGQDWSQPPWHPVRLAEEGYIPWRNLLRTVLRHSGGIRVDHVLGLFRLFVMPRMSPATG 480
mutant50-11      QGQDWSQPPWHPVRLAEEGYIPWRNLLRTVLRHSGGIRVDHVLGLFRLFVMPRMSPATG 480
*****
                                     D460
                                     [ ]
                                     [ ]
                                     [ ]
                                     [ ]

WT-CgAM          TYIRFDHNALVGILALEAELAGAVVIGEIDLGTFFPWQDALAQRGIMGTSILWFEHSPSQ 540
mutant50-11      TYIRFDHNALVGILALEAELAGAVVIGEIDLGTFFPWQDALAQRGIMGTSILWFEHSPSQ 540
*****
                                     E508
                                     [ ]
                                     [ ]
                                     [ ]
                                     [ ]

WT-CgAM          PGP RRQE EYRPLALT TVTTHDL PPTAGYLEGEHIALRERLGV LNTDPA AE LAEDLQWQAE 600
mutant50-11      PGP RRQE EYRPLALT TVTTHDL PPTAGYLEGEHIALRERLGV LNTDPA AE LAEDLQWQAE 600
*****
                                     D561
                                     [ ]
                                     [ ]
                                     [ ]
                                     [ ]

WT-CgAM          ILDVAASANALPAREYVGLERDQRGELAEELLEGLHTFVAKTPSALTCVCLVDMVGEKRAQ 660
mutant50-11      ILDVAASANALPAREYVGLERDQRGELAEELLEGLHTFVAKTPSALTCVCLVDMVGEKRAQ 660
*****

WT-CgAM          NQPGTTRDMYPNWCIPLCDSEGNSVLIESLRENELYHRVAKASKRD 706
mutant50-11      NQPGTTRDMYPNWCIPLCDSEGNSVLIESLRENELYHRVAKASKRD 706
*****

```

Figure 3. 7 The deduced amino acid sequence of MT-CgAM (from clone number 50-11) compared with that of the WT-CgAM using Clustal Omega O (1.2.1) multiple sequence alignment. Catalytic residues are shown in the boxes.

3.2 Site directed mutagenesis at A406V and A406L-CgAM

To confirm this mutation and further investigate the effect of hydrophobic substitution at this position on thermostability of CgAM, site-directed mutagenesis as described in section 2.7 was performed whereby A406 was replaced by Val as well as Leu (L). To confirm the mutated AM constructed, the nucleotide sequence was investigated. The result indicated that the mutated position had GTT (Val) and CTG (Leu) instead of GCT (Ala) thus confirmed that both mutations were correct. The mutated A406V and A406L-CgAMs were used for further experiments.

3.3 The expression of recombinant wild-type WT- and MT-CgAMs

The *E. coli* BL21 (DE3) containing recombinant plasmid *CgAM* was cultivated in LB broth containing 100 µg/ml of ampicillin antibiotic. The enzyme production was induced with 0.4 mM IPTG for 0, 1, 2, 3, 4, 5 and 6 h. The growth rate was followed by A_{600} . The cells were harvested and disproportionation activity in crude extract was assayed as described in section 2.10.3. When recombinant clone was cultured without IPTG induction, the expression of amylomaltase gene was rather low and activity was undetectable. The highest expression of the WT-, A406V- and A406L-CgAMs were obtained after induction with 0.4 mM IPTG for 4, 2 and 4 h. (Figures 3.8, 3.10 and 3.12), respectively. The specific activity of the crude enzyme from A406V-CgAM was 2-fold higher than that of the WT-CgAM. This condition was thus chosen for enzyme induction in further experiments.

3.4 Protein pattern of crude amyloamylase

The 1.5 ml of cell suspension was taken from recombinant clone *CgAMs* grown at 0.4 mM IPTG at various times as described in 2.9 and then harvested by centrifugation. The cell pellets were resuspended in 150 μ l of extraction buffer, then sonicated and centrifuged to get crude supernatant. The 8 μ g protein of crude enzymes from WT-, A406V- and A406L-*CgAMs* were subjected to electrophoresis on 7.5% SDS-polyacrylamide gel. The results in Figures 3.9, 3.11 and 3.13 showed intensity of the major protein band of cells at each induction time at around 84 kDa was quite corresponded to the expected size of amyloamylase from *C. glutamicum*.



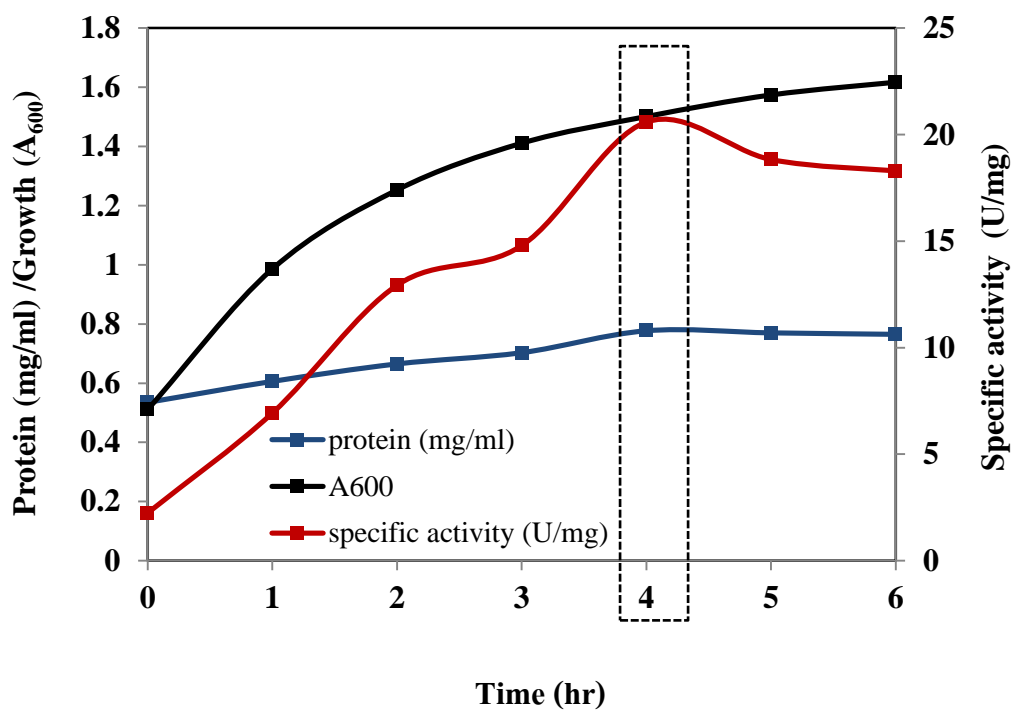


Figure 3. 8 Expression of recombinant WT-CgAM in *E. coli* BL21 (DE3) at 0.4 mM IPTG. The activity of CgAM was determined by disproportionation assay.

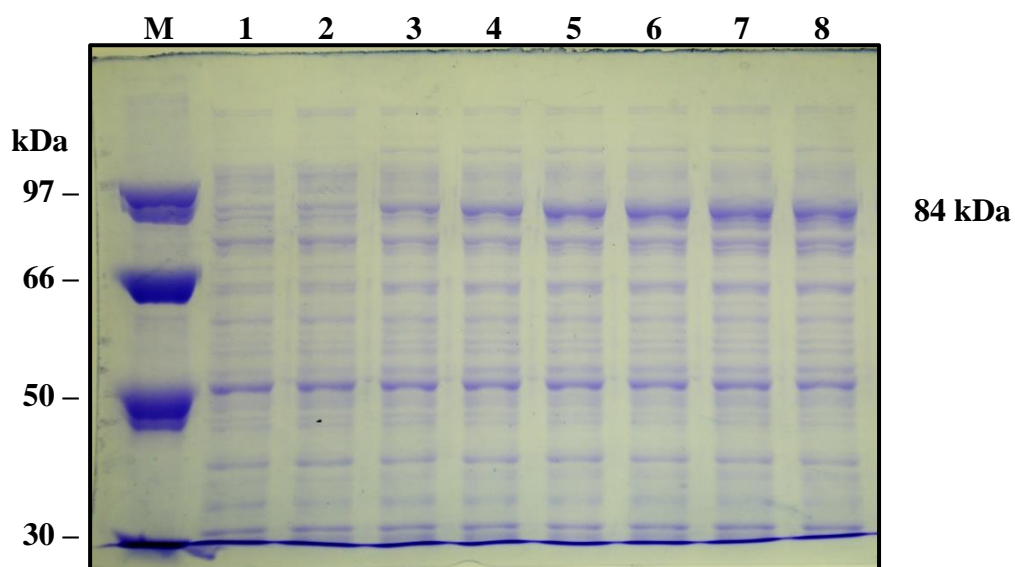


Figure 3. 9 SDS-PAGE of crude enzyme from WT-*CgAM* induced by 0.4 mM IPTG at various times.

Lane M = Low molecular weight protein marker

Lane 1 = crude enzyme from pET-19b vector without *CgAM* gene after induced by 0.4 mM IPTG for 2 h.

Lane 2-8 = crude enzyme from WT-*CgAM* at various induction times: 0, 1, 2, 3, 4, 5 and 6 h, respectively

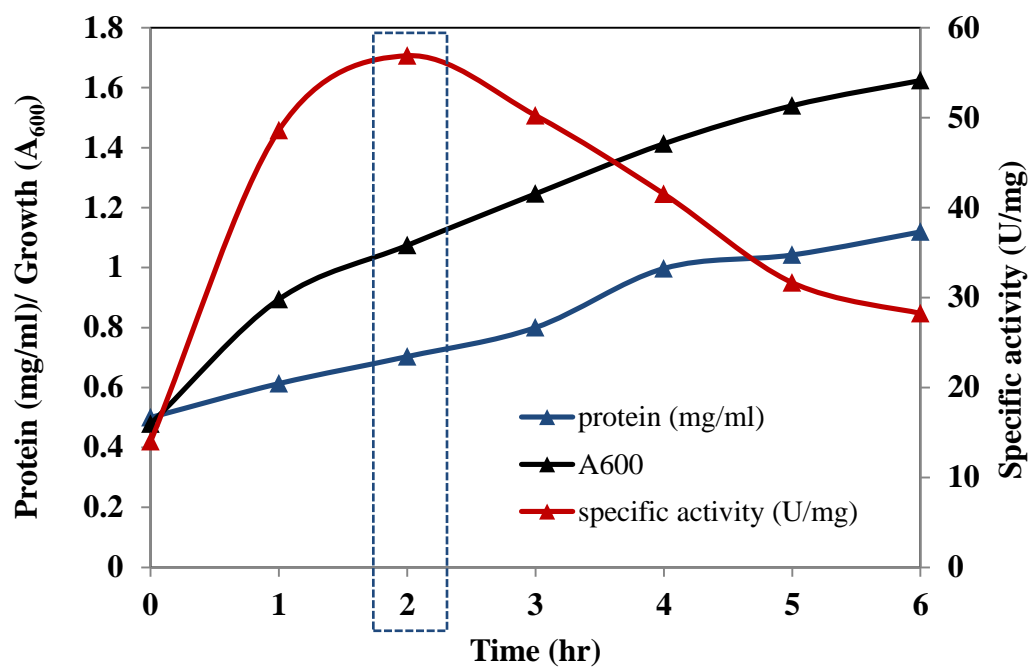


Figure 3. 10 Expression of recombinant A406V-CgAM in *E. coli* BL21 (DE3) at 0.4 mM IPTG. The activity of CgAM was determined by disproportionation assay.

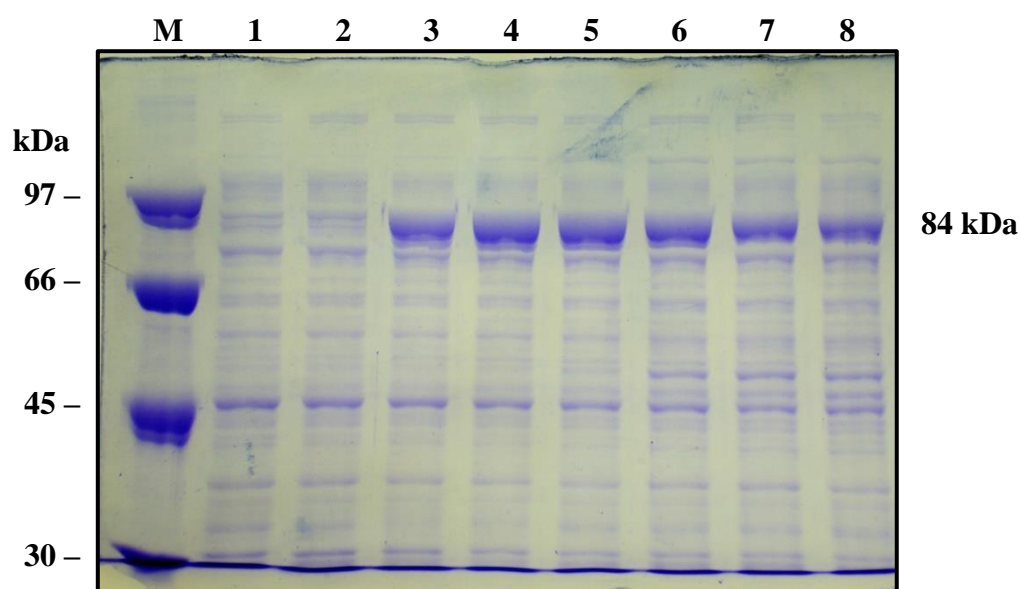


Figure 3. 11 SDS-PAGE of crude enzyme from A406V-CgAM induced by 0.4 mM IPTG at various times.

Lane M = Low molecular weight protein marker

Lane 1 = crude enzyme from pET-19b vector without *CgAM* gene after induced by 0.4 mM IPTG for 2 h.

Lane 2-8 = crude enzyme from A406V-CgAM at various induction times: 0, 1, 2, 3, 4, 5 and 6 h, respectively

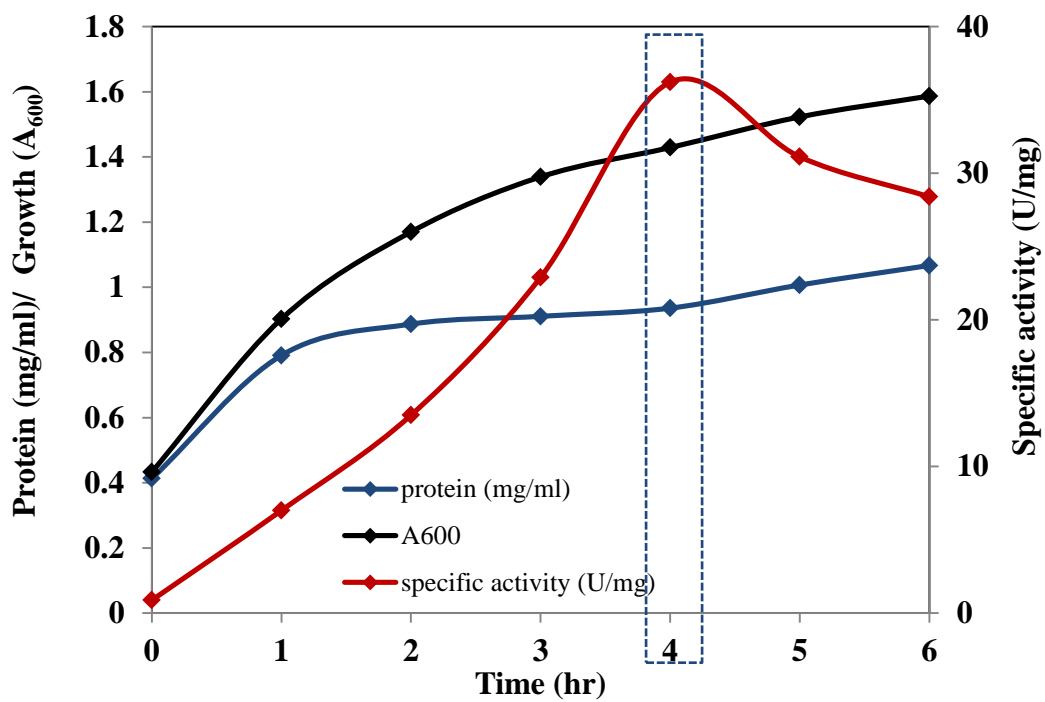


Figure 3. 12 Expression of recombinant A406L-CgAM in *E. coli* BL21 (DE3) at 0.4 mM IPTG. The activity of CgAM was determined by disproportionation assay.

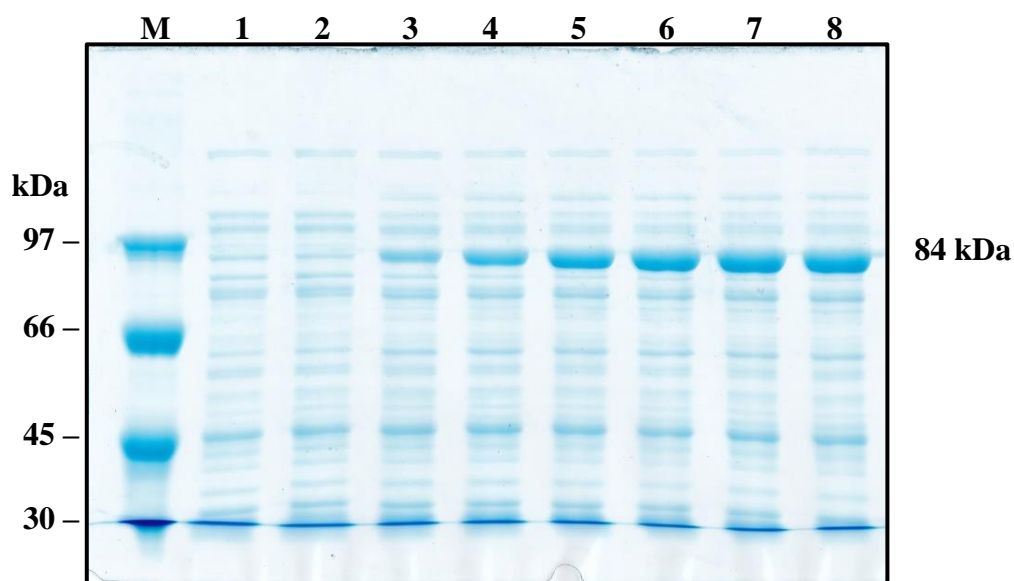


Figure 3. 13 SDS-PAGE of crude enzyme from A406L-CgAM induced by 0.4 mM IPTG at various times.

Lane M = Low molecular weight protein marker

Lane 1 = crude enzyme from pET-19b vector without *CgAM* gene after induced by 0.4 mM IPTG for 2 h.

Lane 2-8 = crude enzyme from A406L-CgAM at various induction times: 0, 1, 2, 3, 4, 5 and 6 h, respectively

3.5 Purification of WT- and MT-CgAMs

3.5.1 Preparation of crude AMs

In the preparation of crude WT-, A406V- and A406L-CgAMs, 5.8, 3.7 and 5.6 g cell pellets of recombinant clones were obtained from 1.2 liters of LB broth medium. Cells were resuspended in extraction buffer (1 g per 2.5 ml), then sonicated and centrifuged to get crude supernatant. Total protein in crude WT-, A406V- and A406L-CgAMs were 362, 376 and 364 mg protein with 15.6, 92.5 and 44.3 Units of disproportionation activity, respectively. Specific disproportionation activity for WT-, A406V- and A406L-CgAMs were 4.30, 24.6 and 12.2 U/mg protein (Table 3.1).

3.5.2 Purification by HisTrap FFTM column

The crude enzyme from recombinant clones was dialyzed against 20 mM phosphate buffer, pH 7.4. The enzyme solution was applied onto a HisTrap FFTM column as described in 2.9.2. The chromatographic profile of WT-CgAM is shown in Figure 3.14. The unbound proteins were washed off the column by the binding buffer as a bulky broad protein peak. Then, the His-tag protein was eluted by elution buffer containing 500 mM imidazole, in a relatively small and narrow protein peak. The fractions that displayed high enzyme activity were pooled and dialyzed against 20 mM phosphate buffer, pH 7.4. The column profiles of A406V- and A406L-CgAMs were similar to that of WT-CgAM. The specific disproportionation activity of the purified WT-, A406V- and A406L-CgAMs were 44.3, 94.5 and 61.0 U/mg protein, respectively (Table 3.1).

3.5.3 Determination of enzyme purity of AMs

All of enzymes from each purification step were examined for protein pattern and purity by SDS-PAGE. The purified WT- and two mutated enzymes showed a single protein band on SDS-PAGE with an apparent molecular mass of 84 kDa (Figure 3.15) indicating the success of purification by only one step of affinity chromatography.



Table 3. 1 Purification of WT-, A406V- and A406L-CgAMs

| Enzyme CgAMs | Purification step | Total protein (mg) | Total activity ^a (U) [10 ²] | Specific activity ^a (U/mg protein) | Yield % | Purification fold |
|-----------------|--------------------------|--------------------------|--|--|------------|----------------------|
| WT | crude extract | 362 | 15.6 | 4.30 | 100 | 1 |
| | HisTrap FF TM | 13.5 | 5.98 | 44.3 | 38.3 | 10.3 |
| A406V | crude extract | 376 | 92.5 | 24.6 | 100 | 1 |
| | HisTrap FF TM | 37.1 | 35.1 | 94.5 | 37.9 | 3.6 |
| A406L | crude extract | 364 | 44.3 | 12.2 | 100 | 1 |
| | HisTrap FF TM | 26.1 | 15.9 | 61.0 | 36.0 | 5.0 |

Crude WT-, A406V- and A406L-CgAMs were prepared from 1.2 liter of cell culture, respectively, which produced 5.8, 3.7 and 5.6 g of wet weight cells.

a = Assayed by disproportionation activity

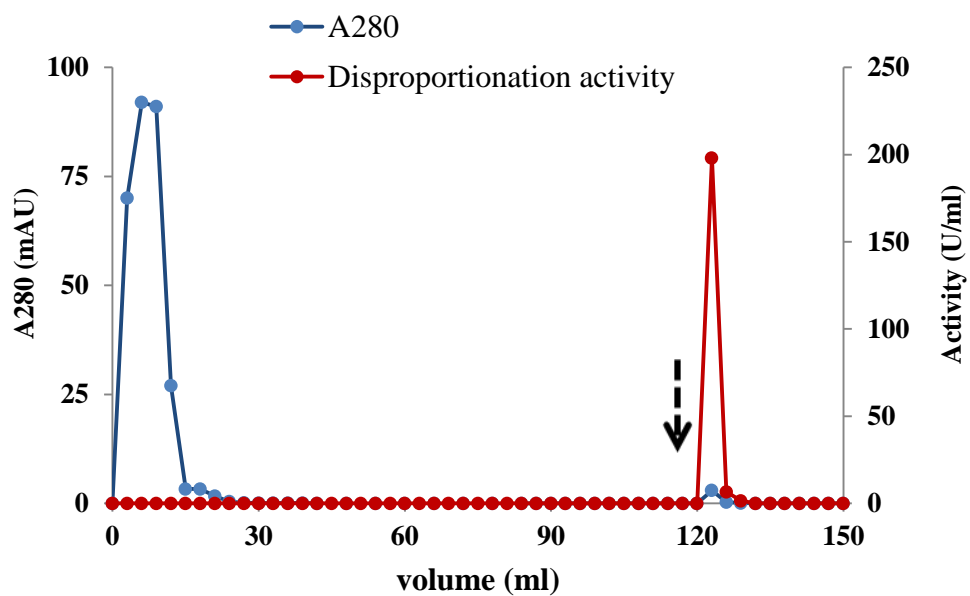


Figure 3. 14 Purification profile of WT-CgAM by HisTrap FFTM column chromatography (1 ml column). Unbound proteins were washed off by binding buffer with 20 mM imidazole, pH 7.4. Elution was by the same buffer containing 500 mM imidazole at a flow rate of 1 ml/min. Fraction size was 3 ml. The arrow indicates the starting point of the elution of bound proteins.

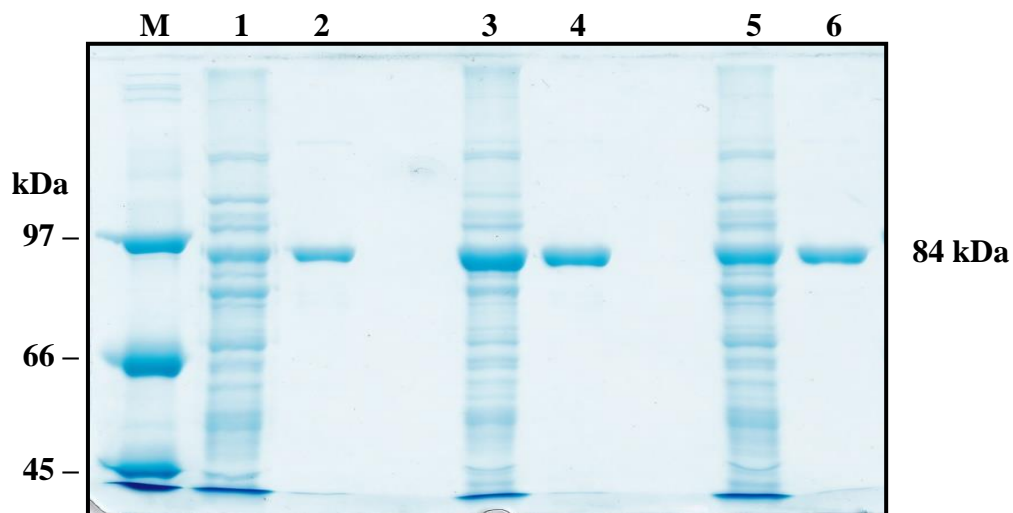


Figure 3. 15 SDS-PAGE of recombinant AMs from each purification step, stained by coomassie blue.

- Lane M = Low molecular weight protein marker
- Lane 1, 3 and 5 = 15 μ g of crude WT, A406V and A406L-CgAMs, respectively
- Lane 2, 4 and 6 = 2 μ g of purified WT, A406V and A406L-CgAMs, respectively

3.6 Effect of mutation on enzyme characteristics

3.6.1 Various activities of amylomaltases

The effect of A406 mutation on various activities of CgAM was investigated. A406V- and A406L-CgAMs showed higher specific activities for starch transglucosylation (2.8 and 2.1-fold) and disproportionation (2.1 and 1.4-fold) than those of the WT, while cyclization, coupling and hydrolysis activities were not different from the WT (Table 3.2). It was observed that coupling and hydrolysis activities were low when compared to the other three activities for both WT- and MT-CgAMs.

3.6.2 Optimum conditions and thermostability

The optimum conditions for two main activities of CgAMs: disproportionation and cyclization, were determined.

3.6.2.1 Effect of temperature

The effect of temperature for disproportionation and cyclization of the three CgAMs were determined. For WT- , A406V- and A406L-CgAMs, the optimum temperature for disproportionation reaction (Figure 3.16A) were 45 °C, 52.5 °C and 50 °C, respectively. The increase of 7.5 °C and 5 °C in optimum temperature was observed for A406V- and A406L-CgAMs, respectively. For cyclization activity, the values were 30 °C, 35 °C and 30 °C for WT- , A406V- and A406L-CgAMs, respectively (Figure 3.17A). Only A406V showed 5 °C higher in optimum cyclization temperature. The upward shift in temperature optimum was obtained by replacing the V and L at position A406.

3.6.2.2 Effect of pH

The optimum pH for disproportionation activity of WT- , A406V- and A406L-CgAMs were pH 6.0, pH 6.5 and pH 6.5, respectively (Figure 3.16B), the slight increase (+ 0.5 pH unit) in optimum pH was observed for A406V- and A406L-CgAMs. In addition, the optimum pH for cyclization activity of WT- , A406V- and A406L-CgAMs was also investigated, the optimum pH were pH 6.0, pH 6.5 and pH 7.0, respectively (Figure 3.17B). A shift of + 0.5 to 1.0 pH unit in optimum pH was observed with A406V- and A406L-CgAMs.

3.6.2.3 Effect of temperature stability

For the effect of mutation on temperature stability for disproportionation reaction, the result showed that thermostability of both MT-CgAMs was significantly higher than that of the WT. At short incubation time for 15 min at 40 °C, the remaining activities of A406V-, A406L- and WT-CgAMs were 68.5%, 60.0% and 39.5%. While for 30 min incubation, the activities remained were 45.6%, 40.2% and 15.2%, respectively. At 35 °C for a longer incubation time of 3 h, the remaining activities of A406V- and A406L-CgAMs were 100% and 84%, while the value for WT was only 45% (Figure 3.18). Substitution of A406 by V led to a higher positive effect on thermostability than substitution by L.

Table 3. 2 Specific activities of WT-, A406V- and A406L-CgAMs ^a

| Activity | Specific activity (U/mg protein) | | |
|---------------------------|----------------------------------|-------------|-------------|
| | WT-CgAM | A406V-CgAM | A406L-CgAM |
| Starch transglucosylation | 39.1 ± 0.64 | 108 ± 1.48 | 80.7 ± 2.33 |
| Disproportionation | 44.3 ± 1.20 | 94.6 ± 0.00 | 60.9 ± 0.42 |
| Cyclization | 0.47 ± 0.01 | 0.50 ± 0.09 | 0.45 ± 0.00 |
| Coupling | 0.03 ± 0.00 | 0.03 ± 0.00 | 0.03 ± 0.00 |
| Hydrolysis | 0.02 ± 0.00 | 0.02 ± 0.00 | 0.02 ± 0.00 |

^aData are mean ± S.D. from three independent repeats.

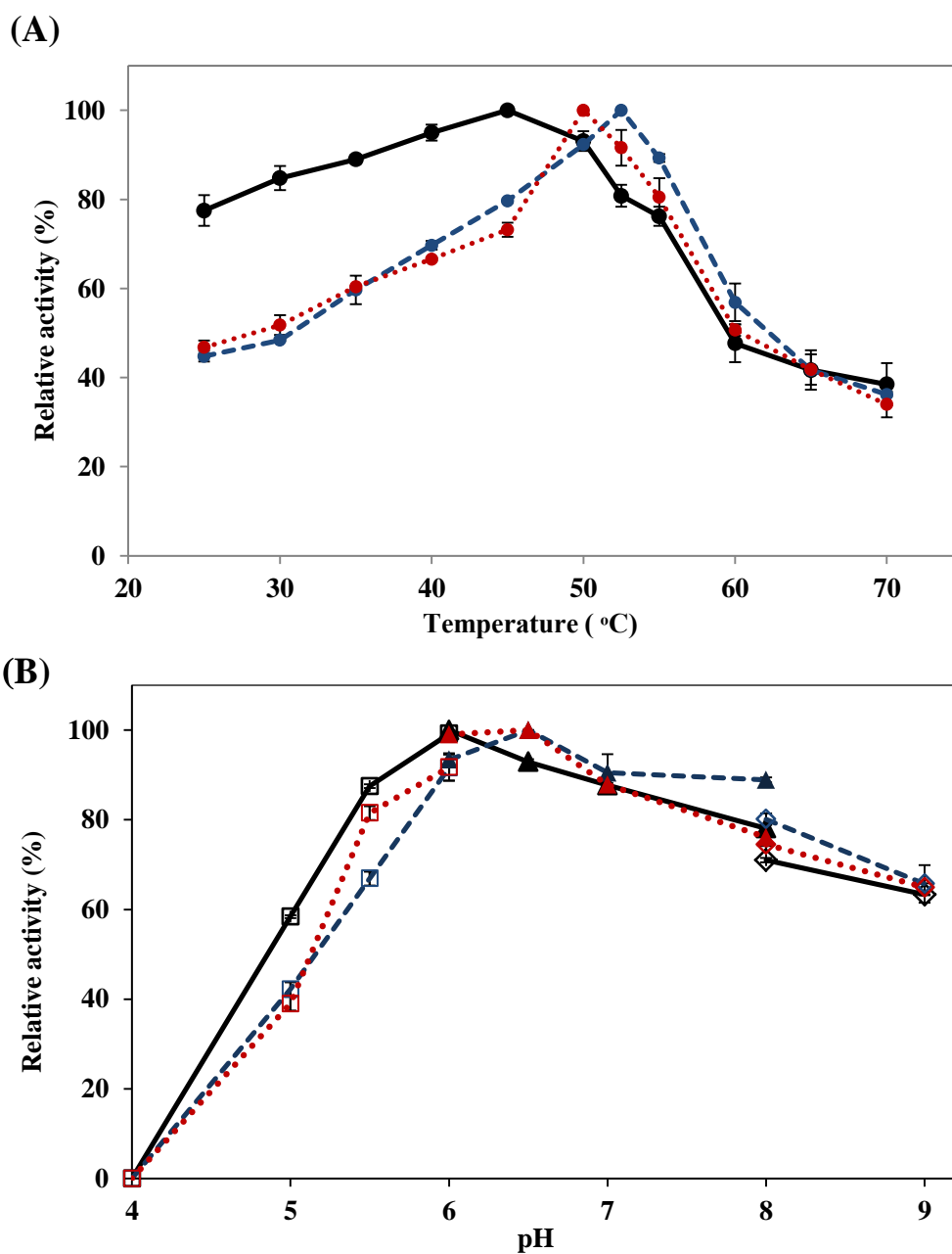


Figure 3.16 Effect of temperature (A) and pH (B) for WT- (solid line), A406V- (dashed line) and A406L- (dotted line) CgAMs on disproportionation reaction. The experiments were performed as described in Section 2.10.3. For effect of pH, the buffers used were: acetate buffer (pH 4.0-6.0; \square), phosphate buffer (pH 6.0-8.0; \blacktriangle) and Tris-HCl buffer (pH 8.0-9.0; \diamond). Data are shown as the mean \pm SD and are derived from three independent repeats.

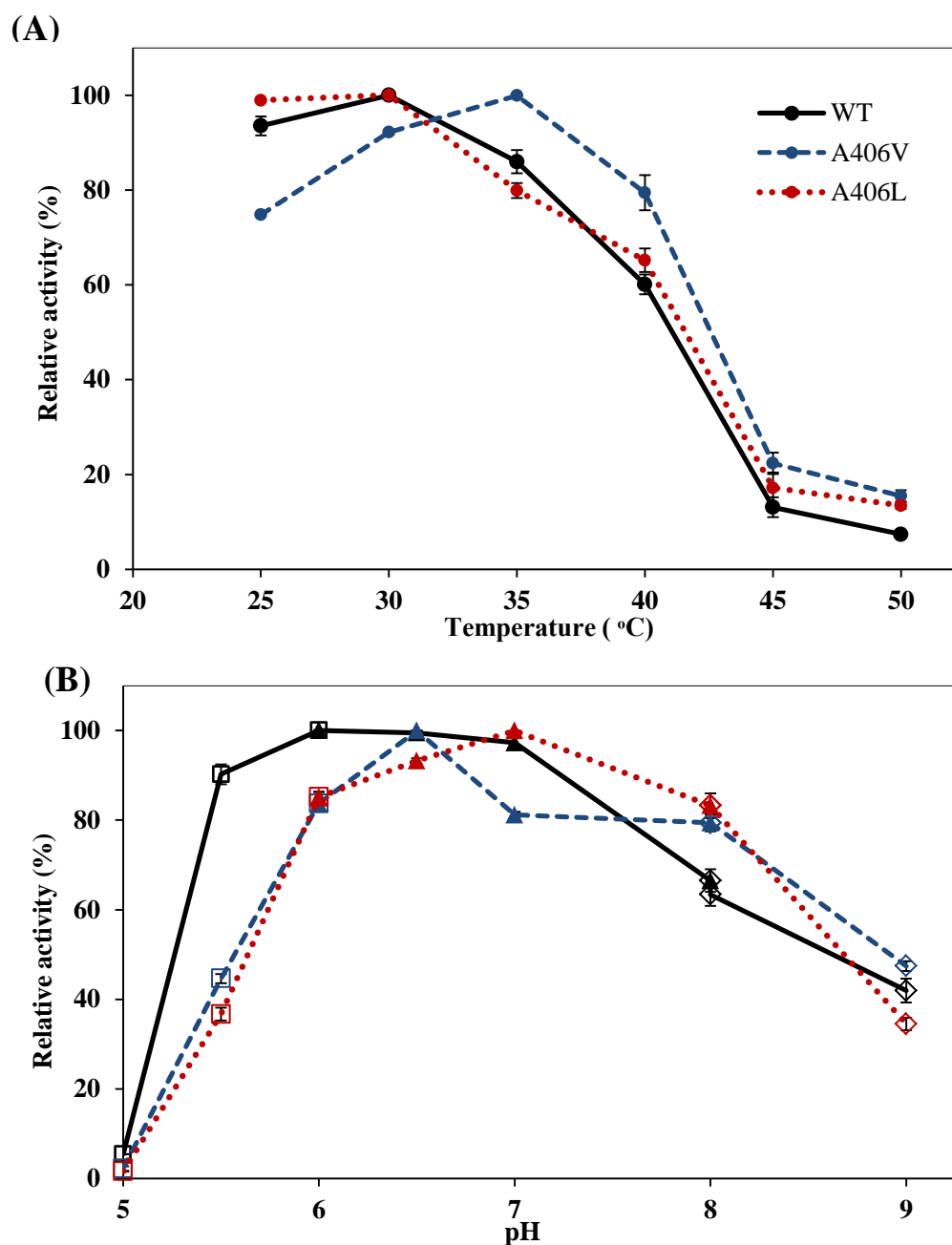


Figure 3. 17 Effect of temperature (A) and pH (B) for WT- (solid line), A406V- (dashed line) and A406L- (dotted line) CgAMs on cyclization reaction. The experiments were performed as described in Section 2.10.4. For effect of pH, the buffers used were: acetate buffer (pH 4.0-6.0; \square), phosphate buffer (pH 6.0-8.0; \blacktriangle) and tris-HCl buffer (pH 8.0-9.0; \diamond). Data are shown as the mean \pm SD and are derived from three independent repeats.

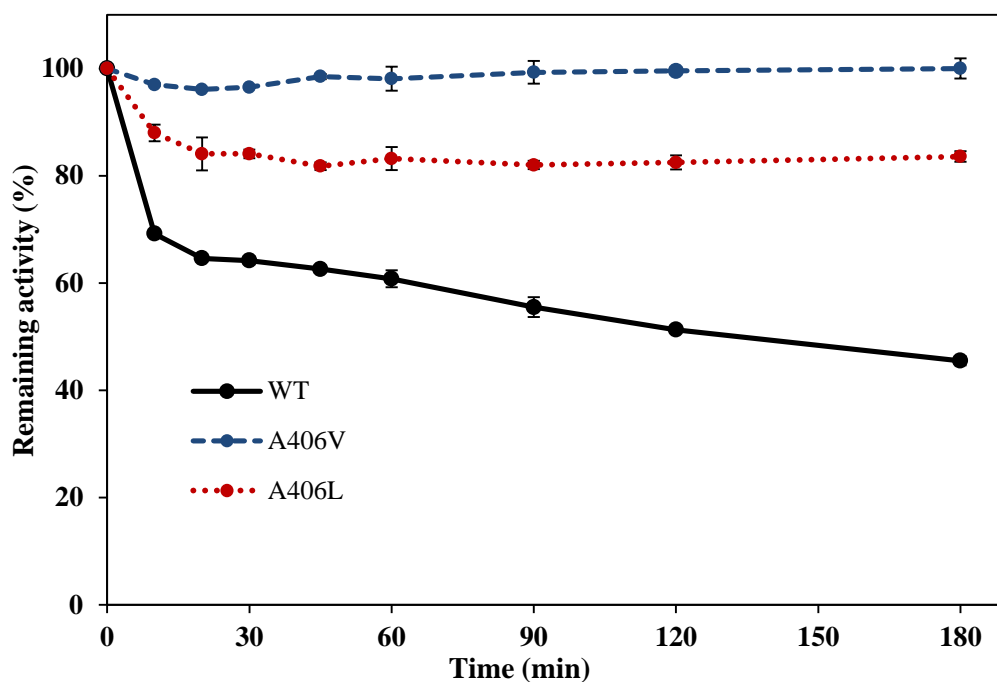


Figure 3. 18 Effect of temperature stability of WT- (solid line), A406V- (dashed line) and A406L- (dotted line) CgAMs on disproportionation reaction. Each CgAM at 15 ug was pre-incubated for various times at 35 °C. Determination of remaining activity was assessed by disproportionation reaction as described in Materials and Methods. Data are shown as the mean \pm SD and are derived from three independent experiments.

3.6.3 Enzyme conformation

To investigate whether A406 mutation results in a conformational change in protein, analysis of secondary structure using circular dichroism technique was performed. The result showed that the CD spectra of both WT- and MT-CgAMs at pH 6.1 were nearly 100% superimposed, the content of α -helix of WT-, A406V- and A406L-CgAMs was 33%, 38% and 35% while the content of β -sheet was 17%, 18% and 18% (Figure 3.19), respectively. The random coil structure of the three AMs was about 44-49%.



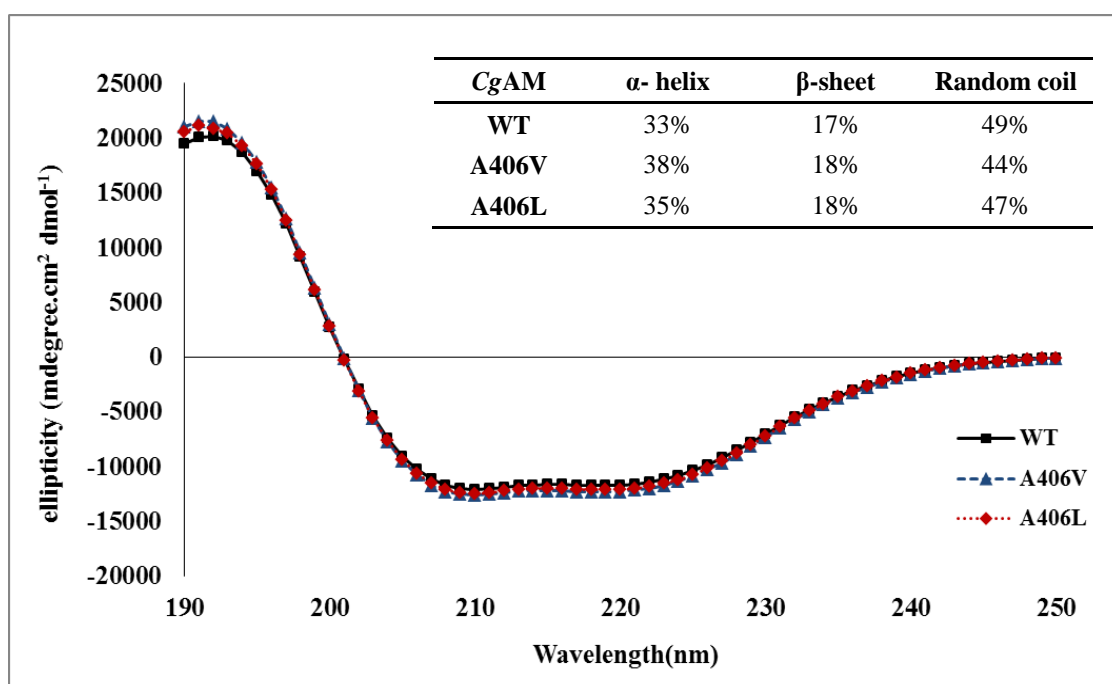
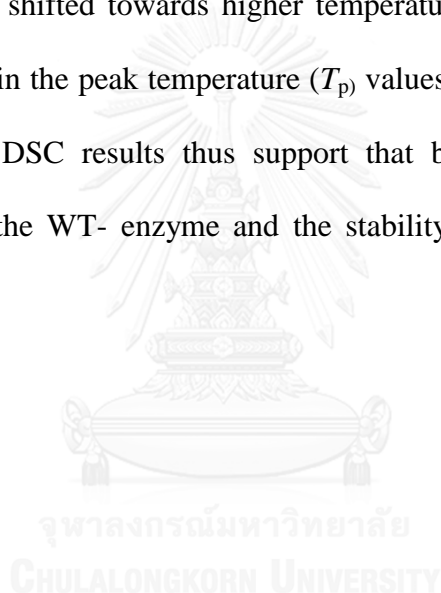


Figure 3. 19 Circular dichroism spectra and the predicted secondary structural compositions of WT (■), A406V- (△) and A406L- (◇) CgAMs

3.6.4 Differential scanning calorimetry

In this work, Differential scanning calorimetry (DSC) was performed in the temperature range of 283 to 373 K in an attempt to compare thermal stability between the WT- and both MT-CgAMs. It was observed that DSC data at all scanning rates for CgAMs indicated the irreversible transition. The thermal transition curves from 285 to 330 K using the scanning rate of 45K/h for the three enzymes at pH 6.1 were plotted (Figure 3.20). It was observed that the heat capacity profiles of the A406V- and A406L-CgAMs were shifted towards higher temperature when compared to that of the WT, the increase in the peak temperature (T_p) values observed were about 1.7 and 1.0 K, respectively. DSC results thus support that both MT-CgAMs had higher thermostability than the WT- enzyme and the stability was more prominent in the A406V.



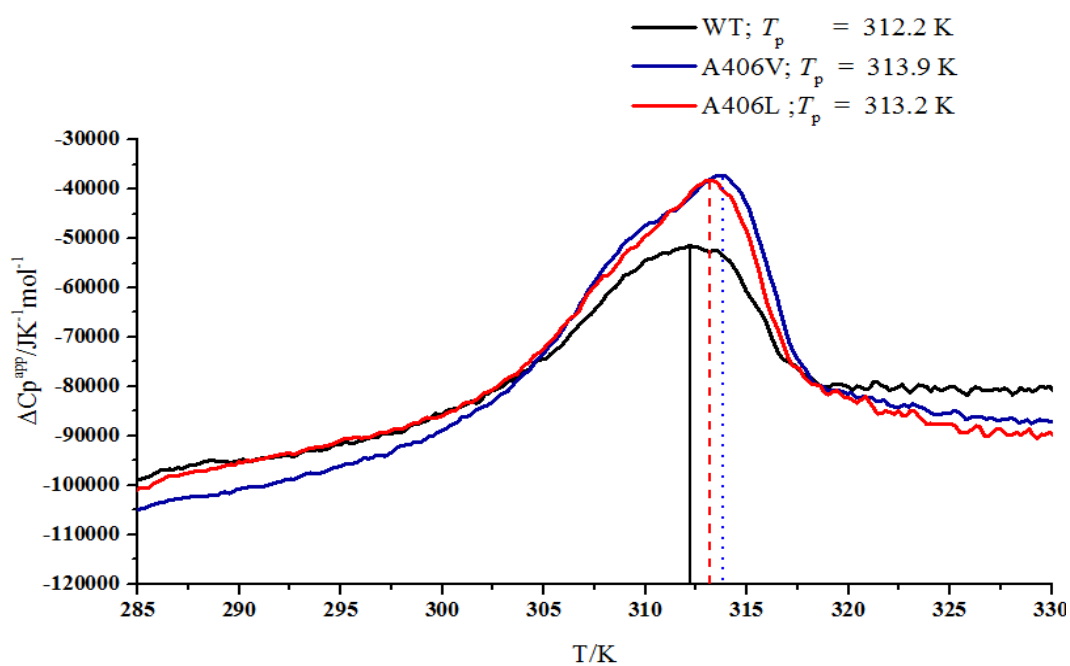


Figure 3. 20 Thermal transition curves of WT- (black line), A406V- (blue line) and A406L- (red line) CgAMs at pH 6.1 with a scan rate of 45 K/h from DSC measurements. T_p = peak temperature

3.6.5 Substrate specificity

The substrate specificity for disproportionation reaction using malto-oligosaccharide substrate (maltose [G2] to maltoheptaose [G7]) was analyzed. Maltotriose (G3) was the most efficient substrate while maltose was poor substrate for both WT- and MT-CgAMs. For WT-CgAM, the substrate specificity was in the order of G3>G4>G5>G6>G7≈G2 while MT-CgAMs showed a preferred substrate order of G3>G4>G5>G6>G7>G2. It was shown that WT-CgAM could use maltose better than MT-CgAMs. In contrast, MT-CgAMs seem to use larger size malto-oligosaccharides (G3-G7) better than the WT (Figure 3.21).

3.6.6 Determination of kinetic parameters

The kinetic analysis of the WT- and both MT-CgAMs for disproportionation reaction on G3 substrate was then performed. Lineweaver-Burk plot using nonlinear least square regression analysis of varying concentrations of maltotriose was shown in Figure 3.22. The result clearly showed that kinetic parameters were affected upon A406 mutation. The catalytic efficiency (k_{cat}/K_m) was 2.9 and 1.4 times increased due to the increase in k_{cat} values (3.3 and 1.3 times) for the A406V- and A406L-CgAMs, respectively (Table 3.3) while their K_m values were similar to that of the WT-CgAM.

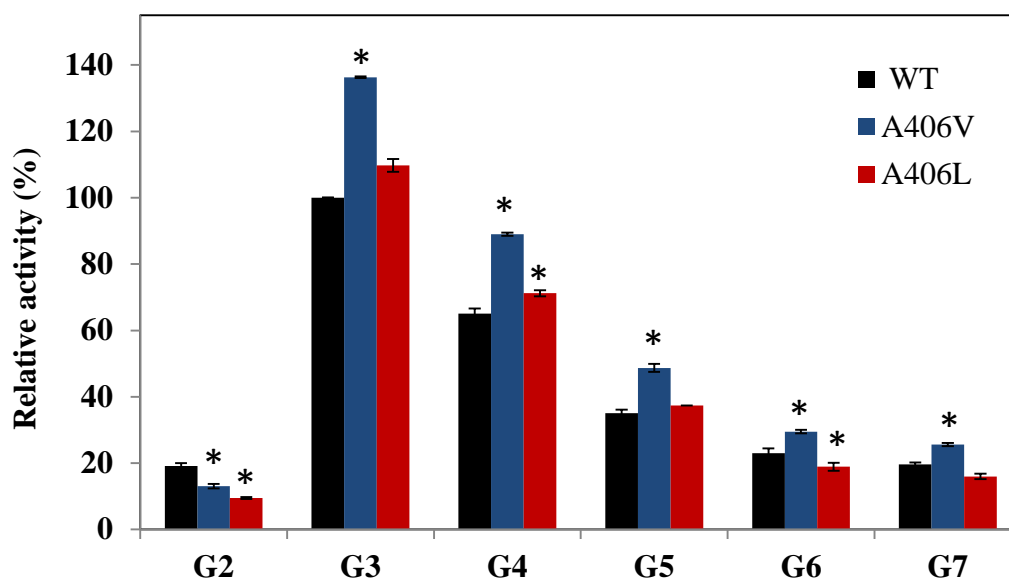


Figure 3. 21 Substrate specificity of WT-, A406V- and A406L-CgAMs in disproportionation reaction using maltooligosaccharide substrate (maltose [G2] to maltoheptaose [G7]). The activity of WT-CgAM on G3 substrate was set as 100%. Data are shown as the mean \pm SD and are derived from three independent experiments. * $P < 0.05$ (Student's *t*-Test) with respect to the disproportionation reaction of WT-CgAM.

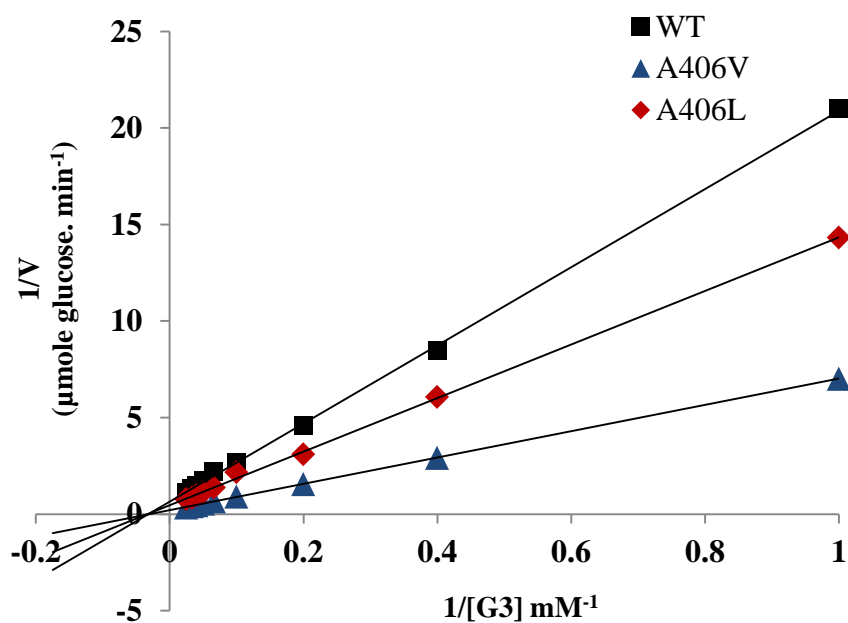


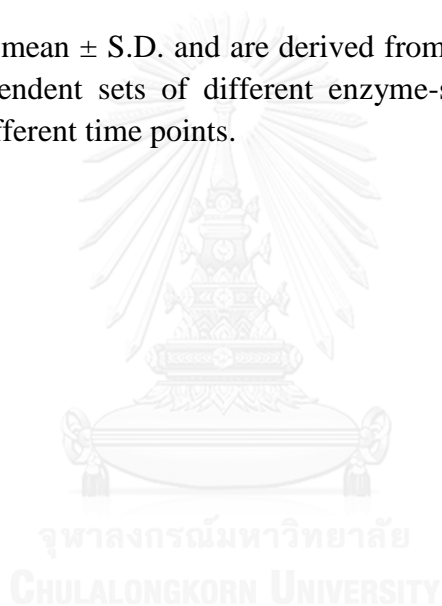
Figure 3. 22 Lineweaver-Burk plot of recombinant WT-, A406V- and A406L-

CgAMs on disproportionation reaction with maltotriose (G3) substrate. All CgAMs were incubated with various concentrations of maltotriose in 50 mM phosphate buffer, pH 6.0 at 45 °C for 5 min. Release of glucose was determined by glucose oxidase assay.

Table 3. 3 Kinetic parameters of WT-, A406V- and A406L-CgAMs derived from the disproportionation reaction using maltotriose as the substrate ^a

| <i>CgAM</i> | <i>K_m</i> (mM) | <i>V_{max}</i> ($\mu\text{mole}\cdot\text{min}^{-1}$) | <i>k_{cat}</i> (min^{-1}) [10^3] | <i>k_{cat}/K_m</i> ($\text{mM}^{-1}\text{min}^{-1}$) [10^3] |
|-------------|------------------------------|--|--|--|
| WT | 31.8 \pm 0.71 | 1.6 \pm 0.04 | 156 \pm 4.25 | 4.9 \pm 0.02 |
| A406V | 35.1 \pm 0.85 | 5.1 \pm 0.12 | 509 \pm 12.0 | 14.5 \pm 0.01 |
| A406L | 26.5 \pm 1.91 | 1.9 \pm 0.08 | 195 \pm 7.78 | 7.1 \pm 0.24 |

^a Data shown are the mean \pm S.D. and are derived from Lineweaver-Burk plot of the result of three independent sets of different enzyme-substrate concentrations with product analysis at different time points.



3.6.7 Synthesis of LR-CDs

3.6.7.1 Effect of pH and temperature on LR-CDs product profiles

To compare the LR-CDs production profile of WT- and both MT-*CgAMs* at different pH and temperature, *CgAMs* (at 0.3 mg protein) were incubated with pea starch substrate as described in section 2.13.1 and LR-CD products were determined by HPAEC-PAD (Figure 3.23). When the product profiles of WT-, A406V- and A406L-*CgAMs* were monitored at various pHs (Figure 3.23A, B and C) a different product pattern was observed, especially at pH 5.5. At pH 5.5, larger size LR-CDs were observed when compared with at other pHs, principal product was CD34 for the WT- and CD38 for both MT-*CgAMs*. The profiles at pH 6.5 and pH 8.0 were relatively similar, the main products were CD30 to CD31 with the rather symmetrical size distribution frequency curve and the higher yield at pH 6.5 for WT- and MT-enzymes. At pH 9.0, a noticeably trace amount of the smaller CDs (CD6-CD17) was observed, with a somewhat broad peak from CD28 to CD38 for all three enzyme forms (Figure 3.23A, B and C). It was also found that A406L gave the lowest product yield.

The pattern of LR-CDs was dependent on the incubation temperature (Figure 3.24A, B and C). LR-CD profiles of the MT-*CgAMs* were different from that of the WT- enzyme. At 30-35 °C, the principal products of the WT- were CD30-CD31 while CD31-CD36 were main products of the two MT-*CgAMs*. At 40-45 °C, a broader peak with a higher level of DPs was obtained, CD30 to CD36 for the WT- and CD31-CD40 for the MT- enzymes. Again, A406L was the enzyme form that gave the lowest product yield.

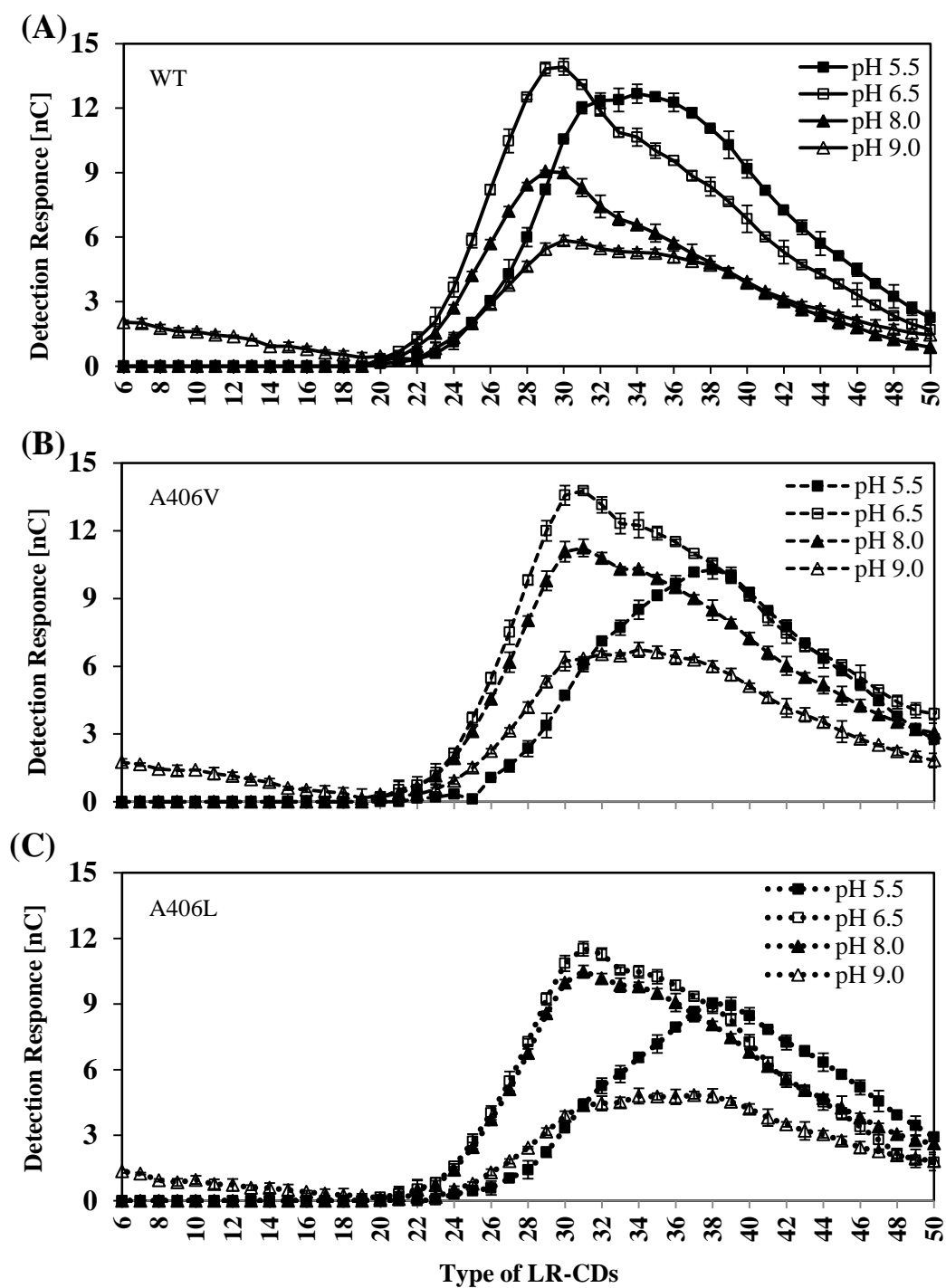


Figure 3. 23 HPAEC analysis of LR-CDs synthesized at different pH by WT- (A, solid line), A406V- (B, dashed line) and A406L-CgAMs (C, dotted line). The buffers used were: acetate buffer (pH 5.5), phosphate buffer (pH 6.5) and Tris-HCl buffer (pH 8.0-9.0). Data are shown as the mean \pm SD and are derived from 3 independent experiments.

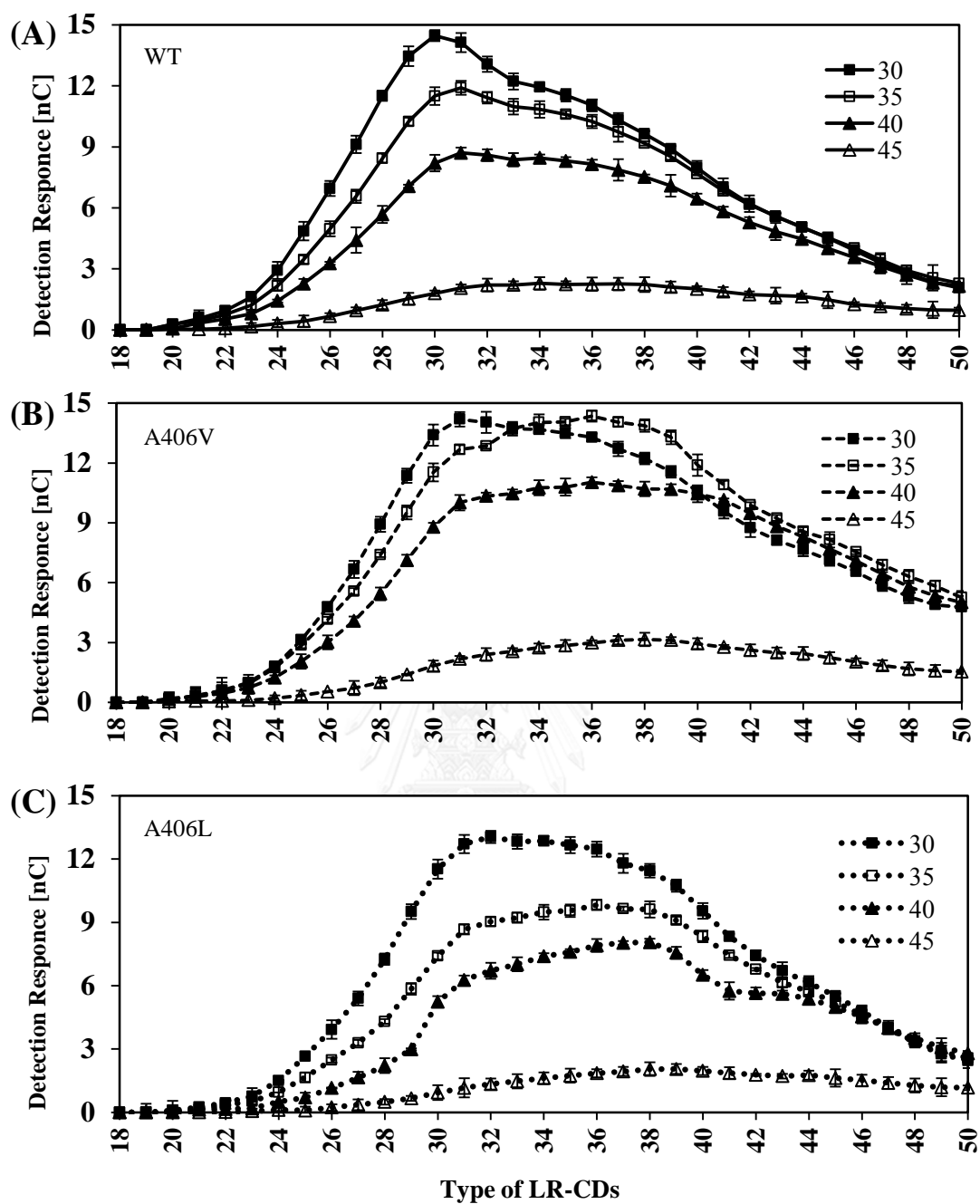


Figure 3.24 HPAEC analysis of LR-CDs synthesized at different temperature (30-45 °C) by WT- (A, solid line), A406V- (B, dashed line) and A406L-CgAMs (C, dotted line). Data are shown as the mean \pm SD and are derived from 3 independent experiments.

3.6.7.2 Effect of incubation time and temperature on LR-CDs production yield

To compare the LR-CDs production yield of WT- and both MT-CgAMs, all enzyme forms (at 0.3 mg protein) were incubated at 30 °C for various incubation times with pea starch substrate as described in section 2.13.1 and LR-CD products were measured by HPAEC-PAD (Figure 3.25A). For WT- and A406L-CgAMs, highest product yield was obtained at 1 h and 4 h incubation time while A406V gave highest product at 8 h. At the highest product yield, each mutated enzyme gave about 12-15% higher yield than its WT counterpart. At long incubation time of 24 h, both mutated enzymes gave up to 60-70% higher yield of LR-CD products than the WT.

Due to the change in optimum temperature and temperature stability of mutated enzymes as shown in Figures 3.17 and 3.18) and described under section 3.6.2, production of LR-CDs was compared at different temperature when incubation time was 90 min. The result (Figure 3.25B) showed that the WT- and A406L-CgAMs gave highest product yield at 30 °C while highest product yield of A406V was at both 30 and 35 °C. A406V gave 33% and 46% higher yield of LR-CDs than the WT at 35 and 40 °C, respectively. This result agrees with the finding that optimum temperature of A406V for cyclization reaction was + 5 °C shifted while that for A406L was about the same as the WT (Figure 3.17B). A406V was also found to have higher stability than A406L and the WT, respectively (Figure 3.18). The results from analysis of LR-CD products thus showed the advantage of A406V- over the WT-CgAM in giving higher product yield, especially when incubated at longer incubation time and higher temperature.

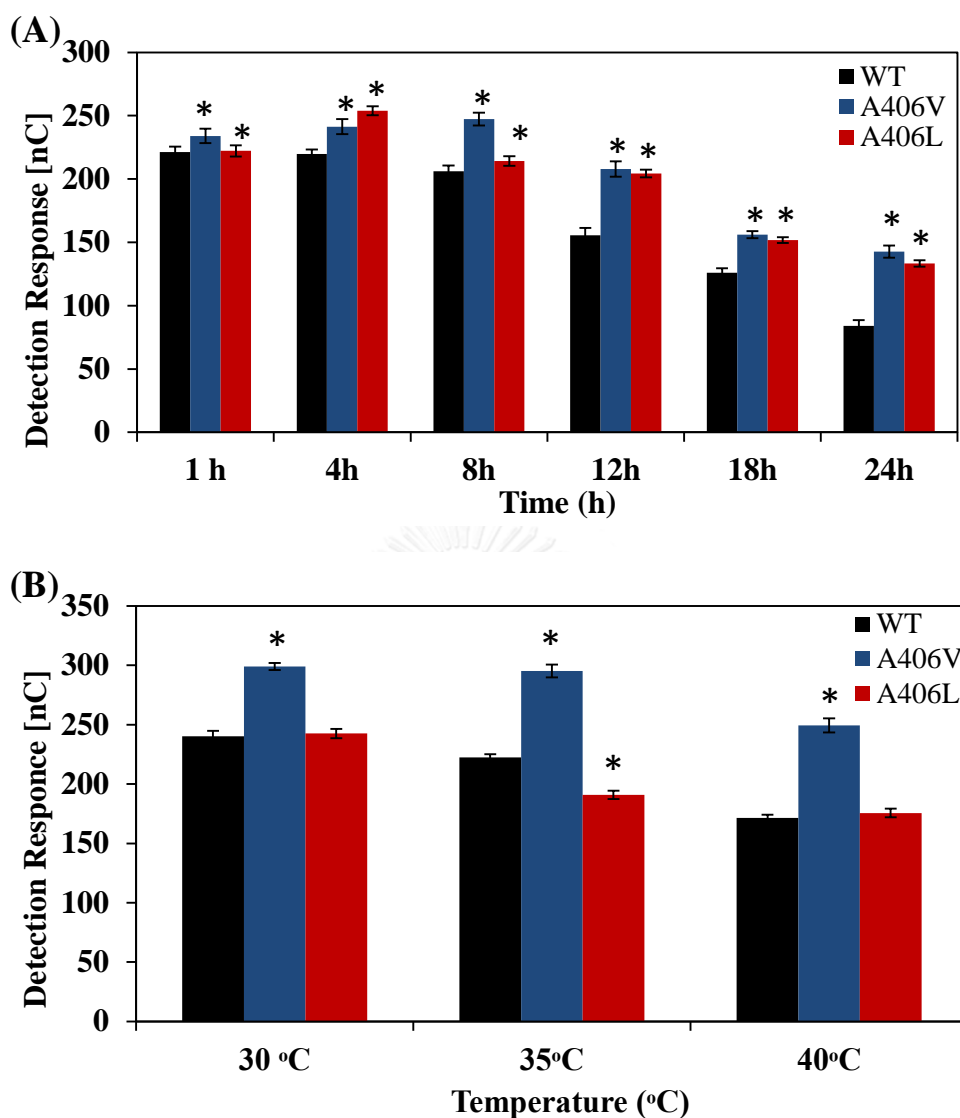


Figure 3. 25 HPAEC analysis of LR-CDs synthesized by WT-, A406V- and A406L-CgAMs at different incubation time (A) and temperature (B). The reaction mixture, consisting of 0.2% (w/v) pea starch and 0.3 mg of each enzyme in 50 mM phosphate buffer, pH 6.0; was incubated at 30 °C for 1-24 h (A) and 30/35/40 °C for 90 min (B). The experiments were performed as described in section 2.14. Data are shown as the mean \pm SD and are derived from three independent experiments. * $P < 0.05$ (Student's t -Test) with respect to the value of LR-CDs of WT-CgAM.

3.7 Site directed mutagenesis for improvement of thermostability of CgAM

From the result in the first part (section 3.1-3.6), A406V-CgAM was obtained from screening for thermostable clones from random mutagenesis, then we had constructed A406V- and A406L-CgAMs by site-directed mutagenesis to investigate the effect of hydrophobic functional group at this position. We found that A406V- and A406L- were more thermostable than the WT- enzyme, and interestingly, the two MT-CgAMs showed higher intermolecular transglucosylation activity. The results drew our interest to explore more on the involvement of the amino acid position at 406 on the enzyme characteristics.

As *C. glutamicum* is a mesophilic bacteria, comparison of amino acid sequence of CgAM with the most well-known amyloamylase from the thermophilic bacteria *T. aquaticus* (TaAM) is attempting. The superimposed structures of CgAM with TaAM (Figure 3.26) showed that Ala406 of CgAM is corresponded to His233 of TaAM. To investigate the effect of this position on thermostability of CgAM, site-directed mutagenesis as described in section 2.7 was performed whereby A406 was replaced by His (H). Mutation to Arg (R) and Phe (F) were also performed since Arg is known to involve with protein stability (Deng *et al.*, 2014) while Phe is aromatic hydrophobic. In addition, the Asn287 of CgAM is in the corresponded position to Tyr101 of TaAM (Fujii *et al.*, 2007) of which the change in this residue was reported to affect cyclization activity of TaAM. In another work, Tyr101 in amyloamylase from *T. thermophilus* (TtAM) in addition to control transglucosylation, also showed a higher thermostability than the mutated Y101S. Thus the involvement of Y101 in enzyme stability towards temperature was suggested (Watanasatitarpa *et al.*, 2014), hence substitution by Tyr (Y) at N287 of CgAM was also performed in this study.

3.7.1 Extraction of recombinant plasmid pET-19b -CgAM

The recombinant plasmid pET-19b CgAM was extracted from *E.coli* DH5 α and checked by agarose gel electrophoresis (Figure 3.27 Lane 1). After double digestion with *Nde* I and *Xho* I, it was found that the size of pET-19b vector and CgAM gene were around 5.7 kb and 2.1 kb, respectively (Figure 3.27 Lane 2). The ratio of A260/280 values was 1.8 indicated that the purity of this extracted recombinant plasmid was sufficient to be used as template for further PCR amplification.

3.7.2 Modification of CgAM gene by a single point mutation

Through site-directed mutagenesis of CgAMs gene, four mutants were constructed by a single point mutation at the position Ala406 as A406H, A406R, A406F and the position Asn287 as N287Y. The recombinant plasmid pET-19b CgAM was used as a DNA template for site directed mutagenesis. The product from the PCR amplification was found as a single band on agarose gel electrophoresis shown in Figure 3.28. The size of PCR product was 7.8 kb as expected for CgAM gene and pET-19b vector.

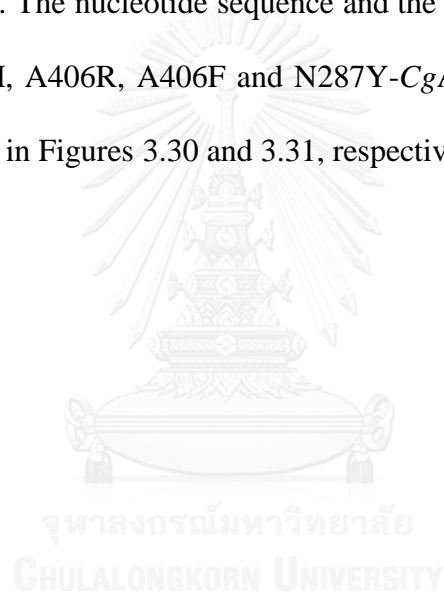
3.7.3 Transformation

The PCR products after digestion with *Dpn* I were purified and transformed into the competent cells of *E. coli* BL21 (DE3) by electroporation as described in section 2.4.7. Five hundred microliters of transformant was spread on LB agar plate containing 100 μ g/ml ampicillin and incubated at 37 °C for overnight. The *E. coli* BL21 (DE3) containing pET-19 vector harboring MT-CgAM gene was grown on the

plate. To confirm the insertion of MT-*CgAM* gene into pET-19b, the transformant was picked for plasmid extraction and digested with *Nde* I and *Xho* I as described in section 2.4.4. The agarose gel electrophoresis pattern of the recombinant plasmid containing *CgAM* gene is shown in Figure 3.29.

3.7.4 Nucleotide sequencing

To confirm the mutated *CgAM* gene, the gene was sequenced as described in section 2.6. and 3.1.5. The nucleotide sequence and the deduced amino acid sequence alignments of A406H, A406R, A406F and N287Y-*CgAM*s were compared with the WT-*CgAM* as shown in Figures 3.30 and 3.31, respectively.



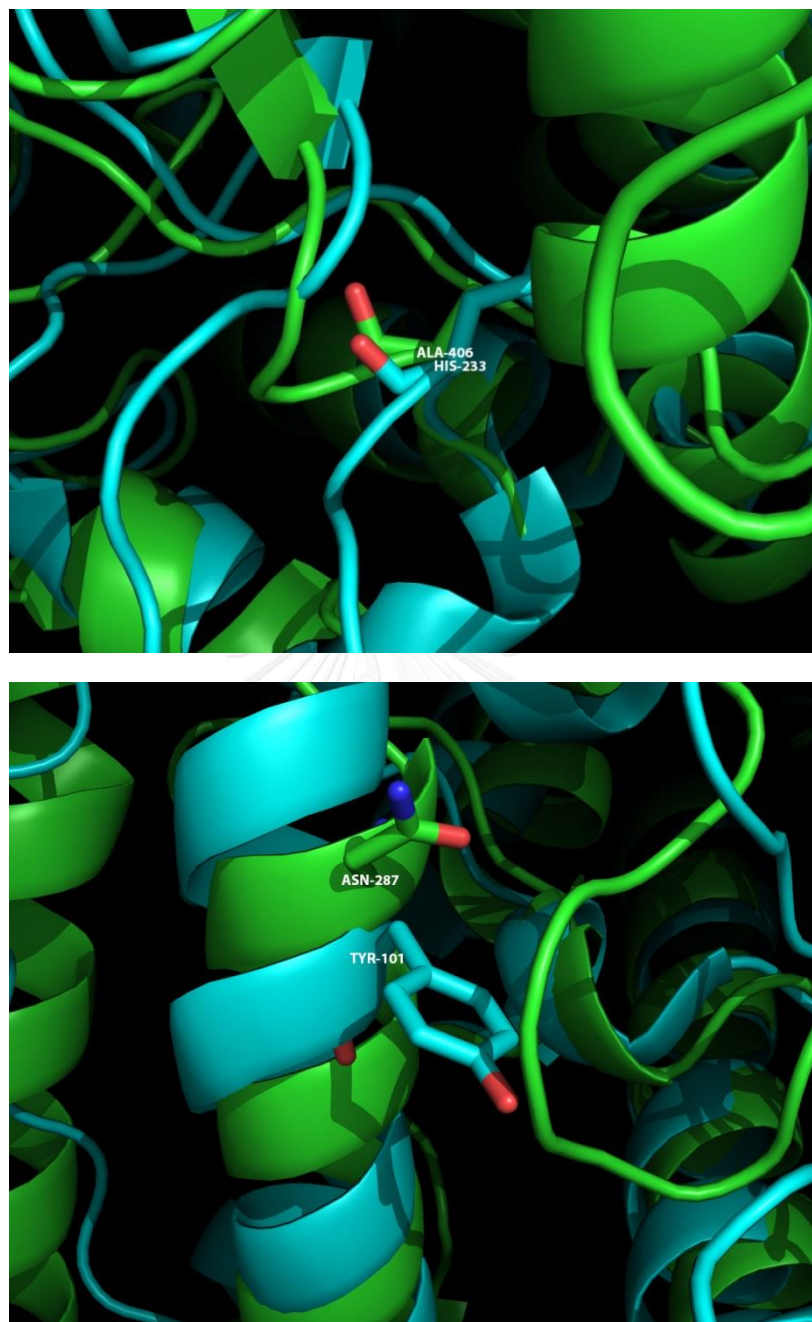


Figure 3. 26 The superimposed structures of *CgAM* (Green) on *T. aquaticus* amyloamylase (*TaAM*) (blue). The enzyme structures are displayed as secondary structure generated by PDB Swiss Viewer Program. Corresponding residues are displayed as stick and colored by atom names: nitrogen and oxygen are shown in blue and red, carbon is shown as stick color, while hydrogen is not shown.

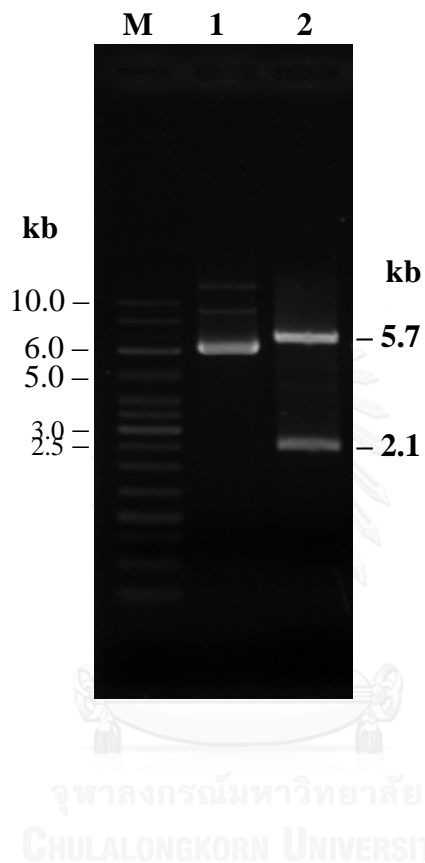


Figure 3. 27 Agarose gel electrophoresis of recombinant plasmid pET-19b *CgAM* extracted from *E.coli* DH5 α . The DNA samples were separated on 1% agarose gel and visualized by ethidium bromide staining.

Lane M = GeneRuler™ 1 kb DNA ladder (Fermentas, Canada)

Lane 1 = Recombinant plasmid *CgAM*

Lane 2 = Recombinant plasmid *CgAM* after double digestion with *Nde* I and *Xho* I

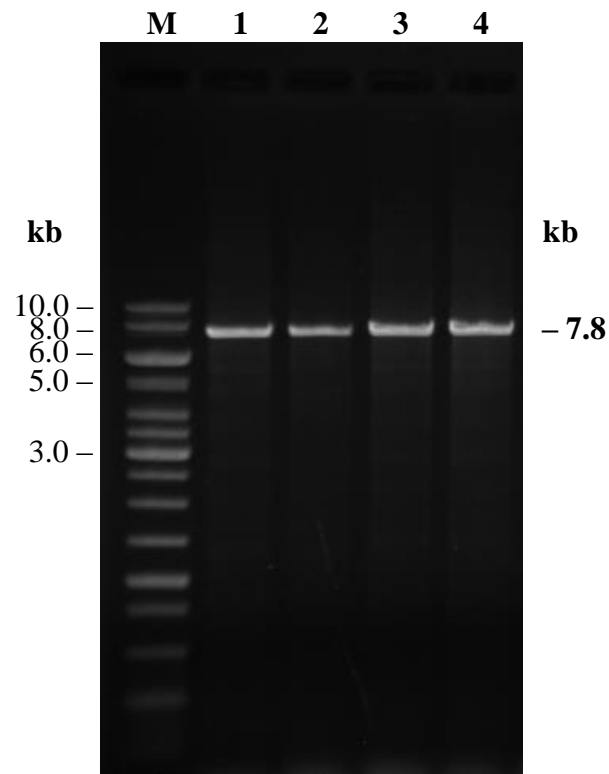


Figure 3. 28 Agarose gel electrophoresis of amplified DNA containing *CgAM* gene with a single point mutation. The DNA samples were separated on 1% agarose gel and visualized by ethidium bromide staining.

Lane M = GeneRuler™ 1 kb DNA ladder (Fermentas, Canada)

Lane 1 = PCR product from a single point mutation at A406H-*CgAM*

Lane 2 = PCR product from a single point mutation at A406R-*CgAM*

Lane 3 = PCR product from a single point mutation at A406F-*CgAM*

Lane 4 = PCR product from a single point mutation at N287Y-*CgAM*

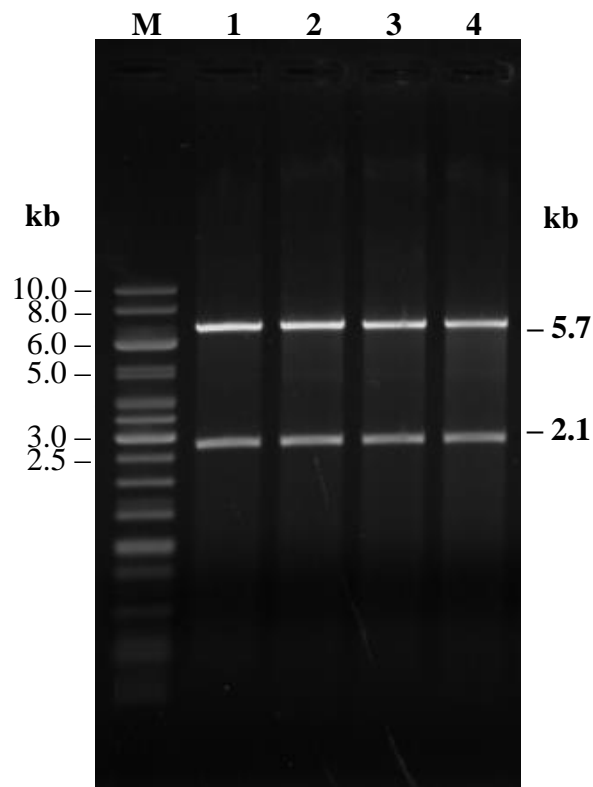


Figure 3. 29 Agarose gel electrophoresis of PCR product from pET-19b vector harboring *CgAM* gene with a single point mutation after digested with *Nde* I and *Xho* I. The DNA samples were separated on 1% agarose gel and visualized by ethidium bromide staining.

Lane M = GeneRuler™ 1 kb DNA ladder (Fermentas, Canada)

Lane 1, 2, 3 and 4 = PCR product from pET-19b vector harboring *CgAM* gene with a single point mutation at A406H, A406R, A406F and N287Y, respectively.

```

WT_CgAM          ATGACTGCTCGCAGATTTTGAATGAACCTCGCCGATCTCTACGGCGTAGCAACTTCTCTAC 60
A406H_CgAM       ATGACTGCTCGCAGATTTTGAATGAACCTCGCCGATCTCTACGGCGTAGCAACTTCTCTAC 60
A406R_CgAM       ATGACTGCTCGCAGATTTTGAATGAACCTCGCCGATCTCTACGGCGTAGCAACTTCTCTAC 60
A406F_CgAM       ATGACTGCTCGCAGATTTTGAATGAACCTCGCCGATCTCTACGGCGTAGCAACTTCTCTAC 60
N287Y_CgAM       ATGACTGCTCGCAGATTTTGAATGAACCTCGCCGATCTCTACGGCGTAGCAACTTCTCTAC 60
*****

WT_CgAM          ACTGATTACAAAGGTGCCCATATTGAGGTCAGCGATGACACATTAGTGAAAATCCTGCGT 120
A406H_CgAM       ACTGATTACAAAGGTGCCCATATTGAGGTCAGCGATGACACATTAGTGAAAATCCTGCGT 120
A406R_CgAM       ACTGATTACAAAGGTGCCCATATTGAGGTCAGCGATGACACATTAGTGAAAATCCTGCGT 120
A406F_CgAM       ACTGATTACAAAGGTGCCCATATTGAGGTCAGCGATGACACATTAGTGAAAATCCTGCGT 120
N287Y_CgAM       ACTGATTACAAAGGTGCCCATATTGAGGTCAGCGATGACACATTAGTGAAAATCCTGCGT 120
*****

WT_CgAM          GCTCTGGGTGTGAATTTAGATACAAGCAACCTCCCCAACGATGACGCTATCCAACGCCAA 180
A406H_CgAM       GCTCTGGGTGTGAATTTAGATACAAGCAACCTCCCCAACGATGACGCTATCCAACGCCAA 180
A406R_CgAM       GCTCTGGGTGTGAATTTAGATACAAGCAACCTCCCCAACGATGACGCTATCCAACGCCAA 180
A406F_CgAM       GCTCTGGGTGTGAATTTAGATACAAGCAACCTCCCCAACGATGACGCTATCCAACGCCAA 180
N287Y_CgAM       GCTCTGGGTGTGAATTTAGATACAAGCAACCTCCCCAACGATGACGCTATCCAACGCCAA 180
*****

WT_CgAM          ATTGCCCTCTTCCATGATCGAGAGTTCACTCGCCCACTGCCTCCATCGGTGGTTGCAGTT 240
A406H_CgAM       ATTGCCCTCTTCCATGATCGAGAGTTCACTCGCCCACTGCCTCCATCGGTGGTTGCAGTT 240
A406R_CgAM       ATTGCCCTCTTCCATGATCGAGAGTTCACTCGCCCACTGCCTCCATCGGTGGTTGCAGTT 240
A406F_CgAM       ATTGCCCTCTTCCATGATCGAGAGTTCACTCGCCCACTGCCTCCATCGGTGGTTGCAGTT 240
N287Y_CgAM       ATTGCCCTCTTCCATGATCGAGAGTTCACTCGCCCACTGCCTCCATCGGTGGTTGCAGTT 240
*****

WT_CgAM          GAAGGTGATGAAC TAGTTTTCCCGGTGCATGTGCACGACGGTTCCCTGCAGATGTCCAC 300
A406H_CgAM       GAAGGTGATGAAC TAGTTTTCCCGGTGCATGTGCACGACGGTTCCCTGCAGATGTCCAC 300
A406R_CgAM       GAAGGTGATGAAC TAGTTTTCCCGGTGCATGTGCACGACGGTTCCCTGCAGATGTCCAC 300
A406F_CgAM       GAAGGTGATGAAC TAGTTTTCCCGGTGCATGTGCACGACGGTTCCCTGCAGATGTCCAC 300
N287Y_CgAM       GAAGGTGATGAAC TAGTTTTCCCGGTGCATGTGCACGACGGTTCCCTGCAGATGTCCAC 300
*****

WT_CgAM          ATCGAATTGGAAGACGGCACGCAGCGGGATGTTTTCTCAGGTGGAAAAC TGGACAGCGCCA 360
A406H_CgAM       ATCGAATTGGAAGACGGCACGCAGCGGGATGTTTTCTCAGGTGGAAAAC TGGACAGCGCCA 360
A406R_CgAM       ATCGAATTGGAAGACGGCACGCAGCGGGATGTTTTCTCAGGTGGAAAAC TGGACAGCGCCA 360
A406F_CgAM       ATCGAATTGGAAGACGGCACGCAGCGGGATGTTTTCTCAGGTGGAAAAC TGGACAGCGCCA 360
N287Y_CgAM       ATCGAATTGGAAGACGGCACGCAGCGGGATGTTTTCTCAGGTGGAAAAC TGGACAGCGCCA 360
*****

WT_CgAM          CGGGAAATTGATGGGATTAGGTGGGGCGAGGCATCGTTTAAAGATTCTTGGTGATCTCCCC 420
A406H_CgAM       CGGGAAATTGATGGGATTAGGTGGGGCGAGGCATCGTTTAAAGATTCTTGGTGATCTCCCC 420
A406R_CgAM       CGGGAAATTGATGGGATTAGGTGGGGCGAGGCATCGTTTAAAGATTCTTGGTGATCTCCCC 420
A406F_CgAM       CGGGAAATTGATGGGATTAGGTGGGGCGAGGCATCGTTTAAAGATTCTTGGTGATCTCCCC 420
N287Y_CgAM       CGGGAAATTGATGGGATTAGGTGGGGCGAGGCATCGTTTAAAGATTCTTGGTGATCTCCCC 420
*****

WT_CgAM          TTGGGTTGGCACAAGCTTACCTTAAATCCAATGAACGCTCAGCTGAGTGC GGTTTGATC 480
A406H_CgAM       TTGGGTTGGCACAAGCTTACCTTAAATCCAATGAACGCTCAGCTGAGTGC GGTTTGATC 480
A406R_CgAM       TTGGGTTGGCACAAGCTTACCTTAAATCCAATGAACGCTCAGCTGAGTGC GGTTTGATC 480
A406F_CgAM       TTGGGTTGGCACAAGCTTACCTTAAATCCAATGAACGCTCAGCTGAGTGC GGTTTGATC 480
N287Y_CgAM       TTGGGTTGGCACAAGCTTACCTTAAATCCAATGAACGCTCAGCTGAGTGC GGTTTGATC 480
*****

```

Figure 3. 30 Nucleotide sequence alignment of A406H, A406R, A406F and N287Y-CgAMs compared with the WT-CgAM using Clustal X (1.81) multiple sequence alignment. Mutated positions are underlined.

```

WT_CgAM          ATCACCCCGGCTCGTCTGTCTACTGCTGATAAGTATCTTGATTCCCCTCGCAGTGGTGTC 540
A406H_CgAM       ATCACCCCGGCTCGTCTGTCTACTGCTGATAAGTATCTTGATTCCCCTCGCAGTGGTGTC 540
A406R_CgAM       ATCACCCCGGCTCGTCTGTCTACTGCTGATAAGTATCTTGATTCCCCTCGCAGTGGTGTC 540
A406F_CgAM       ATCACCCCGGCTCGTCTGTCTACTGCTGATAAGTATCTTGATTCCCCTCGCAGTGGTGTC 540
N287Y_CgAM       ATCACCCCGGCTCGTCTGTCTACTGCTGATAAGTATCTTGATTCCCCTCGCAGTGGTGTC 540
*****

WT_CgAM          ATGGCGCAGATCTACTCTGTGCGTTCCACGTTGTCGTGGGGCATGGGTGATTTCAATGAT 600
A406H_CgAM       ATGGCGCAGATCTACTCTGTGCGTTCCACGTTGTCGTGGGGCATGGGTGATTTCAATGAT 600
A406R_CgAM       ATGGCGCAGATCTACTCTGTGCGTTCCACGTTGTCGTGGGGCATGGGTGATTTCAATGAT 600
A406F_CgAM       ATGGCGCAGATCTACTCTGTGCGTTCCACGTTGTCGTGGGGCATGGGTGATTTCAATGAT 600
N287Y_CgAM       ATGGCGCAGATCTACTCTGTGCGTTCCACGTTGTCGTGGGGCATGGGTGATTTCAATGAT 600
*****

WT_CgAM          TTAGGAAACTTGGCAAGTGTGGTTGCCAGGATGGAGCAGACTTCCTGCTCATCAACCCC 660
A406H_CgAM       TTAGGAAACTTGGCAAGTGTGGTTGCCAGGATGGAGCAGACTTCCTGCTCATCAACCCC 660
A406R_CgAM       TTAGGAAACTTGGCAAGTGTGGTTGCCAGGATGGAGCAGACTTCCTGCTCATCAACCCC 660
A406F_CgAM       TTAGGAAACTTGGCAAGTGTGGTTGCCAGGATGGAGCAGACTTCCTGCTCATCAACCCC 660
N287Y_CgAM       TTAGGAAACTTGGCAAGTGTGGTTGCCAGGATGGAGCAGACTTCCTGCTCATCAACCCC 660
*****

WT_CgAM          ATGCACGCTGCAGAGCCGCTGCCTCCTACTGAGGACTCTCCTTATCTGCCACAACCAGG 720
A406H_CgAM       ATGCACGCTGCAGAGCCGCTGCCTCCTACTGAGGACTCTCCTTATCTGCCACAACCAGG 720
A406R_CgAM       ATGCACGCTGCAGAGCCGCTGCCTCCTACTGAGGACTCTCCTTATCTGCCACAACCAGG 720
A406F_CgAM       ATGCACGCTGCAGAGCCGCTGCCTCCTACTGAGGACTCTCCTTATCTGCCACAACCAGG 720
N287Y_CgAM       ATGCACGCTGCAGAGCCGCTGCCTCCTACTGAGGACTCTCCTTATCTGCCACAACCAGG 720
*****

WT_CgAM          CGCTTTATCAACCCGATCTACATTCGGGTAGAAGATATTCGGAGTTTAATCAGCTTGAG 780
A406H_CgAM       CGCTTTATCAACCCGATCTACATTCGGGTAGAAGATATTCGGAGTTTAATCAGCTTGAG 780
A406R_CgAM       CGCTTTATCAACCCGATCTACATTCGGGTAGAAGATATTCGGAGTTTAATCAGCTTGAG 780
A406F_CgAM       CGCTTTATCAACCCGATCTACATTCGGGTAGAAGATATTCGGAGTTTAATCAGCTTGAG 780
N287Y_CgAM       CGCTTTATCAACCCGATCTACATTCGGGTAGAAGATATTCGGAGTTTAATCAGCTTGAG 780
*****

WT_CgAM          ATTGATCTACGCGATGATATCGCAGAGATGGCTGCGGAATFCCGCGAACGCAATCTGACC 840
A406H_CgAM       ATTGATCTACGCGATGATATCGCAGAGATGGCTGCGGAATFCCGCGAACGCAATCTGACC 840
A406R_CgAM       ATTGATCTACGCGATGATATCGCAGAGATGGCTGCGGAATFCCGCGAACGCAATCTGACC 840
A406F_CgAM       ATTGATCTACGCGATGATATCGCAGAGATGGCTGCGGAATFCCGCGAACGCAATCTGACC 840
N287Y_CgAM       ATTGATCTACGCGATGATATCGCAGAGATGGCTGCGGAATFCCGCGAACGCAATCTGACC 840
*****

WT_CgAM          TCAGACATCATTGAGCGCAATGACGCTACGCTGCAAAGCTTCAAGTGTGCGCGCCATT 900
A406H_CgAM       TCAGACATCATTGAGCGCAATGACGCTACGCTGCAAAGCTTCAAGTGTGCGCGCCATT 900
A406R_CgAM       TCAGACATCATTGAGCGCAATGACGCTACGCTGCAAAGCTTCAAGTGTGCGCGCCATT 900
A406F_CgAM       TCAGACATCATTGAGCGCAATGACGCTACGCTGCAAAGCTTCAAGTGTGCGCGCCATT 900
N287Y_CgAM       TCAGACATCATTGAGCGCAATGACGCTACGCTGCAAAGCTTCAAGTGTGCGCGCCATT 900
*****

WT_CgAM          TTTGAAATGCCTCGTTCAGCGAACGTGAAGCCAACCTTTGTCTCCTTCGTGCAACGGGAA 960
A406H_CgAM       TTTGAAATGCCTCGTTCAGCGAACGTGAAGCCAACCTTTGTCTCCTTCGTGCAACGGGAA 960
A406R_CgAM       TTTGAAATGCCTCGTTCAGCGAACGTGAAGCCAACCTTTGTCTCCTTCGTGCAACGGGAA 960
A406F_CgAM       TTTGAAATGCCTCGTTCAGCGAACGTGAAGCCAACCTTTGTCTCCTTCGTGCAACGGGAA 960
N287Y_CgAM       TTTGAAATGCCTCGTTCAGCGAACGTGAAGCCAACCTTTGTCTCCTTCGTGCAACGGGAA 960
*****

```

Figure 3.30 (continued) Nucleotide sequence alignment of A406H, A406R, A406F and N287Y-CgAMs compared with the WT-CgAM using Clustal X (1.81) multiple sequence alignment. Mutated positions are underlined.

```

WT_CgAM          GGCCAAGGTCTTATTGATTTGCGCCACCTGGTGC GCGGACCGCGAAACTGCACAGTCTGAA 1020
A406H_CgAM      GGCCAAGGTCTTATTGATTTGCGCCACCTGGTGC GCGGACCGCGAAACTGCACAGTCTGAA 1020
A406R_CgAM      GGCCAAGGTCTTATTGATTTGCGCCACCTGGTGC GCGGACCGCGAAACTGCACAGTCTGAA 1020
A406F_CgAM      GGCCAAGGTCTTATTGATTTGCGCCACCTGGTGC GCGGACCGCGAAACTGCACAGTCTGAA 1020
N287Y_CgAM      GGCCAAGGTCTTATTGATTTGCGCCACCTGGTGC GCGGACCGCGAAACTGCACAGTCTGAA 1020
*****

WT_CgAM          TCTGTCCACGGAAC TGAGCCAGACCGCGATGAGCTGACCATGTTCTACATGTGGTTGCAG 1080
A406H_CgAM      TCTGTCCACGGAAC TGAGCCAGACCGCGATGAGCTGACCATGTTCTACATGTGGTTGCAG 1080
A406R_CgAM      TCTGTCCACGGAAC TGAGCCAGACCGCGATGAGCTGACCATGTTCTACATGTGGTTGCAG 1080
A406F_CgAM      TCTGTCCACGGAAC TGAGCCAGACCGCGATGAGCTGACCATGTTCTACATGTGGTTGCAG 1080
N287Y_CgAM      TCTGTCCACGGAAC TGAGCCAGACCGCGATGAGCTGACCATGTTCTACATGTGGTTGCAG 1080
*****

WT_CgAM          TGGCTATGTGATGAGCAGCTGGCGGCAGCTCAA AAGCGCGTGTTCGATGCCGGAATGTCG 1140
A406H_CgAM      TGGCTATGTGATGAGCAGCTGGCGGCAGCTCAA AAGCGCGTGTTCGATGCCGGAATGTCG 1140
A406R_CgAM      TGGCTATGTGATGAGCAGCTGGCGGCAGCTCAA AAGCGCGTGTTCGATGCCGGAATGTCG 1140
A406F_CgAM      TGGCTATGTGATGAGCAGCTGGCGGCAGCTCAA AAGCGCGTGTTCGATGCCGGAATGTCG 1140
N287Y_CgAM      TGGCTATGTGATGAGCAGCTGGCGGCAGCTCAA AAGCGCGTGTTCGATGCCGGAATGTCG 1140
*****

WT_CgAM          ATCGGCATCATGGCAGACCTGGCAGTTGGTGTGC ATCCAGGTGGTGTGATGCCCAGAAC 1200
A406H_CgAM      ATCGGCATCATGGCAGACCTGGCAGTTGGTGTGC ATCCAGGTGGTGTGATGCCCAGAAC 1200
A406R_CgAM      ATCGGCATCATGGCAGACCTGGCAGTTGGTGTGC ATCCAGGTGGTGTGATGCCCAGAAC 1200
A406F_CgAM      ATCGGCATCATGGCAGACCTGGCAGTTGGTGTGC ATCCAGGTGGTGTGATGCCCAGAAC 1200
N287Y_CgAM      ATCGGCATCATGGCAGACCTGGCAGTTGGTGTGC ATCCAGGTGGTGTGATGCCCAGAAC 1200
*****

WT_CgAM          CTCAGCCACGTA CTTGCTCCGGATGCGTCAGTGGGCGCCCCACCAGATGGATAACAACCAG 1260
A406H_CgAM      CTCAGCCACGTA CTTGCTCCGGATGCGTCAGTGGGCGCCCCACCAGATGGATAACAACCAG 1260
A406R_CgAM      CTCAGCCACGTA CTTGCTCCGGATGCGTCAGTGGGCGCCCCACCAGATGGATAACAACCAG 1260
A406F_CgAM      CTCAGCCACGTA CTTGCTCCGGATGCGTCAGTGGGCGCCCCACCAGATGGATAACAACCAG 1260
N287Y_CgAM      CTCAGCCACGTA CTTGCTCCGGATGCGTCAGTGGGCGCCCCACCAGATGGATAACAACCAG 1260
*****

WT_CgAM          CAGGGCCAAGACTGGTCCCAGCCACCATGGCATCC AGTGCGTCTTGCAGAGGAAGGCTAC 1320
A406H_CgAM      CAGGGCCAAGACTGGTCCCAGCCACCATGGCATCC AGTGCGTCTTGCAGAGGAAGGCTAC 1320
A406R_CgAM      CAGGGCCAAGACTGGTCCCAGCCACCATGGCATCC AGTGCGTCTTGCAGAGGAAGGCTAC 1320
A406F_CgAM      CAGGGCCAAGACTGGTCCCAGCCACCATGGCATCC AGTGCGTCTTGCAGAGGAAGGCTAC 1320
N287Y_CgAM      CAGGGCCAAGACTGGTCCCAGCCACCATGGCATCC AGTGCGTCTTGCAGAGGAAGGCTAC 1320
*****

WT_CgAM          ATTCCGTGGCGTAATCTGCTGCGCACTGTGCTGCGTCACTCCGGCGGAATCCGCGTGGAC 1380
A406H_CgAM      ATTCCGTGGCGTAATCTGCTGCGCACTGTGCTGCGTCACTCCGGCGGAATCCGCGTGGAC 1380
A406R_CgAM      ATTCCGTGGCGTAATCTGCTGCGCACTGTGCTGCGTCACTCCGGCGGAATCCGCGTGGAC 1380
A406F_CgAM      ATTCCGTGGCGTAATCTGCTGCGCACTGTGCTGCGTCACTCCGGCGGAATCCGCGTGGAC 1380
N287Y_CgAM      ATTCCGTGGCGTAATCTGCTGCGCACTGTGCTGCGTCACTCCGGCGGAATCCGCGTGGAC 1380
*****

WT_CgAM          CACGTTCTTGGTTTGTTCAGGCTCTTTGTGCATGCCACGCATGCAATCCCCTGCTACGGGC 1440
A406H_CgAM      CACGTTCTTGGTTTGTTCAGGCTCTTTGTGCATGCCACGCATGCAATCCCCTGCTACGGGC 1440
A406R_CgAM      CACGTTCTTGGTTTGTTCAGGCTCTTTGTGCATGCCACGCATGCAATCCCCTGCTACGGGC 1440
A406F_CgAM      CACGTTCTTGGTTTGTTCAGGCTCTTTGTGCATGCCACGCATGCAATCCCCTGCTACGGGC 1440
N287Y_CgAM      CACGTTCTTGGTTTGTTCAGGCTCTTTGTGCATGCCACGCATGCAATCCCCTGCTACGGGC 1440
*****

```

Figure 3.30 (continued) Nucleotide sequence alignment of A406H, A406R, A406F and N287Y-CgAMs compared with the WT-CgAM using Clustal X (1.81) multiple sequence alignment. Mutated positions are underlined.


```

WT_CgAM          ACCTATATCCGCTTCGACCATAATGCGTTGGTAGGCATTCTAGCCCTAGAAGCAGAACTC 1500
A406H_CgAM       ACCTATATCCGCTTCGACCATAATGCGTTGGTAGGCATTCTAGCCCTAGAAGCAGAACTC 1500
A406R_CgAM       ACCTATATCCGCTTCGACCATAATGCGTTGGTAGGCATTCTAGCCCTAGAAGCAGAACTC 1500
A406F_CgAM       ACCTATATCCGCTTCGACCATAATGCGTTGGTAGGCATTCTAGCCCTAGAAGCAGAACTC 1500
N287Y_CgAM       ACCTATATCCGCTTCGACCATAATGCGTTGGTAGGCATTCTAGCCCTAGAAGCAGAACTC 1500
*****

WT_CgAM          GCAGGCGCCGTTGTCATTGGTGAAGATCTGGGAACGTTTGAGCCTTGGGTACAAGATGCA 1560
A406H_CgAM       GCAGGCGCCGTTGTCATTGGTGAAGATCTGGGAACGTTTGAGCCTTGGGTACAAGATGCA 1560
A406R_CgAM       GCAGGCGCCGTTGTCATTGGTGAAGATCTGGGAACGTTTGAGCCTTGGGTACAAGATGCA 1560
A406F_CgAM       GCAGGCGCCGTTGTCATTGGTGAAGATCTGGGAACGTTTGAGCCTTGGGTACAAGATGCA 1560
N287Y_CgAM       GCAGGCGCCGTTGTCATTGGTGAAGATCTGGGAACGTTTGAGCCTTGGGTACAAGATGCA 1560
*****

WT_CgAM          TTGGCTCAGCGTGGCATCATGGGCACCTCGATCCTATGGTTCGAGCATTCCCAAGCCAG 1620
A406H_CgAM       TTGGCTCAGCGTGGCATCATGGGCACCTCGATCCTATGGTTCGAGCATTCCCAAGCCAG 1620
A406R_CgAM       TTGGCTCAGCGTGGCATCATGGGCACCTCGATCCTATGGTTCGAGCATTCCCAAGCCAG 1620
A406F_CgAM       TTGGCTCAGCGTGGCATCATGGGCACCTCGATCCTATGGTTCGAGCATTCCCAAGCCAG 1620
N287Y_CgAM       TTGGCTCAGCGTGGCATCATGGGCACCTCGATCCTATGGTTCGAGCATTCCCAAGCCAG 1620
*****

WT_CgAM          CCGGGTCCTCGCCGCCAGGAAGAGTATCGTCCGCTGGCCTTGACCACTGTGACCACTCAT 1680
A406H_CgAM       CCGGGTCCTCGCCGCCAGGAAGAGTATCGTCCGCTGGCCTTGACCACTGTGACCACTCAT 1680
A406R_CgAM       CCGGGTCCTCGCCGCCAGGAAGAGTATCGTCCGCTGGCCTTGACCACTGTGACCACTCAT 1680
A406F_CgAM       CCGGGTCCTCGCCGCCAGGAAGAGTATCGTCCGCTGGCCTTGACCACTGTGACCACTCAT 1680
N287Y_CgAM       CCGGGTCCTCGCCGCCAGGAAGAGTATCGTCCGCTGGCCTTGACCACTGTGACCACTCAT 1680
*****

WT_CgAM          GATCTCCCTCCGACTGCTGGTTATTTGGAGGGCGAGCACATTGCTCTTCGTGAGCGATTG 1740
A406H_CgAM       GATCTCCCTCCGACTGCTGGTTATTTGGAGGGCGAGCACATTGCTCTTCGTGAGCGATTG 1740
A406R_CgAM       GATCTCCCTCCGACTGCTGGTTATTTGGAGGGCGAGCACATTGCTCTTCGTGAGCGATTG 1740
A406F_CgAM       GATCTCCCTCCGACTGCTGGTTATTTGGAGGGCGAGCACATTGCTCTTCGTGAGCGATTG 1740
N287Y_CgAM       GATCTCCCTCCGACTGCTGGTTATTTGGAGGGCGAGCACATTGCTCTTCGTGAGCGATTG 1740
*****

WT_CgAM          GGGGTGCTCAACACTGATCCTGCTGCAGAACTCGCTGAGGATCTGCAGTGGCAAGCGGAG 1800
A406H_CgAM       GGGGTGCTCAACACTGATCCTGCTGCAGAACTCGCTGAGGATCTGCAGTGGCAAGCGGAG 1800
A406R_CgAM       GGGGTGCTCAACACTGATCCTGCTGCAGAACTCGCTGAGGATCTGCAGTGGCAAGCGGAG 1800
A406F_CgAM       GGGGTGCTCAACACTGATCCTGCTGCAGAACTCGCTGAGGATCTGCAGTGGCAAGCGGAG 1800
N287Y_CgAM       GGGGTGCTCAACACTGATCCTGCTGCAGAACTCGCTGAGGATCTGCAGTGGCAAGCGGAG 1800
*****

WT_CgAM          ATCCTTGATGTCGACGATCTGCCAACGCATTGCCAGCCCGGGAATACGTGGGACTCGAA 1860
A406H_CgAM       ATCCTTGATGTCGACGATCTGCCAACGCATTGCCAGCCCGGGAATACGTGGGACTCGAA 1860
A406R_CgAM       ATCCTTGATGTCGACGATCTGCCAACGCATTGCCAGCCCGGGAATACGTGGGACTCGAA 1860
A406F_CgAM       ATCCTTGATGTCGACGATCTGCCAACGCATTGCCAGCCCGGGAATACGTGGGACTCGAA 1860
N287Y_CgAM       ATCCTTGATGTCGACGATCTGCCAACGCATTGCCAGCCCGGGAATACGTGGGACTCGAA 1860
*****

WT_CgAM          CGCGATCAGCGCGGTGAGTTGGCTGAGCTGTTGGAAGGCCTGCACACTTTCGTTGCGAAA 1920
A406H_CgAM       CGCGATCAGCGCGGTGAGTTGGCTGAGCTGTTGGAAGGCCTGCACACTTTCGTTGCGAAA 1920
A406R_CgAM       CGCGATCAGCGCGGTGAGTTGGCTGAGCTGTTGGAAGGCCTGCACACTTTCGTTGCGAAA 1920
A406F_CgAM       CGCGATCAGCGCGGTGAGTTGGCTGAGCTGTTGGAAGGCCTGCACACTTTCGTTGCGAAA 1920
N287Y_CgAM       CGCGATCAGCGCGGTGAGTTGGCTGAGCTGTTGGAAGGCCTGCACACTTTCGTTGCGAAA 1920
*****

```

Figure 3.30 (continued) Nucleotide sequence alignment of A406H, A406R, A406F and N287Y-CgAMs compared with the WT-CgAM using Clustal X (1.81) multiple sequence alignment. Mutated positions are underlined.

```

WT_CgAM          ACCCCTTCAGCACTGACCTGTGTCTGCTTGGTAGACATGGTCGGTGAAAAGCGGGCACAG 1980
A406H_CgAM       ACCCCTTCAGCACTGACCTGTGTCTGCTTGGTAGACATGGTCGGTGAAAAGCGGGCACAG 1980
A406R_CgAM       ACCCCTTCAGCACTGACCTGTGTCTGCTTGGTAGACATGGTCGGTGAAAAGCGGGCACAG 1980
A406F_CgAM       ACCCCTTCAGCACTGACCTGTGTCTGCTTGGTAGACATGGTCGGTGAAAAGCGGGCACAG 1980
N287Y_CgAM       ACCCCTTCAGCACTGACCTGTGTCTGCTTGGTAGACATGGTCGGTGAAAAGCGGGCACAG 1980
*****

WT_CgAM          AATCAGCCGGGCACAACGAGGGATATGTATCCCAACTGGTGTATCCCACTGTGTGACAGC 2040
A406H_CgAM       AATCAGCCGGGCACAACGAGGGATATGTATCCCAACTGGTGTATCCCACTGTGTGACAGC 2040
A406R_CgAM       AATCAGCCGGGCACAACGAGGGATATGTATCCCAACTGGTGTATCCCACTGTGTGACAGC 2040
A406F_CgAM       AATCAGCCGGGCACAACGAGGGATATGTATCCCAACTGGTGTATCCCACTGTGTGACAGC 2040
N287Y_CgAM       AATCAGCCGGGCACAACGAGGGATATGTATCCCAACTGGTGTATCCCACTGTGTGACAGC 2040
*****

WT_CgAM          GAAGGCAACTCCGTGCTCATTGAATCGCTGCGTGAAAATGAGCTGTATCACCGTGTGGCA 2100
A406H_CgAM       GAAGGCAACTCCGTGCTCATTGAATCGCTGCGTGAAAATGAGCTGTATCACCGTGTGGCA 2100
A406R_CgAM       GAAGGCAACTCCGTGCTCATTGAATCGCTGCGTGAAAATGAGCTGTATCACCGTGTGGCA 2100
A406F_CgAM       GAAGGCAACTCCGTGCTCATTGAATCGCTGCGTGAAAATGAGCTGTATCACCGTGTGGCA 2100
N287Y_CgAM       GAAGGCAACTCCGTGCTCATTGAATCGCTGCGTGAAAATGAGCTGTATCACCGTGTGGCA 2100
*****

WT_CgAM          AAGGCAAGCAAGCGAGATTAG 2121
A406H_CgAM       AAGGCAAGCAAGCGAGATTAG 2121
A406R_CgAM       AAGGCAAGCAAGCGAGATTAG 2121
A406F_CgAM       AAGGCAAGCAAGCGAGATTAG 2121
N287Y_CgAM       AAGGCAAGCAAGCGAGATTAG 2121
*****

```

Figure 3.30 (continued) Nucleotide sequence alignment of A406H, A406R, A406F and N287Y-CgAMs compared with the WT-CgAM using Clustal X (1.81) multiple sequence alignment. Mutated positions are underlined.

```

WT_CgAM          MTARRFLNELADLYGVATSQYTDYKGAHIEVSDDTLVKILRALGVNLDTSNLPNDDAIQRQ 60
A406H_CgAM      MTARRFLNELADLYGVATSQYTDYKGAHIEVSDDTLVKILRALGVNLDTSNLPNDDAIQRQ 60
A406R_CgAM      MTARRFLNELADLYGVATSQYTDYKGAHIEVSDDTLVKILRALGVNLDTSNLPNDDAIQRQ 60
A406F_CgAM      MTARRFLNELADLYGVATSQYTDYKGAHIEVSDDTLVKILRALGVNLDTSNLPNDDAIQRQ 60
N287Y_CgAM      MTARRFLNELADLYGVATSQYTDYKGAHIEVSDDTLVKILRALGVNLDTSNLPNDDAIQRQ 60
*****

WT_CgAM          IALFHDREFTRPLPPSVVAVEGDELVFPVHVHDGSPADVHIELEDGTQRDVSQVENWTAP 120
A406H_CgAM      IALFHDREFTRPLPPSVVAVEGDELVFPVHVHDGSPADVHIELEDGTQRDVSQVENWTAP 120
A406R_CgAM      IALFHDREFTRPLPPSVVAVEGDELVFPVHVHDGSPADVHIELEDGTQRDVSQVENWTAP 120
A406F_CgAM      IALFHDREFTRPLPPSVVAVEGDELVFPVHVHDGSPADVHIELEDGTQRDVSQVENWTAP 120
N287Y_CgAM      IALFHDREFTRPLPPSVVAVEGDELVFPVHVHDGSPADVHIELEDGTQRDVSQVENWTAP 120
*****

WT_CgAM          REIDGIRWGEASFKIPGDLPLGWHLHLKSNERSAECGLIITPARLSTADKYLDSFRSGV 180
A406H_CgAM      REIDGIRWGEASFKIPGDLPLGWHLHLKSNERSAECGLIITPARLSTADKYLDSFRSGV 180
A406R_CgAM      REIDGIRWGEASFKIPGDLPLGWHLHLKSNERSAECGLIITPARLSTADKYLDSFRSGV 180
A406F_CgAM      REIDGIRWGEASFKIPGDLPLGWHLHLKSNERSAECGLIITPARLSTADKYLDSFRSGV 180
N287Y_CgAM      REIDGIRWGEASFKIPGDLPLGWHLHLKSNERSAECGLIITPARLSTADKYLDSFRSGV 180
*****

WT_CgAM          MAQIYSVRSTLSWGMGDFNDLGNLASVVAQDGADFLINPMHAAEPLPPTEDSPYLPPTTR 240
A406H_CgAM      MAQIYSVRSTLSWGMGDFNDLGNLASVVAQDGADFLINPMHAAEPLPPTEDSPYLPPTTR 240
A406R_CgAM      MAQIYSVRSTLSWGMGDFNDLGNLASVVAQDGADFLINPMHAAEPLPPTEDSPYLPPTTR 240
A406F_CgAM      MAQIYSVRSTLSWGMGDFNDLGNLASVVAQDGADFLINPMHAAEPLPPTEDSPYLPPTTR 240
N287Y_CgAM      MAQIYSVRSTLSWGMGDFNDLGNLASVVAQDGADFLINPMHAAEPLPPTEDSPYLPPTTR 240
*****

WT_CgAM          RFINPIYIRVEDIPEFNQLEIDLRRDDIAEMAAEFRENRNLTSDIERNDVYAAKLQVLRAI 300
A406H_CgAM      RFINPIYIRVEDIPEFNQLEIDLRRDDIAEMAAEFRENRNLTSDIERNDVYAAKLQVLRAI 300
A406R_CgAM      RFINPIYIRVEDIPEFNQLEIDLRRDDIAEMAAEFRENRNLTSDIERNDVYAAKLQVLRAI 300
A406F_CgAM      RFINPIYIRVEDIPEFNQLEIDLRRDDIAEMAAEFRENRNLTSDIERNDVYAAKLQVLRAI 300
N287Y_CgAM      RFINPIYIRVEDIPEFNQLEIDLRRDDIAEMAAEFRENRNLTSDIERNDVYAAKLQVLRAI 300
*****

WT_CgAM          FEMPRSSEREANFVSFVQREGQGLIDFATWCADRETAQSESVHGTEPDRDELTMFYMWLQ 360
A406H_CgAM      FEMPRSSEREANFVSFVQREGQGLIDFATWCADRETAQSESVHGTEPDRDELTMFYMWLQ 360
A406R_CgAM      FEMPRSSEREANFVSFVQREGQGLIDFATWCADRETAQSESVHGTEPDRDELTMFYMWLQ 360
A406F_CgAM      FEMPRSSEREANFVSFVQREGQGLIDFATWCADRETAQSESVHGTEPDRDELTMFYMWLQ 360
N287Y_CgAM      FEMPRSSEREANFVSFVQREGQGLIDFATWCADRETAQSESVHGTEPDRDELTMFYMWLQ 360
*****

WT_CgAM          WLCDEQLAAAQKRAVDAGMSIGIMADLAVGVHPPGGADAQNLSHVLAPDASVGPDPGYNQ 420
A406H_CgAM      WLCDEQLAAAQKRAVDAGMSIGIMADLAVGVHPPGGADAQNLSHVLAPDASVGPDPGYNQ 420
A406R_CgAM      WLCDEQLAAAQKRAVDAGMSIGIMADLAVGVHPPGGADAQNLSHVLAPDASVGPDPGYNQ 420
A406F_CgAM      WLCDEQLAAAQKRAVDAGMSIGIMADLAVGVHPPGGADAQNLSHVLAPDASVGPDPGYNQ 420
N287Y_CgAM      WLCDEQLAAAQKRAVDAGMSIGIMADLAVGVHPPGGADAQNLSHVLAPDASVGPDPGYNQ 420
*****

WT_CgAM          QGQDWSQPPWHPVRLAEEGYIPWRNLLRTVLRHSGGIRVDHVLGLFRLFMVPRMQSPATG 480
A406H_CgAM      QGQDWSQPPWHPVRLAEEGYIPWRNLLRTVLRHSGGIRVDHVLGLFRLFMVPRMQSPATG 480
A406R_CgAM      QGQDWSQPPWHPVRLAEEGYIPWRNLLRTVLRHSGGIRVDHVLGLFRLFMVPRMQSPATG 480
A406F_CgAM      QGQDWSQPPWHPVRLAEEGYIPWRNLLRTVLRHSGGIRVDHVLGLFRLFMVPRMQSPATG 480
N287Y_CgAM      QGQDWSQPPWHPVRLAEEGYIPWRNLLRTVLRHSGGIRVDHVLGLFRLFMVPRMQSPATG 480
*****

WT_CgAM          TYIRFDHNALVGI LALEAELAGAVVIGEDLGTTFEPWVQDALAQRGIMGTSILWFEHSPSQ 540
A406H_CgAM      TYIRFDHNALVGI LALEAELAGAVVIGEDLGTTFEPWVQDALAQRGIMGTSILWFEHSPSQ 540
A406R_CgAM      TYIRFDHNALVGI LALEAELAGAVVIGEDLGTTFEPWVQDALAQRGIMGTSILWFEHSPSQ 540
A406F_CgAM      TYIRFDHNALVGI LALEAELAGAVVIGEDLGTTFEPWVQDALAQRGIMGTSILWFEHSPSQ 540
N287Y_CgAM      TYIRFDHNALVGI LALEAELAGAVVIGEDLGTTFEPWVQDALAQRGIMGTSILWFEHSPSQ 540
*****

```

Figure 3. 31 The deduced amino acid sequence alignment of A406H, A406R, A406F and N287Y-CgAMs compared with the WT-CgAM using Clustal Omega (1.2.1) multiple sequence alignment. Mutated amino acids are highlighted. Catalytic residues are show in the boxes.

D561

```

WT_CgAM          PGPRRQEEYRPLALTTVTTHDL PPTAGYLEGEHIALRERLGVNLTPAAELAEDLQWQAE 600
A406H_CgAM      PGPRRQEEYRPLALTTVTTHDL PPTAGYLEGEHIALRERLGVNLTPAAELAEDLQWQAE 600
A406R_CgAM      PGPRRQEEYRPLALTTVTTHDL PPTAGYLEGEHIALRERLGVNLTPAAELAEDLQWQAE 600
A406F_CgAM      PGPRRQEEYRPLALTTVTTHDL PPTAGYLEGEHIALRERLGVNLTPAAELAEDLQWQAE 600
N287Y_CgAM      PGPRRQEEYRPLALTTVTTHDL PPTAGYLEGEHIALRERLGVNLTPAAELAEDLQWQAE 600
*****

WT_CgAM          ILDVAASANALPAREYVGLERDQRGELAEELLEGLHTFVAKTPSALTCVCLVDMVGKRAQ 660
A406H_CgAM      ILDVAASANALPAREYVGLERDQRGELAEELLEGLHTFVAKTPSALTCVCLVDMVGKRAQ 660
A406R_CgAM      ILDVAASANALPAREYVGLERDQRGELAEELLEGLHTFVAKTPSALTCVCLVDMVGKRAQ 660
A406F_CgAM      ILDVAASANALPAREYVGLERDQRGELAEELLEGLHTFVAKTPSALTCVCLVDMVGKRAQ 660
N287Y_CgAM      ILDVAASANALPAREYVGLERDQRGELAEELLEGLHTFVAKTPSALTCVCLVDMVGKRAQ 660
*****

WT_CgAM          NQPGTTRDMPNWCIPLCDSEGNVLIESLRENELYHRVAKASKRD          706
A406H_CgAM      NQPGTTRDMPNWCIPLCDSEGNVLIESLRENELYHRVAKASKRD          706
A406R_CgAM      NQPGTTRDMPNWCIPLCDSEGNVLIESLRENELYHRVAKASKRD          706
A406F_CgAM      NQPGTTRDMPNWCIPLCDSEGNVLIESLRENELYHRVAKASKRD          706
N287Y_CgAM      NQPGTTRDMPNWCIPLCDSEGNVLIESLRENELYHRVAKASKRD          706
*****

```

Figure 3.31 (continued) The deduced amino acid sequence alignment of A406H, A406R, A406F and N287Y-CgAMs compared with the WT-CgAM using Clustal Omega (1.2.1) multiple sequence alignment. Mutated amino acids are highlighted. Catalytic residues are show in the boxes.

3.7.5 The expression of recombinant wild-type WT- and four MT-CgAMs

The *E. coli* BL21 (DE3) containing recombinant WT-, A406H, A406R, A406F and N287Y-CgAMs were cultivated in LB broth containing 100 µg/ml of ampicillin antibiotic. The enzyme production was induced with 0.4 mM IPTG for 0, 1, 2, 3, 4, 5 and 6 hours. The cell pellets were resuspended in 150 µl of extraction buffer, then sonicated and centrifuged to get crude supernatant. The 8 µg protein of crude enzymes from A406H, A406R, A406F and N287Y-CgAMs were subjected to electrophoresis on a 7.5% SDS-polyacrylamide gel (Figures 3.32, 3.33 and 3.34, respectively, data not shown for A406F). Unfortunately, the mutated CgAM proteins were not overexpressed in soluble fraction, the major protein band at around 84 kDa could not be observed with appropriate intensity, at all induction times. They were found to express as insoluble aggregates, more than 90% of the protein was aggregated in cell pellets (Figure 3.35B). It was noticed that the WT-, A406V- and A406L-CgAMs showed higher expression in the soluble protein form at around 20-30% (Figure 3.35A).

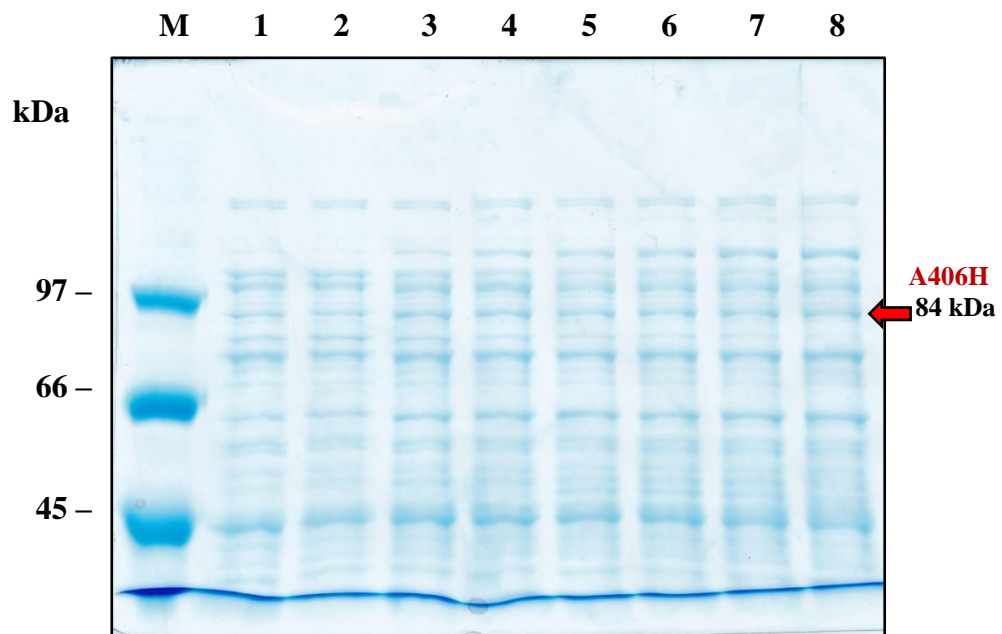


Figure 3. 32 SDS-PAGE of crude enzyme from A406H-CgAM induced by 0.4 mM IPTG at various times

Lane M = Low molecular weight protein marker

Lane 1 = crude enzyme from pET-19b vector without *CgAM* gene after induced by 0.4 mM IPTG for 2 h.

Lane 2-8 = crude enzyme from A406H-CgAM at various induction times: 0, 1, 2, 3, 4, 5 and 6 h, respectively.

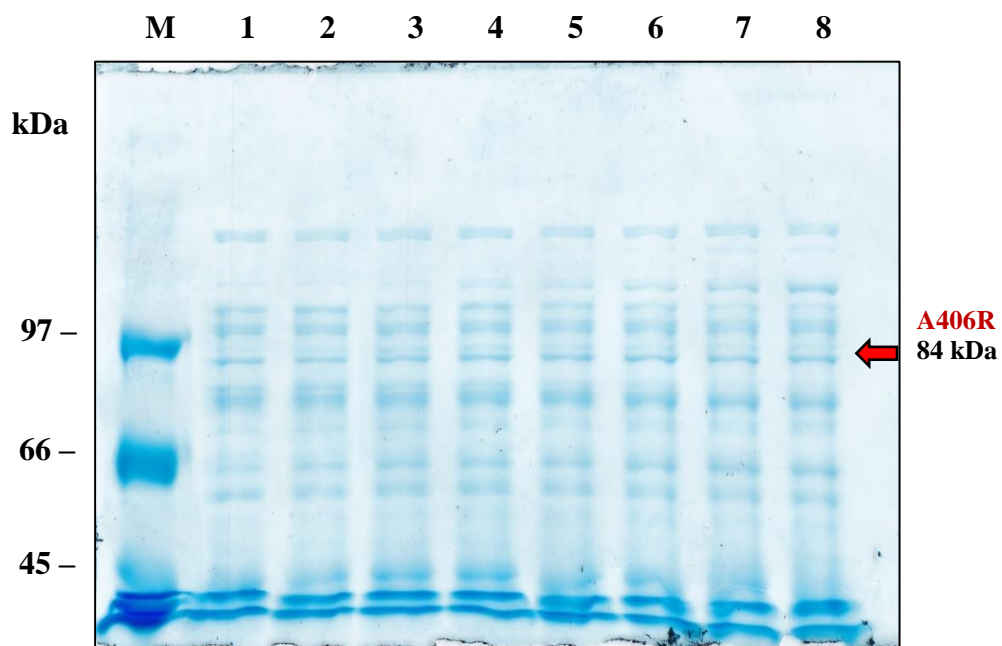


Figure 3. 33 SDS-PAGE of crude enzyme from A406R-CgAM induced by 0.4 mM IPTG at various times

Lane M = Low molecular weight protein marker

Lane 1 = crude enzyme from pET-19b vector without *CgAM* gene after induced by 0.4 mM IPTG for 2 h.

Lane 2-8 = crude enzyme from A406R-CgAM at various induction times: 0, 1, 2, 3, 4, 5 and 6 h, respectively.

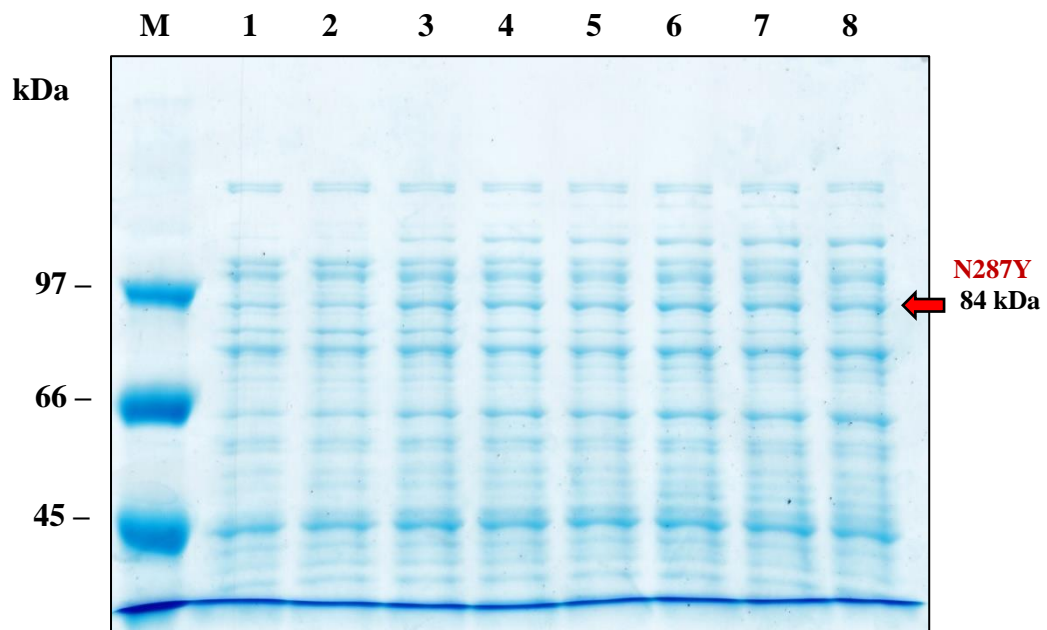


Figure 3. 34 SDS-PAGE of crude enzyme from N287Y-CgAM induced by 0.4 mM IPTG at various times

Lane M = Low molecular weight protein marker

Lane 1 = crude enzyme from pET-19b vector without *CgAM* gene after induced by 0.4 mM IPTG for 2 h.

Lane 2-8 = crude enzyme from N287Y-CgAM at various induction times: 0, 1, 2, 3, 4, 5 and 6 h, respectively.

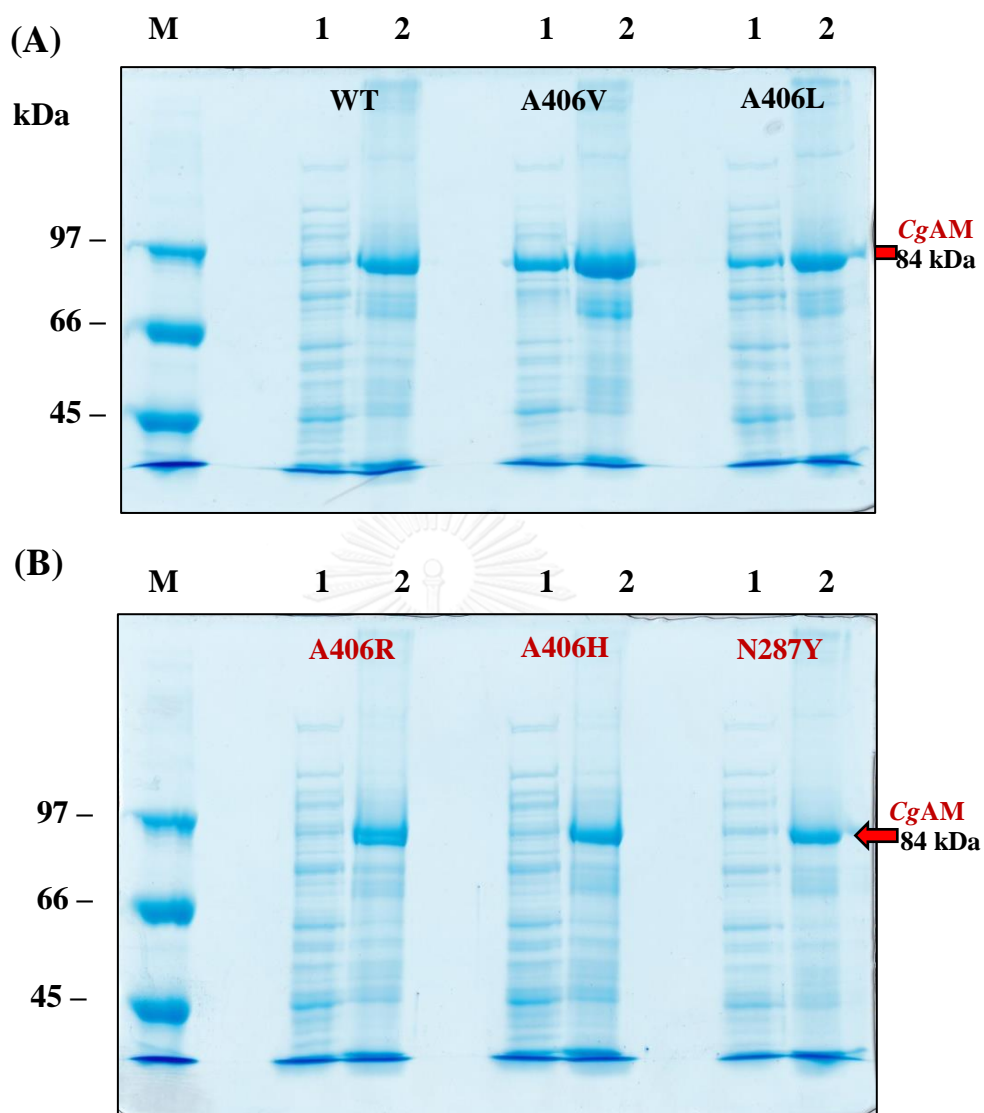


Figure 3.35 SDS-PAGE of crude enzymes and cell pellets from WT- and MT-CgAMs after induced with 0.4 mM IPTG at 37 °C for 2 h

Lane M = Low molecular weight protein marker

Lane 1 = crude enzymes from WT- and MT-CgAMs after induced with 0.4 mM IPTG for 2 h

Lane 2 = cell pellets from WT- and MT-CgAMs after induced with 0.4 mM IPTG for 2 h

3.7.5.1 The condition for soluble protein expression

Thus, the change of the condition for protein expression of the four mutated enzymes was investigated. A406R-CgAM was used to study the protein expression by cultivation in 4 conditions ; condition 1 and 2 : cells were cultivated at 37 °C in LB broth and LB broth containing 1% of glucose, respectively, cell growth was monitored by measuring optical density at 600 nm, cells were grown until A_{600} reached 0.4-0.6, the enzyme production was induced with 0.4 mM IPTG; condition 3 : cells were cultivated at 37 °C in LB broth containing 1% of glucose, cells were grown until A_{600} reached 0.4-0.6, the enzyme production was induced with 1 mM IPTG, then the temperature was changed to 16 °C for protein expression at induction time 0, 2, 4, 6, 8, 14 and 18 h (Figures 3.36, 3.38 and 3.40). In condition 4: cells were cultivated at 37 °C in Auto Induction Media (AIM) containing lactose until A_{600} reached 0.4-0.6, the temperature was then changed to 16 °C for protein expression at induction time 0, 2, 4, 6, 8, 14 and 18 h without IPTG induction (Figure 3.42).

The protein pattern of crude enzymes was investigated. The 1.5 ml cell suspension was taken from A406R-CgAM grown at various times when cultivated in 4 conditions as described in 2.9 and then harvested by centrifugation. The cell pellets were resuspended in 150 μ l of extraction buffer, then sonicated and centrifuged to get crude supernatant. The 15 μ g protein of crude enzyme from A406R-CgAM were subjected to electrophoresis on 7.5% SDS-polyacrylamide gel. The results in Figures 3.37, 3.39, 3.41 and 3.43, the condition 1 and 4 showed good intensity of the major protein band at around 84 kDa of cells at each induction time, corresponding to the expected size of CgAM enzyme while the condition 2 and 3 show lower expression.

However, the highest enzyme activity was detected from condition 4 after growing cells at 16 °C for 14 h. Thus, the condition 4 was selected for enzyme induction in further experiments for A406H-, A406F- and N287Y-CgAMs.



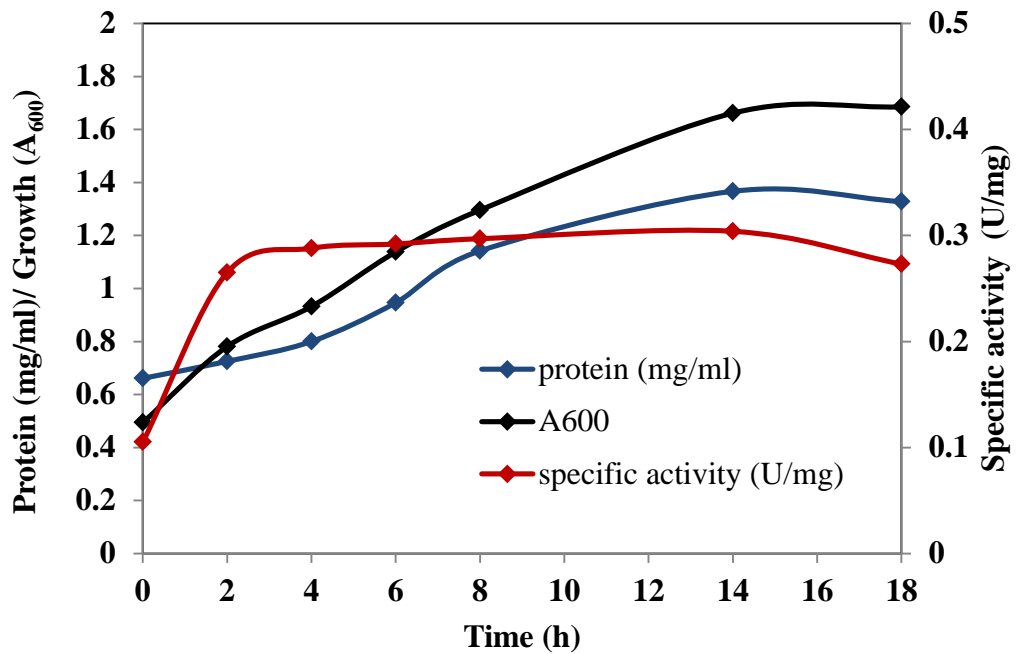


Figure 3. 36 Expression of recombinant A406R-CgAM in *E. coli* BL21 (DE3)

by cultivation in LB broth after induced with 0.4 mM IPTG at 16 °C for various times (condition 1). The activity of CgAM was determined by disproportionation assay.

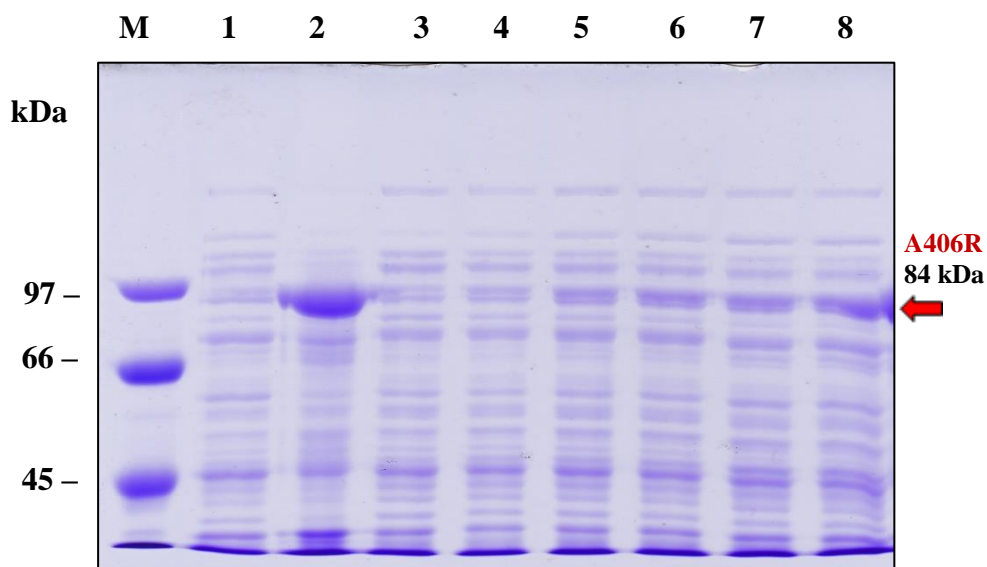


Figure 3. 37 SDS-PAGE of crude enzyme expressed from cells harboring A406R-CgAM. Cells were cultivated in LB broth after induced with 0.4 mM IPTG at various times (condition1).

Lane M = Low molecular weight protein marker

Lane 1 = 15 μ g protein of crude enzyme from A406R-CgAM after induced with 0.4 mM IPTG at 37 °C for 2 h

Lane 2 = 15 μ g protein of cell pellets from A406R-CgAM after induced with 0.4 mM IPTG at 37 °C for 2 h

Lane 3-8 = 15 μ g protein of crude enzyme from A406R-CgAM after induced with 0.4 mM IPTG at 16 °C for 2, 4, 6, 8, 14 and 18 h, respectively

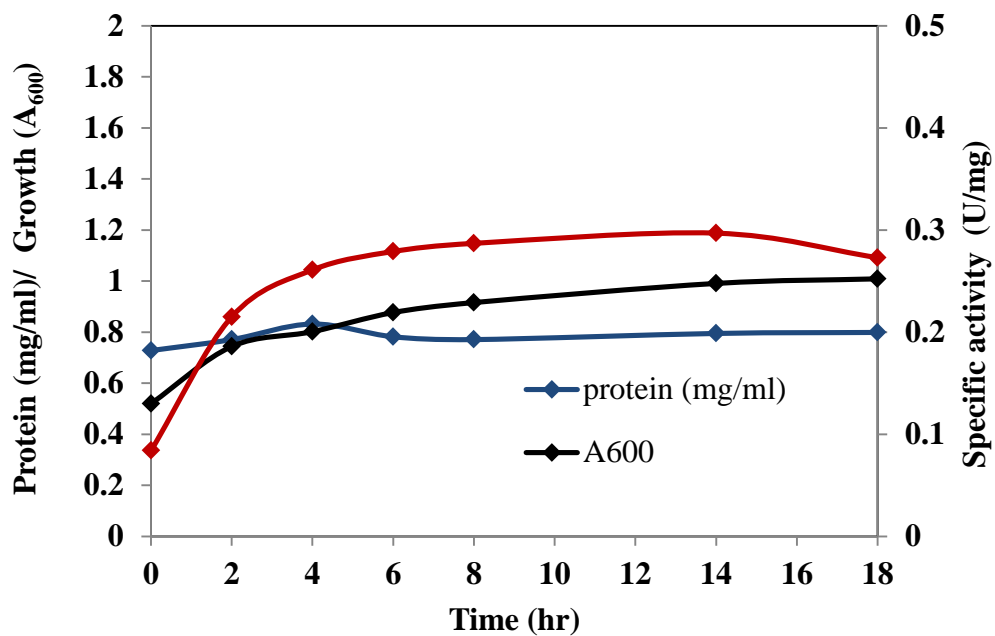


Figure 3. 38 Expression of recombinant A406R-CgAM in *E. coli* BL21 (DE3)

by cultivation in LB broth containing 1% of glucose after induced with 0.4 mM IPTG at 16 °C for various times (condition 2). The activity of CgAM was determined by disproportionation assay.

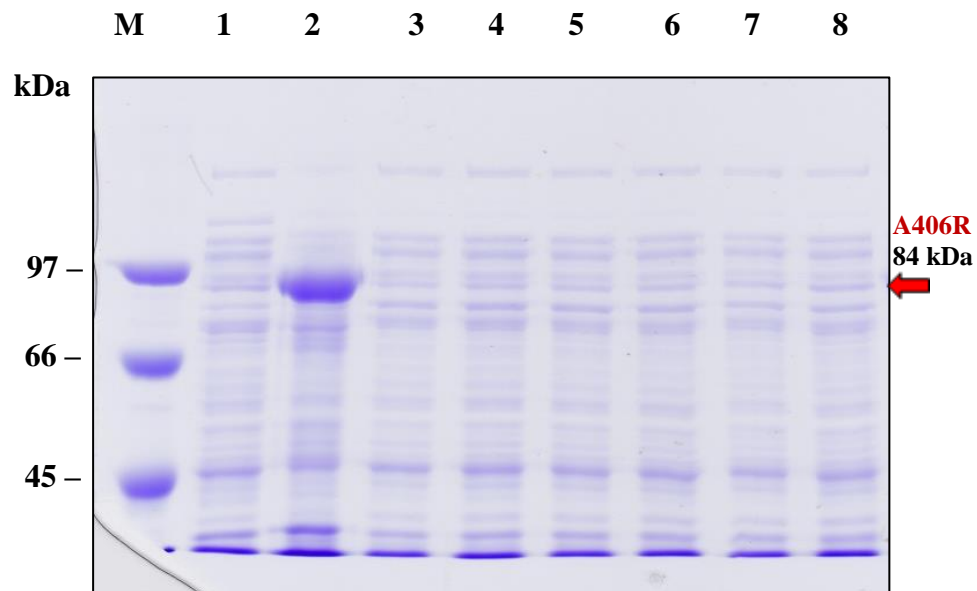


Figure 3. 39 SDS-PAGE of crude enzyme expressed from cells harboring A406R-CgAM. Cells were cultivated in LB broth containing 1% of glucose after induced with 0.4 mM IPTG at various times (condition 2)

Lane M = Low molecular weight protein marker

Lane 1 = 15 μ g protein of crude enzyme from A406R-CgAM after induced with 0.4 mM IPTG at 37 $^{\circ}$ C for 2 h

Lane 2 = 15 μ g protein of cell pellets from A406R-CgAM after induced with 0.4 mM IPTG at 37 $^{\circ}$ C for 2 h

Lane 3-8 = 15 μ g protein of crude enzyme from A406R-CgAM after induced with 0.4 mM IPTG at 16 $^{\circ}$ C for 2, 4, 6, 8, 14 and 18 h, respectively

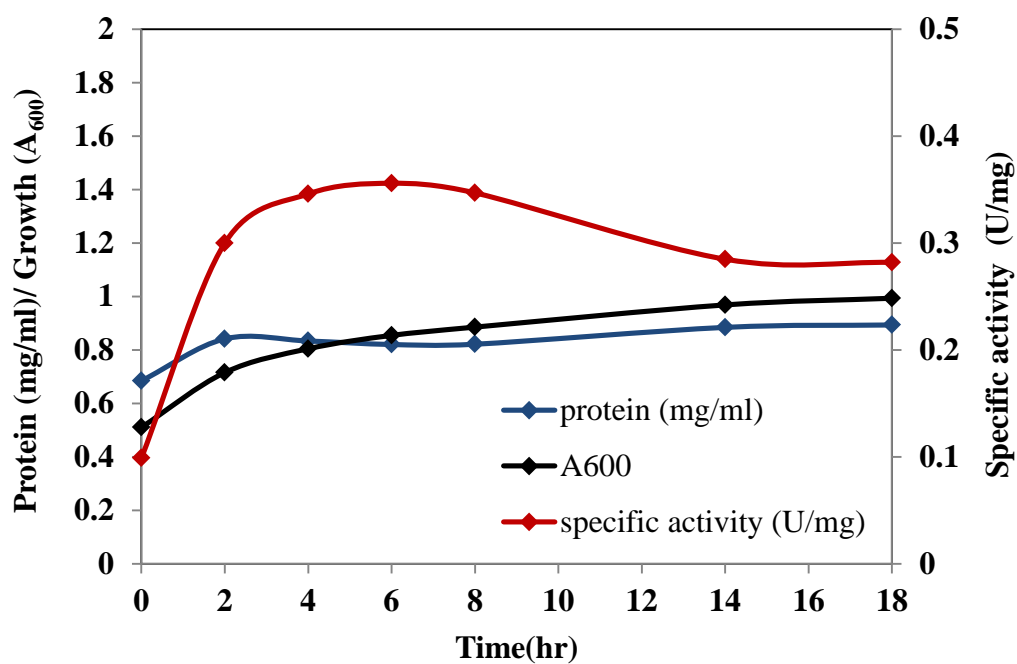


Figure 3. 40 Expression of recombinant A406R-CgAM in *E. coli* BL21 (DE3)

by cultivation in LB broth containing 1% of glucose after induced with 1 mM IPTG at 16 °C for various times (condition 3). The activity was measured by disproportionation assay

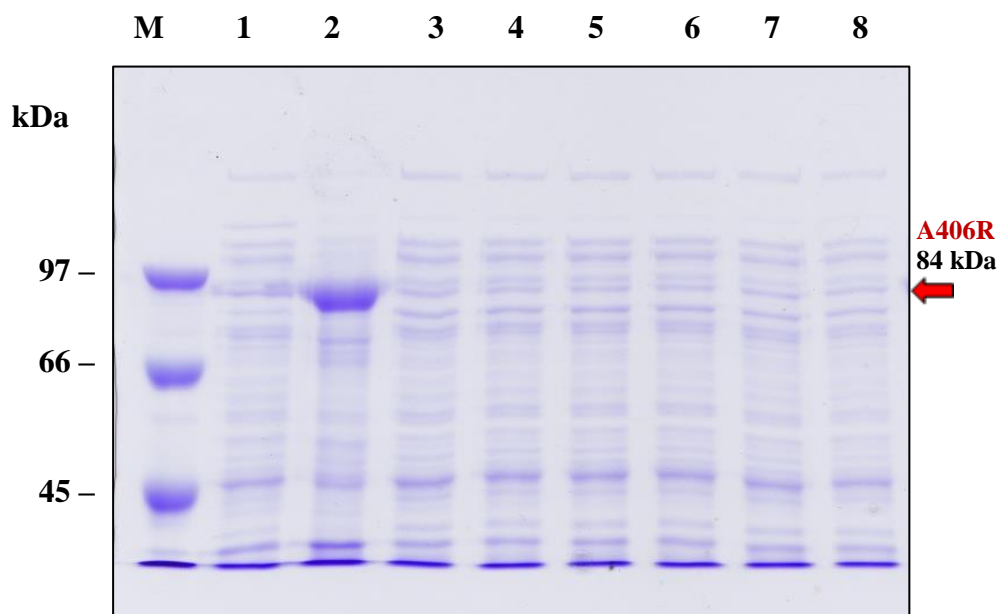


Figure 3. 41 SDS-PAGE of crude enzyme expressed from cells harboring A406R-CgAM. Cells were cultivated in LB broth containing 1% of glucose after induced with 1 mM IPTG at various times (condition 3)

Lane M = Low molecular weight protein marker

Lane 1 = 15 μ g protein of crude enzyme from A406R-CgAM after induced with 1.0 mM IPTG at 37 $^{\circ}$ C for 2 h

Lane 2 = 15 μ g protein of cell pellets from A406R-CgAM after induced with 1.0 mM IPTG at 37 $^{\circ}$ C for 2 h

Lane 3-8 = 15 μ g protein of crude enzymes from A406R-CgAM after induced with 1 mM IPTG at 16 $^{\circ}$ C for 2,4 6,8,14 and 18 h, respectively

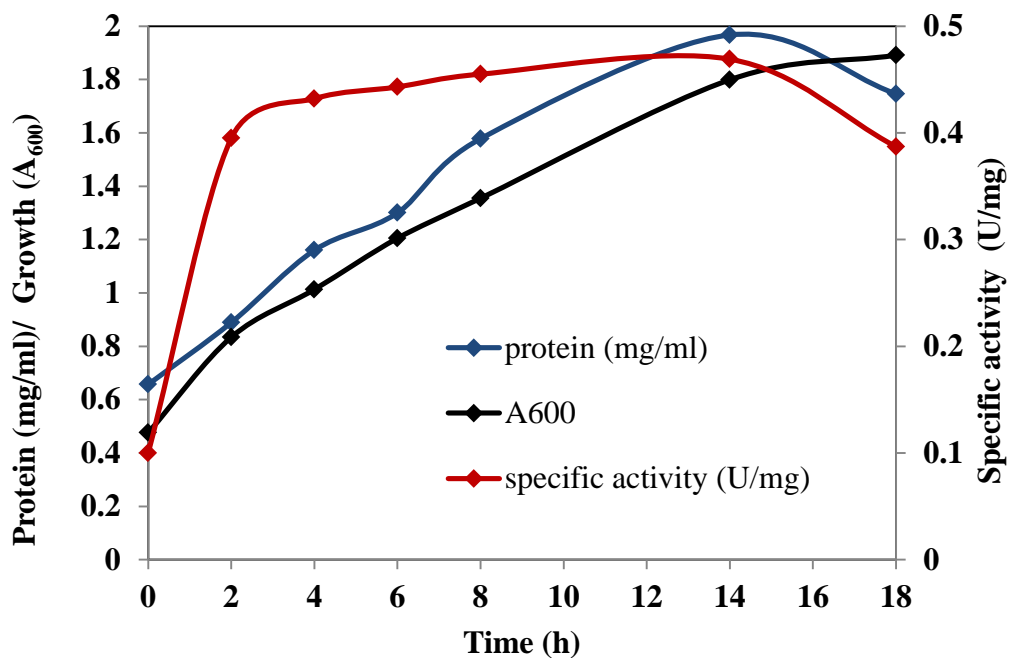


Figure 3. 42 Expression of recombinant A406R-CgAM in *E. coli* BL21 (DE3) by cultivation in Auto Induction Media (AIM) containing lactose without IPTG induction at 16 °C for various times (condition 4). The activity was measured by disproportionation assay.

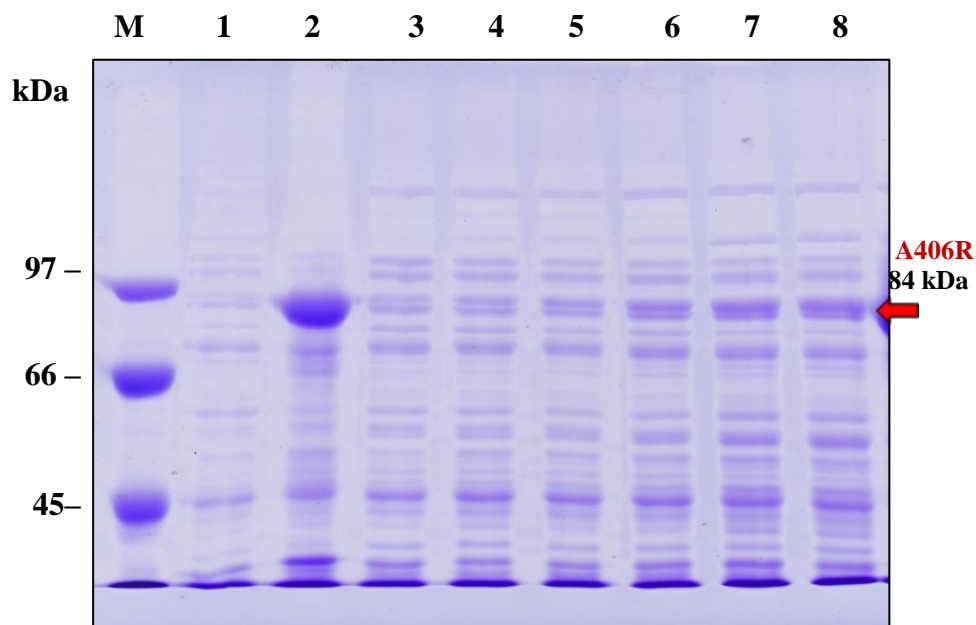


Figure 3. 43 SDS-PAGE of crude enzyme expressed from cells harboring A406R-CgAM. Cells were cultivated in Auto Induction Media (AIM) containing lactose without IPTG induction at 16 °C for various times (condition 4)

Lane M = Low molecular weight protein marker

Lane 1 = 15 µg protein of crude enzyme from A406R-CgAM after induced with 0.4 mM IPTG at 37 °C for 2 h

Lane 2 = 15 µg protein of cell pellets from A406R-CgAM after induced with 0.4 mM IPTG at 37 °C for 2 h

Lane 3-8 = 15 µg protein of crude enzyme from A406R-CgAM without IPTG induction at 16 °C for various times at 16 °C for 2, 4, 6, 8, 14 and 18 h, respectively

3.7.6 Purification of WT- and the four MT-CgAMs

3.7.6.1 Preparation of crude AMs

In the preparation of crude CgAMs, Auto Induction Media (AIM) containing lactose as described in section 2.9 was used for cultivation of WT-, A406H-, A406R-, A406F- and N287Y-CgAMs, cell pellets of recombinant clones at 12, 10.2, 10.2, 10.2 and 10.3 g were obtained from 1.2 liters of LB broth medium, respectively. Cells were resuspended in extraction buffer (1 g per 2.5 ml), then sonicated and centrifuged to get crude supernatant. Total protein in crude WT-, A406H-, A406R-, A406F- and N287Y-CgAMs were 701.3, 615.1, 628.6, 634.7 and 687.5 mg protein with 9482, 217.6, 202.4, 243.4 and 170.8 Units of disproportionation activity, respectively. Specific disproportionation activity for WT-, A406H-, A406R-, A406F- and N287Y-CgAMs were 13.5, 0.354, 0.322, 0.383 and 0.248 U/mg protein, respectively (Table 3.4).

3.7.6.2 Purification by HisTrap FFTM column

The crude enzyme from recombinant clones was dialyzed against 20 mM phosphate buffer, pH 7.4. The enzyme solution was applied onto a HisTrap FFTM column as described in 2.9.2. The chromatographic profile of WT-, A406H-, A406R-, A406F- and N287Y-CgAMs were similar to profile of WT-CgAM as shown in Figure 3.14. The unbound proteins were washed off the column by the binding buffer as a bulky broad protein peak. Then, the His-tag protein was eluted by elution buffer containing 500 mM imidazole, in a relatively small and narrow protein peak. The fractions that displayed high enzyme activity were pooled and dialyzed against 20 mM phosphate buffer, pH 7.4. The specific disproportionation activity of the

purified WT-, A406H-, A406R-, A406F- and N287Y-CgAMs were 45.6, 0.12, 0.03, 0.03 and 0.33 U/mg protein, respectively (Table 3.4).

3.7.6.3 Determination of enzyme purity of AMs

All of enzymes from each purification step were examined for protein pattern and purity by SDS-PAGE. All four purified MT-CgAMs showed a single protein band on SDS-PAGE with an apparent molecular mass of 84 kDa as similar to the WT- (Figure 3.44) indicating the success of purification by only one step of affinity chromatography.



Table 3. 4 Purification of WT-, A406H-, A406R-, A406F- and N287Y-CgAMs

| Enzyme CgAMs | Purification step | Total protein (mg) | Total activity ^a (U) [10 ²] | Specific activity ^a (U/mg protein) | Yield % | Purification fold |
|--------------|--------------------------|--------------------|--|---|---------|-------------------|
| WT | crude extract | 701 | 94.8 | 13.5 | 100 | 1 |
| | HisTrap FF TM | 74.6 | 34.0 | 45.6 | 36 | 3.4 |
| A406H | crude extract | 615 | 2.2 | 0.35 | 100 | 1 |
| | HisTrap FF TM | 23.0 | 0.03 | 0.12 | 1.4 | 0.34 |
| A406R | crude extract | 629 | 2.0 | 0.32 | 100 | 1 |
| | HisTrap FF TM | 26.6 | 0.01 | 0.03 | 0.5 | 0.1 |
| A406F | crude extract | 635 | 2.4 | 0.38 | 100 | 1 |
| | HisTrap FF TM | 18.2 | 0.01 | 0.03 | 0.4 | 0.1 |
| N287Y | crude extract | 688 | 1.7 | 0.25 | 100 | 1 |
| | HisTrap FF TM | 49.4 | 0.16 | 0.33 | 9.4 | 1.3 |

Crude of WT-, A406H-, A406R-, A406F- and N287Y-CgAMs were prepared from 1.2 liters of cell culture, respectively, which produced 12, 10.2, 10.2, 10.2 and 10.3 g of wet weight cells.

a = Assayed by disproportionation activity

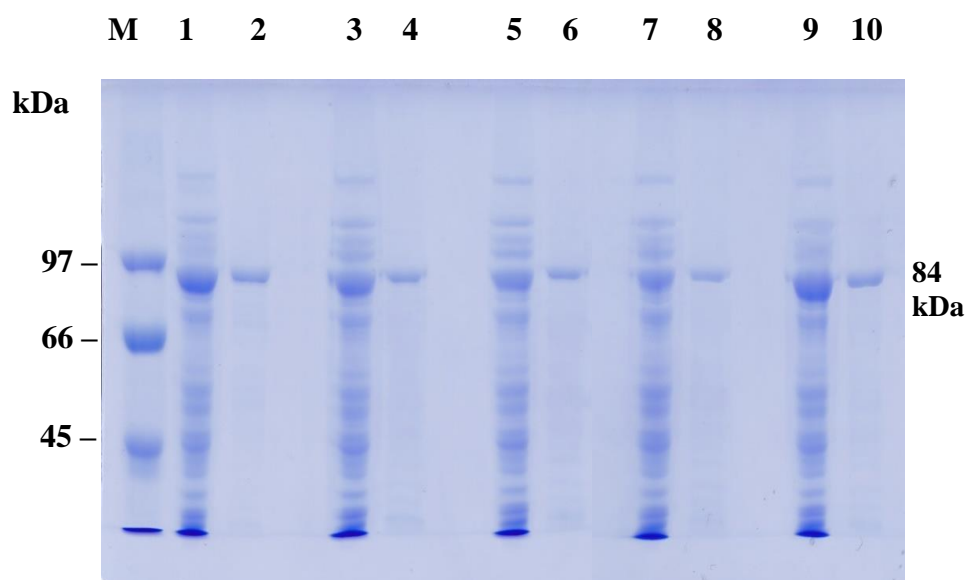


Figure 3. 44 SDS-PAGE of recombinant AMs stained by coomassie blue from each purification step

- Lane M = Low molecular weight protein marker;
- Lane 1, 3, 5, 7 and 9 = 15 μ g of crude WT-, A406H-, A406R-, A406F-, and N287Y-CgAMs, respectively
- Lane 2, 4, 6, 8 and 10 = 2 μ g of purified WT-, A406H-, A406R-, A406F-, and N287Y-CgAMs, respectively

3.8 Effect of mutation on enzyme characteristics

3.8.1 Various activities of amylomaltase

The effect of A406 and N287 mutations on various activities of CgAM was investigated, transglucosylation activities of the enzymes including starch transglucosylation and disproportionation of the A406H-, A406R-, A406F- and N287Y-CgAMs were diminished. In addition, cyclization activity of all MT-CgAMs could not be detected while hydrolysis activities were not different from that of the WT. It was observed that coupling and hydrolysis activities were low when compared to the other three activities for both WT- and MT-CgAMs (Table 3.5).

3.8.2 Optimum conditions and thermostability

In this experiment, the optimum conditions for two main activities, disproportionation and cyclization, of CgAMs were determined.

3.8.2.1 Effect of temperature

The effect of temperature for disproportionation of CgAMs were determined. For WT-, A406H-, A406R- and A406F-CgAM, the optimum temperature for disproportionation reaction (Figure 3.45A) was 45 °C, while for N287Y-CgAM, the value was 50 °C. The increase of 5 °C in optimum temperature was observed for N287Y-CgAM. The cyclization activity of CgAMs were also investigated, the optimum temperature of WT was 30 °C, the same result as described under section 3.6.2, while for MT-CgAMs, the cyclization activity at various temperatures could not be detected.

3.8.2.2 Effect of pH

The optimum pH for disproportionation activity of WT-, A406H-, A406R-, A406F- and N287Y-CgAMs were pH 6.0, pH 7.0, pH 7.0, pH 7.0 and pH 6.5, respectively (Figure 3.45B). The slight increase (+0.5 pH unit) in optimum pH was observed for N287Y-CgAMs while a shift of 1.0 pH unit in optimum pH was also observed with A406H-, A406R- and A406F-CgAMs, respectively. In addition, the optimum pH for cyclization activity of WT- and all MT-CgAMs were also investigated, the optimum pH of WT-CgAM was pH 6.0, the same result as described under section 3.6.2. While the cyclization activity of A406H-, A406R-, A406F- and N287Y-CgAMs could not be observed when incubated at pH 6.0 for various temperatures, small peaks of cyclization products from A406R and N287Y-CgAM at pH 8.0 and pH 9.0 could be detected. However, for A406H- and A406F-CgAMs, there were no cyclization activity at various pHs tested. (Figure 3.46).

3.8.2.3 Effect of temperature stability

For the effect of mutation on temperature stability, all the crude MT-CgAMs were more stable than the WT when starch transglycosylation activity was investigated (Table 3.6). Mutation at A406 to V, L, F and H resulted in stability increase at 40 °C for about two times at 30 min incubation while five to fifty times when incubated at 45 °C. Interestingly, A406R- and N287Y-CgAMs gave three times higher stability at 40 °C and sixty times higher at 45 °C when compared to the WT-enzyme. At 60 min incubation at 40 °C, the activity of all the MTs was stayed at the same level as those at 30 min, except for the A406V- and the WT-CgAMs of which about half of the activity was dropped.

When the purified enzymes were examined for thermostability, disproportionation reaction was measured. The result for A406V and A406L was shown in section 3.6.2.3. For A406H-, A406R-, A406F- and N287Y-CgAMs, thermostability was significantly higher than that of the WT. At 35 °C for a longer incubation time of 3 h, the remaining activities of WT-, A406H-, A406R-, A406F- and N287Y-CgAMs were 50.0%, 69.3%, 89.8%, 95.8% and 92.4%, respectively (Figure 3.47). At short incubation time for 30 min at 40 °C, the remaining activities of WT-, A406H-, A406R-, A406F- and N287Y-CgAMs were 10.0% , 17.7%, 39.0%, 56.0% and 35.8% while for a longer incubation time of 3 h, the remaining activities of WT-, A406H-, A406R-, A406F- and N287Y-CgAMs were 0%, 11.0% , 32.4%, 40.0% and 32%, respectively(Figure 3.48). In addition, at 45 °C for short incubation time of 10 min, the remaining activities of WT-, A406H-, A406R-, A406F- and N287Y-CgAMs were 0% , 10.0%, 30.0%, 50% and 29%, respectively, while for a longer incubation time of 3 h, the remaining activities of A406H-, A406R-, A406F- and N287Y-CgAMs were 7.5% , 23.4%, 29.0% and 25.8%, respectively (Figure 3.49). The single point mutation by substitution of A406 by F, R and H, and substitution of N287 by Y led to a higher effect on themstability.at 35 °C, 40 °C and 45 °C than that of WT-CgAM at a longer incubation for 3 h.

Table 3. 5 Specific activities of WT-, A406H-, A406R-, A406F- and N287Y- CgAMs

| Activity | Specific activity (U/mg) | | | | |
|---------------------------|--------------------------|-------------|-------------|-------------|-------------|
| | WT | A406H | A406R | A406F | N287Y |
| Starch transglucosylation | 54.3 ± 1.27 | 0.43 ± 0.04 | 0.2 ± 0.01 | 0.29 ± 0.02 | 0.82 ± 0.03 |
| Disproportionation | 44.9 ± 0.99 | 0.13 ± 0.01 | 0.04 ± 0.00 | 0.03 ± 0.00 | 0.34 ± 0.01 |
| Cyclization | 0.41 ± 0.03 | ND | ND | ND | ND |
| Coupling | 0.03 ± 0.00 | 0.01 ± 0.00 | 0.01 ± 0.00 | 0.01 ± 0.00 | 0.01 ± 0.00 |
| Hydrolysis | 0.02 ± 0.00 | 0.02 ± 0.00 | 0.02 ± 0.00 | 0.02 ± 0.00 | 0.02 ± 0.00 |

ND = not detectable

^aData are mean ± S.D. from three independent repeats.

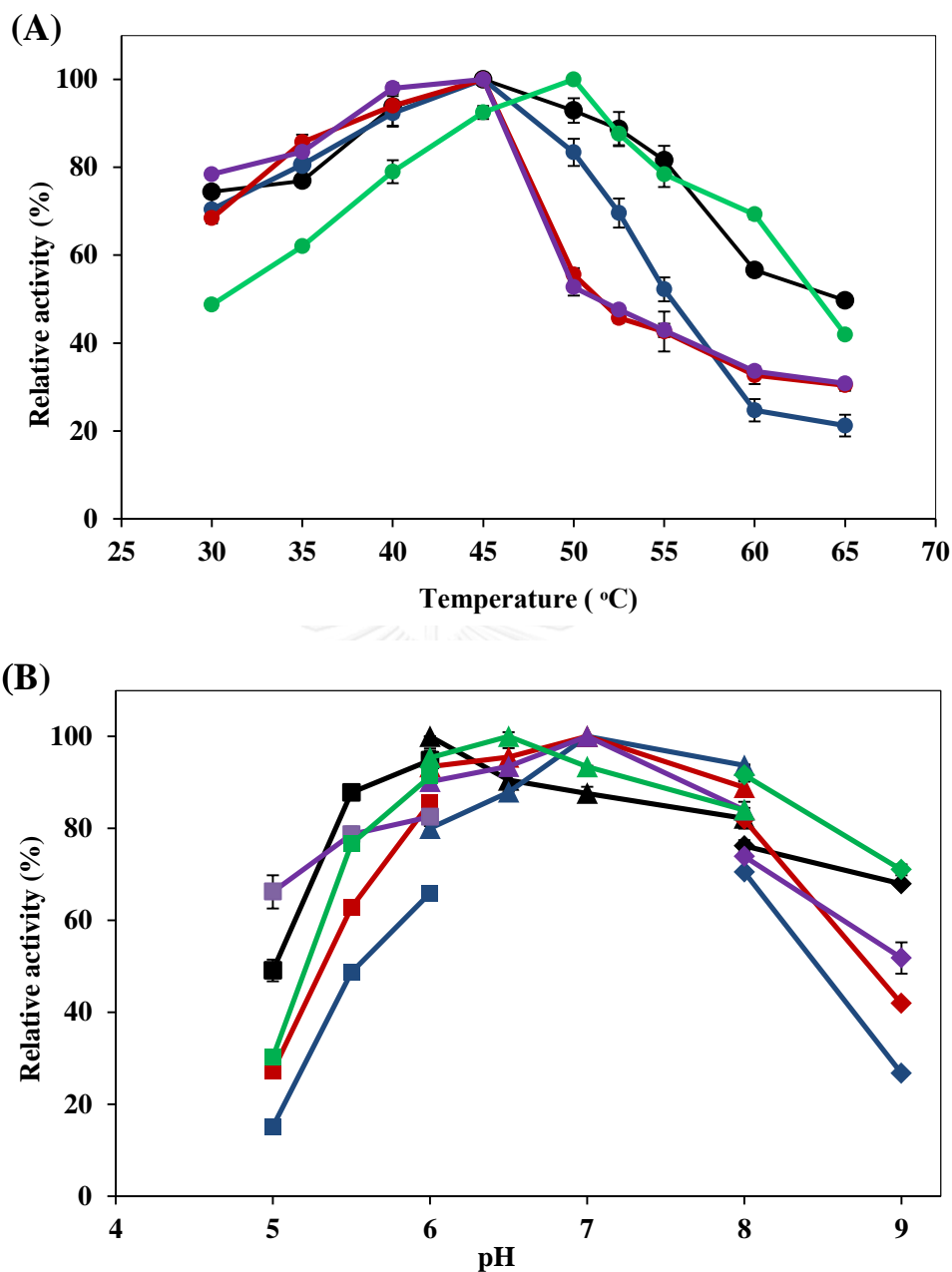


Figure 3.45 Effect of temperature (A) and pH (B) for WT- (black line), A406H- (blue line) A406R- (red line), A406F- (purple line) and N287Y- (green line) CgAMs on disproportionation reaction. The experiments were performed as described in Section 2.13.1. The buffers used were: acetate buffer (pH 4.0-6.0 ; ■), phosphate buffer (pH 6.0-8.0 ; ▲) and Tris-HCl buffer (pH 8.0-9.0 ; ◆). Data are shown as the mean \pm SD and are derived from three independent repeats.

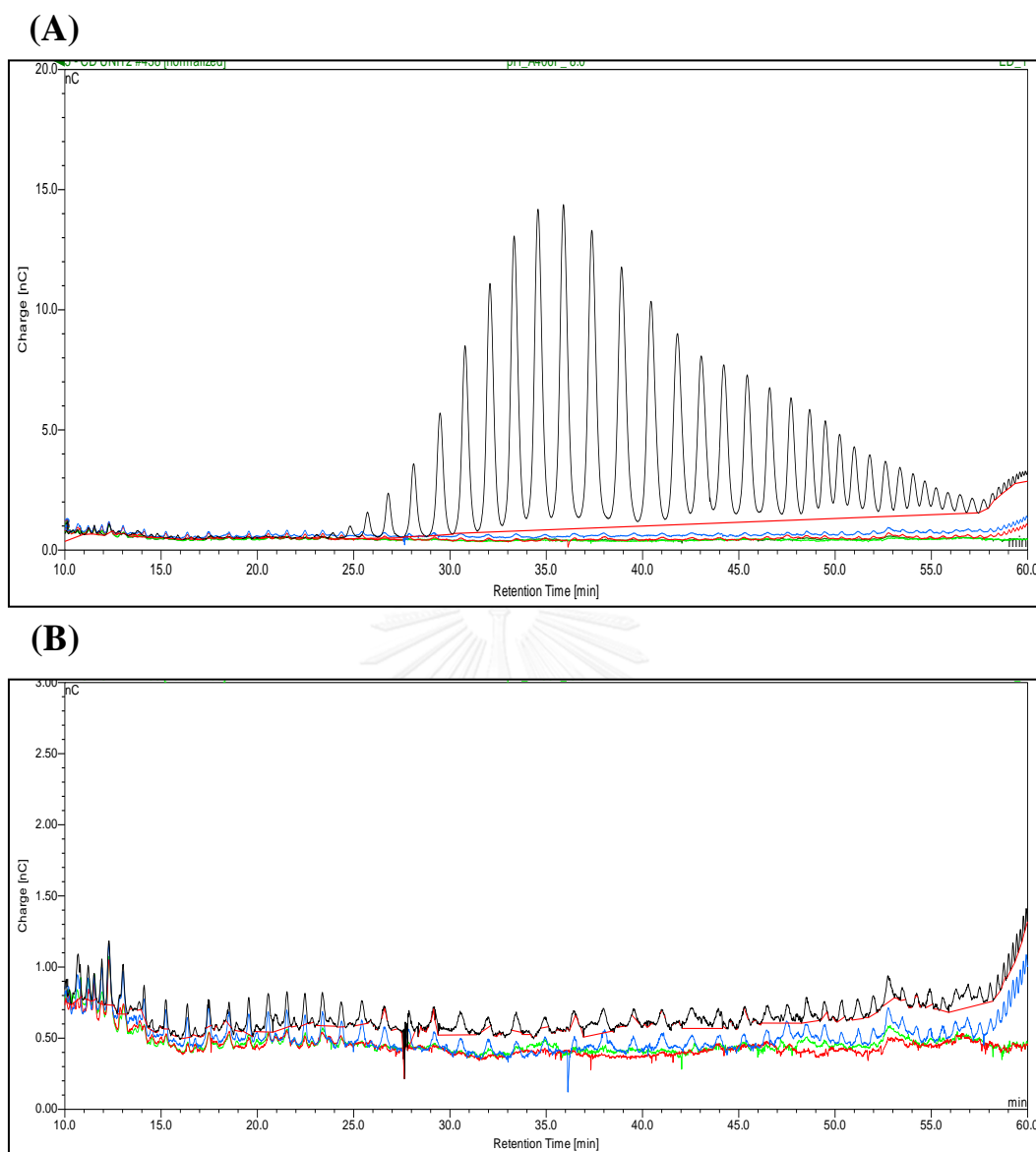


Figure 3. 46 (A) HPAEC analysis of the LR-CD products. 0.2% (w/v) pea starch was incubated with 0.3 mg protein of enzyme at 30 °C , pH 8.0 for 90 min. The profile with high peaks is products from the WT while the trace lines are from MT-CgAMs (B) The LR-CD products from (A) when the high peaks from WT-CgAM was left out, A406H- (green line), A406R- (blue line), A406F- (red line) and N287Y- (black line) CgAMs.

Table 3. 6 Temperature stability of crude WT- and MT-CgAMs.

Crude enzymes at 5U/mg protein were pre-incubated at 40 °C /45 °C for 30 or 60 min, then starch transglucosylation assay was determined.

| CgAM | Remaining activity (%) | | |
|-------|------------------------|--------|--------|
| | 40 °C | | 45 °C |
| | 30 min | 60 min | 30 min |
| WT | 45 | 20 | 2.0 |
| A406V | 79 | 39 | 10 |
| A406L | 80 | 60 | 37 |
| A406H | 90 | 80 | 90 |
| A406R | 149 | 151 | 130 |
| A406F | 67 | 61 | 87 |
| N287Y | 155 | 149 | 119 |

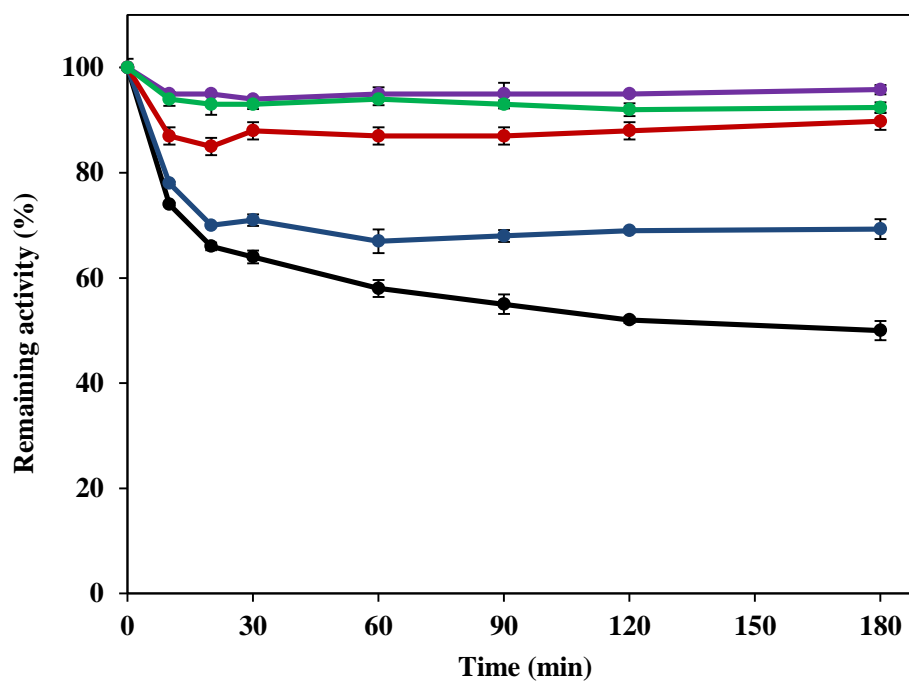


Figure 3. 47 Effect of temperature stability of WT- (black line), A406H- (blue line) A406R- (red line), A406F- (purple line) and N287Y- (green line) CgAMs on disproportionation reaction. Each purified CgAM at 75 ug was pre-incubated for various times at 35 °C. Determination of remaining activity was assessed by disproportionation reaction as described in Materials and Methods. Data are shown as the mean \pm SD and are derived from three independent experiments.

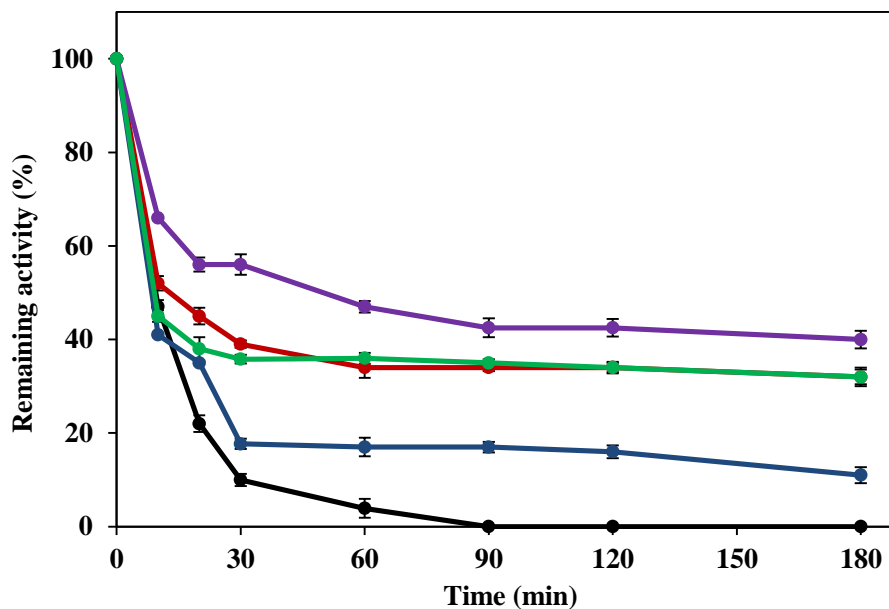


Figure 3. 48 Effect of temperature stability of WT- (black line), A406H- (blue line) A406R- (red line), A406F- (purple line) and N287Y- (green line) CgAMs on disproportionation reaction. Each purified CgAM at 75 ug was pre-incubated for various times at 40 °C. Determination of remaining activity was assessed by disproportionation reaction as described in Materials and Methods. Data are shown as the mean \pm SD and are derived from three independent experiments.

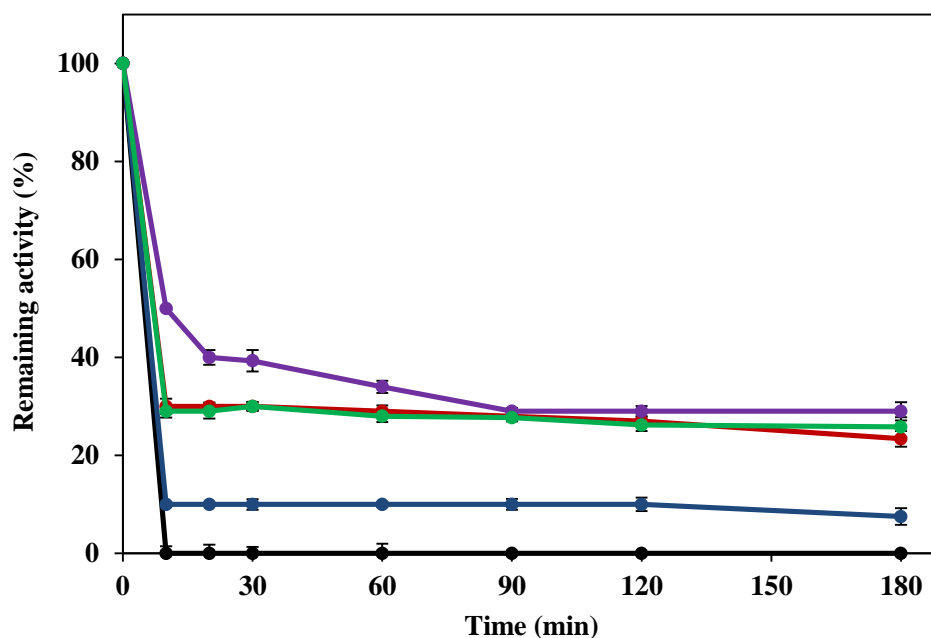
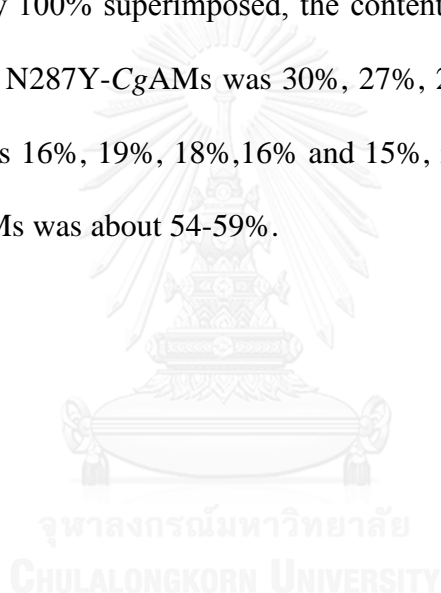


Figure 3. 49 Effect of temperature stability of WT- (black line), A406H- (blue line) A406R- (red line), A406F- (purple line) and N287Y- (green line) CgAMs on disproportionation reaction. Each purified CgAM at 75 ug was pre-incubated for various times at 45 °C. Determination of remaining activity was assessed by disproportionation reaction as described in Materials and Methods. Data are shown as the mean \pm SD and are derived from three independent experiments.

3.8.3 Enzyme conformation

To investigate whether A406H-, A406R-, A406F- and N287Y mutation results in a conformational change in protein, analysis of secondary structure was performed using circular dichroism (CD) spectrometer scanning from 190 to 250 nm. The CD spectra of all mutated and the WT-CgAMs were compared at pH 6.1 (Figure 3.50). The result showed that the spectral difference from the WT was clearly seen for all MT-CgAMs, while the CD spectra of A406H-, A406R-, A406F- and N287Y-CgAMs at pH 6.1 were nearly 100% superimposed, the content of α -helix of WT-, A406H-, A406R-, A406F- and N287Y-CgAMs was 30%, 27%, 26%, 26% and 26% while the content of β -sheet was 16%, 19%, 18%, 16% and 15%, respectively. The random coil structure of the all AMs was about 54-59%.



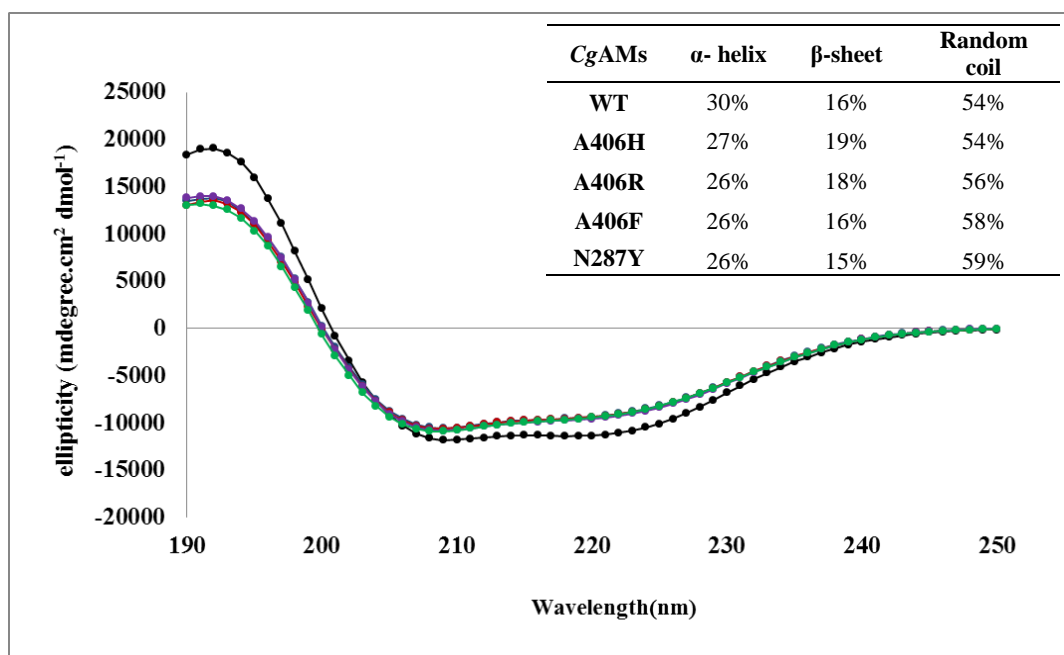
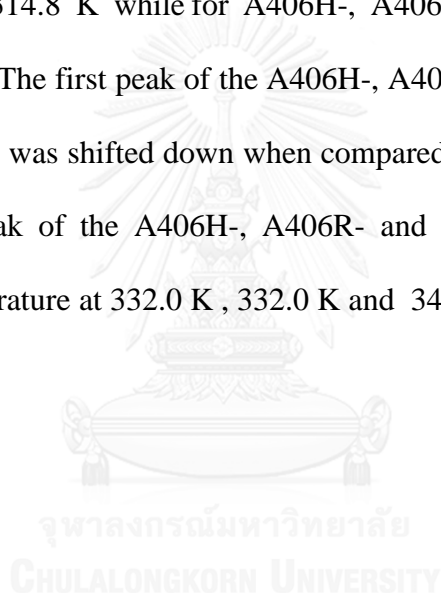


Figure 3. 50 Circular dichroism spectra and the predicted secondary structural compositions of WT- (black line), A406H- (blue line) A406R- (red line), A406F- (purple line) and N287Y- (green line) CgAMs

3.8.4 Differential scanning calorimetry

In this work, DSC was performed in the temperature range of 283 to 373 K in an attempt to compare thermal stability between the WT- and MT-CgAMs. It was observed that DSC data at all scanning rates for CgAMs indicated the irreversible transition. The thermal transition curves from 285 to 365K using the scanning rate of 90 K/h for WT and MT-CgAMs at pH 6.1 were plotted (Figure 3.51), The result showed that, the heat capacity profiles of the WT-CgAMs gave only one main peak temperature (T_p) at 314.8 K while for A406H-, A406R- and N287Y-CgAMs, two peaks were obtained. The first peak of the A406H-, A406R- and N287Y-CgAMs was observed at 310 K, T_p was shifted down when compared to the one main peak of WT, while the second peak of the A406H-, A406R- and N287Y-CgAMs were shifted towards higher temperature at 332.0 K, 332.0 K and 340.5 K, respectively



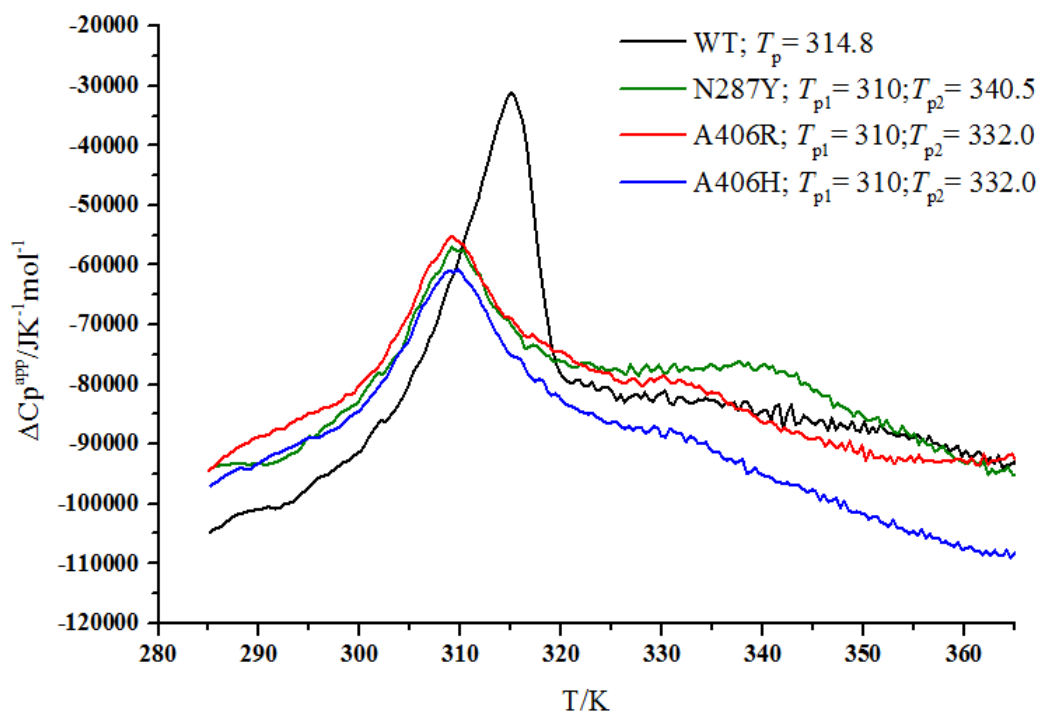


Figure 3. 51 Thermal transition curves of WT- (black line), A406H- (blue line) and A406R- (red line) and N287Y- (green line) CgAMs at pH 6.1 with a scan rate of 90 K/h from DSC measurements. T_p = peak temperature

3.8.5 Substrate specificity

The substrate specificity for disproportionation reaction using malto-oligosaccharide substrates (maltose [G2] to maltoheptaose [G7]) was analyzed. Maltotriose (G3) was the most efficient substrate while maltose was poor substrate for both WT- and MT-CgAMs. For WT-CgAMs, the substrate specificity was in the order of $G3 > G4 > G5 > G6 > G7 \approx G2$ while the A406H-CgAMs showed a preferred substrate order of $G3 > G5 > G4 > G6 > G7 > G2$. In addition, A406R-, A406F- and N287Y showed the same preferred substrate order of $G3 = G5 > G4 > G6 > G7 > G2$. (Figure 3.52).



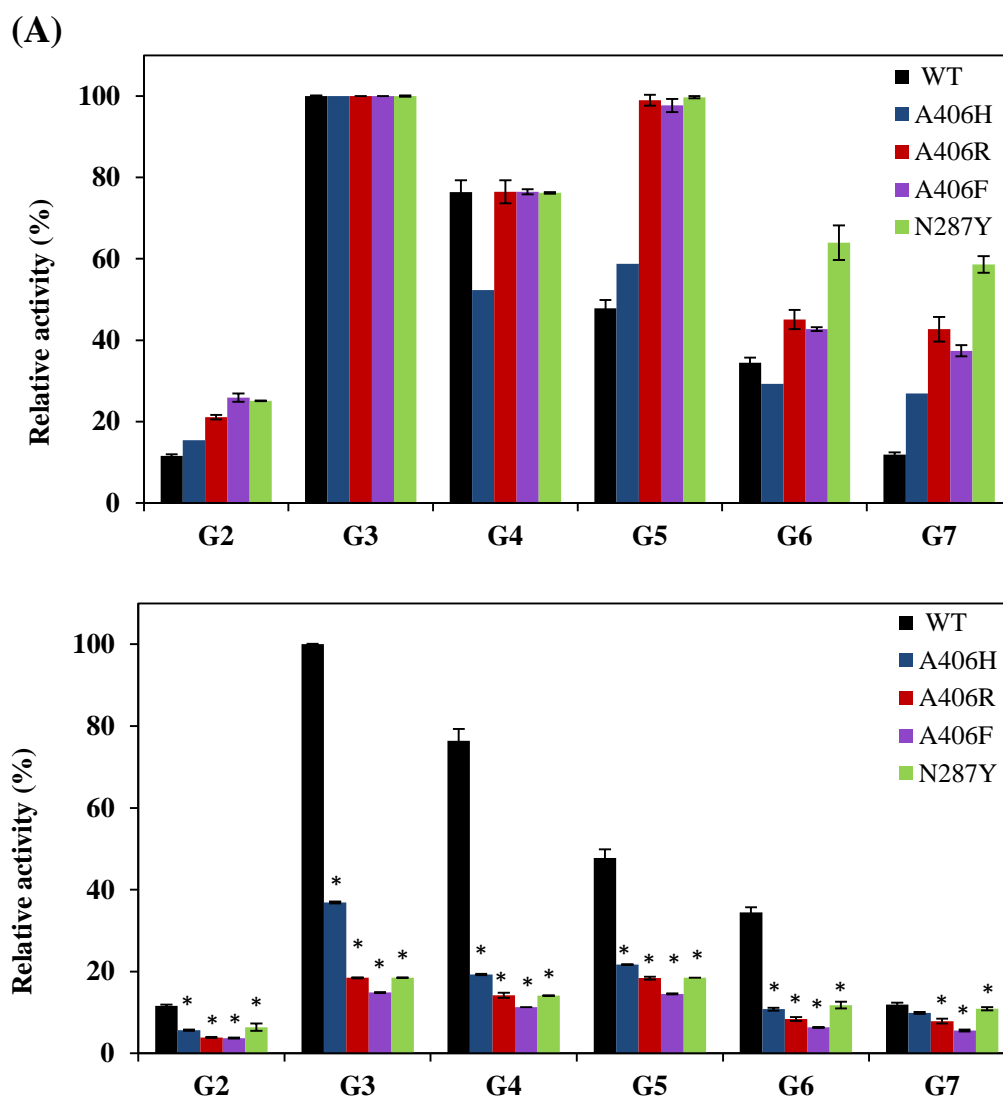


Figure 3. 52 Substrate specificity of WT-, A406H-, A406R-, A406F- and N287Y-CgAMs in disproportionation reaction using maltooligosaccharide (maltose [G2] to maltoheptaose [G7]) as the substrate. (A) The highest activity of each CgAM was set as 100% (B) The activity of WT-CgAM on G3 substrate was set as 100%. Data are shown as the mean \pm SD and are derived from three independent experiments. * $P < 0.05$ (Student's *t*-Test) with respect to the disproportionation reaction of WT-CgAM.

CHAPTER IV

DISCUSSION

In our previous study, a novel AM from *C. glutamicum* (a mesophilic bacteria) was cloned and characterized. The *C. glutamicum* amyloamylase gene (*CgAM*) had an ORF of 2,121 bp and was deduced into a protein with 706 amino acids. The enzyme *CgAM* is larger in size and has a low amino acid sequence identity to those well characterized AMs from *Thermus*. Our group had successfully crystallized this enzyme (Srisimarath *et al.*, 2013) and at present is prepared to publish the three-dimensional structure. *CgAM* could produce LR-CDs with a DP of 18-55 and the enzyme was stable at temperature only up to 30 °C (Srisimarath *et al.*, 2012; Srisimarath *et al.*, 2011). It is well accepted that the thermostable enzymes with favorable properties have a great potential for industrial use e.g. as stable catalysts in food processing: clarification of fruit juice, dough making and starch processing (Lehmann *et al.*, 2000). In this work, our aim is to increase thermostability of *CgAM*, however, due to low similarity of *CgAM* to AMs from *Thermus* with known 3D-structures, random mutagenesis through the error-prone PCR is a method of choice for introducing mutation in this enzyme (Fujii *et al.*, 2005b; Pritchard *et al.*, 2005). We here describe screening for the highest thermostable mutated clone from random mutagenesis, sequencing to identify the site of mutation, investigating the importance of this residue by site directed mutagenesis, and comparing properties of the mutated *CgAMs* to that of the wild-type enzyme.

4.1 Mutagenesis for the improvement of thermostability of *CgAM* gene

4.1.1 Modification of *CgAM* gene using error-prone PCR technique

Error-prone PCR is a technique commonly used for random mutagenesis in the attempt to improve the protein or enzyme functions of interest, without a structural understanding of the target protein/enzyme. The technique involves reducing the fidelity of DNA polymerase during PCR of the targeting gene by adding manganese ion (MnCl_2) and biasing the dNTP concentration (Mabrouk *et al.*, 2013; Melzer *et al.*, 2015; Pritchard *et al.*, 2005). Previously, several enzymatic properties such as activity (Fujii *et al.*, 2005a; Kobayashi *et al.*, 2010), thermostability (Batra and Mishra, 2013; Mabrouk *et al.*, 2013; Nakaniwa *et al.*, 2004), alkali- or acid-stability (Melzer *et al.*, 2015), and product selectivity were improved by this technique (Fujii *et al.*, 2005b; Melzer *et al.*, 2015).

In this work, random mutagenesis of *CgAM* gene using error-prone PCR technique was firstly employed in the aim to increase thermostability of the enzyme *CgAM*. The various concentrations of MnCl_2 (50, 100 and 200 μM) were added into PCR reaction. The Mn^{2+} doping reaction yielded higher amount of PCR product than those of the control reaction without the addition of MnCl_2 (Figure 3.2), this may due to the fact that Mn^{2+} also acts as a cofactor for *Taq* DNA polymerase, subsequently enhanced the polymerase activity and resulted in higher amount of PCR product (Nakapong, 2011) In addition, the mutation frequency could be controlled by varying the concentration of Mn^{2+} . After thirty mutated clones from each MnCl_2 concentration were randomly screened for thermostability of *CgAM*, the disproportionation activity of the crude enzymes from WT- and MT-*CgAM*s were determined. The enzyme activity was observed from ten, five and two mutated clones that were obtained from

error-prone PCR using 50, 100 and 200 μM of MnCl_2 , respectively while other clones showed no activity, possibly due to the higher MnCl_2 concentration added in PCR reaction, the higher frequency of mutation in *CgAM* gene (Fujii *et al.*, 2004). Thus, 50 μM of MnCl_2 was appropriated for random mutation in *CgAM* gene. In this study a MT-*CgAM* clone (number 50-11) obtained from error-prone PCR using 50 μM of MnCl_2 was selected for further characterization because it showed highest activity and thermostability, significantly higher than the wild-type which showed no activity at 50 °C. The nucleotide sequence of the MT-*CgAM* gene from this clone was then determined as a single mutation at residue 406 from Ala (A) to Val (V).

4.1.2 Site directed mutagenesis

For site directed mutagenesis, the PCR reaction and conditions were employed using Quick Change site-directed mutagenesis protocol. The whole plasmid implication and incorporation of mismatch nucleotides were simultaneously performed using DNA polymerase with proof-reading activity (*pfu* DNA polymerase) because it is useful for polymerization reaction requiring high fidelity synthesis (Lundberg *et al.*, 1991). Only 16-18 PCR cycles were performed to minimize PCR error. To remove the parental DNA, the dam methylated DNAs were digested with *DpnI*, following by directly transformed in to *E. coli* competent.

A406V-*CgAM* was obtained from screening for thermostable clones using random mutagenesis. To confirm this mutation and further investigate the effect of hydrophobic substitution at this position on thermostability of *CgAM*, site-directed mutagenesis was performed whereby A406 was replaced by Val as well as Leu (L). We found that A406V- and A406L- were more thermostable than the WT- enzyme, and

interestingly, the two MT-CgAMs showed higher intermolecular transglucosylation activity. The results drew our interest to explore more on the involvement of the amino acid position at 406 on the enzyme characteristics. The superimposed structures of CgAM with TaAM (Figure 3.27) showed that Ala406 of CgAM is corresponded to His233 of TaAM, site-directed mutagenesis was then performed whereby A406 was replaced by His (H). Mutation to Arg (R) and Phe (F) were also performed since Arg is known to involve with protein stability (Deng *et al.*, 2014) while Phe is aromatic hydrophobic. In addition, the Asn287 of CgAM is in the corresponded position to Tyr101 of TaAM (Fujii *et al.*, 2007) of which the change in this residue was reported to affect thermostability and cyclization activity of TaAM, hence substitution by Tyr (Y) at N287 of CgAM was also performed in this study. In previous reports on other enzymes, the thermostability of L-asparaginase from *E. chrysanthemi* was improved significantly by replacement of Asp133 with Val (Kotzia and Labrou, 2009), a single amino acid substituted in four mutated haloperoxidase G106S, R114H, N146H and V148I from *Streptomyces aureofaciens* BPO-A1 was shown to improve thermostability and organic solvent stability of this enzyme (Yamada *et al.*, 2014).

4.1.3 Expression of WT- and MT-CgAMs

E. coli has been commonly used as host for AMs expression, gene expression was induced by appropriate concentration of IPTG for each AM source. All expressed AMs by our research group are intracellular enzyme as previously reported (Kaewpathomsri *et al.*, 2015; Srisimarath *et al.*, 2011; Tantanarat *et al.*, 2014). The recombinant WT-CgAM, A406V-, A406L-, A406H-, A406R-, A406F- and N287Y-CgAMs were expressed in *E. coli* BL21 (DE3) using expression vector pET-19, gene

expression was induced by adding 0.4 mM of IPTG. Unfortunately, in this condition, A406H-, A406R-, A406F- and N287Y-CgAMs were not overexpressed in soluble fraction, the enzymes was observed as inclusion body (Figure 3.36B), while WT-, A406V- and A406L-CgAMs showed higher expression in the soluble protein form at around 20-30% (Figure 3.36A). The expression of some proteins in *E. coli* may yield insoluble aggregates that are known as inclusion bodies. The insoluble proteins are in general misfolded that might be possibly caused from the overexpression of recombinant protein. To overcome this problem, the expression conditions were improved by choosing an alternative *E. coli* strain or performing induction at low temperature (Esposito and Chatterjee, 2006). Thus, the change of the condition for protein expression of the four mutated enzymes was investigated by cultivation in 4 conditions as decried in section 3.7.5.1. The lowering temperature expression was successful to obtain soluble protein from condition 1 and 4 when the cells were cultivated at 37 °C in LB broth and Auto Induction Media (AIM) containing lactose, respectively, and then changed to 16 °C for protein expression. However, the highest enzyme activity was detected from condition 4 after growing cells at 16 °C for 14 h without IPTG induction. Thus, the condition 4 was selected for enzyme induction in further experiments for WT-, A406H-, A406R-, A406F- and N287Y-CgAMs. These results suggest that the overexpression might influence the initial folding of enzyme resulting in the failure of the molecule to reach the native state at 37 °C.

4.2 Purification of recombinant WT- and MT-CgAMs

The recombinant WT- and MT-CgAMs containing pET-19b inserted with *CgAM* gene were expressed as enzyme containing his-tag residues at N-terminal. All

enzymes were purified by HisTrap FFTM which is a prepacked column containing 90 μm highly cross-linked agarose bead with an immobilized chelating group. The matrix has been charged with Ni^{2+} -ion. This column selectively binds histidine-tag protein which has specific affinity for Ni^{2+} . The WT- and all MT- enzymes were purified to homogeneity with about 36 to 38% yield for the WT-, A406V- and A406L-, 9% yield for N287Y- and very low yield of 0.4 to 1.4% yield for A406H-, A406R-, A406F-CgAMs, respectively (Table 3.1 and Table 3.4). In previous reports, the WT-AM from *C. glutamicum* ATCC 13032 was 10.8-fold purified with 30.2% yield (Srisimarat *et al.*, 2011), while AM from *Synechocystis* sp. PCC 6803 was 2.9-fold purified with 84.5% yield (Lee *et al.*, 2009) and that from *T. brockianus* was 35-fold purified with 67% yield after heat treatment and Ni^{2+} -NTA column chromatography (Bo-young *et al.*, 2006).

4.3 Characterization of recombinant WT- and MT-CgAMs

4.3.1 Molecular weight

In SDS-PAGE analysis, the purified enzyme showed a single protein band on the gel (Figure 3.15 and Figure 3.45). This result indicated that the enzyme was highly purified. The molecular weight of WT- and MT-CgAMs containing his-tag residues was 84 kDa, similar to previous report (Srisimarat *et al.*, 2011). The size of CgAM was closed to $4\alpha\text{GTase}$ from *Thermococcus litoralis* (79 kDa, (Xavier *et al.*, 1999)), but different from *T. aquaticus* (57 kDa, (Terada *et al.*, 1999)), *Synechocystis* sp. PCC 6893 (57 kDa, (Lee *et al.*, 2009)) and *T. filiformis* JCM 11600 (55 kDa, (Kaewpathomsri *et al.*, 2015)), as well as plant D-enzymes from potatoes which was 60 kDa (Takahashi *et al.*, 1993). The result indicated that, AM from a mesospheric

bacteria *C. glutamicum* is bigger in size than that of the AMs from thermophilic bacteria *Thermus* sp.

4.3.2 Various activities of amyloamylase

The effect of A406 and N287 mutations on various activities of CgAM was investigated, A406V- and A406L-CgAMs showed higher specific activities for starch transglucosylation (2.8 and 2.1-fold) and disproportionation (2.1 and 1.4-fold) than those of the WT, while cyclization, coupling and hydrolysis activities were not different from the WT (Table 3.2). It was observed that coupling and hydrolysis activities were low when compared to the other three activities for both WT- and MT-CgAMs, this behavior is known as a characteristic of amyloamylase in general (Fujii *et al.*, 2007; Hansen *et al.*, 2008; Kaewpathomsri *et al.*, 2015; Przylas *et al.*, 2000b; Srisimararat *et al.*, 2011).

Residue A406 is buried inside the protein structure and approximately 14 Å away from the active site (Figure 4.1A). The amino group of A406 forms a H-bond with the carboxyl group of P429 (with a distance of 3.0 Å) while the carboxyl group of A406 forms a H-bond with the amino group of A409 (with a distance of 3.2 Å) (Figure 4.1B). It is unlikely that substitution of alanine at position 406 of CgAM to valine or leucine will create new H-bond formation with other amino acid residues, we found that the H- bonding to nearby residues of A/V/L at position 406 was the same (Figure 4.2). However, it is previously shown that hydrophobic interactions are important for stability of globular conformations (Pace *et al.*, 2011; Takano *et al.*, 1998). Therefore, it is possible that a change of hydrophobic interactions around this position may contribute to improvement of conformation stability. In Table 3.3,

A406V and A406L mutants showed higher catalytic efficiency than the wild-type enzyme. A406V and A406L mutants had much higher k_{cat} than that of the wild-type enzyme, while their K_m values were similar to that of the WT-CgAM. It is likely that improvement of conformation stability of A406V- and A406L-CgAMs affected the turnover rate of the enzyme but not the binding affinity. A406 is distant from the substrate binding site and hence it is unlikely that A406V and A406L mutation will directly interfere with substrate binding. Instead, A406V and A406L mutation might increase protein stability and this affects the turnover rate of the enzyme.

However, transglucosylation activities of the enzymes including starch transglucosylation, and disproportionation of the A406H-, A406R-, A406F- and N287Y-CgAMs were diminished. In addition, cyclization activity of all these four MT-CgAMs could not be detected while hydrolysis activities were not different from that of the WT (Table 3.5). It is possible that substitution of alanine at position 406 of CgAM by His (H), Arg (R) and Phe (F) changed hydrophobic interactions around this position and might contribute to conformational change of the enzymes, thus led to the change in substrate binding site and enzyme activity.

In addition, the N287 of CgAM is in the corresponded position to Tyr101 of TaAM which locates in the secondary binding site (Fujii *et al.*, 2007). The change in this residue was reported to affect cyclization activity of TaAM. Our structural analysis comparing the structures between N287Y and WT-CgAMs is described in Section 4.3.3. The result showed that substitution by Tyr (Y) at N287 of CgAM resulted in conformational change and be a cause of the decrease in enzyme activity.

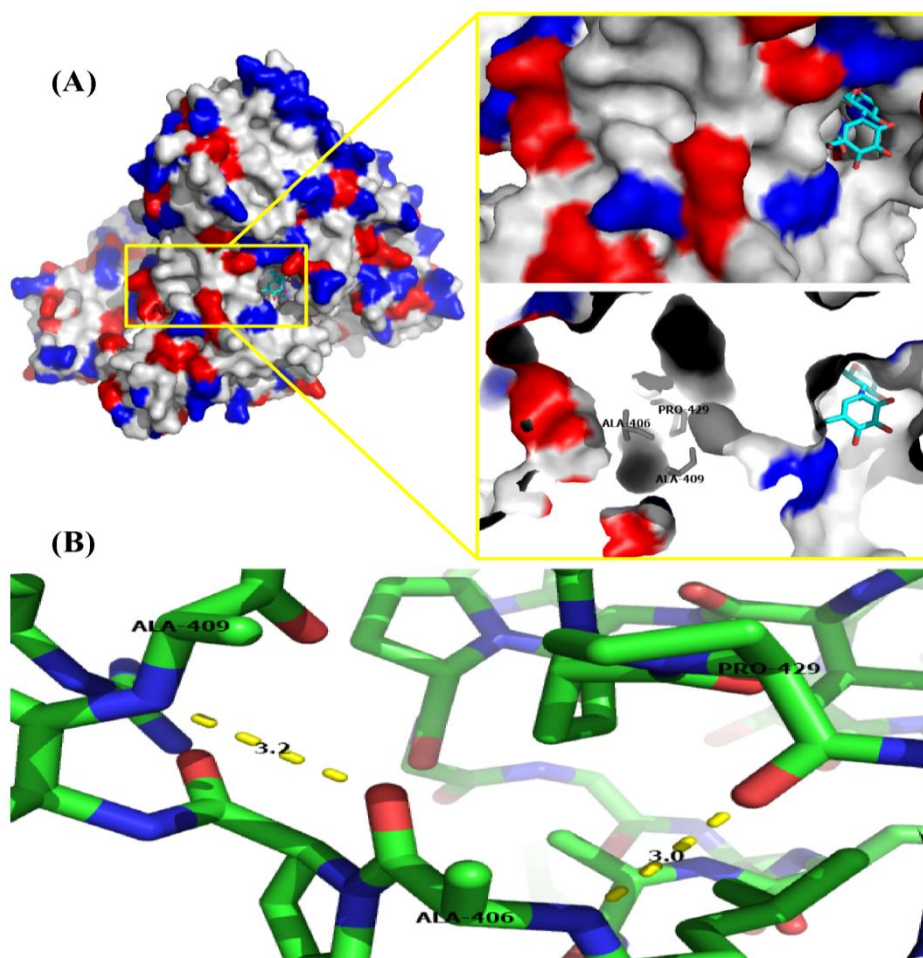


Figure 4.1 Proposed binding of acarbose in the active site of CgAM

(superimposed of PDB entry 1ESW on CgAM structure (Przylas *et al.*, 2000a). (A) Surface of CgAM is displayed with hydrophobic and polar residues in grey, negative residues in blue and positive residues in red. A406 is buried within the protein structure and approximately 14 Å away from the active site. Acarbose is shown in cyan. (B) The amino group of A406 forms a H-bond with the carboxyl group of P429 while the carboxyl group of A406 forms a H-bond with the amino group of A409. The important residues are displayed as stick, amino and carboxyl groups are shown in blue and red, respectively. Hydrogen bonds are shown as dashed yellow line.

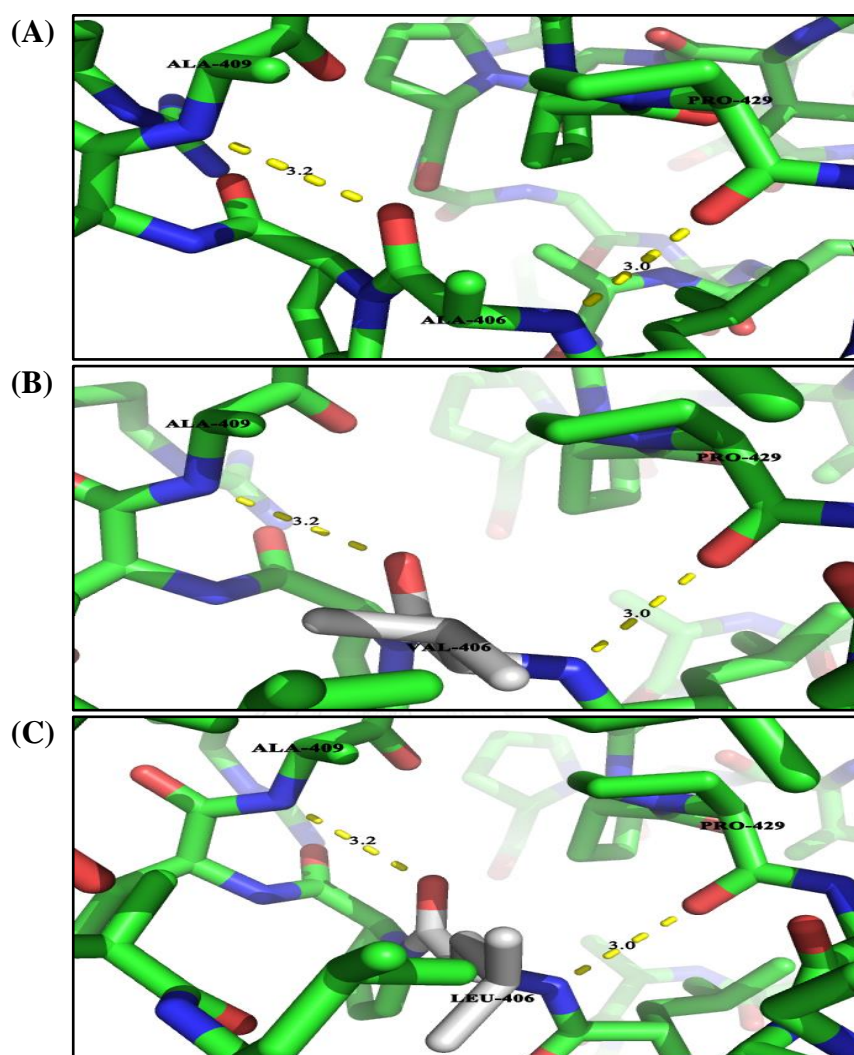


Figure 4.2 Proposed of the hydrogen bonding interactions between the amino group of (A) A406, (B) V406 and (C) L406 with the carboxyl group of P429 and the carboxyl group of (A) A406, (B) V406 and (C) L406 with the amino group of A409. The important residues are displayed as stick, amino and carboxyl groups are shown in blue and red, respectively, hydrogen bonding interactions are shown by dashed yellow line.

4.3.3 Enzyme conformation

To investigate whether A406 and N287 mutation results in a conformational change of protein, analysis of secondary structure of CgAMs was performed by circular dichroism technique. The result showed that the CD spectra of WT-, A406V- and A406L-CgAMs at pH 6.1 were nearly 100% superimposed (Figure 3.19). The composition of the secondary structure of WT-CgAM obtained is the same as that previously reported (Rachadech *et al.*, 2015). The change in transglucosylation activities of the A406V- and A406L-CgAMs shown in Table 3.2 thus did not result from the change in the secondary structure of the enzymes. However, in the superimposed structures of WT- (cyan), A406V- (purple) and A406L-CgAMs (red) (Figure 4.3), a few parts are not superimposed especially the cyan and purple in the closer area to active site where acarbose binds (beta strands to the lower right and the coil in upper right and also coil in the left, together with structure around position 406), while differences of A406L (red) and WT (cyan) are seen only in area around position 406. These evidences suggest some conformation change did occur especially in A406V-CgAM.

The somewhat spectral difference from the WT was seen for A406H-, A406R-, A406F- and N287Y-CgAMs while the CD spectra of all four MT-CgAMs at pH 6.1 were nearly 100% superimposed (Figure 3.51). However, the content of the secondary structures determined for all enzymes was not much different from the WT. When three-dimensional modeling structure of WT- and N287Y-CgAMs were compared (Figure 4.4), we could not obtain the superimposed structures due to model error. Thus both structures were separately shown, differences in some parts were observed, especially around position 287 and the active site region. It is likely that, the change

in transglucosylation activities of the A406H-, A406R-, A406F- and N287Y-CgAMs shown in Table 3.5 thus resulted from the change in conformation of the enzymes.



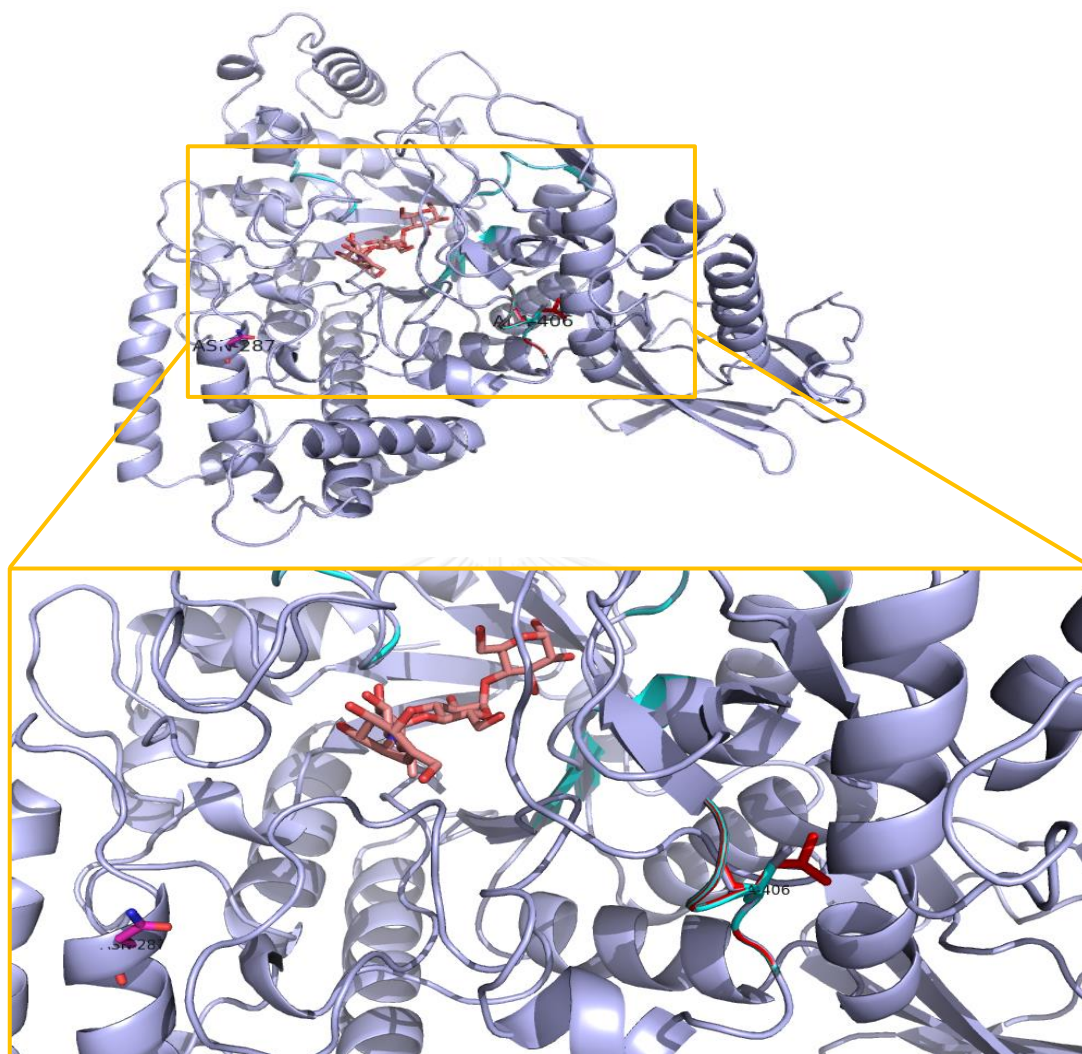


Figure 4.3 The superimposed structures of WT- (cyan), A406V- (purple) and A406L-CgAMs (red). The enzyme structures are displayed as secondary structure generated by PDB Swiss Viewer Program. The important residues 406 are displayed as stick and colored. The active center of CgAM is located at the center of the modeled oligosaccharide shown in red.

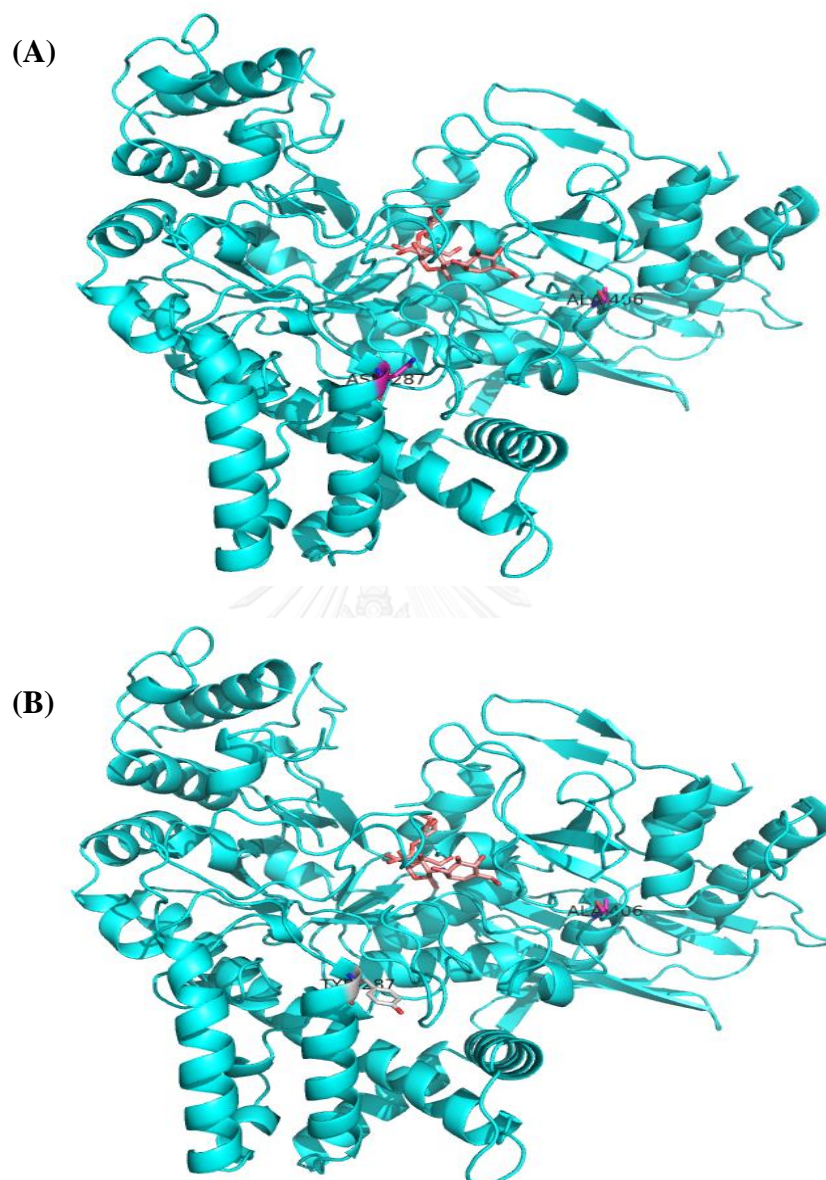


Figure 4.4 Three-dimensional modeling structure of AM from *C. glutamicum* (CgAM) generated by PDB Swiss Viewer Program (A) WT-CgAM and (B) N287Y-CgAM. The active center of CgAM is located at the center of acarbose shown in red.

4.3.4 Optimum conditions and thermostability

The increase of 7.5 °C and 5 °C in optimum disproportionation temperature was observed for A406V- and A406L-CgAM, respectively, with the slight increase (+ 0.5 pH unit) in optimum pH. Only A406V showed 5 °C higher in optimum cyclization temperature (Figure 3.17A). A shift of + 0.5 to 1.0 pH unit in optimum pH for cyclization was also observed with A406V- and A406L-CgAMs (Figure 3.17B). The effect of amino acid residues on higher thermostability were followed in the order V > L > A, the same order of activities as described under section 3.6.1. Substitution by V and L could contribute to a more compact core of the protein structure, thus increase temperature stability and leads to a higher optimum temperature than that of A406. Several works reported that, the increase in hydrophobic interactions, salt bridge or side chain-side chain H-bond has been suggested as the principal determinants in enhancing thermostability (Guo *et al.*, 2014; Guo *et al.*, 2015; Kumar *et al.*, 2000; Liu *et al.*, 2013; Ragone, 2001; Vogt *et al.*, 1997). The slight increase (+ 0.5 pH unit) in optimum pH was observed for N287Y-CgAMs while a shift of 1.0 pH unit in optimum pH was also observed with A406H-, A406R- and A406F-CgAMs, respectively. In previous reports with other enzymes, the variant S35 was obtained by random mutagenesis of the γ -CGTase from *Bacillus* sp. G1, all of nine amino acid substitutions of S35 were located distant from the active site, the substitutions of S461G and E472G were in the C-domain, while V605A, N606K and R648H were in the E-domain and thus much further away from the active site. However, these substitutions did obviously contribute to the observed changes in pH activity of the CGTase (Melzer *et al.*, 2015). By site-directed mutagenesis at five positions based on sequence comparisons of cellulases with different pH optimum, the

pH activity of a cellobiohydrolase from the filamentous fungus *Trichoderma reesei* could be shifted to the alkaline pH range (Boer and Koivula., 2003).

Moreover, the increase of 5 °C in optimum disproportionation temperature was observed for N287Y-CgAM, while WT-, A406H-, A406R- and A406F-CgAMs was 45 °C. However, A406H-, A406R-, A406F- and N287Y-CgAMs also indicated a higher effect on thermostability at 35 °C, 40 °C and 45 °C than that of WT-CgAM at a longer incubation of 3 h. It has been previously reported from the study of the effect of replaced amino acids on thermostability that in the thermal inactivation study with increased pre-incubation time intervals carried out at 50 °C, the enzyme activity decreased sharply in the first 10 min and then showed small changes with the increase in pre-incubation time (Zhang *et al.*, 2013). From the CD spectra of A406H-, A406R-, A406F- and N287Y-CgAMs, the secondary structure of the enzymes was changed. It is possible that substitution of alanine (A) at position 406 of CgAM to His (H), Arg (R) and Phe (F), and of asparagine (N) at position 287 to Tyr (Y)-CgAMs may be beneficial not only because it affected changes in hydrophobic and cationic interactions but also because it removes a potential deamidation residue, thereby stabilizing the secondary structure and enhancing its rigidity. This means that the thermostability improvement was caused by secondary structure changes. A single amino acid substituted in four mutated haloperoxidase G106S, R114H, N146H and V148I from *Streptomyces aureofaciens* BPO-A1 was shown to improve thermostability and organic solvent stability of this enzyme (Yamada *et al.*, 2014). The thermostability of L-asparaginase from *E. chrysanthemi* was improved significantly by replacement of Asp133 with Val (Georgia and Nikolaos, 2009). For amyloamylase, only one work on the increase in thermostability has been reported, a

single mutation as E27R-*TfAM* was more stable than its counterpart WT (Kaewpathomsri *et al.*, 2015).

4.3.5 Differential scanning calorimetry

Differential scanning calorimetry (DSC) is one of the most frequently used techniques to determine thermal stability of protein. Its fundamental is to measure heat capacity (C_p) when molecules unfold due to increase in temperature, generally performed in the range of $-10\text{ }^{\circ}\text{C}$ to $130\text{ }^{\circ}\text{C}$. The transition midpoint or melting temperature (T_m) is considered as the temperature, where 50% of the protein owns its native conformation, and the rest remains denatured. Higher T_m values would be representative of a more stable molecule. Besides T_m , the T_p value which represents the DSC peak temperature is easily obtained and also can be used to designate thermostability (Gill *et al.*, 2010; Islam *et al.*, 2009; Wen *et al.*, 2012). In this work, it was observed that the heat capacity profiles of the WT-, A406V- and A406L-CgAMs gave only one main peak temperature (T_p), and the profiles of the A406V- and A406L-CgAMs were shifted towards higher temperature when compared to that of the WT (Figure 3.20). However, two peaks were obtained from A406H-, A406R- and N287Y-CgAMs. The first peak of A406H-, A406R- and N287Y-CgAMs was observed at 310 K, T_p was downshifted when compared to the one main peak of WT, while the second peak of these three mutants, A406H-, A406R- and N287Y-CgAMs, was upshifted towards higher temperature at 330K, 333K and 340K, respectively (Figure 3.20). DSC results thus support that all MT-CgAMs had higher thermostability than the WT-CgAM. Previous study by our group on the amyloamylase from *T. filiformis* also revealed that, the heat capacity profiles of E27R

-*TfAM* were upward shifted to higher temperature in the temperature range of 350-360 K as compared to the WT, the increase in the T_p value observed was about 3 K (Kaewpathomsri *et al.*, 2015). The DSC result thus supported higher thermostability of E27R-*TfAM* than the WT.

4.4 Synthesis of LR-CDs

4.4.1 Effect of pH and temperature on LR-CD product profiles

When the product profiles of WT-, A406V- and A406L-*CgAMs* were monitored at various pHs (Figure 3.23A, B and C) a different product pattern was observed. At pH 5.5, larger size LR-CDs were obtained when compared with at other pHs, principal product was CD34 for the WT- and CD38 for both MT-*CgAMs*. The profiles at pH 6.5 and pH 8.0 were relatively similar, the main products were CD30 to CD31 with the rather symmetrical size distribution frequency curve and the higher yield at pH 6.5 for WT- and MT-enzymes. At pH 9.0, a noticeably trace amount of the smaller CDs (CD6-CD17) was observed, with a somewhat broad peak from CD28 to CD38 for WT-, A406V- and A406L- *CgAMs* (Figure 3.23A, B and C). The change in product pattern and product yield observed at different pHs is possibly due to conformational change of the enzymes, which led to the change in substrate binding site and enzyme activity. From previous reports, the formation of productive enzyme-substrate complexes with longer α -glucan substrates not only is mediated by the active-site cleft but also is enhanced by starch binding sites (Przylas *et al.*, 2000). The 3D-structures of AMs have been determined from a few species of *Thermus*. All comprise of two Asp (Asp293 and Asp395) and one Glu (Glu340) (*T. aquaticus* numbering) as catalytic residues at the active sites. The loop structure around residues

250s (residues 247-255) of AM from *T. aquaticus* lies over the active site and proposed to be important for binding of substrates, dissociation of products and supports the ring size of cyclic product (Przylas *et al.*, 2000). From the CD spectra of WT- and E27R-*Tf*AM, the change in enzyme conformation was observed only at pH 9.0 but not at pH 5.0 and pH 7.0 (Kaewpathomsri *et al.*, 2015).

In addition, the slight difference in product pattern was also observed at different incubation temperature (Figure 3.24A, B and C) which might be due to the change in optimum temperature and temperature stability of A406V- and A406L- CgAMs. At 30-35 °C, the principal products of the WT- were CD30-CD31 while CD31-CD36 were main products of both A406V- and A406L-CgAMs, At 40-45 °C, a broader peak with a higher level of DPs was obtained, CD30 to CD36 for the WT- and CD31-CD40 for both MT-enzymes.

4.4.2 Effect of incubation time and temperature on LR-CD production

yield

When incubation time was varied (Figure 3.25A), the highest product yield of WT- and A406L-CgAMs, was obtained at 1 h and 4 h incubation while A406V- gave highest yield at 8 h. At the highest product yield, each mutated enzyme gave about 12-15% higher yield than its WT counterpart. At long incubation time of 24 h, both mutated enzymes gave up to 60 -70 % higher yield of LR-CD products than the WT. From previous reports on *T. aquaticus* AM, Y54G mutated enzyme with dramatically decreased hydrolytic activity gave 30% higher yield of LR-CDs than that of the WT at 24 h incubation (Prichard *et al.*, 2005). In our work, higher product yield should be

the result of higher thermostability of the mutated enzymes, no change in hydrolysis activity was observed upon A406 mutation (Table 3.2).

From the change in optimum temperature and temperature stability of mutated enzymes as shown in Figures 3.17 and 3.18 and described under section 3.6.2, production of LR-CDs was compared at different temperatures when incubation time was 90 min. The result (Figure 3.25B) showed that the WT- and A406L-CgAMs gave highest product yield at 30 ° C while highest product yield of A406V was at both 30 and 35 ° C. A406V gave 33% and 46% higher yield of LR-CDs than the WT at 35 and 40 ° C, respectively. This result agrees with the finding that optimum temperature of A406V for cyclization reaction was + 5 ° C shifted while that for A406L was about the same as the WT (Figure 3.17B). A406V was also found to have higher stability than A406L and the WT, respectively (Figure 3.18). The increase in product yield, enzyme activity and thermostability had been reported with aminotransferase from a mesophilic *Athrobacter citreus* of which error-prone PCR technique was used to generate a mutated enzyme with 17 amino acid residues out of 480 being replaced. The mutated aminotransferase was able to operate at temperature greater than 50 ° C for an extended period of time (Martin *et al.*, 2007). For amyloamylase, thermostability of the E27R-TfAM (Kaewpathomsri *et al.*, 2015) and Y101S-TtAM (Watanasatitarpa *et al.*, 2014) was reported to be increased over their WT counterparts. The results from analysis of LR-CD products in this work thus showed the advantage of A406V- over the WT-CgAM in giving higher product yield, especially when incubated at longer incubation time and higher temperature.

CHAPTER V

CONCLUSIONS

1. From error prone PCR, a mutated CgAM with higher thermostability at 50 °C compared to the wild-type was selected and sequenced. The result showed that the mutant contains a single mutation of A406V.
2. Site-directed mutagenesis was then performed to construct A406V and A406L. Both mutated CgAMs showed higher intermolecular transglucosylation activity with an upward shift in optimum temperature and a slight increase in optimum pH for disproportionation and cyclization reactions.
3. Thermostability of both mutated CgAMs at 35-40 °C was significantly increased with a higher peak temperature from DSC spectra when compared to the wild-type. A406V had a higher effect on activity and thermostability than A406L.
4. The catalytic efficiency values k_{cat}/K_m of A406V- and A406L-CgAMs were 2.9 and 1.4 times higher than that of the wild-type, mainly due to a significant increase in k_{cat} .

5. LR-CD products analysis demonstrated that A406V gave higher product yield, especially at longer incubation time and higher temperature, in comparison to the wild-type enzyme. The shift towards larger size of LR-CDs was observed.
6. Since no change in secondary structure was observed, possible explanations of the mechanism related to the improvement of thermostability and catalytic efficiency may be the change in enzyme conformation related to hydrophobic interactions of A406V and A406L-CgAMs as evidenced by results from DSC and kinetic analysis.
7. Four more mutated enzymes, A406H, A406R, A406F and N287Y-CgAMs, were constructed. Intermolecular transglucosylation activities of all these mutants were diminished while cyclization activity could not be detected.
8. For disproportionation activity, the slight increase (+0.5 pH unit) in optimum pH was observed for N287Y-CgAM while a shift of 1.0 pH unit in optimum pH was also observed with A406H, A406R and A406F-CgAMs, respectively.
9. A406H-, A406R-, A406F- and N287Y-CgAM showed higher thermostability at 35 °C, 40 °C and 45 °C when incubated for 3 h than the WT-CgAM, a shift of +5 °C in optimum temperature was observed for N287Y-CgAM. DSC result also confirmed the higher thermostability of these mutants than the WT.

10. From all the six mutants, A406V was the best mutated enzyme in terms of high thermostability and transglucosylation activity compared to the WT.



REFERENCES

- Abe, J.-i., Ushijima, C., and Hizukuri, S. (1999). Expression of the isomylase gene of *Flavobacterium odoratum* KU in *Escherichia coli* and identification of essential residues of the enzyme by site-directed mutagenesis. *Applied and Environmental Microbiology* **65**, 4163-4170.
- Alting, A. C., Van de Velde, F., Kanning, M. W., Burgering, M., Mulleners, L., Sein, A., and Buwalda, P. (2009). Improved creaminess of low-fat yoghurt: The impact of amyloamylase-treated starch domains. *Food Hydrocolloids* **23**, 980-987.
- Barends, T. R., Bultema, J. B., Kaper, T., van der Maarel, M. J., Dijkhuizen, L., and Dijkstra, B. W. (2007). Three-way stabilization of the covalent intermediate in amyloamylase, an α -amylase-like transglycosylase. *Journal of Biological Chemistry* **282**, 17242-17249.
- Batra, J., and Mishra, S. (2013). Organic solvent tolerance and thermostability of a β -glucosidase co-engineered by random mutagenesis. *Journal of Molecular Catalysis B: Enzymatic* **96**, 61-66.
- Ben Messaoud, E., Ben Ammar, Y., Mellouli, L., and Bejar, S. (2002). Thermostable pullulanase type I from new isolated *Bacillus thermoleovorans* US105: cloning, sequencing and expression of the gene in *E. coli*. *Enzyme and Microbial Technology* **31**, 827-832.
- Bhuiyan, S. H., Kitaoka, M., and Hayashi, K. (2003). A cycloamylose-forming hyperthermostable 4- α -glucanotransferase of *Aquifex aeolicus* expressed in *Escherichia coli*. *Journal of Molecular Catalysis B: Enzymatic* **22**, 45-53.

- Bloch, M. A., and Raibaud, O. (1986). Comparison of the malA regions of *Escherichia coli* and *Klebsiella pneumoniae*. *Journal of Bacteriology* **168**, 1220-1227.
- Bo-young, B., Kim, H., Baik, M., Ahn, S., Kim, C., and Park, C. (2006). Cloning and overexpression of 4- α -glucanotransferase from *Thermus brockianus* (TBGT) in *E. coli*. *Journal of Microbiology and Biotechnology* **16**, 1809-1813.
- Boer, H., and Koivula. (2003). The relationship between thermal stability and pH optimum studies with wild-type and mutant *Trichoderma reesei* cellobiohydrolase Cel7A. *European Journal of Biochemistry* **270**, 841-848.
- Bollag, D. M., and Edelstein, S. J. (1991). "Protein Method," A John Wiley & Son, INC., Publication, New York.
- Bradford, M. M. (1976). A rapid and sensitive method for the quantitation of microgram quantities of protein utilizing the principle of protein dye binding. *Analytical Biochemistry* **274**, 248-254.
- Deckert, G., Warren, P. V., Gaasterland, T., W.G., Y., Lenox, A. L., Graham, D. E., Overbeek, R., Snead, M. A., Keller, M., Aujay, M., Huber, R., Feldman, R. A., Short, J. M., Olsen, G. J., and Swanson, R. V. (1998). The complete genome of hyperthermophilic bacterium *Aquifex aeolicus*. *Nature* **392**, 353-358.
- Deng, Z., Yang, H., Shin, H.-d., Li, J., and Liu, L. (2014). Structure-based rational design and introduction of arginines on the surface of an alkaline α -amylase from *alkalimonas amylolytica* for improved thermostability. *Applied Microbiology and Biotechnology* **98**, 8937-8945.

- Endo, T. (2011). Large-ring cyclodextrin. *Trend in Glycoscience and Glycotechnology* **23**, 79-92.
- Endo, T., Zheng, M., and Zimmermann, W. (2002). Enzymatic synthesis and analysis of large-ring cyclodextrins. *Australian Journal of Chemistry* **55**, 39-48.
- Esposito, D., and Chatterjee, D. K. (2006). Enhancement of soluble protein expression through the use of fusion tags. *Current Opinion in Biotechnology* **17**, 353-358.
- Fleischmann, R. D., Adams, M. D., White, O., Clayton, R. A., Kirkness, E. F., Kerlavage, A. R., Bult, C. J., Tomb, J. F., Dougherty, B. A., and Merrick, J. M. (1995). Whole-genome random sequencing and assembly of *Haemophilus influenzae* Rd. *Science* **269**, 496-512.
- Fujii, K., Minagawa, H., Terada, Y., Takaha, T., Kuriki, T., Shimada, J., and Kaneko, H. (2005a). Improvement of amyloamylase from *Thermus aquaticus* by random and saturation mutageneses. *Journal of Applied Glycoscience* **52**, 137-143.
- Fujii, K., Minagawa, H., Terada, Y., Takaha, T., Kuriki, T., Shimada, J., and Kaneko, H. (2005b). Use of random and saturation mutageneses to improve the properties of *Thermus aquaticus* amyloamylase for efficient production of cycloamyloses. *Applied and Environmental Microbiology* **71**, 5823-5827.
- Fujii, K., Minagawa, H., Terada, Y., Takaha, T., Kuriki, T., Shimada, J., and Kaneko, H. (2007). Function of second glucan binding site including tyrosines 54 and 101 in *Thermus aquaticus* amyloamylase. *Journal of Bioscience and Bioengineering* **103**, 167-173.

- Fujii, R., Kitaoka, M., and Hayashi, K. (2004). One-step random mutagenesis by error-prone rolling circle amplification. *Nucleic Acids Research* **32**, 145.
- Furuishi, T., Endo, T., Nagase, H., Ueda, H., and Nagai, T. (1998). Solubilization of C70 into water by complexation with α -cyclodextrin. *Chemical & Pharmaceutical Bulletin* **46**, 1658-1659.
- Georgia, A. K., and Nikolaos, E. L. (2009). Engineering thermal stability of L-asparaginase by in vitro directed evolution. *FEBS Journal* **276**, 1750-1761.
- Gill, P., Moghadam, T. T., and Ranjbar, B. (2010). Differential scanning calorimetry techniques: applications in biology and nanoscience. *Journal of Biomolecular Techniques: JBT* **21**, 167.
- Goda, S. K., Eissa, O., Akhtar, M., and Minton, N. P. (1997). Molecular analysis of a *Clostridium butyricum* NCIMB 7423 gene encoding 4- α -glucanotransferase and characterization of the recombinant enzyme produced in *Escherichia coli*. *Microbiology* **143**, 3287-3294.
- Gotsev, M. G., and Ivanov, P. M. (2007). Large-ring cyclodextrins. A molecular dynamics study of the conformational dynamics and energetics of CD10, CD14 and CD26. *ARKIVOC* **13**, 167-189.
- Guo, F., Zhang, C., Bie, X., Zhao, H., Diao, H., Lu, F., and Lu, Z. (2014). Improving the thermostability and activity of lipoxygenase from *Anabaena* sp. PCC 7120 by directed evolution and site-directed mutagenesis. *Molecular Catalysis B: Enzymatic* **107**, 23-30.
- Guo, J., Rao, Z., Yang, T., Man, Z., Xu, M., Zhang, X., and Yang, S.-T. (2015). Enhancement of the thermostability of *Streptomyces kathirae* SC-1 tyrosinase

- by rational design and empirical mutation. *Enzyme and Microbial Technology* **77**, 54-60.
- Hansen, M. R., Blennow, A., Pedersen, S., Nørgaard, L., and Engelsen, S. B. (2008). Gel texture and chain structure of amyloamylase-modified starches compared to gelatin. *Food Hydrocolloids* **22**, 1551-1566.
- Henrissat, B. (1991). A classification of glycosyl hydrolases based on amino acid sequence similarities. *Biochem J* **280**, 309-316.
- Imamura, H., Fushinobu, S., Yamamoto, M., Kumasaka, T., Jeon, B.-S., Wakagi, T., and Matsuzawa, H. (2003). Crystal structures of 4- α -glucanotransferase from *Thermococcus litoralis* and its complex with an inhibitor. *Journal of Biological Chemistry* **278**, 19378-19386.
- Islam, M. M., Sohya, S., Noguchi, K., Kidokoro, S. i., Yohda, M., and Kuroda, Y. (2009). Thermodynamic and structural analysis of highly stabilized BPTIs by single and double mutations. *Proteins: Structure, Function, and Bioinformatics* **77**, 962-970.
- Jung, J. H., Jung, T. Y., Seo, D. H., Yoon, S. M., Choi, H. C., Park, B. C., Park, C. S., and Woo, E. J. (2011). Structural and functional analysis of substrate recognition by the 250s loop in amyloamylase from *Thermus brockianus*. *Proteins: Structure, Function, and Bioinformatics* **79**, 633-644.
- Kaewpathomsri, P., Takahashi, Y., Nakamura, S., Kaulpiboon, J., Kidokoro, S., Murakami, S., Krusong, K., and Pongsawasdi, P. (2015). Characterization of amyloamylase from *Thermus filiformis* and the increase in alkaline and thermo-stability by E27R substitution. *Process Biochemistry*.

- Kaper, T., Leemhuis, H., Uitdehaag, J. C., van der Veen, B. A., Dijkstra, B. W., van der Maarel, M. J., and Dijkhuizen, L. (2007). Identification of acceptor substrate binding subsites+ 2 and+ 3 in the amyloamylase from *Thermus thermophilus* HB8. *Biochemistry* **46**, 5261-5269.
- Kaper, T., Talik, B., Ettema, T. J., Bos, H., van der Maarel, M. J., and Dijkhuizen, L. (2005). Amyloamylase of *Pyrobaculum aerophilum* IM2 produces thermoreversible starch gels. *Applied and Environmental Microbiology* **71**, 5098-5106.
- Kaper, T., van der Maarel, M., Euverink, G., and Dijkhuizen, L. (2004). Exploring and exploiting starch-modifying amyloamylases from thermophiles. *Biochemical Society Transactions* **32**, 279-282.
- Kelly, S. M., Jess, T. J., and Price, N. C. (2005). How to study proteins by circular dichroism. *Biochimica et Biophysica Acta (BBA)-Proteins and Proteomics* **1751**, 119-139.
- Kobayashi, R., Hirano, N., Kanaya, S., Saito, I., and Haruki, M. (2010). Enhancement of the enzymatic activity of *Escherichia coli* acetyl esterase by random mutagenesis. *Journal of Molecular Catalysis B: Enzymatic* **67**, 155-161.
- Kotzia, G. A., and Labrou, N. E. (2009). Engineering thermal stability of L-asparaginase by in vitro directed evolution. *Febs Journal* **276**, 1750-1761.
- Krusong, K., Srisimararat, W., and Pongsawasdi, P. X-ray structure of amyloamylase from *Corynebacterium glutamicum*, unpublished manuscript.
- Kumar, S., Tsai, C.-J., and Nussinov, R. (2000). Factors enhancing protein thermostability. *Protein Engineering* **13**, 179-191.

- Kuriki, T., Takata, H., Yanase, M., Ohdan, K., Fujii, K., Terada, Y., Takaha, T., Hondoh, H., Matsuura, Y., and Imanaka, T. (2006). The concept of the α -amylase family: A rational tool for interconverting glucanohydrolase/glucanotransferases, and their specificities. *Journal of Applied Glycoscience* **53**, 155-161.
- Lamour, V., Hogan, B. P., Erie, D. A., and Darst, S. A. (2006). Crystal structure of *Thermus aquaticus* Gfh1, a Gre-factor paralog that inhibits rather than stimulates transcript cleavage. *Journal of Molecular Biology* **356**, 179-188.
- Larsen, K. L. (2002). Large cyclodextrins. *Journal of Inclusion Phenomena and Macrocyclic Chemistry* **43**, 1-13.
- Lee, B.-H., Oh, D.-K., and Yoo, S.-H. (2009). Characterization of 4- α -glucanotransferase from *Synechocystis* sp. PCC 6803 and its application to various corn starches. *New Biotechnology* **26**, 29-36.
- Lee, H.-S., Auh, J.-H., Yoon, H.-G., Kim, M.-J., Park, J.-H., Hong, S.-S., Kang, M.-H., Kim, T.-J., Moon, T.-W., and Kim, J.-W. (2002). Cooperative action of α -glucanotransferase and maltogenic amylase for an improved process of isomaltooligosaccharide (IMO) production. *Journal of Agricultural and Food Chemistry* **50**, 2812-2817.
- Lee, K. Y., Kim, Y.-R., Park, K. H., and Lee, H. G. (2006). Effects of α -glucanotransferase treatment on the thermo-reversibility and freeze-thaw stability of a rice starch gel. *Carbohydrate Polymers* **63**, 347-354.
- Lehmann, M., Pasamontes, L., Lassen, S., and Wyss, M. (2000). The consensus concept for thermostability engineering of proteins. *Biochimica et Biophysica Acta (BBA)-Protein Structure and Molecular Enzymology* **1543**, 408-415.

- Li, D., Roh, S.-A., Shim, J.-H., Mikami, B., Baik, M.-Y., Park, C.-S., and Park, K.-H. (2005). Glycosylation of genistin into soluble inclusion complex form of cyclic glucans by enzymatic modification. *Journal of Agricultural and Food Chemistry* **53**, 6516-6524.
- Liu, B., Zhang, J., Fang, Z., Gu, L., Liao, X., Du, G., and Chan, J. (2013). Enhanced thermostability of keratinase by computational design and empirical mutation. *Journal of Industrial Microbiology & Biotechnology* **40**, 697-704.
- Lundberg, K. S., Shoemaker, D. D., Adams, M. W. W., Short, J. M., Sorge, J. A., and Mathur, E. J. (1991). High-fidelity amplification using a thermostable DNA polymerase isolated from *Pyrococcus furiosus*. *Gene* **108**, 1-6.
- Mabrouk, S. B., Ayadi, D. Z., Hlima, H. B., and Bejar, S. (2013). Thermostability improvement of maltogenic amylase MAUS149 by error prone PCR. *Journal of Biotechnology* **168**, 601-606.
- Machida, S., Hayashi, K., Tokuyasu, T., and Takaba, T. (2003). Refolding method of antibody. *Japanese Patent*, 2003-128699.
- Machida, S., Ogawa, S., Xiaohua, S., Takaha, T., Fujii, K., and Hayashi, K. (2000). Cycloamylose as an efficient artificial chaperone for protein refolding. *FEBS letters* **486**, 131-135.
- Machius, M., Vertesy, L., Huber, R., and Wiegand, G. (1996). Carbohydrate and protein-based inhibitors of porcine pancreatic α -amylase: structure analysis and comparison of their binding characteristics. *Journal of Molecular Biology* **260**, 409-421.
- Martin, A. R., DiSanto, R., Plotnikov, I., Kamat, S., Shonnard, D., and Pannuri, S. (2007). Improved activity and thermostability of (S)-aminotransferase by

- error-prone polymerase chain reaction for the production of a chiral amine. *Biochemical Engineering Journal* **37**, 246-255.
- Melzer, S., Sonnendecker, C., Föllner, C., and Zimmermann, W. (2015). Stepwise error-prone PCR and DNA shuffling changed the pH activity range and product specificity of the cyclodextrin glucanotransferase from an alkaliphilic *Bacillus* sp. *FEBS open bio* **5**, 528-534.
- Miwa, I., Okuda, J., Maeua, K., and Okuda, G. (1972). Mutarotase effect on colorimetric determination of blood glucose with β -D-glucose oxidase. *Clinica Chimica Acta* **37**, 538-540.
- Miyazawa, S. (1994). A reliable sequence alignment method based on probabilities of residue correspondences. *Protein Engineering* **8**, 999-1009.
- Monod, J., and Torriani, A.-M. (1950). Amylomaltase of *Escherichia coli*. Paper presented at: *Annales de l'Institut Pasteur*.
- Mun, S., Kim, Y.-L., Kang, C.-G., Park, K.-H., Shim, J.-Y., and Kim, Y.-R. (2009). Development of reduced-fat mayonnaise using 4 α GTase-modified rice starch and xanthan gum. *International Journal of Biological Macromolecules* **44**, 400-407.
- Nakaniwa, T., Tada, T., Takao, M., Sakai, T., and Nishimura, K. (2004). An in vitro evaluation of a thermostable pectate lyase by using error-prone PCR. *Journal of Molecular Catalysis B: Enzymatic* **27**, 127-131.
- Nakapong, S. (2011). Biochemical and structural characterization of levansucrase from *Bacillus licheniformis* RN-01. *PhD. Thesis, Chulalongkorn University, Bangkok, Thailand*.

- Pace, C. N., Fu, H., Fryar, K. L., Landua, J., Trevino, S. R., Shirley, B. A., Hendricks, M. M., Iimura, S., Gajiwala, K., and Scholtz, J. M. (2011). Contribution of hydrophobic interactions to protein stability. *Journal of Molecular Biology* **408**, 514-528.
- Palmer, T. N., Ryman, B. E., and Whelan, W. J. (1976). The action pattern of amyloamylase from *Escherichia coli*. *European Journal of Biochemistry* **69**, 105-115.
- Park, J.-H., Kim, H.-J., Kim, Y.-H., Cha, H., Kim, Y.-W., Kim, T.-J., Kim, Y.-R., and Park, K.-H. (2007). The action mode of *Thermus aquaticus* YT-1 4- α -glucanotransferase and its chimeric enzymes introduced with starch-binding domain on amylose and amylopectin. *Carbohydrate Polymers* **67**, 164-173.
- Pritchard, L., Corne, D., Kell, D., Rowland, J., and Winson, M. (2005). A general model of error-prone PCR. *Journal of theoretical biology* **234**, 497-509.
- Przylas, I., Terada, Y., Fujii, K., Takaha, T., Saenger, W., and Sträter, N. (2000a). X-ray structure of acarbose bound to amyloamylase from *Thermus aquaticus*. *European Journal of Biochemistry* **267**, 6903-6913.
- Przylas, I., Tomoo, K., Terada, Y., Takaha, T., Fujii, K., Saenger, W., and Sträter, N. (2000b). Crystal structure of amyloamylase from *Thermus aquaticus*, a glycosyltransferase catalysing the production of large cyclic glucans. *Journal of Molecular Biology* **296**, 873-886.
- Pugsley, A., and Dubreuil, C. (1988). Molecular characterization of malQ, the structural gene for the *Escherichia coli* enzyme amyloamylase. *Molecular Microbiology* **2**, 473-479.

- Qi, Q., Mokhtar, M. N., and Zimmermann, W. (2007). Effect of ethanol on the synthesis of large-ring cyclodextrins by cyclodextrin glucanotransferases. *Journal of Inclusion Phenomena and Macrocyclic Chemistry* **57**, 95-99.
- Rachadech, W., Nimpiboon, P., Naumthong, W., Nakapong, S., Krusong, K., and Pongsawasdi, P. (2015). Identification of essential tryptophan in amyломaltase from *Corynebacterium glutamicum*. *International Journal of Biological Macromolecules* **76**, 230-235.
- Ragone, R. (2001). Hydrogen-bonding classes in proteins and their contribution to the unfolding reaction. *Protein Science* **10**, 2075-2082.
- Roujeinikova, A., Raasch, C., Sedelnikova, S., Liebl, W., and Rice, D. W. (2002). Crystal structure of *Thermotoga maritima* 4- α -glucanotransferase and its acarbose complex: implications for substrate specificity and catalysis. *Journal of Molecular Biology* **321**, 149-162.
- Saeu, S., Srisimarat, W., Prousoontorn, M. H., and Pongsawasdi, P. (2013). Transglucosylation reaction of amyломaltase for the synthesis of anticariogenic oligosaccharides. *Journal of Molecular Catalysis B: Enzymatic* **88**, 77-83.
- Schmidt, A. K., Cottaz, S., Driguez, H., and Schulz, G. E. (1998). Structure of cyclodextrin glycosyltransferase complexed with a derivative of its main product β -cyclodextrin. *Biochemistry* **37**, 5909-5915.
- Schwartz, M. (1987). The maltose regulon. In F.C. Neidhardt, *et al.*, (eds), *Escherichia coli* and *Salmonella typhimurium*. *Cellular and Molecular Biology*, 1482-1502.

- Srisimarat, W., Kaulpiboon, J., Krusong, K., Zimmermann, W., and Pongsawasdi, P. (2012). Mutation at Tyr-172 in the amyloamylase from *Corynebacterium glutamicum* leads to a change in large-ring cyclodextrin products profile. *Applied and Environmental Microbiology* **AEM**, 01366-01312.
- Srisimarat, W., Murakami, S., Pongsawasdi, P., and Krusong, K. (2013). Crystallization and preliminary X-ray crystallographic analysis of the amyloamylase from *Corynebacterium glutamicum*. *Acta Crystallographica Section F: Structural Biology and Crystallization Communications* **69**, 1004-1006.
- Srisimarat, W., Powviriyakul, A., Kaulpiboon, J., Krusong, K., Zimmermann, W., and Pongsawasdi, P. (2011). A novel amyloamylase from *Corynebacterium glutamicum* and analysis of the large-ring cyclodextrin products. *Journal of Inclusion Phenomena and Macrocyclic Chemistry* **70**, 369-375.
- Stassi, D. L., Lopez, P., Espinosa, M., and Lacks, S. A. (1981). Cloning of chromosomal genes in *Streptococcus pneumoniae*. *Proceedings of the National Academy of Sciences* **78**, 7028-7032.
- Taira, H., Nagase, H., Endo, T., and Ueda, H. (2006). Isolation, Purification and Characterization of Large-Ring Cyclodextrins (CD36~CD39). *Journal of Inclusion Phenomena and Macrocyclic Chemistry* **56**, 23-28.
- Takaha, T., and Smith, S. M. (1999). The functions of 4- α -glucanotransferases and their use for the production of cyclic glucans. *Biotechnology and Genetic Engineering Reviews* **16**, 257-280.
- Takaha, T., Yanase, M., Okada, S., and Smith, S. M. (1993). Disproportionating enzyme (4- α -glucanotransferase; EC 2.4.1.25) of potato. Purification,

- molecular cloning, and potential role in starch metabolism. *The Journal of Biological Chemistry* **268**, 1391-1396.
- Takano, K., Yamagata, Y., and Yutani, K. (1998). A general rule for the relationship between hydrophobic effect and conformational stability of a protein: stability and structure of a series of hydrophobic mutants of human lysozyme. *Journal of Molecular Biology* **280**, 749-761.
- Takata, H., Kuriki, T., Okada, S., Takesada, Y., Iizuka, M., Minamiura, N., and Imanaka, T. (1992). Action of neopullulanase. Neopullulanase catalyzes both hydrolysis and transglycosylation at alpha-(1→4)-and alpha-(1→6)-glucosidic linkages. *Journal of Biological Chemistry* **267**, 18447-18452.
- Tantanarat, K., O'Neill, E. C., Rejzek, M., Field, R. A., and Limpaseni, T. (2014). Expression and characterization of 4- α -glucanotransferase genes from *Manihot esculenta* Crantz and *Arabidopsis thaliana* and their use for the production of cycloamyloses. *Process Biochemistry* **49**, 84-89.
- Terada, Y., Fujii, K., Takaha, T., and Okada, S. (1999). *Thermus aquaticus* ATCC 33923 amyloamylase gene cloning and expression and enzyme characterization: production of cycloamylose. *Applied and Environmental Microbiology* **65**, 910-915.
- Tomono, K., Mugishima, A., Suzuki, T., Goto, H., Ueda, H., Nagai, T., and Watanabe, J. (2002). Interaction between cycloamylose and various drugs. *Journal of Inclusion Phenomena and Macrocyclic Chemistry* **44**, 267-270.
- Turner, P., Mamo, G., and Karlsson, E. N. (2007). Potential and utilization of thermophiles and thermostable enzymes in biorefining. *Microbial Cell Factories* **6**, 9.

- Ueda, H., Wakisaka, M., Nagase, H., Takaha, T., and Okada, S. (2002). Physicochemical properties of large-ring cyclodextrins (CD18-CD21). *Journal of Inclusion Phenomena and Macrocyclic Chemistry* **44**, 403-405.
- Uitdehaag, J. C. M., Euverink, G. J., Van Der Veen, B. A., Van Der Maarel, M., and Dijkstra, B. W. (1999). Structure and mechanism of the amylomaltase from *Thermus thermophilus* HB8.
- Van Der Maarel, M. J., Van Der Veen, B., Uitdehaag, J. C., Leemhuis, H., and Dijkhuizen, L. (2002). Properties and applications of starch-converting enzymes of the α -amylase family. *Journal of Biotechnology* **94**, 137-155.
- Voet, D., and Voet, J. G. (2004). "Biochemistry," J. Wiley & Sons, New York.
- Vogt, G., Woell, S., and Argos, P. (1997). Protein thermal stability, hydrogen bonds, and ion pairs. *Journal of Molecular Biology* **269**, 631-643.
- Watanasatitarpa, S., Rudeekulthamrong, P., Krusong, K., Srisimarat, W., Zimmermann, W., Pongsawasdi, P., and Kaulpiboon, J. (2014). Molecular mutagenesis at Tyr-101 of the amylomaltase transcribed from a gene isolated from soil DNA. *Applied Biochemistry and Microbiology* **50**, 243-252.
- Wen, J., Arthur, K., Chemmalil, L., Muzammil, S., Gabrielson, J., and Jiang, Y. (2012). Applications of differential scanning calorimetry for thermal stability analysis of proteins: qualification of DSC. *Journal of Pharmaceutical Sciences* **101**, 955-964.
- Xavier, K. B., Peist, R., Kossmann, M., Boos, W., and Santos, H. (1999). Maltose metabolism in the hyperthermophilic archaeon *Thermococcus litoralis*: Purification and characterization of key enzymes. *Journal of Bacteriology* **181**, 3358-3367.

- Yamada, R., Higo, T., Yoshikawa, C., China, H., and Ogino, H. (2014). Improvement of the stability and activity of the BPO-A1 haloperoxidase from *Streptomyces aureofaciens* by directed evolution. *Journal of Biotechnology* **192**, 248-254.
- Yoshio, N., Maeda, I., Taniguchi, H., and Nakamura, M. (1986). Purification and properties of D-enzyme from malted barley. *Journal of The Japanese Society of Starch Science* **33**, 244-252.
- Zhang, J., Fang, Z., Gu, L., Liao, X., Du, G., and Chen, J. (2013). Enhanced thermostability of keratinase by computational design and empirical mutation. *Journal of Industrial Microbiology & Biotechnology* **40**, 697-704.





APPENDICES

จุฬาลงกรณ์มหาวิทยาลัย
CHULALONGKORN UNIVERSITY

APPENDIX 1: Preparation for polyacrylamide gel electrophoresis**1) Stock reagents****30% Acrylamide, 0.8% bis-acrylamide, 100 ml**

Acrylamide 29.2 g

N, N'-methylene-bis-acrylamide 0.8 g

Adjusted volume to 100 ml with distilled water

1.5 M Tris-HCl pH 8.8

Tris (hydroxymethyl)-aminomethane 18.17 g

Adjusted pH to 8.8 with 1 M HCl and adjusted volume to 100 ml with distilled water

2 M Tris-HCl pH 8.8

Tris (hydroxymethyl)-aminomethane 24.2 g

Adjusted pH to 8.8 with 1 M HCl and adjusted volume to 100 ml with distilled water

0.5 M Tris-HCl pH 6.8

Tris (hydroxymethyl)-aminomethane 6.06 g

Adjusted pH to 6.8 with 1 M HCl and adjusted volume to 100 ml with distilled water

1 M Tris-HCl pH 6.8

Tris (hydroxymethyl)-aminomethane 12.1 g

Adjusted pH to 6.8 with 1 M HCl and adjusted volume to 100 ml with distilled water

Solution B (SDS-PAGE)

| | | |
|---------------------|----|----|
| 2 M Tris-HCl pH 8.8 | 75 | ml |
| 10% SDS | 4 | ml |
| Distilled water | 21 | ml |

Solution C (SDS-PAGE)

| | | |
|---------------------|----|----|
| 1 M Tris-HCl pH 6.8 | 50 | ml |
| 10% SDS | 4 | ml |
| Distilled water | 46 | ml |

2) Denaturing PAGE (SDS-PAGE)**10.0 % separating gel**

| | | |
|---|------|---------------|
| 30% Acrylamide solution | 2.50 | ml |
| Solution B (SDS-PAGE) | 2.50 | ml |
| Distilled water | 2.39 | ml |
| 10% $(\text{NH}_4)_2\text{S}_2\text{O}_8$ | 100 | μl |
| TEMED | 10 | μl |

5.0% stacking gel

| | | |
|---|------|---------------|
| 30% Acrylamide solution | 0.84 | ml |
| Solution C (SDS-PAGE) | 1.0 | ml |
| Distilled water | 3.1 | ml |
| 10% $(\text{NH}_4)_2\text{S}_2\text{O}_8$ | 50 | μl |
| TEMED | 10 | μl |

5X Sample buffer

| | | |
|---------------------|-----|----|
| 1 M Tris-HCl pH 6.8 | 0.6 | ml |
| 50% Glycerol | 5.0 | ml |
| 10% SDS | 2.0 | ml |
| 2-Mercaptoethanol | 0.5 | ml |
| 1% Bromophenol blue | 1.0 | ml |
| Distilled water | 0.9 | ml |

One part of sample buffers was added to four parts of sample. The mixture was heated for 5 min in boiling water prior to loading to the gel.

Electrophoresis buffer, 1 litre

| | | |
|----------------------------------|------|---|
| Tris (hydroxymethyl)-aminometane | 3.0 | g |
| Glycine | 14.4 | g |
| SDS | 1.0 | g |

Adjusted volume to 1 litre with distilled water (pH should be approximately

8.3)

Coomassie Gel Stain, 1 litre

| | | |
|----------------------|-----|----|
| Coomassie Blue R-250 | 1 | g |
| Methanol | 450 | ml |
| Distilled water | 450 | ml |
| Glacial acetic acid | 100 | ml |

Coomassie Gel Destain, 1 litre

| | | |
|---------------------|-----|----|
| Methanol | 100 | ml |
| Glacial acetic acid | 100 | ml |
| Distilled water | 800 | ml |

APPENDIX 2: Preparation for buffer solution**0.2 M Sodium Acetate pH 4.0, 5.0 and 6.0**

| | | |
|-----------------------|------|---|
| CH ₃ COONa | 1.21 | g |
|-----------------------|------|---|

Adjusted volume to 100 ml with distilled water. Adjusted to pH 4, 5 or 6 by

0.2 M acetic acid

0.2 M Phosphate pH 6.0

| | | |
|---------------------------------|------|---|
| KH ₂ PO ₄ | 3.28 | g |
|---------------------------------|------|---|

| | | |
|---------------------------------|------|---|
| K ₂ HPO ₄ | 0.16 | g |
|---------------------------------|------|---|

| | | |
|-----------------|-----|----|
| Distilled water | 100 | ml |
|-----------------|-----|----|

0.2 M Phosphate pH 7.0

| | | |
|---------------------------------|------|---|
| KH ₂ PO ₄ | 1.35 | g |
|---------------------------------|------|---|

| | | |
|---------------------------------|------|---|
| K ₂ HPO ₄ | 1.67 | g |
|---------------------------------|------|---|

| | | |
|-----------------|-----|----|
| Distilled water | 100 | ml |
|-----------------|-----|----|

0.2 M Phosphate pH 8.0

| | | |
|---------------------------------|------|---|
| KH ₂ PO ₄ | 0.48 | g |
|---------------------------------|------|---|

| | | |
|---------------------------------|------|---|
| K ₂ HPO ₄ | 2.34 | g |
|---------------------------------|------|---|

| | | |
|-----------------|-----|----|
| Distilled water | 100 | ml |
|-----------------|-----|----|

0.2 M Tris-Glycine NaOH pH 8.0, 9.0 and 10.0

| | | |
|---------|-----|---|
| Glycine | 1.5 | g |
|---------|-----|---|

Adjusted to pH 8.0, 9.0 and 10.0 by 1 M NaOH and adjusted volume to 100 ml with distilled water.

APPENDIX 3: Preparation of solution for cell preparation and enzyme purification

1) Stock solution

1 M Monopotassium phosphate (100 ml)

The pellet of monopotassium phosphate 13.6 g was dissolved in distilled water to final 100 ml

1 M Dipotassium hydrogen phosphate (500 ml)

The pellet of dipotassium phosphate 87.1 g was dissolved in distilled water to final 500 ml

1 M potassium phosphate buffer, pH 7.4

1 M potassium phosphate buffer, pH 7.4 was prepared by mixing 401 ml of 1 M Dipotassium hydrogen phosphate with 99 ml of Monopotassium phosphate.

2) Extraction buffer

| | | |
|--|---|----|
| 1 M potassium phosphate buffer, pH 7.4 | 5 | ml |
|--|---|----|

| | | |
|-------------------------------------|-----|----|
| 0.1 mM PMSF in 95% absolute ethanol | 0.1 | ml |
|-------------------------------------|-----|----|

| | | |
|-------------------------------------|----|---------|
| 100% (v/v) β -mercaptoethanol | 10 | μ l |
|-------------------------------------|----|---------|

| | | |
|------------|-----|----|
| 0.5 M EDTA | 0.2 | ml |
|------------|-----|----|

Adjusted volume to 100 ml with distilled water

3) 0.85% (w/v) NaCl

| | | |
|-----------------|------|---|
| Sodium chloride | 0.85 | g |
|-----------------|------|---|

Adjusted volume to 100 ml with distilled water

4) Binding buffer

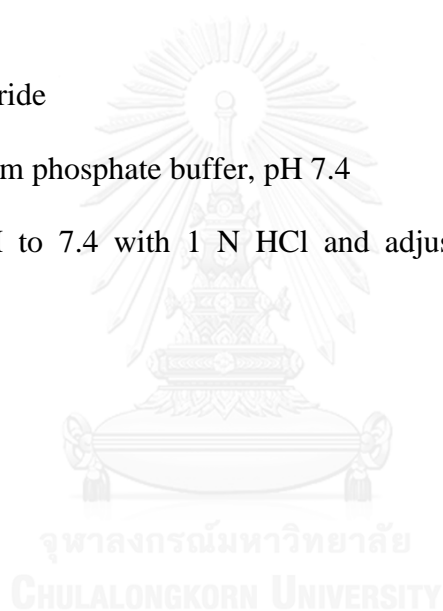
| | | |
|--|-----|----|
| Imidazole | 0.3 | g |
| Sodium chloride | 5.8 | g |
| 1 M potassium phosphate buffer, pH 7.4 | 4.0 | ml |

Adjusted pH to 7.4 with 1 N HCl and adjusted volume to 200 ml with distilled water

5) Elution buffer

| | | |
|--|-----|----|
| Imidazole | 6.8 | g |
| Sodium chloride | 5.8 | g |
| 1 M potassium phosphate buffer, pH 7.4 | 4.0 | ml |

Adjusted pH to 7.4 with 1 N HCl and adjusted volume to 200 ml with distilled water



APPENDIX 4: Preparation for Iodine solution**10X Stock solution (100 ml)**0.2 (w/v) I₂ in 2.0 % (w/v) KI

Potassium iodide 2 g

Iodine 0.2 g

Adjusted to 100 ml with distilled water

1X Iodine solution (100 ml)0.2 (w/v) I₂ in 2.0 % (w/v) KI 10 ml

Distilled water 90 ml



APPENDIX 5: Preparation of Bradford solution**(Bollag and Edelstein, 1991)****1) Stock solution**

| | | |
|----------------------|-----|----|
| Ethanol | 100 | ml |
| Phosphoric acid | 200 | ml |
| Coomassie blue G-250 | 350 | mg |

Stable indefinite at room temperature

2) Working solution

| | | |
|-----------------|-----|----|
| Ethanol | 15 | ml |
| Phosphoric acid | 30 | ml |
| Stock solution | 30 | ml |
| Distilled water | 425 | ml |

Filter through Whatman No. 1 paper, store at room temperature in brown glass bottle. Unstable for several weeks but may need to be refiltrated.

APPENDIX 6: Preparation for bicinchoninic acid assay**Bicinchoninic acid reagent****Solution A**

4,4'-Dicarboxy-2,2'-biquinoline 0.1302 g

Dissolved in 85 ml of distilled water

NaCO₃ 6.2211 g

Adjusted to 100 ml with distilled water

Solution B

Component (1)

L-aspartic acid 0.642 g

NaCO₃ 0.8681 g

Dissolved in 15 ml of distilled water

Component (2)

CuSO₄ 0.1736 g

Dissolved in 5 ml of distilled water

Mixed component (1) and (2), then adjusted to 25 ml with distilled water

Mixed 24 ml of solution A and 1 ml of solution B and used within 24 hours

APPENDIX 7: Preparation for DNS reagent**DNS reagent**

| | | |
|---------------------------------------|-----|----|
| 2-hydroxy-3,5-dinitrobenzoic acid | 5 | g |
| 2 N NaOH | 100 | ml |
| Potassium sodium tartrate | 150 | g |
| Adjust to 500 ml with distilled water | | |



APPENDIX 8: Bacterial media culture**LB (Luria-Bertani) Medium and Plates**

| | | |
|---------------|----|---|
| Tryptone | 10 | g |
| Yeast extract | 5 | g |
| NaCl | 5 | g |

Adjust to 1,000 ml with distilled water (add 15 g/L agar for agar plate) The medium was sterilized by autoclaving at 15 lb/in² for 15 min

Auto Induction Media (AIM) formular (g/L)

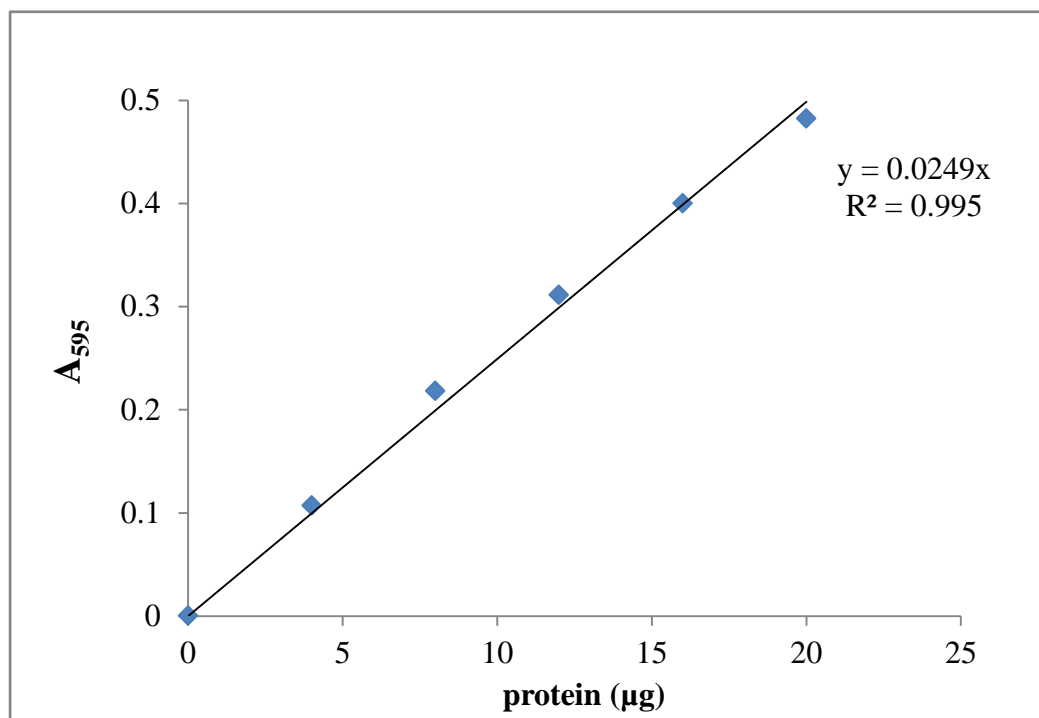
| | | |
|---|------|---|
| Tryptone | 10 | g |
| Yeast extract | 5 | g |
| (NH ₄) ₂ SO ₄ | 3.3 | g |
| KH ₂ PO ₄ | 6.8 | g |
| Na ₂ HPO ₄ | 7.1 | g |
| Glucose | 0.5 | g |
| α-Lactose | 2 | g |
| MgSO ₄ | 0.15 | g |

Adjust to 1,000 ml with distilled water (add 15 g/L agar for agar plate) The medium was sterilized by autoclaving at 110° C, 15 lb/in² for 15 min

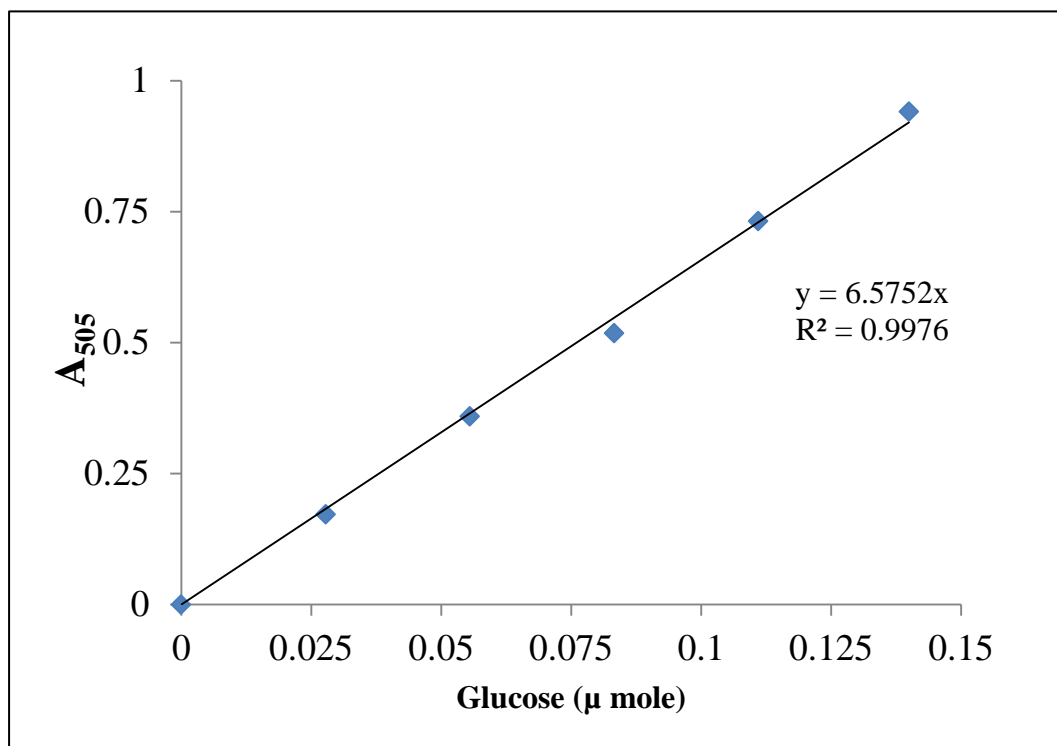
APPENDIX 9: Abbreviation for amino acid residues

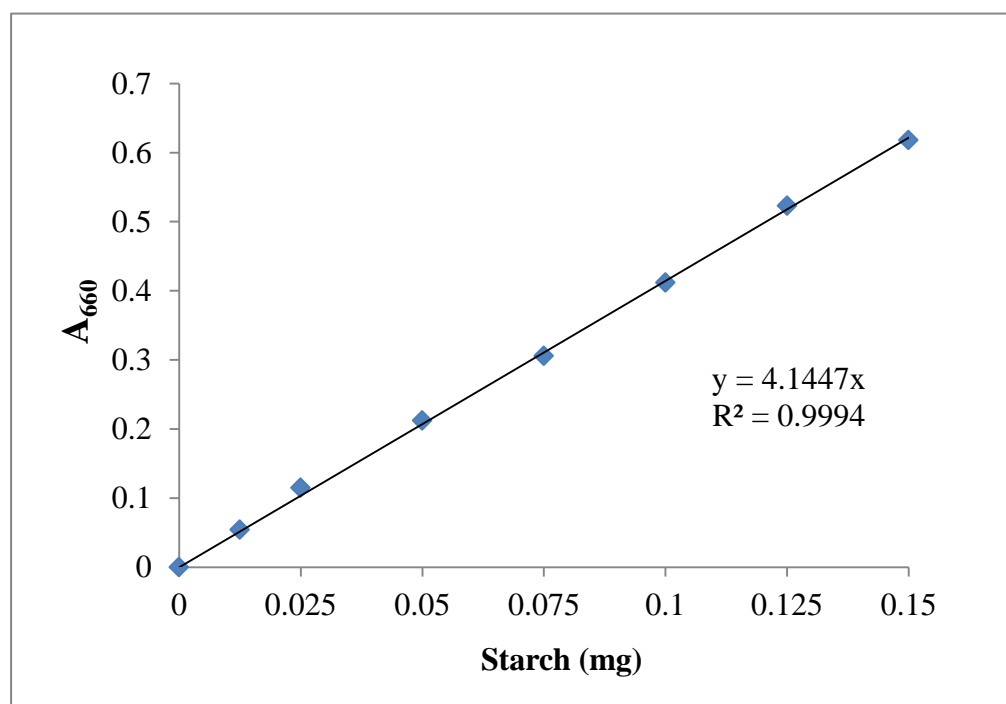
(Voet and Voet, 2004)

| Amino acid | 3 Letter-Abbreviation | 1 Letter-Abbreviation |
|-------------------|------------------------------|------------------------------|
| Alanine | Ala | A |
| Arginine | Arg | R |
| Asparagine | Asn | N |
| Aspartic acid | Asp | D |
| Cystein | Cys | C |
| Glutamine | Gln | Q |
| Glutamic acid | Glu | E |
| Glycine | Gly | G |
| Histidine | His | H |
| Isoleucine | Ile | I |
| Leucine | Leu | L |
| Lysine | Lys | K |
| Methionine | Met | M |
| Phenylalanine | Phe | F |
| Proline | Pro | P |
| Serine | Ser | S |
| Threonine | Thr | T |
| Tryptophan | Trp | W |
| Tyrosine | Tyr | Y |
| Valine | Val | V |
| Unknown | - | X |

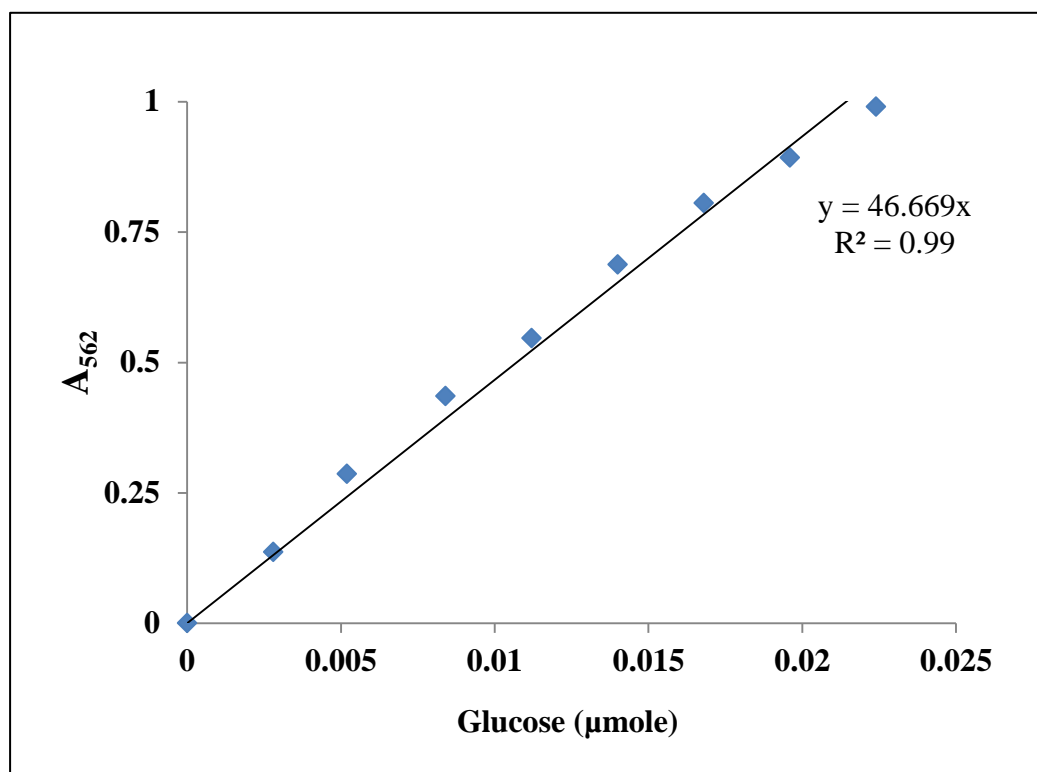
APPENDIX 10: Standard curve for protein determination by Bradford's method

APPENDIX 11: Standard curve of glucose determination by glucose oxidase assay

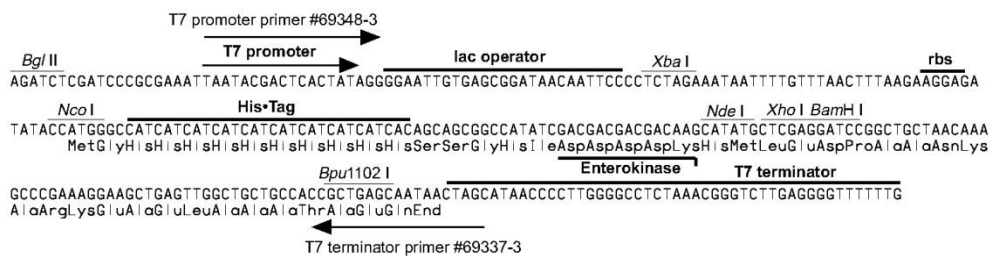
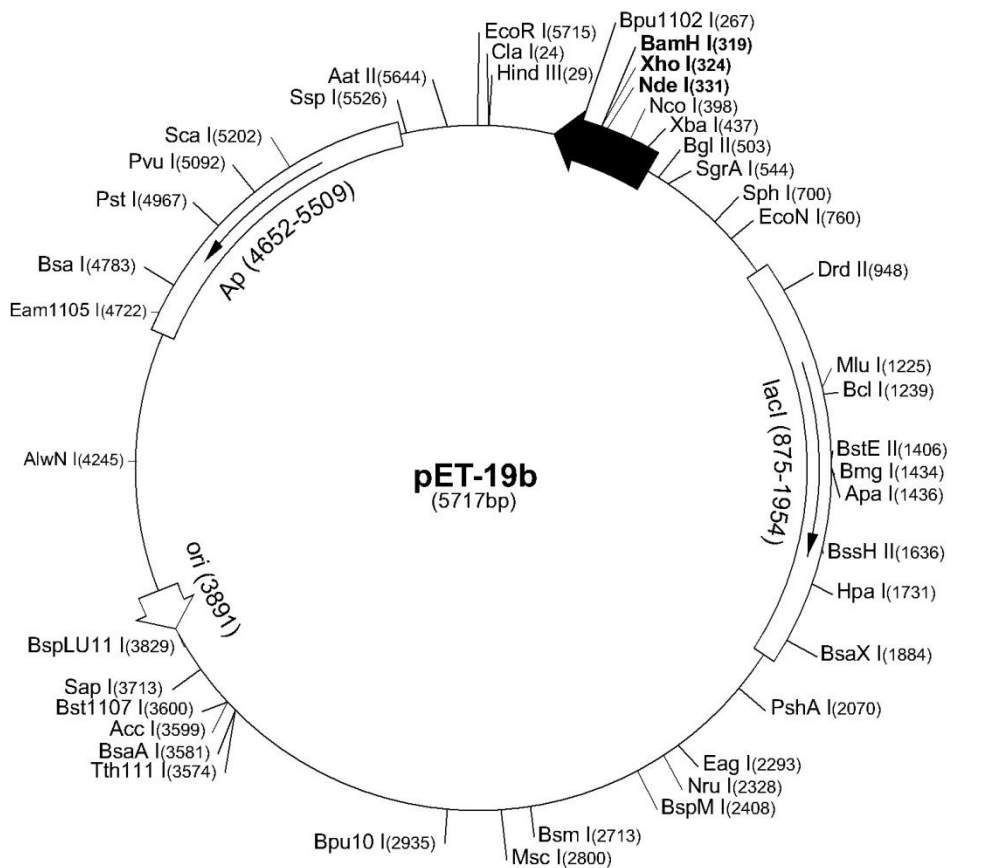


APPENDIX 12: Standard curve of starch degrading activity assay

APPENDIX 13: Standard curve for glucose determination by bicinchoninic acid assay

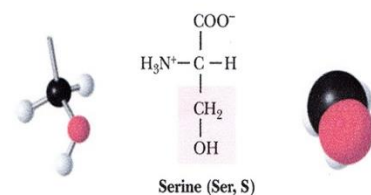
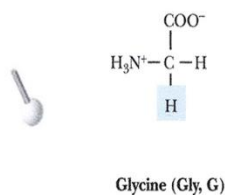
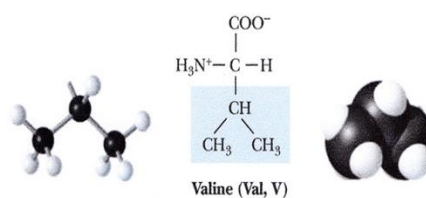
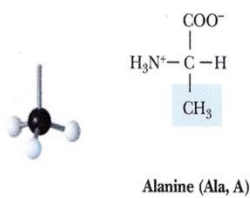
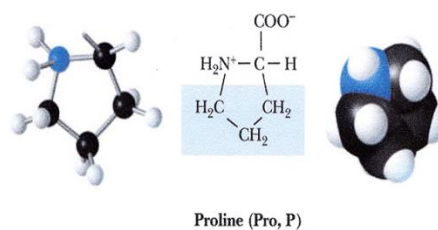
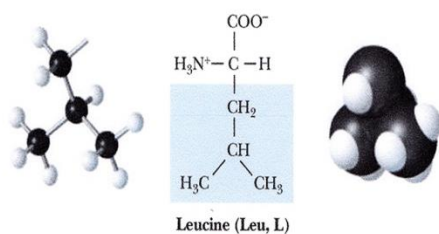


APPENDIX 14: Restriction map of pET-19b

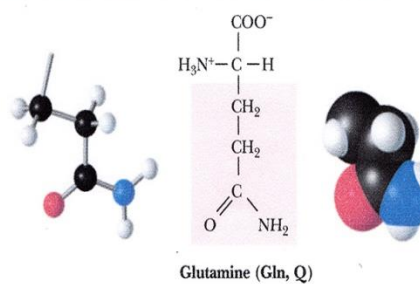
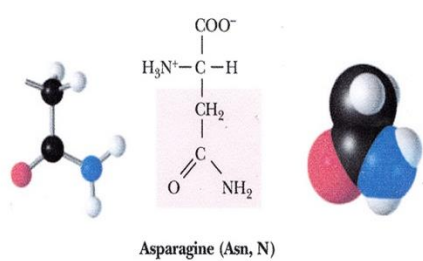


APPENDIX 15: Structures of the amino acids commonly found in protein

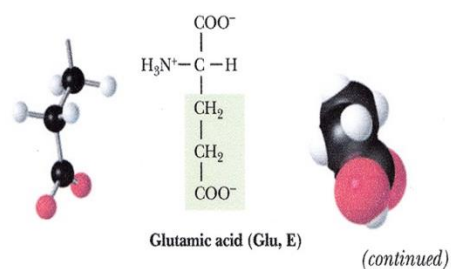
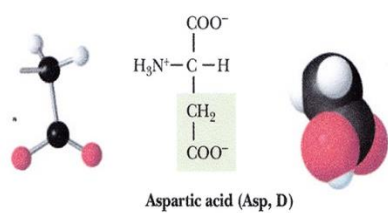
A Non-polar (hydrophobic)



B Polar, uncharged



C Acidic

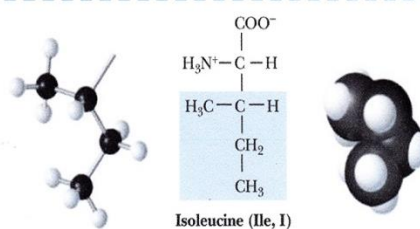
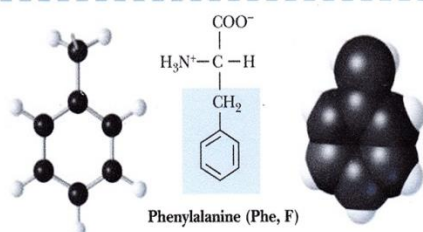
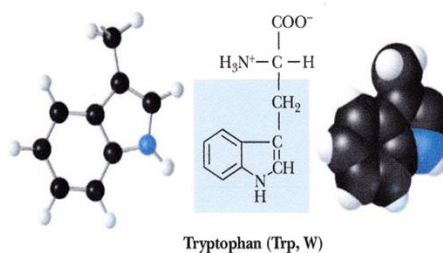
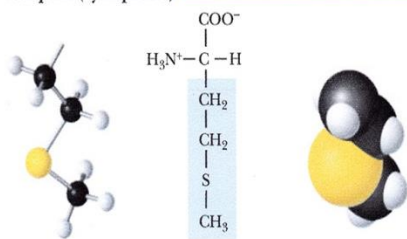


(continued)

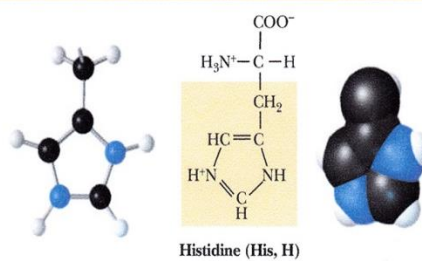
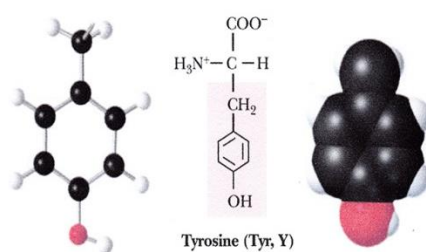
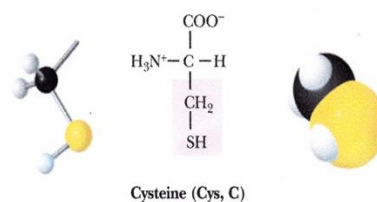
APPENDIX 15: (continued) Structures of the amino acids commonly found in protein

(continued)

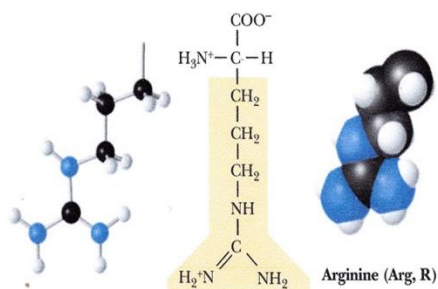
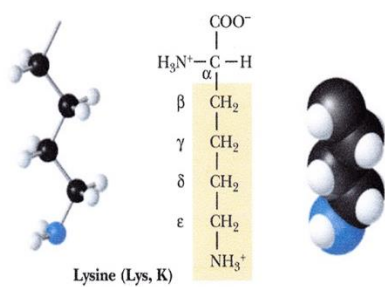
A Non-polar (hydrophobic)



B Polar, uncharged



D Basic



VITA

Miss Pitchanan Nimpiboon was born on September 18th, 1980. She graduated with the Bachelor's degree of Science from the Department of Biotechnology from Ramkhamhang University in 2003 and the Master degree of Science in Biotechnology from Chulalongkorn University in 2008. Then, she continued studying Ph.D. in Biotechnology program, faculty of Science at Chulalongkorn University.

Pubilcation:

1. Nimpiboon, P., Kaulpiboon, J., Krusong, K., Nakamura, S., Kidokoro, S Pongsawasdi, P. Mutagenesis for improvement of activity and thermostability of amyloamylase from *Corynebacterium glutamicum* (Manuscript submitted to *Int. J. Biol. Macromol*)
2. Nimpiboon, P., Kaulpiboon, J., Krusong, K., Nakamura, S., Kidokoro, S Pongsawasdi, P. Alteration in transglucosylation activity and thermostability of N287Y mutated amyloamylase from *Corynebacterium glutamicum* (Manuscript submitted to *Appl. Environ. Microbiol*)

Academic Conference:

1. Nimpiboon, P., Kaulpiboon, J., Pongsawasdi, P. Random mutagenesis of amyloamylase from *Corynebacterium glutamicum* by error-prone PCR for the improvement of enzyme thermostability (Poster presentation) 2012. 13th FAOBMB International Congress of Biochemistry and Molecular Biology, 25-29 November 2012, Bangkok, Thailand.
2. Nimpiboon, P., Kaulpiboon, J., Pongsawasdi, P. A mutation to improve thermostability of *Corynebacterium glutamicum* amyloamylase and to alter large-ring cyclodextrin products profile (Poster presentation) 2013. 7th Asian Cyclodextrin Conference, 27-29 November 2013, Chulalongkorn University, Bangkok, Thailand.
3. Nimpiboon, P., Kaulpiboon, J., Pongsawasdi, P. Random mutagenesis by error-prone PCR for the improvement of thermostability of amyloamylase from *Corynebacterium glutamicum* (Oral presentation) 2014. 18th Biological Sciences Graduate Congress (BSGC), 6-8 January 2014, University of Malaya, Kuala Lumpur, Malaysia.
4. Nimpiboon, P., Kaulpiboon, J., Pongsawasdi, P. A thermostable mutated amyloamylase from *Corynebacterium glutamicum* : Random mutagenesis and enzyme characterization (Poster presentation) 2014. 7th Asia Oceania Human Proteome Organization (AOHUPO) Congress, 6-8 August 2014, Bangkok, Thailand.
5. Nimpiboon, P., Kaulpiboon, J., Pongsawasdi, P. The improvement of thermostability of amyloamylase from *Corynebacterium glutamicum* : random mutagenesis and enzyme characterization (Oral presentation) 2014. NUT-CU Materials Science and Technology Colloquium 2014, 17-18 November 2014, Nagaoka University of Technology, Japan.
6. Nimpiboon, P., Kaulpiboon, J., Pongsawasdi, P. Mutation at Ala-406 in Amyloamylase from *Corynebacterium glutamicum* leads to changes in thermostability and cyclodextrin product profile (Oral and Poster presentation) 2015. 8th Asian Cyclodextrin Conference, 14-16 May 2015, Kumamoto, Japan.